Epac's (exchange protein directly activated by cAMP) role in obesity-induced cardiovascular diseases

by

ZIBELE NDLOVU

A thesis in fulfilment of the requirements for the degree

Doctor of Philosophy

Division of Medical physiology, Faculty of Medicine and Health Sciences,

Stellenbosch University

Supervisor: Dr Erna Marais

Co-supervisor: Prof Hans Strijdom

March 2020

DECLARATION

By submitting this dissertation electronically, I declare that the entirety of the work contained therein is my own, original work, that I am the sole author thereof (save to the extent explicitly otherwise stated), that reproduction and publication thereof by Stellenbosch University will not infringe any third-party rights and that I have not previously in its entirety or in part submitted it for obtaining any qualification.

Mr Zibele Ndlovu
Date March 2020

ABSTRACT

Introduction and aims: The strong association between obesity and cardiovascular diseases (CVD) stresses the necessity of elucidating the underlying molecular mechanisms linking these pathologies. Evidence suggests that Epac (exchange protein directly activated by cAMP) could be a new therapeutic target for obesity and CVD. This study aimed to elucidate the role of Epac in (i) myocardial I/R injury of *ex vivo* hearts from normal weight; and diet-induced obese rats; (ii) vascular reactivity of *ex vivo* aortas from diet-induced obese rats and (iii) free fatty acid (FFA)-induced endothelial dysfunction in rat aortic endothelial cells (RAECs).

Methods: Male Wistar rats of normal weight (250 to 350 g) or receiving a high-calorie diet (HC) for 16 weeks or age-matched controls (CD), were used. Mechanical function of isolated perfused working rat hearts were evaluated. Regional ischaemia (35 minutes) was followed by 60 minutes reperfusion and infarct size determination. Hearts were perfused with a selective Epac1 agonist (8-CPT-2'-O-Me-cAMP, CPT, 2 µM) or antagonist (ESI-09, 5 µM) for 10 minutes before (pre-treatment) or after (post-treatment) regional ischaemia and also post-treated with MEK-ERK inhibitor (PD98059, 10 µM) or PKB inhibitor (A6730, 2.5 µM). Thoracic aortas were isolated from rats fed either the HC or CD diet. Aortas were pre-incubated for 15 min with CPT, ESI-09 or nitric oxide synthase (NOS) inhibitor (L-NAME, 100 µM). Vascular reactivity was evaluated by phenylephrine-precontraction followed by acetylcholine-induced relaxation. Cardiac and aortic signalling proteins were detected with Western blotting. Cultured RAECs were supplemented with FFAs (Palmitic acid and Oleic acid) to induce endothelial injury. The effects of FFAs, CPT and ESI-09 on intracellular levels of NO, superoxide (ROS) and cell viability were determined with fluorescence-based assays.

Results: After 16 weeks the HC animals presented with significantly increased body weight and visceral fat. In hearts, HC diet had no deleterious effects on post-ischaemic cardiac function and infarct size. Post-treatment with CPT (2 µM) reduced infarct size and improved cardiac recovery. This protection was abolished by post-treatment with A6730 in HC hearts, but not with PD98059. Furthermore, CPT increased CaMKII

activation but reduced eNOS phosphorylation. Epac inhibitor (ESI-09, 5 μM) was detrimental to cardiac function. This was associated with: decreased phosphorylated ERK1/2 and GSK-3β; increased phosphorylated AMPK, ULK-1 and PARP cleavage. HC diet did not adversely affect vascular reactivity. CPT significantly improved vasorelaxation in both diets which were abolished by ESI-09. CPT induced vasorelaxation in a dose-dependent manner in both diets via NOS. ESI-09 reduced PKB phosphorylation in CD aortas and increased AMPK phosphorylation in both diets. In normal RAECs CPT improved NO production and reduced intracellular ROS. CPT could not reverse the detrimental effect of FFAs on RAECs.

Conclusion: Post-ischaemic Epac activation is cardioprotective against I/R injury in *ex vivo* isolated rat hearts from HC, partially via the PKB pathway. Epac activation improved vasorelaxation via NOS in *ex vivo* aortas from both diets. In addition, Epac activation increased NO production and reduced ROS generation in normal RAECs. Therefore Epac may be a potential therapeutic target in the protection against CVD.

ABSTRAK

Inleiding en doelstellings: Die sterk verband tussen vetsug en kardiovaskulêre siektes (KVS) beklemtoon die noodsaaklikheid om die onderliggende molekulêre meganismes wat hierdie patologieë verbind, te verklaar. Bewyse dui daarop dat Epac ('n uitruil-proteïen wat direk deur cAMP geaktiveer word) 'n nuwe terapeutiese teiken vir vetsug en KVS kan wees. Hierdie studie het ten doel gehad om die rol van Epac in (i) miokardiale isgemie-herperfusie (I/R)-besering van *ex vivo*-harte van óf normale gewig óf dieet-geïnduseerde vetsugtige rotte; (ii) vaskulêre reaktiwiteit van *ex vivo* aortas van dieet-geïnduseerde vetsugtige rotte en (iii) vrye vetsuur (VVS) geïnduseerde endoteel disfunksie in rot aorta endoteelselle (RAEC), te ondersoek.

Metodes: Manlike Wistar-rotte van 'n normale gewig (250 tot 350 g) of 'n hoë-kalorie-dieet (HC) vir 16 weke of 'n ouderdomskontrole (CD), is gebruik. Meganiese funksie van geïsoleerde geperfuseerde werkende rot harte is geëvalueer. Streeks-isgemie (35 minute) is gevolg deur herperfusie (60 minute) en infarkt-grootte bepaling. Harte is behandel met 'n selektiewe Epac1-agonis (8-CPT-2'-O-Me-cAMP, CPT, 2 μM) of 'n antagonis (ESI-09, 5 μM) vir 10 minute voor (pre-behandeling) of na (post-behandeling) streeks-isgemie en ook post-behandeling met MEK-ERK-inhibitor (PD98059, 10 μM) of PKB-inhibitor (A6730, 2.5 μM). Torakale aortas is geïsoleer van rotte wat óf die HC- óf CD-dieet gevoer is. Aortas is 15 minute vooraf geïnkubeer met CPT, ESI-09 of stikstofoksied sintase (NOS) inhibitor (L-NAME, 100 μM). Vaskulêre reaktiwiteit is geëvalueer deur fenielefrien-prekontraksie gevolg deur asetielkolien-geïnduseerde ontspanning. Met Western blot analise is hart- en aorta-seineproteïene bepaal. Gekultuurde RAEC is gesupplementeer met VVSe (Palmitaat en Oleaat) om endoteelbesering te veroorsaak. Die effekte van VVSe, CPT en ESI-09 op intrasellulêre vlakke van NO, superoksied (ROS) en sel-oorlewing is bepaal met behulp van fluoressensie-gebaseerde toetse.

Resultate: Na 16 weke het die HC-diere se liggaamsgewig en viserale vet aansienlik vermeerder. In die harte het HC-dieet geen nadelige gevolge gehad op post-isgemiese hartfunksie en infarkt-grootte nie. Post-behandeling met CPT (2 μM) het

infarkt-grootte verminder en die funksionele herstel verbeter. Hierdie beskerming is opgehef deur post-behandeling met A6730 in HC-harte, maar nie met PD98059 nie. Verder het CPT die aktivering van CaMKII verhoog, maar eNOS-fosforilering verminder. Epac-antagonis (ESI-09, 5 μM) was nadelig vir die hartfunksie. Dit was geassosieer met: verminderde gefosforileerde ERK1/2 en GSK-3β; verhoogde gefosforileerde AMPK, ULK-1 en PARP splitsing. HC-dieet het nie die vaskulêre reaktiwiteit benadeel nie. CPT het in beide diëte vaso-verslapping aansienlik verbeter, wat deur ESI-09 opgehef is. CPT het vaso-verslapping op 'n dosis-afhanklike manier in beide diëte via NOS, veroorsaak. ESI-09 verminder PKB-fosforilering in CD-aortas en verhoog AMPK-fosforilering in beide diëte. In normale RAEC's het CPT die NO produksie verbeter en die intrasellulêre ROS verminder. CPT kon nie die nadelige uitwerking van VVSe op RAEC's omkeer nie.

Gevolgtrekking: Post-iskemiese Epac-aktivering is kardiobeskermend teen I/R-beserings in *ex vivo* geïsoleerde rotteharte van HC, gedeeltelik via die PKB-pad. Epac-aktivering het vaso-verslapping, via NOS in *ex vivo* aortas van beide diëte, verbeter. Boonop het Epac-aktivering NO produksie verhoog en ROS-ontwikkeling in RAEC's verminder. Daarom kan Epac 'n potensiële terapeutiese teiken in die beskerming teen KVS wees.

ACKNOWLEDGEMENTS

I would like to express my deep gratitude to **Dr. Erna Marais** and **Prof. Hans Strijdom**, my research supervisors, for their patient guidance, enthusiastic encouragement and useful critiques of this research work.

I am also thankful for:

- Prof. Barbara Huisamen and Prof. Amanda Lochner for their assistance throughout the project.
- Dr. Amanda Genis for her assistance in tissue culture experiments.
- Dr. Corli Westcott for her assistance in vascular reactivity experiments.
- The entire Division of Medical Physiology staff and students for their continued support during this project.
- **National Research Foundation (NRF)**, Harry Crossley Foundation and the University of Stellenbosch for funding throughout my PhD studies.
- My parents, Mr. Elliot D. Ndlovu and Mrs. Nokhaya Ndlovu, and my family for their endless love, support and encouragement.
- I would also like to thank **God** for who without everything could have been impossible to achieve.

OUTPUTS DURING THE COURSE OF THE STUDY

PRESENTATIONS AT SCIENTIFIC MEETING

Title of Proceeding	**Society for Heart and Vascular Metabolism (SHVM)**
Title of Conference	15th Annual Scientific Sessions: The Power of Metabolism
Title of Contribution	*Vascular alterations in diet-induced obese rats: role of exchange protein directly activated by cyclic AMP (Epac)*
All Authors	**Zibele Ndlovu**, H Strijdom, A Lochner, E Marais
Status	Presented
Year	2017
City/Country	Weimar, Germany

Title of Proceeding	**18th Annual Congress of the South African Heart Association**
Title of Conference	18th Annual Congress of the South African Heart Association
Title of Contribution	*Cardioprotection in hearts from obese rats is mediated via an Exchange protein directly activated by cyclic AMP (Epac) - ERK pathway*
All Authors	**Zibele Ndlovu**, H Strijdom, A Lochner, E Marais
Status	Presented
Year	2017
City/Country	Sandton (JHB), South Africa

Title of Proceeding	**Physiology Society Of South Africa (PSSA) (2016)**
Title of Contribution	*High fat diet-induced obesity: the role of Epac (Exchange protein directly activated by cyclic AMP) in myocardial ischaemia/reperfusion of ex vivo rat hearts.*
All Authors	**Zibele Ndlovu**, Prof H Strijdom, Prof A Lochner, Dr E Marais
Status	Presented
Year	2016
City/Country	Cape Town, South Africa

Title of Proceeding	**South African Society for Cardiovascular Research (SASCAR) (2016)**
Title of Contribution	*High fat diet-induced obesity: the role of Epac (Exchange protein directly activated by cyclic AMP) in myocardial ischaemia/reperfusion of ex vivo rat hearts.*
All Authors	**Zibele Ndlovu**, H Strijdom, A Lochner, E Marais
Status	Presented
Year	2016
City/Country	Cape Town, South Africa

Title of Proceeding	**Academic Year Day, Stellenbosch University, Faculty of Medicine and Health Sciences (2016)**
Title of Contribution	*High fat diet-induced obesity: the role of Epac (Exchange protein directly activated by cyclic AMP) in myocardial ischaemia/reperfusion of ex vivo rat hearts.*
All Authors in Order	**Zibele Ndlovu**, H G Strijdom, A Lochner, E Marais
Status	Presented
Year	2016
City/Country	Cape Town, South Africa

Title of Proceeding	**SA Heart Annual congress (2016)**
Title of Contribution	*The role of Epac (exchange protein directly activated by cAMP) in obesity-induced cardiovascular dysfunction.*
All Authors	E Marais, **Zibele Ndlovu**, H Strijdom
Status	Co-author
Year	2016
City/Country	Cape Town, South Africa

Title of Conference	**Department of Science and Technology, and National Research Foundation (DST-NRF Research Day 2015)**
Title of Contribution	*Selective Epac modulation mediates cardioprotection during ischaemia/reperfusion*
All Authors	**Zibele Ndlovu**, Dr E Marais, Prof A Lochner
Status	Presented and won 1st prize for oral presentation
Year	2015
City/Country	Cape Town, South Africa

TABLE OF CONTENT

List of figures

List of tables

Units of measurements and symbols

% percentage
°C degree celcius
bpm beats per minute
cm centimeter
g gram
h hour
Hg mercury
IU International unit
kDa kilo Daltons
kg kilogram
kJ kilojoules
L litre
M molar
mg milligram
min minute
mM millimolar
mm millimeter
mWatts milliwatts
p pico
rpm revolutions per minute
sec second
v volume
V volt
W work
α alpha
β beta
µ micro
µL microlitre
µM micromolar

List of abbreviations

5'-AMP: 5'-adenosine monophosphate
8-pCPT/CPT: 8-(4-Chlorophenylthio)-2′-O-methyladenosine-3′,5′-cyclic monophosphate
AC: adenylate cyclase
ACh: acetylcholine
AF: aortic flow
AIDS: acquired immunodeficiency syndrome
AMPK: adenosine monophosphate-activated protein kinase
ANOVA: one-way analysis of variance
ATP: adenosine triphosphate
ATPase: adenosine triphosphatase
Bad: Bcl-2-associated death promoter
Bak: Bcl-2 homologous antagonist/killer
Bax: Bcl-2-associated X protein
Bcl-2: B-cell lymphoma 2
BcL-xL: B-cell lymphoma-extra large
bFGF: basic fibroblast growth factor
BK_{Ca}: Ca^{2+} -sensitive large-conductance K^+ channels
BMI: body mass index
Ca^{2+}: calcium ion
CAD: coronary artery disease
CaM: calmodulin
CaMKII: calmodulin kinase II
cAMP: cyclic adenosine 3',5' monophosphate
CaN: calcineurin
CD: control diet
CF: coronary flow
cGMP: cyclic guanosine monophosphate
CMEC: cardiac microvascular endothelial cells
CNBD: cyclic-nucleotide-binding domain
CO: cardiac output
cPLA2: cytosolic phospholipase A2
CVD : cardiovascular disease
DAF-2/DA: 4,5-diaminofluorescein-2/diacetate
DAG: diacylglycerol
DEA/NO: Diethylamine NONOate diethylammonium salt
DEP: Dishevelled, Egl-10, Pleckstrin
DHE: Dihydroethidium
DMSO: dimethyl sulfoxide
DRP1: Dynamin related protein 1
EAT: epicardial adipose tissue
ECL: enhanced chemiluminescence
ED: endothelial dysfunction
EDTA: Ethylene diamine tetra acetic acid
EGTA: Ethylene glycol tetra acetic acid
E_{max}: maximal tension/ contraction
eNOS: endothelial nitric oxide synthase
Epac: exchange protein directly activated by cAMP
Erg1: early growth response protein 1
ERK1/2: extracellular signal-regulated kinase 1 and 2
ESI-09: 3-(5-Tert-butyl-isoxazol-3-yl)-2-[(3-chloro-phenyl)-hydrazno]-3-oxo-propionitrile
FBS: Foetal bovine serum
FFAs: free fatty acids
GEFs: guanine nucleotide exchange factors

GLUT2: Glucose transporter 2
GPCR: G-protein-coupled receptors
GSK3β: glycogen synthase kinase 3 beta
GTP: guanosine-5'-triphosphate
HC: high calorie diet
HDL: high-density lipoprotein
HFD: high fat diet
HIV: human immunodeficiency virus
HOMA-IR: homeostatic model for insulin resistance
I/R: ischaemia/reperfusion
IC: ischaemic conditioning
IHD: ischaemic heart disease
IL6: interleukin 6
I_{NaL}: late sodium current
iNOS: inducible nitric oxide synthase
IP_3: inositol trisphosphate
IPosC: ischaemic postconditioning
IPreC: ischaemic preconditioning
ISO: isoproterenol
JNK: c-Jun N-terminal kinase
K^+: potassium ion
L-NAME: N(ω)-nitro-L-arginine methyl ester
LAD: left anterior descending
LDL: low-density lipoprotein
LV: left ventricular
LVH: left ventricular hypertrophy
mK_{ATP}; mitochondrial ATP-dependent potassium channel
MLC: myosin light chain
mPTP: mitochondrial permeability transition pore
mRNA: messenger RNA
mTOR: mammalian target of rapamycin
Na^+: sodium ion
NCDs: non-communicable diseases
NFAT: nuclear factor of activated T-cells
nNOS: neuronal nitric oxide synthase
NO: nitric oxide
NOS: nitric oxide synthase
OA: Oleic acid
OGTT: oral glucose tolerance test
p38 MAPK: p38 mitogen-activated protein kinases
PA: Palmitic acid
PARP: Poly (ADP-ribose) polymerase
PBS: Phosphate-buffered saline
PDE: phosphodiesterase
PDE3: phosphodiesterase 3
PDE4: phosphodiesterase 4
PDGF: platelet-derived growth factor
PDGFR: platelet-derived growth factor receptor
PDX-1: pancreatic and duodenal homeobox 1
PI: Propidium Iodide
PI3K: phosphoinositide-dependent kinase
PIP_2: phosphatidylinositol 4,5-bisphosphate
PKA: protein kinase A
PKB/Akt: protein kinase B
PKG: protein kinase G
PLB: phospholamban
PLCε: phospholipase Cε
PMSF: phenylmethylsulfonyl fluoride
PSP: peak systolic pressure
PVAT: perivascular adipose tissue
PVDF: polyvinylidene fluoride
RAECs: rat aortic endothelial cells
Ral GDS: Ral Guanine Nucleotide Dissociation Stimulator
Rap1: Ras-related protein 1
Rap2: Ras-related protein 2
RBD: Rap1-binding domain

Rheb: Ras homolog enriched in brain
RhoA: Ras homolog gene family, member A
RIP1: receptor-interacting protein 1
RISK: reperfusion injury salvage kinase
R_{max} : maximal relaxation
ROS: reactive oxygen species
RPosC: remote ischaemic post conditioning
RyR: ryanodine receptor
SAFE: survivor activating factor enhancement
SANS: South African National Standard
SDS: sodium dodecyl sulphate
SEM: standard error of the mean
Ser: Serine
SERCA: sarcoplasmic reticulum Ca2+ ATPase
Skp2: s-phase kinase-associated protein 2
SOCS-3: suppressor of cytokine signalling 3
STAT-3: signal transducer and activator of transcription 3
STAT-5: signal transducer and activator of transcription 5
T-cells: T-lymphocytes
T2D: type 2 diabetes mellitus
TGF-β1: transforming growth factor beta 1
Thr : threonine
TNF-α: tumour necrosis factor alpha
TPF: 1,3,5-triphenylformazan
TTC: triphenyl tetrazolium chloride
TW: Total work performance
ULK1: Unc-51 like autophagy activating kinase 1
VECs: vascular endothelial cells
VSMCs: vascular smooth muscle cells
WHO: World Health Organisation
β-arr: beta-arrestin

Chapter One

Literature Review

1. Cardiovascular disease (CVD)

1.1 General introduction and epidemiology

Cardiovascular disease (CVD) is a broad term used to describe a range of disorders that affect the heart and the circulatory system; such disorders include coronary artery disease (CAD), cardiac dysrhythmias, hypertension, congenital heart defects and cerebrovascular disease (British Heart Foundation, 2019; Sanchis-Gomar *et al*., 2016).

CVD is the most common causes of death worldwide. In the year 2016, the World Health Organisation (WHO) estimated about 17.9 million people died from CVDs each year, which contributed to 31% of all deaths globally (WHO, 2018a). Of these deaths, CAD and stroke were the major contributors with an estimated 7.4 million deaths due to CAD and 6.7 million deaths due to stroke respectively (WHO, 2018a). In 2015, an estimated 82% of premature deaths in underdeveloped (low income) and developing (middle income) countries were due to non-communicable diseases (NCDs), and 37% were caused by CVDs (WHO, 2018a).

In Africa, the challenges of communicable diseases such as malaria, HIV/AIDS, and tuberculosis are well known (Kandala *et al*., 2014). However, the rapid increase in chronic NCDs such as CAD and stroke, due to risk factors like obesity, hypertension, and type 2 diabetes mellitus (T2D) are becoming a major public health problem, especially in Sub-Saharan Africa (Kandala *et al*., 2014). Epidemiological transition driven by urbanisation, globalization and social changes is the major contributor to the development of these chronic NCDs (Mathers and Loncar, 2006; Oni *et al*., 2015).

South Africa is the most urbanised developing country with an estimated 62% of the country's population living in the cities (Oni *et al*., 2015; Prados-Torres *et al*., 2014) and that number has increased to 65.78% in 2017 (Statista, 2017). This rapid and unplanned demographic shift can affect lifestyle choices such as unhealthy dietary patterns due to the high cost of living in the cities (Kandala *et a*l., 2014; Mathers and Loncar, 2006).

Therefore in South Africa, NCDs particular CVD are already among the top causes of death (Nojilana *et al.*, 2016). In 2010, NCDs accounted for 39% of total deaths in the country and more than a third (36%) of these deaths occurred before the age of 60 years (Nojilana *et al*., 2016). In addition, the number of deaths due to NCDs was similar to the number from HIV/AIDS and tuberculosis combined (Nojilana *et al*., 2016).

Recently, NCDs were estimated to account for more than 50% of all deaths in South Africa and CVD (19%) as the major contributor (WHO, 2018b). Furthermore, the major risk factors for NCDs in South Africa include excessive use of alcohol, physical inactivity, increased salt/sodium intake, tobacco use, high blood pressure and obesity (WHO, 2018b).

1.2 Risk factors of CVD

There are two types of CVD risk factors: non-modifiable and modifiable. The "non-modifiable" risk factors cannot be changed and they include age, gender and family history. Other risk factors can be changed ("modifiable''), which include dyslipidaemia (altered levels of blood cholesterol and raised triglycerides with low HDL-cholesterol), hypertension/high blood pressure, diabetes, excessive stress, sedentary lifestyle, smoking, excessive alcohol consumption and being overweight/ obesity (Díaz-Vegas *et al*., 2018; Grundy, 2012; Mandini *et al*., 2018; Puddey *et al*., 1999). For the purpose of this study, the focus will be on obesity as a modifiable CVD risk factor.

1.3 Obesity as a CVD risk factor

Obesity is persistently increasing worldwide, and it affects all age groups. Obesity is defined by or classified using an anthropometric measurement, the body mass index (BMI). An individual is classified overweight with a BMI of 25–29.9 kg/m^2 and obese with a BMI of ≥ 30 kg/m^2 or waist to hip ratio of >0.9 (male) or >0.85 (females) (Lanktree and Hegele, 2017; Poirier *et al.*, 2009). However, it has been reported that BMI is not the gold standard measure of body fat and there is no clear association between body weight, mortality and cardiovascular events (Romero-Corral *et al.*, 2006). Generally, excess body fat is closely associated with cardiovascular abnormalities (Wormser *et al*., 2011). Therefore, although BMI influences cardiovascular risk, one should argue that other adiposity indices should be taken into consideration such as the waist circumference and waist-to-hip ratio (Bastien *et al.*, 2014). These adiposity indices may further influence the intermediate risk factors (high blood pressure, diabetes, dyslipidaemia, insulin resistance and inflammation) which may lead to increased cardiovascular events (Bastien *et al.*, 2014; Poirier, 2007; Romero-Corral *et al*., 2007, 2006). It has been reported that among patients with CVDs, the overweight and obese patients often counterintuitively show an improvement in cardiovascular events and mortality, and this controversy is called the “obesity paradox” (Bastien *et al*., 2014; Carbone *et al*., 2019). Therefore, despite the influence of obesity on cardiovascular health, normal-weight patients can also develop metabolic abnormalities that may increase cardiovascular events and mortality.

1.3.1 Excessive visceral adiposity and CVD

Visceral fat or abdominal fat is located within the abdominal cavity and it surrounds the major organs e.g. stomach, liver, kidneys and intestines. Regardless of BMI, excess abdominal fat is strongly associated with a number of diabetogenic and atherogenic abnormalities such as an increase in peripheral tissue insulin resistance, plasma free fatty acid (FFA) release, inflammatory cytokines, decrease in adiponectin, a decrease in cardiac output and a decrease in endothelium-dependent vasorelaxation (Bastien *et al*., 2014). In the vasculature, an excess in perivascular adipose tissue (PVAT) can cause local inflammation, impaired vascular function,

vascular remodelling and an increase in macrophage infiltration into atherosclerotic lesions (Horimatsu *et al*., 2017; Lastra and Manrique, 2015; Ozen. *et al.*, 2015)

1.3.2 Cardiac remodelling and obesity

Cardiac remodelling also known as the ventricular remodelling is defined as a change in size, shape and function of the heart. This can occur due to exercise or after an injury to the heart muscle (pathological remodelling). Obesity is associated with increased myocardial fat and impair myocardial metabolism which can induce cardiac remodelling whereby the heart is trying to adapt to the new environment as well as to maintain the whole body's blood supply (Bastien *et al*., 2014). Therefore, the heart maintains this adaptive state by increasing the cardiac output and decreasing peripheral resistance (Bastien *et al.*, 2014; Kaltman and Goldring, 1976; Messerli *et al*., 1987). Furthermore, excess myocardial fat can lead to impaired myocardial metabolism and reduced metabolic activity. This could lead to heart failure (with a decreased diastolic chamber compliance, an increase in the left ventricular (LV) mass, a concentric LV remodelling and fatty infiltration of the right ventricle (Iacobellis et al., 2014; Iacobellis and Sharma, 2007).

In obese patients, an increased cardiac output can be a determinant of the amount of blood pumped out in each ventricle due to contraction (Bastien *et al*., 2014). Excessive blood volume contributes to an increase in heart preload and if this happens for a longer duration it can cause left ventricular wall thickening (ventricular remodelling) and subsequently left ventricular hypertrophy (LVH) (Ku *et al.*, 1994). LVH, muscle degeneration, systolic and diastolic dysfunction are major factors that contribute to heart failure in obese patients (Alpert *et al*., 1995; Lauer *et al.*, 2010). Furthermore, increased epicardial fat is associated with obesity and atherosclerosis (Shimabukuro *et al.*, 2013; Vela *et al*., 2007). Epicardial fat is closely associated with the amount of visceral fat deposits which may produce proinflammatory cytokines and macrophages involved in CAD (Iacobellis and Sharma, 2007; Shimabukuro et al., 2013).

1.4 Ischaemic heart disease (IHD)

The term ischaemia refers to an inadequate blood supply to organs (such as the heart, brain, liver, kidney and intestine) due to narrowing or obstruction of the arterial flow as a result of atherosclerotic plaque development (NIH, 2019). Myocardial ischaemia is defined as a narrowing of the coronary arteries, which is also known as coronary artery disease (CAD) (NIH, 2019). Therefore, a reduction in blood supply causes an insufficient supply of oxygen and reduces the availability of nutrients to the myocardium (see “Ischaemic phase” in section 1.4.3.1).

1.4.1 Process of atherosclerosis

1.4.1.1 Endothelial cells in the heart

The heart is a complex organ and is made up of different cell types, including cardiomyocytes, endothelial cells, inflammatory cells, stem cells, and fibroblasts (Kamo *et al*., 2015; Perin and Silva, 2004). These cells are highly organised in the myocardium and secrete autocrine, juxtacrine, and paracrine factors that modulate the function of neighbouring cells (Segers *et al*., 2018). Intercellular communication is pivotal in cardiac development, normal cardiac function and in pathophysiology of cardiac remodelling and heart failure development (Segers *et al*., 2018). In particular, cardiac microvascular endothelial cells (CMEC), which are part of cardiac endothelium, secrete factors that play a vital role in normal cardiac function and during cardiac remodelling (Segers, Brutsaert and De Keulenaer, 2018).

The myocardium is a highly metabolic tissue and it receives blood supply from a dense vascular and capillary network (Duncker and Bache, 2008). The CMECs line these capillaries and serve as a barrier between blood and the myocardial tissue. But they also communicate with adjacent cardiomyocytes by exchanging small molecules, peptides, proteins, microvesicles, and microRNAs (Brutsaert, 2015). Similar to cardiac endothelium, the endothelial cells are located in the pericardial coronary arteries, which are part of coronary vascular endothelium, that plays a crucial role in modulating vascular smooth muscle function (Brutsaert, 2015). Endothelial cells in the microcirculation of the heart produce paracrine factors which can regulate

cardiomyocyte contractility, growth and survival (Segers *et al*., 2018). These paracrine factors include prostacyclin, angiotensin II, endothelin 1 and nitric oxide (NO) (Brutsaert, 2015).

1.4.1.2 Nitric oxide as an early precursor of endothelium dysfunction and eventually atherosclerosis

NO and endothelium function

NO is a soluble gas synthesised from the amino acid L-arginine in endothelial cells by the constitutive Ca^{2+}-calmodulin-dependent enzyme and endothelial nitric oxide synthase (eNOS) (Behrendt and Ganz, 2002; Palmer *et al*., 1988). Endothelial nitric oxide is one of the three distinct isoforms of NOS, including neuronal NOS (nNOS) and inducible NOS (iNOS). Endothelial NOS is constitutively expressed and it is referred to as Ca^{2+}-dependent enzyme even though eNOS can be activated in a Ca^{2+}-independent manner (Behrendt and Ganz, 2002; Förstermann and Kleinert, 1995). Endothelium shear stress (blood flow) is the main trigger of NO production under physiological conditions in a Ca^{2+}-independent manner (Figure 1.1) (Behrendt and Ganz, 2002; Zhao *et al.*, 2015). On the other hand, agonists including acetylcholine (ACh), serotonin, thrombin and bradykinin act on specific receptors on the endothelial cell membrane to increase the intracellular concentration of Ca^{2+}, which binds to calmodulin (CaM) and leads to the activation of calmodulin-binding domain of eNOS to produce NO (Figure1.1 Behrendt and Ganz, 2002; Zhao *et al.*, 2015). The vasodilatory effect of NO on vascular smooth muscle is through activation of guanylate cyclase, an enzyme that catalyses the synthesis of cyclic guanosine monophosphate (cGMP) from guanosine-5'-triphosphate (GTP) in response to low intracellular Ca^{2+} levels (Behrendt and Ganz, 2002; Förstermann and Kleinert, 1995).

Subsequently, it was discovered that endocardial endothelial cells produce NO which modulates growth, contractility and rhythmicity of cardiomyocytes (Brutsaert, 2015). NO has a positive inotropic effect in smaller concentration, however, in higher concentrations, it has negative inotropic effects (Balligand *et al*., 2009; Brutsaert, 2015; Mohan *et al*., 1996).

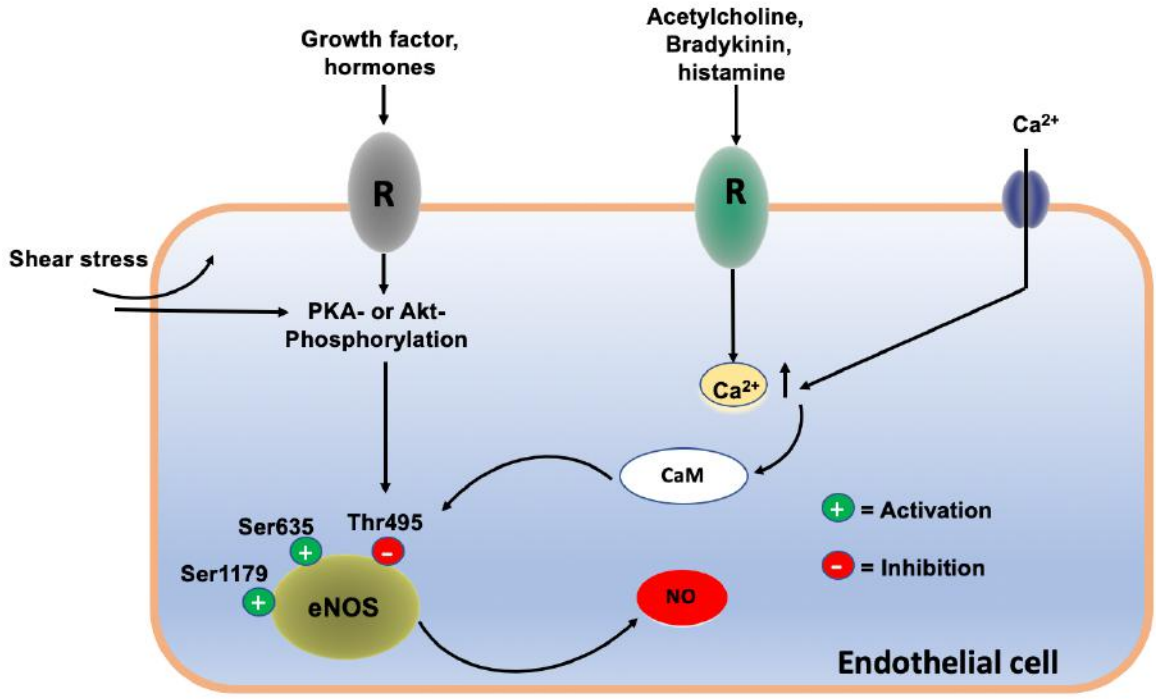

Figure 1. 1 Endothelial nitric oxide synthase (eNOS).

Endothelial NOS can be activated in Ca^{2+}-dependent or- independent ways. The Ca^{2+}-dependent pathway involves agonist such Ach, bradykinin and histamine which act on receptors (R) to increase intracellular Ca^{2+}, which binds to CaM and leads to activation of calmodulin-binding domain of eNOS to produce NO. On the other hand, phosphorylation of eNOS independently of the calcium concentration is also important for the activation of the enzyme. Thr495 is an inhibitory site but Ser635 and Ser1179 are activation sites. The responses to hemodynamic shear stress and hormones are mediated mainly through this calcium-independent pathway. Taken from (Zhao *et al.*, 2015).

1.4.1.3 Endothelial dysfunction

Endothelial dysfunction (ED) is a major pathophysiological phenomenon that leads to coronary artery disease, and other atherosclerotic diseases (Higashi, 2015). A reduction in the bioavailability of pro-vasodilatory factors, predominantly NO, is a key indicator of endothelial dysfunction. (Grover-Páez and Zavalza-Gómez, 2009; Lerman and Zeiher, 2005). Thus, ED is mainly an imbalance in between factors with pro-vasodilatory, anti-mitogenic and anti-thrombogenic properties (endothelium-derived relaxing factors such as NO) and factors with pro-vasoconstrictory, pro-thrombotic and proliferative characteristics (endothelium-derived contracting factors such as endothelin-1)(Flammer and Lüscher, 2010; Higashi, 2015).

1.4.1.4 The role of endothelial cells in the process of atherosclerosis

Atherosclerosis is a disease characterised by thickening of the intimal layer of arteries, accumulation of fat (due to hyperlipidaemia), lipid oxidation, inflammation and other factors (Rafieian-Kopaei *et al.*, 2014). It is a vascular disease that can affect the aorta and coronary arteries (Baradaran, 2012). Several studies have demonstrated that fatty streaks are the first indicators of atherosclerosis (Skålén *et al*., 2002; Tavafi, 2013). Increased accumulation of lipoprotein particles (proteins, phospholipids, cholesterol and triglycerides) in the vascular intimal layer of arteries initiates an atherosclerotic lesion (Rafieian-Kopaei *et al.*, 2014). Low-density lipoprotein (LDL) is also known for its major role in the development of atherosclerotic lesions (Figure 1.2) (Diaz *et al.*, 2002). LDL can easily infiltrate the endothelium or adhere to extracellular matrix components such as proteoglycans and be trapped in the vascular intima (Hajjar and Gotto, 2013; Leitinger, 2003). This leads to the activation of endothelial cells, which causes an increase in the expression of leukocyte adhesion molecules and inflammatory genes (Leitinger, 2003). This causes the blood cells to migrate to the area of activation. Monocytes infiltrate the area of activation and differentiate macrophages leading to plaque development. This activates the immune system, followed by T-cell, antigen-presenting dendritic cell, monocyte, macrophage, and mast cell infiltration (Hansson, 2001). Macrophages secrete meta proteases that contribute to lysis of the extracellular matrix. T-cells (T-lymphocytes) produce a pro-inflammatory cytokine, tumour necrosis factor-alpha (TNF-α), which prevents collagen synthesis in the smooth muscle cells (Rafieian-Kopaei *et al*., 2014). This process weakens the fibrous cap of the plaque resulting in plaque rupture, which leads to blood clot formation in the arteries and blockage of blood flow (Rafieian-Kopaei et al., 2014). This results in an inadequate blood supply (ischaemia) to the vital organs such as heart, brain and kidneys. Furthermore, lipolysis in visceral adipose tissues increases nonesterified fatty acids (NEFA), which in turn increase insulin resistance and eventually an increase in oxidative stress (Hajjar and Gotto, 2013). Oxidative stress and adipokines further exacerbate the vascular pro-oxidant and pro-inflammatory environment which worsen endothelial dysfunction (Hajjar and Gotto, 2013).

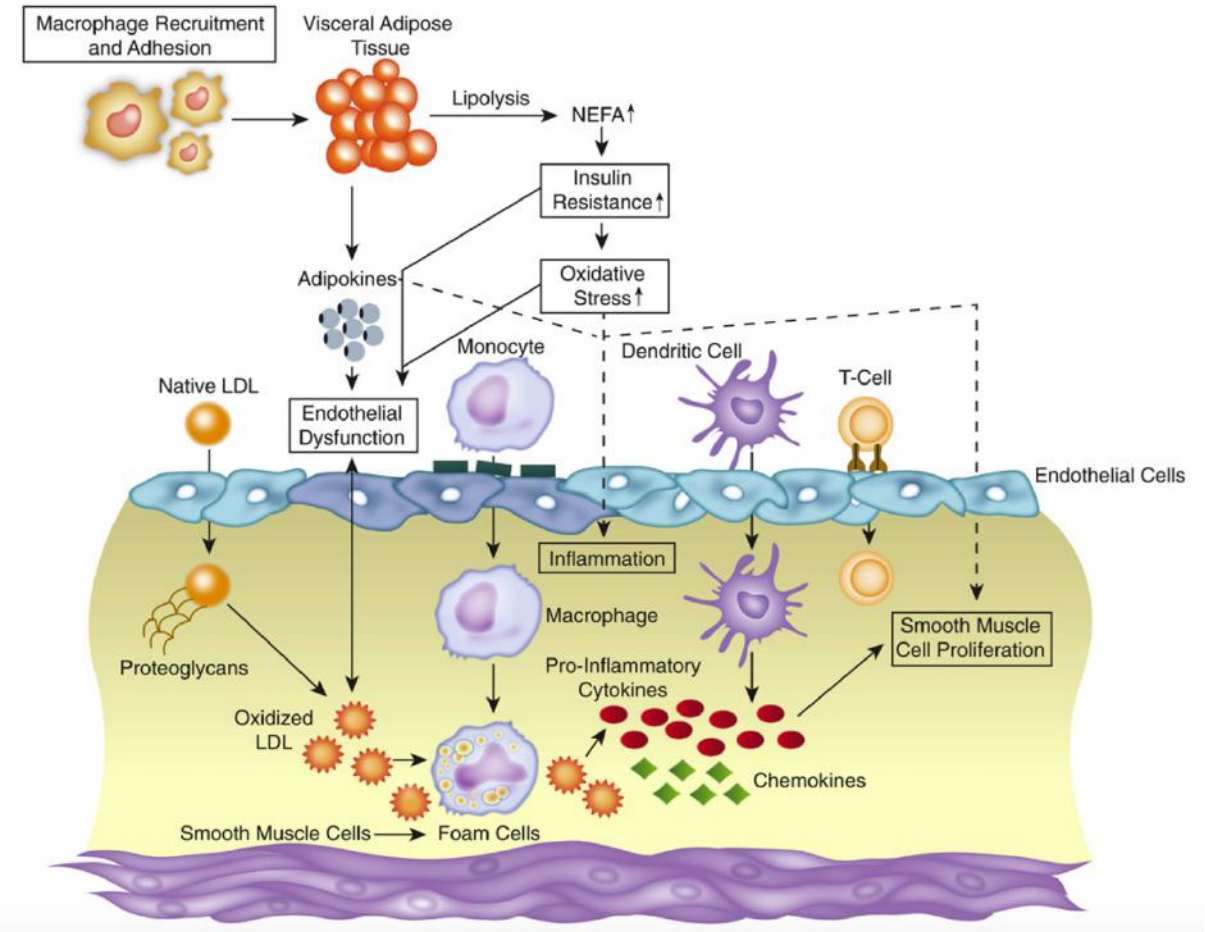

Figure 1. 2 Mechanisms of disease in atherosclerosis and obesity.

Taken from (Hajjar and Gotto, 2013).

1.4.2 Pathophysiology of myocardial infarction

The acute occlusion of coronary arteries through a build-up of atherosclerotic plaque causes a reduction in oxygen and nutrient supply to the myocardium (Ambrose and Singh, 2015). Cardiomyocytes are very sensitive to changes in intracellular oxygen as they rely on oxidative metabolism and therefore a slight reduction in oxygen can result in ischaemic injury to cardiomyocytes (Ardehali *et al.*, 2012). Therefore, myocardial infarction can be defined be as myocardial cell death due to prolonged ischaemia (Frangogiannis, 2015).

1.4.3 Ischaemia-reperfusion (I/R) injury

1.4.3.1 Ischaemic phase

The oxygen tension in cells decreases during ischaemia. There is a decrease in mitochondrial energy production (adenosine triphosphate, ATP, synthesis) due to a loss of oxidative phosphorylation (de Groot and Rauen, 2007). ATP depletion impairs cellular ion homeostasis, resulting in the activation of hydrolases, and increasing the permeability of cellular membranes (de Groot and Rauen, 2007). In addition, ATP depletion induces cellular acidosis which alters the activity of the sodium (Na^+)/potassium (K^+) adenosine triphosphatase (ATPase) pump, which favours an increase in exchange of Ca^{2+} for Na^+ by the antiporter (Buja, 2005; de Groot and Rauen, 2007; Turer and Hill, 2010). An increase in intracellular Ca^{2+} activates phospholipases and hydrolases which disrupt the cellular structure by degrading their substrates and eventually leading to cell death (Turer and Hill, 2010). Furthermore, an increase in intercellular Ca^{2+} causes osmotic swelling and further disruption of the cellular structures. This type of injury would result in necrotic cell death (Buja, 2005).

1.4.3.2 Reperfusion phase:

This may start from macrophages, neutrophils and endothelial cells which are activated by cell debris (constituents of damaged cells) and reoxygenation. The restoration of oxygen supply to the ischaemic area generates the release of several factors including reactive oxygen species (ROS), TNF-α, Ca^{2+} overload and high concentrations of nitric oxide (Lejay *et al.*, 2016; Li and Jackson, 2013; Turer and Hill, 2010; Zweier and Talukder, 2006). These factors contribute to cytotoxicity, the opening of the mitochondrial permeability transition pore (mPTP), disruption of cellular structure and eventually cell death (Buja, 2005; Turer and Hill, 2010).

1.4.3.3 Mechanisms of myocardial cell death

Apoptosis

Apoptosis or programmed cell death is characterized by cell shrinking, chromatin condensation and nuclear fragmentation, and eventual phagocytosis of the cells by

macrophages (Zitvogel *et al*., 2010). Apoptosis is induced by a death ligand tumour TNF-α, the same TNF-α may induce both apoptosis and necrosis (Galluzzi *et al*., 2012). The binding of the ligand to a death receptor is called an extrinsic apoptotic pathway (Galluzzi et al., 2012). The intrinsic or mitochondrial apoptotic pathway is induced by various stimuli including oxidative stress, growth factor deprivation and hypoxia. In response to the stimuli, the members of the Bcl-2 family proteins (antiapoptotic: Bcl-2, Bcl-xl and proapoptotic: Bax, Bak and Bad) are recruited to the mitochondria and sarcoplasmic reticulum to trigger apoptotic proteins (Chipuk *et al*., 2010). Furthermore, Cytochrome C initiates the assembly of the so-called apoptosome in which procaspase-9 is cleaved and caspase-9 activates the downstream caspase-3 which leads to apoptosis (Acehan *et al*., 2004).

In vivo studies have demonstrated that cardiac overexpression of Bcl-2 reduces both infarct size (a small localized area of dead tissue resulting from the failure of blood supply) and cardiac dysfunction following I/R injury (Brocheriou *et al*., 2000; Chen *et al*., 2001). On the other hand, deletion of Bax reduced infarct size in isolated hearts subjected to an I/R injury (Hochhauser et al., 2015) and reported to induce a moderate reduction in the infarct size after a permanent coronary artery occlusion (Hochhauser *et al*., 2007). Therefore, the members of the Bcl-2 family modulate infarct size.

Necrosis

Necrosis is a form of premature cell death due to injury and is characterized morphologically by cell and organelle swelling, and eventually, plasma membrane rupture resulting in a loss of intracellular contents. Unlike apoptosis, this process of cell death is considered merely accidental, however, evidence suggests that necrosis may also be programmed or tightly regulated (Degterev *et al*., 2005; Marín-García, 2016; Vandenabeele *et al*., 2010).

Several studies have demonstrated that regulated or programmed necrosis plays a role in myocardial necrosis. For example, *in vivo*, the inhibition of Receptor-interacting protein 1 (RIP1), a kinase that regulates inflammation and cell death, showed a reduction in infarct size in hearts subjected to I/R (Lim *et al*., 2007; Ofengeim and Yuan, 2013). It has been suggested that the RIP1 cardioprotective role is depended

on the presence of cyclophilin D, a positive regulator of mPTP (Lim *et al*., 2007). In addition, cyclophilin D knock out mice, as well pharmacological inhibition of cyclophilin D, showed a significant reduction in infarct size in hearts subjected to I/R injury (Argaud *et al.*, 2005; Baines *et al*., 2005; Clarke *et al*., 2002; Nakagawa *et al*., 2005). Furthermore, Bax and Bak have been demonstrated to play a role in necrosis, and the silencing of Bax and Bak showed a reduction in the degree of necrosis in mice subjected to I/R (Whelan *et al*., 2012). Therefore, RIP1, Bax and Bak play a major role in regulated myocardial necrosis. Altogether, both apoptosis and necrosis contribute to the pathogenesis of myocardial infarction.

Autophagy

Autophagy or "self-eating" is a physiological process in which the cell destroys its own damaged organelles to generate new ones. Under stressful conditions such as starvation or mild ischaemia, the cell digests its own proteins and lipids to provide energy for cell survival (Mizushima *et al*., 2008). Cardiomyocyte autophagy is induced in both I/R as well as in permanent occlusion of the coronary artery.

Adenosine monophosphate-activated protein kinase (AMPK) is a kinase that plays a role in energy homeostasis. During ischaemia, AMPK is activated and inhibits mammalian target of rapamycin (mTOR), a potent inhibitor of autophagy (Matsui *et al*., 2007). However, inhibition of AMPK suppresses autophagy and increases infarct size (Matsui *et al*., 2007). Similar results were found when autophagy was decreased through overexpression of Ras homolog enriched in brain (Rheb) (Sciarretta *et al*., 2012) and deletion of one allele of glycogen synthase kinase 3 beta (GSK3β) (Zhai *et al*., 2011). However, other studies suggest that autophagy protects the myocardium against I/R (Hamacher-Brady *et al.*, 2007, 2006). On the other hand, prolonged ischaemia may induce too much autophagy that may be detrimental to the myocardium (Gustafsson and Gottlieb, 2009; Zhu *et al*., 2007).

1.4.4 I/R and cardioprotective mechanisms

Time is a very important factor in cardioprotection. The shorter the time of thrombotic coronary artery occlusion, the less severe the myocardial infarction and the better the

outcome for the patient (Gersh *et al.*, 2005; Heusch and Gersh, 2017). Although restoration of oxygen to the myocardium (myocardial reperfusion) is essential to protect and rescue the viable myocardium, it comes at a high price that causes more damage to the myocardium and it is called I/R injury (Vinten-Johansen *et al*., 2013). Several animal and human studies have demonstrated the significant contribution of I/R injury on myocardial infarct size. Therefore, current cardioprotective studies are looking at the mechanisms of I/R injury to develop new therapies (Rossello and Yellon, 2016).

1.4.4.1 Ischaemic conditioning (IC)

It has been over 20 years since Murry and colleagues demonstrated that repeated short cycles of non-injurious I/R significantly protects the myocardium from subsequent prolonged ischaemia (Murry *et al*., 1986). Therefore, myocardial IC is the is a powerful form of endogenous protection against myocardial infarction. This phenomenon has been widely studied in organs, different animal species as well as in humans (Wever *et al*., 2015, 2012; Yellon *et al*., 1993). The IC cardioprotective strategies are further divided into **ischaemic preconditioning (IPreC) and ischaemic postconditioning (IPosC).** IPreC is a cardioprotective strategy that includes repeated short episodes of I/R just before a sustained period of I/R (Ferdinandy *et al*., 2014).

There are two forms of postconditioning: **IPosC** and remote ischaemic postconditioning **(RPosC)** (Ferdinandy *et al*., 2014). **IPosC** is defined as brief episodes of ischaemia after a sustained ischaemia insult. **RPosC** is also subdivided in the forms of pre (before), per (during evolving infarction), and post (after) conditioning (Heusch, 2015).

Cardioprotection by IPosC is mediated through a delayed reversed acidosis and it involves activation of signalling transduction cascades such as adenosine and mediation of protein kinases. This intervention has been shown to reduce infarct size significantly, most likely through the activation of pro-survival kinases and the final step of ischaemic postconditioning is the inhibition of the mPTP. The applicability of IPosC is limited clinically, therefore, activation of pro-survival kinases with

pharmacologic agents/drugs at reperfusion to mimic IPosC could be beneficial. Figure 1.3 illustrates the potential targets for pharmacological interventions during early reperfusion (Hausenloy and Yellon, 2007).

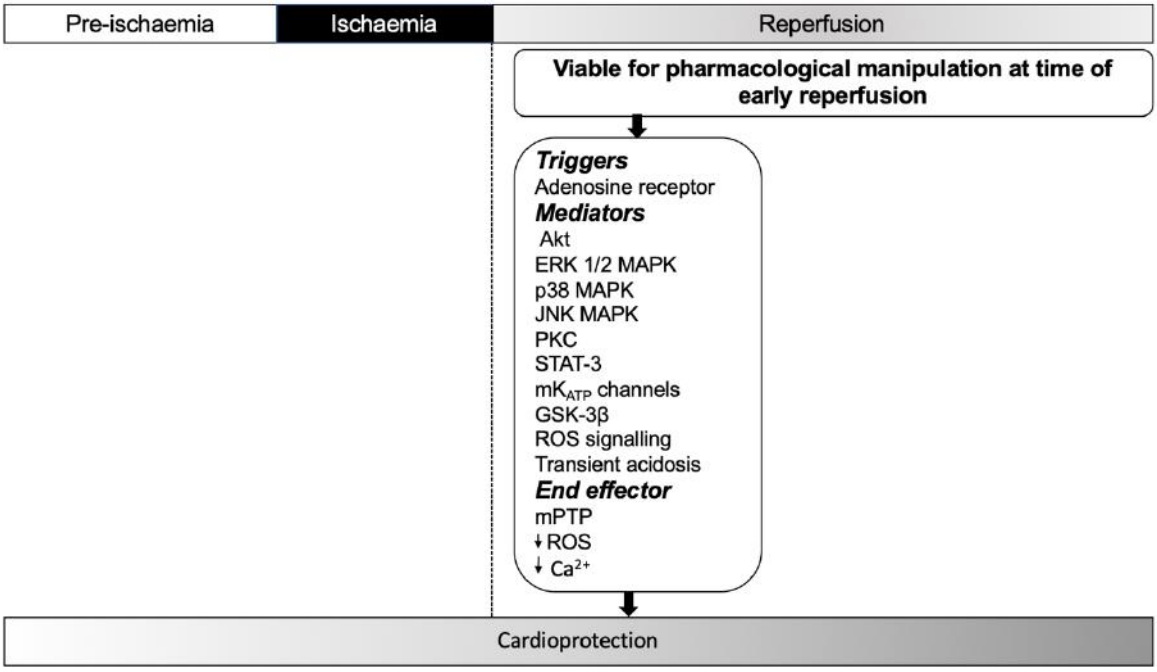

Figure 1. 3 The common signalling mechanisms and signalling cascades though to be involved in cardioprotection at the time of reperfusion

Adapted from (Hausenloy and Yellon, 2007).

1.4.4.2 Reperfusion Injury Salvage Kinase (RISK) pathway

Earlier studies on cardioprotection against I/R injury were targeting pro-apoptotic signalling cascades. This was based on the hypothesis that antagonising these pro-apoptotic signalling cascades could save the cardiomyocytes that were already committed to undergo cell death through apoptosis. It was, therefore, demonstrated that by inhibiting caspases, at the time of reperfusion, the infarct size could be reduced in animal models (Mocanu *et al*., 2000). Furthermore, the apoptotic processes were not only inhibited through antagonising of pro-apoptotic caspases but also through activation of pro-survival protein kinases such as phosphoinositide-dependent kinase (PI3K), protein kinase B (PKB) and extracellular signal-regulated kinase 1/2 (ERK 1/2) – mitogen-activated protein kinase (MAPK), also called the RISK pathway (Baxter *et al*., 2001; Yellon and Baxter, 1999). Schulman and colleagues, further demonstrated that the administration of urocortin (a growth factor) at reperfusion, protects the heart

from I/R injury through upregulation of the ERK 1/2 signalling pathway (Schulman *et al*., 2015). Co-administration of PD98059 (ERK 1/2 inhibitor) and urocortin at reperfusion abolished protection (increased infarct size), thus confirming the cardioprotective role of ERK 1/2. Furthermore, insulin and transforming growth factor-beta 1 (TGF-β1) was also found to protect against myocardial infarction and apoptotic cell death through activation of the RISK pathway at reperfusion (Baxter *et al*., 2001; Jonassen *et al*., 2001).

Activation of both PI3K-PKB and ERK1/2, using growth factors and cytokines, could mediate cell survival through activation of anti-apoptotic mechanisms (Schulman *et al*., 2015). This led to more investigations on these pro-survival protein kinases during reperfusion, using pharmacological agents/drugs (Heusch, 2015). The proposed main end effector of myocardial protection against I/R injury is the mPTP which opens within the first 15 minutes of reperfusion (Hausenloy *et al*., 2003). The RISK pathway cardioprotective mechanism has been linked to the closure of the mPTP in rat myocytes (Davidson *et al*., 2006). In addition, in IPreC, PI3K-PKB phosphorylation inhibits GSK3β activity thus inhibiting mPTP opening during reperfusion (Heusch, 2015; Juhaszova *et al*., 2004; Tong *et al*., 2002).

1.4.4.3 Survivor activating factor enhancement (SAFE) pathway

The RISK pathway is considered the universal signalling pathway for cardioprotection, however, there are other cardioprotective signalling cascades including the survivor activating factor enhancement (SAFE) pathway (Heusch, 2015). Lecour and co-workers discovered that pharmacological preconditioning **(PPreC)** with TNF-α was cardioprotective without involving the RISK pathway (Lecour, 2009). The same group further investigated the effects of administering TNF-α at reperfusion and discovered that TNF-α recruited an alternative signalling cascade, called the SAFE pathway (Lacerda *et al*., 2010). The SAFE pathway is also known to be involved in the trigger phase of ischaemic preconditioning which involves dual activation of signal transducer and activator of transcription 3 (STAT-3) and PKB (Boengler *et al.*, 2010). In the clinical setting, it seems that the signal transducer and activator of transcription 5 (STAT-5) and STAT-3 play a crucial role in cardioprotection (Wu *et al*., 2018).

1.4.4.4 Second messengers in cardioprotection

Second messengers are small lipid or water-soluble molecules that are produced in response to stimuli (i.e. protein hormones, growth factors) and transmit signals from ~~a~~ membrane receptors to downstream effectors (i.e. signalling proteins). Second messengers amplify the signal strength received by the receptors to target receptors in the cytosol and/or nucleus. Cyclic adenosine 3',5' monophosphate (cAMP) and cyclic guanosine 3',5' monophosphate (cGMP) are cyclic nucleotides which are two of the major second messengers.

In the cGMP signalling pathway, phosphorylated PI3K and PKB can phosphorylate eNOS to produce NO (Dimmeler *et al*., 1999). NO activates a soluble guanylate cyclase to form cGMP, which then activates PKG (Cohen and Downey, 2007). PKG targets mitochondrial ATP-dependent potassium channels (mK_{ATP}) and redox signalling (Oldenburg *et al*., 2004; Penna *et al*., 2007). In addition, mK_{ATP} channel dysfunction leads to a loss of cardioprotection (Lejay *et al*., 2016).

The β-adrenoceptors, on the other hand, play a crucial role in the regulation of cardiac function in both the normal and diseased state (Port and Bristow, 2001). Stimulation of these receptors activates adenyl cyclase to form cAMP from ATP. It has been demonstrated that the *β*-adrenergic-cAMP signalling pathway is involved in several cardioprotective events including IPreC (Khaliulin *et al*., 2014, 2010; Lochner *et al*., 1999). An increase in tissue cAMP during preconditioning is cardioprotective against I/R injury (Lochner *et al*., 1999).

1.5. Cyclic adenosine 3',5' monophosphate (cAMP)

As early as in 1958, cAMP was the first second messenger to be identified and to play a crucial role in cellular responses to hormone signalling and neurotransmitters (Sutherland and Rall, 1958). cAMP plays a vital role in cardiovascular processes such as the regulation of cardiac contractility, cardiac relaxation, endothelial barrier function and vasodilation (Patterson *et al*., 2000; Roberts and Dart, 2014). Cellular levels of

cAMP are controlled and regulated by changes in the activity of a transmembrane enzyme, adenylate cyclase (AC), as well as cyclic nucleotide phosphodiesterase (PDE). AC activity is controlled through stimulation or inhibition of G-protein-coupled receptors (GPCR) such as the β adrenoceptor by interactions with the α subunit of the G_s protein (α_s - stimulating activity) or a β adrenoceptor by interactions with the α subunit of the G_i protein (α_i - inhibiting it) (Sassone-Corsi, 2012). Binding of an agonist ligand (e.g. epinephrine in the case of β adrenoceptors) to GPCR complexes causes a release of an α subunit of the G_s protein (α_s) from the GPCR complexes to bind and activate AC (Sassone-Corsi, 2012). Therefore, cAMP production depends not only on the AC activation or inhibition by ligands from GPCR-α_s to GPCR-α_I, but also on its degradation by PDEs, which catalyse the hydrolysis of cAMP to adenosine monophosphate (5'-AMP) (Lezoualc'H *et al*., 2016; Mika *et al*., 2012). ACs catalyses the conversion of adenosine triphosphate (ATP) (a substrate) in the presence of magnesium as a co-factor to produce cAMP and pyrophosphate. The cAMP generated through AC activation can serve as a regulatory signal via protein kinase A (PKA) which is one of the most studied cAMP-dependent proteins (Pierce *et al.*, 2002). Over the years, all cAMP-mediated effects were attributed to the activation of PKA (Patterson *et al*., 2000; Vossler *et al*., 1997), however cAMP-induced activation of the small GTPase, Rap1, was unresponsive to PKA inhibitors. This led to the discovery of a new cAMP effector protein, namely exchange protein directly activated by cAMP (Epac) (De Rooij *et al*., 1998; Kawasaki *et al.*, 1998).

1.6 Exchange protein directly activated by cAMP (Epac)

1.6.1 Epac structure and the mechanism of activation

Recent evidence suggests that Epac, independent of PKA, plays an important role in many cellular functions, including in the cardiovascular system. Epac proteins are a family of cAMP guanine nucleotide exchange factors (GEFs) for the small GTPases, Rap1 and Rap2. There are two Epac isoforms namely, cAMP-GEF-1 (Epac1) and cAMP-GEF-2 (Epac2), which are GEFs for Rap1 and Rap2, respectively (Bos, 2006; De Rooij *et al*., 1998; Kawasaki *et al.*, 1998). Epac proteins are encoded differently by Rapgef3 (Epac1) and Rapgef4 (Epac2) genes although they display a similar genetic make-up (Banerjee and Cheng, 2015).

Epac1 and Epac2 are multi-domain proteins that contain an N-terminal regulatory region and a C-terminal catalytic region. These proteins have a cyclic-nucleotide-binding domain (CNBD) at the N-terminal regulatory region that is homogenous to that of PKA R-subunit (see Figure 1.4) (Cheng *et al*., 2008). The CNBD is a high-affinity cAMP-binding domain (Epac activation) and activates the Ras superfamily of small GTPases Rap1 and Rap2. Epac1 has one N-terminal CNBD whereas Epac2 is further subdivided into three isoforms: (i) Epac2A (brain/β-cell type) which has an additional N-terminal CNBD acting as a low affinity cAMP-binding domain, (ii) Epac2B (adrenal type) which is similar to Epac1 in domain structure and (iii) Epac2C (De Rooij *et al*., 2000; Lewis *et al*., 2016; Niimura *et al*., 2009). The regulatory region of Epac also contains a Dishevelled, Egl-10, Pleckstrin (DEP) domain which is involved in Epac localization. A cytosolic localization was observed with Epac1 through deletion of the DEP domain but that did affect the regulation of Epac by cAMP (Ponsioen *et al*., 2004). The catalytic region of Epac contains a Ras-exchange motif domain, RAS association domain and a CDC25 homology domain which controls the nucleotide exchange activity (Cheng *et al*., 2008).

Binding of a ligand (extracellular signal) to the GPCR complexes leads to activation of AC, which catalyses the conversion of ATP to cAMP (Figure 1.4). The binding of cAMP to Epac's CNBD allows the regulatory region to rotate and expose the CDC25 homology domain for Rap to bind. The active Epac complex catalyses the exchange of inactive Rap- guanosine diphosphate (GDP) to an active Rap-guanosine triphosphate (GTP) and controls Rap-mediated biological functions (Métrich *et al*., 2010).

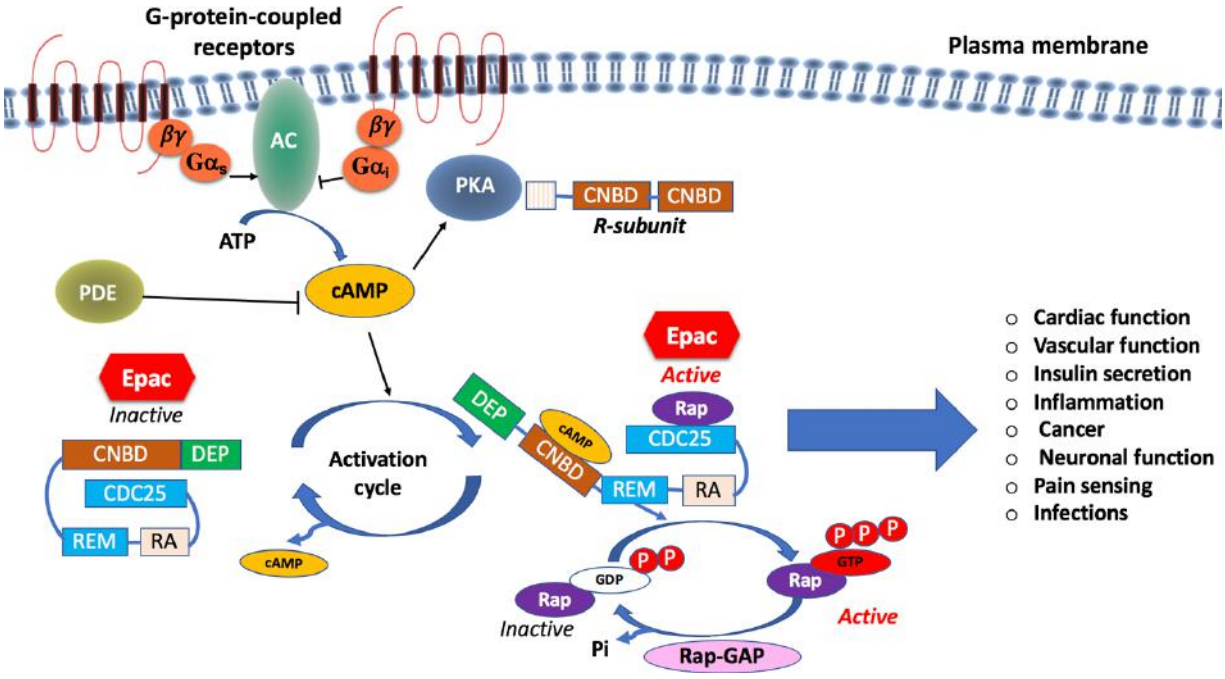

Figure 1. 4 Mechanisms of Epac activation and its associated biological functions.

Intracellular cAMP is produced from ATP by the enzyme adenyl cyclase (AC) in response to binding of the ligand (e.g. norepinephrine) to the $G\alpha_s$ -coupled G-protein-couples receptors. cAMP can bind to the cyclic-nucleotide-binding domain (CNBD) of Epac (alternative PKA CNBD) and this allows the regulatory region to rotate and expose the catalytic CDC25 homology domain for Rap to bind. The active Epac complex catalyses the exchange of inactive Rap-guanosine diphosphate (GDP) to an active Rap-guanosine triphosphate (GTP) and controls Rap-mediated biological functions. Adapted from (Lezoualc'H *et al.*, 2016; Métrich *et al.*, 2010; Schmidt *et al.*, 2013).

1.6.2 Epac protein tissue expression

Epac1 messenger RNA (mRNA) is expressed in relatively high levels in the heart, thyroid gland, ovary, blood vessels, proximal tubules of the kidney and in some parts of the brain (De Rooij *et al.*, 1998; Honegger *et al.*, 2006; Kawasaki *et al.*, 1998; Li *et al.*, 2008). Previous studies suggest that the regulation of Epac1 and Epac2 mRNA expression depends on developmental stages and pathophysiological conditions. In foetal organs (heart, brain, kidney, and lungs), Epac1 and Epac2 mRNA can be detected at an early stage of development, suggesting that both proteins play a major role in organ development and function (Ulucan *et al.*, 2007). Both isoforms have shown to be highly expressed in adulthood in these organs, with only renal Epac2

showing a decline in mRNA expression in adulthood (Ulucan *et al*., 2007). In the heart, Epac1 and Epac2 mRNA expression have shown to be upregulated in isoproterenol-induced left ventricular hypertrophy whereas only Epac1 mRNA was expressed in pressure overload-induced hypertrophy (Ulucan *et al*., 2007).

1.6.3 Pharmacological modulators of Epac

The development of Epac selective analogues is summarised in Figure 1.5.

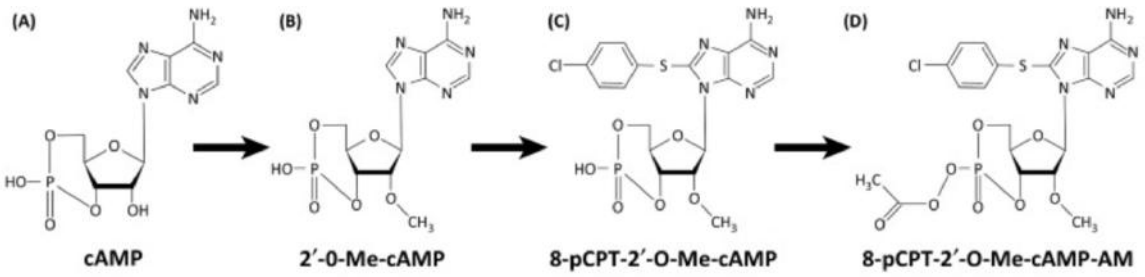

Figure 1. 5 Development of exchange protein activated by cAMP (EPAC)-selective cAMP analogues.

(A) cAMP. **(B)** cAMP methylated at the ribose 2′oxygen (2′O) yields 2′-O-Me-cAMP. **(C)** Addition of parachlorophenylthio (pCPT) to carbon 8 of the base yields 8-pCPT-2′O-Me-cAMP (007) **(CPT)** (Enserink *et al*., 2002). **(D)** Masking the phosphate group of 007 with an acetoxymethyl ester (8-pCPT-2′O-Me-cAMP-AM) improves membrane permeability (intracellular esterases remove this to allow binding to cAMP-binding domains) (Vliem *et al*., 2008). From (Parnell *et al*., 2015).

The discovery of Epac-selective agonist and antagonists for both Epac1 and/or Epac2 have enhanced the study of Epac signalling in different cell types, including cardiovascular cells (Table 1.1) (Lezoualc'H *et al*., 2016)

Table 1.1: Epac's agonists and antagonists

Agonist chemical name	Isoform targeted	*In vitro* studies	*In vivo* studies	Reference
8-pCPT (CPT) 8-(4-Chlorophenylthio)-2′-O-methyladenosine-3′,5′-cyclic monophosphate	Epac1 (preferentially) and Epac2	Used in most cell types (including cardiovascular cells)	Induces positive inotropic and pro-arrhythmic effects (ex-vivo rodents)	(Md Hashim, 2015; Rehmann *et al.*, 2003; Ruiz-Hurtado *et* al., 2012)
Sulfonylurea drugs (Tolbutamide, Glibenclamide, and Gliclazide)	Epac2	Stimulates β-cell insulin secretion	Stimulates insulin secretion in mice	(Tsalkova *et al.*, 2010; Zhang *et al.*, 2009)
Scottish Biomedical (SB) compounds (Undisclosed)	Epac1 and Epac2	Able to compete for ^{3}H cAMP-binding to CNBDs Not validated for inhibition of EPAC GEF activity	-	(McPhee *et al.*, 2005)
Sp-8-BnT-cAMPS (S-220) 8- Benzylthioadenosine- 3', 5'- cyclic monophosphorothioate, Sp- isomer	Epac2	Potentiates glucose-induced insulin secretion in human pancreatic cells	-	(Schwede *et al.*, 2015)

Antagonist chemical name	Isoform targeted	*In vitro* studies	*In vivo* studies	Reference
CE3F4 5,7-Dibromo-6-fluoro-2-methyl-1,2,3,4-tetrahydroquinoline-1-carbaldehyde	Epac1	Inhibits Epac1-induced hypertrophy markers and autophagy in cardiomyocytes	-	(Courilleau *et al.*, 2012)
ESI-05 (4-Methyl-2,4,6-trimethylphenylsulfone) **ESI-07** (Undisclosed)	Epac2	ESI-05 inhibits Epac-induced proarrhythmic Ca^{2+} in rat cardiomyocytes	-	(Domínguez-Rodríguez *et al.*, 2015; Tsalkova *et al.*, 2012)
ESI-08 5-Cyano-6-oxo-1,6-dihydrocyclohexyl **HJC0197** 5-Cyano-6-oxo-1,6-dihydrocyclopentyl **HJC0198** 5-Cyano-6-oxo-1,6-dihydrocyclopropyl	Epac1/Epac2 Epac1/Epac2	HJC0197 and HJC0198 block Epac1 Epac2-mediated PKB phosphorylation in HEK293T cells	-	(Chen *et al.*, 2012; Tsalkova *et al.*, 2012)
ESI-09 3-(5-Tert-butyl-isoxazol-3-yl)-2-[(3-chloro-phenyl)-hydrazno]-3-oxo-propionitrile	Epac1/Epac2	Supresses pancreatic cancer cell migration and invasion	Protect mice against rickettsia infection	(Almahariq *et al.*, 2012; Chen *et al.*, 2013; Gong *et al.*, 2013)
5376753	Epac1	5376753 inhibits Epac1-mediated migration of rat cardiac fibroblast	-	(Brown *et al.*, 2014)

Adapted from: (Lezoualc'H *et al.*, 2016; Parnell *et al.*, 2015)

1.7 Epac and vascular function

The integrity of blood vessels is critical to vascular homeostasis (Murakami and Simons, 2009). Vascular smooth muscle cells (VSMCs) and vascular endothelial cells (VECs) play a crucial role in regulation of vascular tone, blood pressure and maintenance of blood vascular integrity (Lezoualc'H *et al*., 2016). In pathological conditions, the abnormal regulation of VSMCs and VECs can lead to development cells with migratory and proliferative phenotypes that can result in the progression of cardiovascular diseases, such as atherosclerosis and restenosis (Gimbrone and García-Cardeña, 2016; Lezoualc'H *et al*., 2016).

1.7.1 Role of Epac on vascular tone

Vascular tone is determined by the balance between cellular signalling pathways that mediate the generation of force (vasoconstriction) and release of force (vasodilation) respectively in the blood vessel (Morgado *et al*., 2012). Vascular tone can be influenced by either *extrinsic* factors such as sympathetic nerves and circulating angiotensin II or *intrinsic* factors such as myogenic mechanisms (which increases tone), endothelial factors (e.g. NO, which modulate vascular tone) and metabolic by-products or hypoxia (which modulate vascular tone).
cAMP and cGMP are considered as the main second messengers that are involved in the regulation of vascular tone through various signalling pathways (Morgado *et al*., 2012). Therefore since the effects of cAMP were previously mainly attributed to PKA, current studies have shifted the focus to the role of Epac.

Current studies have demonstrated that Epac activation could be a potential therapeutic target in vascular diseases (Barker *et al*., 2017; Parnell *et al*., 2015). Pharmacological activation of Epac with its selective agonists such as 8- pCPT [8-(4-chlorophenylthio)-2′ -O-methyladenosine 3′,5′ - cyclic monophosphate] has shown promising results about role of Epac in the regulation of vasorelaxation. In primary human tracheal smooth muscle cells, Epac1 via Rap1 relaxes airway smooth muscles by inhibiting Ras homolog gene family member A (RhoA) activity, leading to dephosphorylation of myosin light chain (MLC) thereby inducing vasorelaxation

(Roscioni *et al*., 2011). Zieba *et al*. (2011) have demonstrated that in both intact and permeabilized vascular, gut, and airway smooth muscle cells, 8- pCPT significantly reduced agonist-induced contractile force and MLC phosphatase phosphorylation independent of PKA and PKG (Zieba *et al*., 2011). Furthermore, silencing Epac1 in rat aortic smooth muscle cells leads to the inhibition of isoproterenol-induced Rap1 activity, which further confirms that cAMP-medicated signalling mechanism through Epac activation is independent of PKA (Zieba *et al*., 2011). Rap1b knockout mice presented with cardiac hypertrophy, elevated blood pressure and endothelial dysfunction (reduced eNOS activity) suggesting that Epac1/Rap1b is required for maintenance of vascular tone and normal blood pressure (Lakshmikanthan *et al*., 2014).

Epac1/Rap1b activation with CPT in vascular endothelial cells stimulates ryanodine receptor (RyR) in sarcoplasmic reticulum to release Ca^{2+}. Ca^{2+} release activates BK_{Ca} (Ca^{2+} -sensitive large-conductance K^{+}) channels causing membrane hyperpolarization and eventually closure of voltage gated Ca^{2+} channels, this leads to a decrease in intracellular Ca^{2+} which induces vasorelaxation (Roberts *et al*., 2013).
In addition, Epac activation through eNOS activity seems to be involved in endothelium-dependent Epac-mediated vasorelaxation (Lakshmikanthan *et a*l., 2014; Roberts *et al*., 2013). However, PKA cannot be excluded in Epac's role in vasorelaxation. Some studies suggested that in smooth muscle the inhibition of RhoA activity is mediated by activation of both Epac and PKA (Zieba *et al*., 2011).

Overall, Epac1/Rap1b activation with its agonist CPT directly induces vasorelaxation in different types of vascular smooth muscle cells through inhibition of RhoA activity and independent of PKA. In addition, Epac induced vasorelaxation in vascular smooth muscle cells may be via the activation of endothelial nitric oxide synthase (eNOS).

1.7.2 Role of Epac in the regulation of VSMC proliferation and migration

Cell proliferation in vascular tissue can be defined by excessive growth of VSMC which can contribute to the development of atherosclerosis and restenosis. Cell proliferation can be controlled by different signalling molecules and cell proliferation is increased

in tumours. The well-known factor influencing VSMC proliferation is the platelet-derived growth factor (PDGF) and its receptor (PDGFR) via downstream signalling effectors (including the Ras/ MAPK-, Src-, PI3K/PKB-, phospholipase C-γ- and JAK/STAT pathways) (Wang *et al.*, 2018; Yu *et al*., 2018). Adenosine A_2(B) receptors have been reported to facilitate an early induction of genes which lead to a decrease in arterial smooth muscle cell proliferation (Mayer *et al.*, 2011). On the other hand, Epac activation with CPT and PKA synergistically inhibits VSMC proliferation via a Rap1 independent mechanism (Hewer *et al*., 2011).

Cell migration is a central process in embryogenesis, bone remodelling and wound healing, it requires all immune responses and other cellular signals for the cells to migrate to the place of injury (Lauffenburger and Horwitz, 1996; Stossel, 1993). cAMP has been implicated in promoting wound healing in VSMC after injury (Palmer *et al*., 1998). Epac1 is upregulated during neointimal thickening and increases VSMC migration. Thus Epac may play a crucial role in vascular remodelling and restenosis upon injury (Yokoyama *et al*., 2008b, 2008a). Furthermore, Yokoyama at al. suggested that both Epac and PKA take part in vascular remodelling (Yokoyama *et al*., 2010). In rat aortas, cAMP-mediated inhibition of VSMC migration is associated with the activity of phosphodiesterase 3 (PDE3) and phosphodiesterase 4 (PDE4) (Palmer *et al*., 1998).

PDE4 inhibition reduced the thickening of arterial walls following vascular injury in an Epac-dependent manner (Lehrke *et al*., 2015). McKean and co-workers have demonstrated that the cAMP producing agonist, beraprost, inhibited migration in human VSMC through Epac and the proposed mechanism was via Rap1 and with subsequent inhibition of RhoA (McKean *et al*., 2015, 2013). Recently, Epac1 deficiency, possible via PKB-GSK3β pathway, inhibited the basic fibroblast growth factor (bFGF)-mediated VSMC migration (Kato *et al*., 2019). Therefore, these studies suggest that Epac may play a crucial role in the regulation of VSMC proliferation and migration.

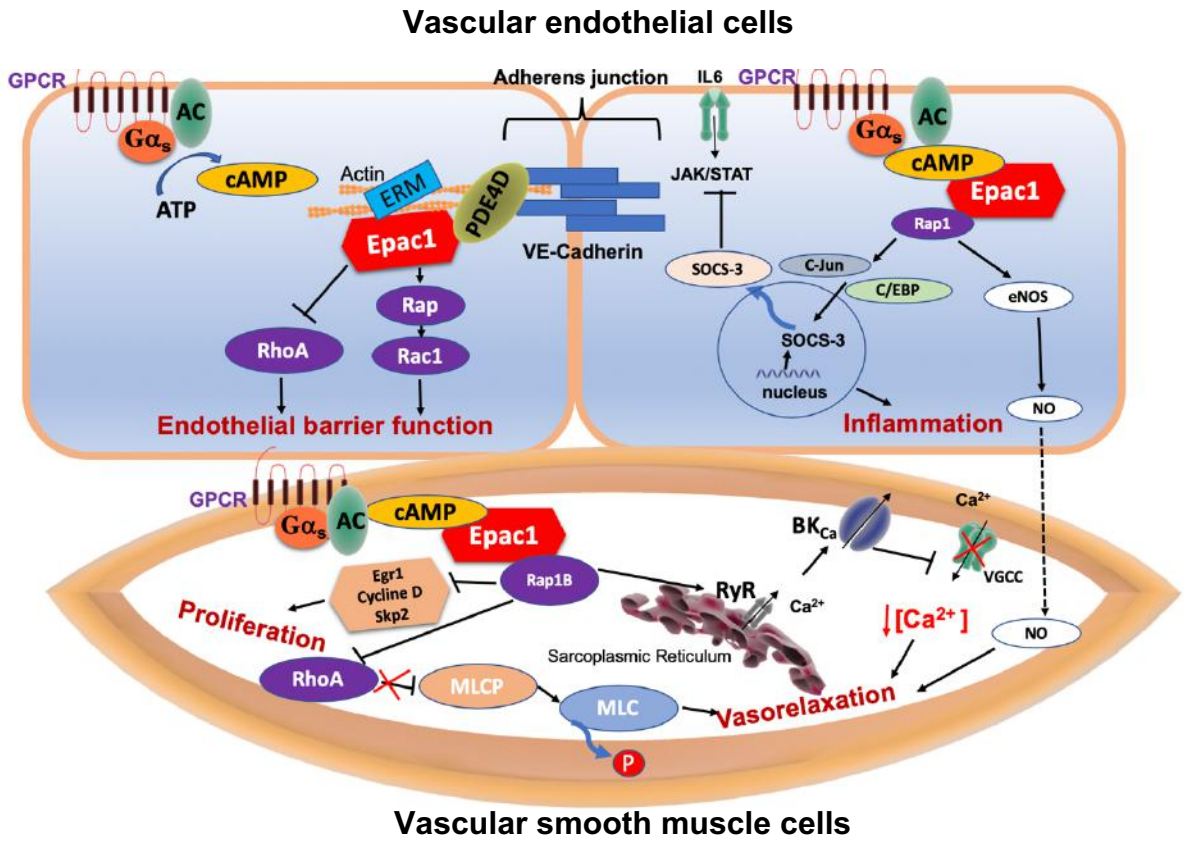

Figure 1. 6 An overview of Epac's role in vascular function.

In endothelial cells, the complex Epac1-PDE4D VE-cadherin-bearing cell to cell contacts and the interaction of Epac1 with ERM molecules stabilize endothelial barrier function. Furthermore, Epac1-Rap1 via c-Jun and C/ERB promotes suppressor of cytokine signalling 3 (SOCS-3) in the nucleus, which blocks proinflammatory cytokine interleukin 6 (IL6). In VSMC, Epac1-Rap1b decreases smooth muscle cells proliferation through inhibition of early growth response protein 1 (Erg1), Cycline D and s-phase kinase-associated protein 2 (Skp2). Epac1 activation also inhibits RhoA which lead to dephosphorylation of MLC and vasorelaxation. Epac1 also stimulates RyR in the sarcoplasmic reticulum and a release of Ca^{2+} which activates BK_{ca} causing membrane hyperpolarization and eventually closure of voltage gated Ca^{2+} channels, this leads to a decrease in intracellular Ca^{2+} concentration which induces VSMC relaxation. In addition, Epac1 induces endothelial-dependent VSMC relaxation via eNOS and NO release. Adapted from (Métrich *et al.*, 2010; Roberts and Dart, 2014; Schmidt *et al.*, 2013)

1.7.3 Role of Epac in vascular endothelial barrier function

The endothelium is defined as a simple squamous layer of vascular endothelial cells which separates all tissues from the blood in the vasculature. The primary function of the endothelium is to control vascular tone and permeability (which allows a selective transport of fluids, ions, macromolecules, and leukocytes across the vessel wall), also to regulate vascular inflammation, prevention of thrombosis and maintenance of vascular integrity (Chavez *et al*., 2011). Inflammation, diabetes, oxidative stress, dyslipidaemia and invasion of pathogens can initiate loss of vascular endothelial function (endothelial dysfunction) which can lead to the development of cardiovascular diseases such as atherosclerosis (Svensjö and Bouskela, 2018). The vascular endothelial barrier function and vascular integrity are highly supported by two major intracellular junctions which join the adjacent endothelial cells (Vestweber, 2012). The adherens junctions composed of mainly vascular endothelial (VE)-cadherin and the membrane proteins (p120, β-catenin, and plakoglobin/γ-catenin) (Dejana and Orsenigo, 2013; Hirase and Node, 2011). The tight junctions are formed by junctional adhesion molecules and membrane proteins (occludin and claudins) and they are involved in the control movement of solutes between adjacent cells (Hirase and Node, 2011; Runkle and Mu, 2013).

Over the years, cAMP/PKA has been known to regulate endothelial cell barrier function. Both *in vivo* and *in vitro* studies have shown cAMP elevation with PDE inhibitors and AC activators can decrease inflammation-induced basal permeability and reverse vascular leakage in endothelial cells.

However, studies with PKA inhibitors generated inconsistent results with regard to the regulation of vascular endothelial cell barrier function. The direct activation of Epac1/Rap1 with its agonist CPT has been shown to regulate endothelial cell barrier function through RhoA inhibition at junctions which induces redistribution of VE-cadherin and tight junctions molecules enhancing barrier function (Figure 1.6) (Cullere *et al*., 2005). However, Birukova *et al*., (2007) have demonstrated that both PKA and Epac/Rap, through activation of Rac1, lead to the enhancement of peripheral actin cytoskeleton and adherens junctions (Birukova *et al*., 2010, 2008, 2007). Furthermore, the vascular endothelial cell barrier permeability depends on the integrity of cell to cell

junctions stability VE-cadherin and tight junctions (Figure 1.6) (Dejana and Orsenigo, 2013; Hirase and Node, 2011; Runkle and Mu, 2013). Therefore, PKA and Epac1 agonists have been shown to reduce vascular endothelial cell barrier permeability and vascular leakage through increased cell to cell junction stability. Both PKA and Epac1, through inhibition of Rho and activation of Rac1, lead to accumulation of intercellular junctional proteins which regulate and stabilize the adherens and tight junction (Aslam *et al*., 2014). Furthermore, phosphodiesterase 4D (PDE4D) enzymes integrate Epac1 to VE-cadherin-signalling complex and control the effects of cAMP on vascular endothelial cell permeability (Figure 1.6) (Rampersad *et al.*, 2010).

1.8 Epac in the heart

The cAMP is a known second messenger that modulates several physiological processes in the heart, including cardiac contractility and relaxation. The β-adrenergic receptors belong to the GPCR superfamily and are known to play a crucial role in cardiac function. There are three β-adrenergic receptor subtypes that are expressed in the mammalian heart namely β1-, β2 - and β3-adrenergic receptor subtypes, with only β1- and β2 adrenergic receptor subtypes known to regulate cardiac performance in response to stress or exercise (Berthouze *et al*., 2011). Cardiac function is controlled by the sympathetic nervous system. Catecholamines (nor-epinephrine and epinephrine) serves as primary agonists of all β-adrenergic receptors. Therefore, binding of catecholamines to β-adrenergic receptors activates AC which increases intracellular cAMP (Sassone-Corsi, 2012). The cAMP produced serves as a regulatory signal that activates PKA, which further phosphorylates the key excitation-contraction coupling proteins including troponin I, cardiac ryanodine receptors (RyR), or phospholamban (PLB) (Aasakiran, 2007; Berthouze *et al*., 2011; Freedman and Lefkowitz, 2004).

1.8.1 Role of Epac in Ca^{2+} handling and cardiac excitation-contraction

Ca^{2+} is a universal intracellular second messenger and it plays a central role in cardiac contraction and relaxation (Bers, 2007). PKA phosphorylates the L-type Ca^{2+} channels located at the sarcolemma, which allows Ca^{2+} to enter the cardiomyocyte, and this

triggers more Ca^{2+} from the sarcoplasmic reticulum to induce myofilament contraction. PKA also phosphorylates RyR resulting in Ca^{2+} leakage from the sarcoplasmic reticulum, thus providing the Ca^{2+} necessary to activate the contraction of the myofibrils (Lezoualc'H *et a*l., 2016). After contraction, PLB phosphorylation by PKA at Ser16 relieves its tonic inhibition on sarcoplasmic reticulum Ca^{2+} ATPase activity, allowing Ca^{2+} uptake in the sarcoplasmic reticulum, thus favouring relaxation (Bers, 2007; Lezoualc'H *et al*., 2016). In addition, the α subunit of the inhibitory G protein ($G_{\alpha i}$), which inhibits AC, activates cytosolic effector molecule phospholipase A2 (cPLA2) leading to a reduced cardiac contractility independent of cAMP (Aasakiran, 2007).

Since Ca^{2+} is a key element that modulates cardiac excitation-contraction, several studies have shown that Epac regulated intracellular Ca^{2+} handling in cardiomyocytes (Cazorla *et al*., 2009; Domínguez-Rodríguez *et al*., 2015; Kaur et al., 2016; Morel et *al*., 2005; Oestreich *et al*., 2009, 2007; Pereira *et al*., 2017, 2012; Ruiz-Hurtado *et al*., 2013, 2012). Initial evidence demonstrated that selective activation of Epac with its analogue CPT increases spontaneous Ca^{2+} transients in cultured rat neonatal ventricular myocytes (Figure 1.7) (Morel *et al*., 2005). Similarly, CPT increased the frequency of Ca^{2+} sparks via Ca^{2+}/calmodulin kinase II (CaMKII)-dependent and independent of PKA in adult rat cardiomyocytes, thus confirming a role of Epac in Ca^{2+} handling (Figure 1.7) (Pereira *et al*., 2007). Like PKA, Epac phosphorylates RyR which results in Ca^{2+} leakage from the sarcoplasmic reticulum independent of PKA but rather require involvement of phospholipase Cε (PLCε) and Ca^{2+}/calmodulin kinase II (CaMKII) activation (Cazorla *et al*., 2009; Oestreich *et al*., 2007; Pereira *et al*., 2012, 2007). Epac activation in rat cardiac muscle increased myofilament Ca^{2+} sensitivity via CaMKII, an effect which was abolished by a CaMKII inhibitor KN-93 (Cazorla *et al*., 2009; Kaur *et al*., 2016). Moreover, Epac activation with CPT showed a positive inotropic effect by boosting extracellular Ca^{2+} influx via L-type Ca^{2+} channels (Ruiz-Hurtado *et al*., 2012). In summary, Epac activates the enzyme PLCε which catalyses the conversion of phosphatidylinositol 4,5-bisphosphate (PIP_2) to produce inositol trisphosphate (IP_3) and diacylglycerol (DAG) leading to the activation of PKC and CaMKII. PKC and CaMKII are involved in contractile protein phosphorylation and myofilament Ca^{2+} sensitivity.

1.8.2 Epac and arrhythmias and hypertrophy

In the heart, Epac1 and Epac2 mRNA expression have shown to be upregulated in isoproterenol-induced left ventricular hypertrophy whereas only Epac1 mRNA was expressed in pressure overload-induced hypertrophy (Ulucan *et al.*, 2007). In addition, Metrich and co-workers (2008) reported that Epac1 is expressed in the human heart and that it's level increases during heart failure (Métrich *et al.*, 2008). However, Epac proteins may exert both anti- and pro-hypertrophic properties in cardiomyocytes (Md Hashim, 2015).

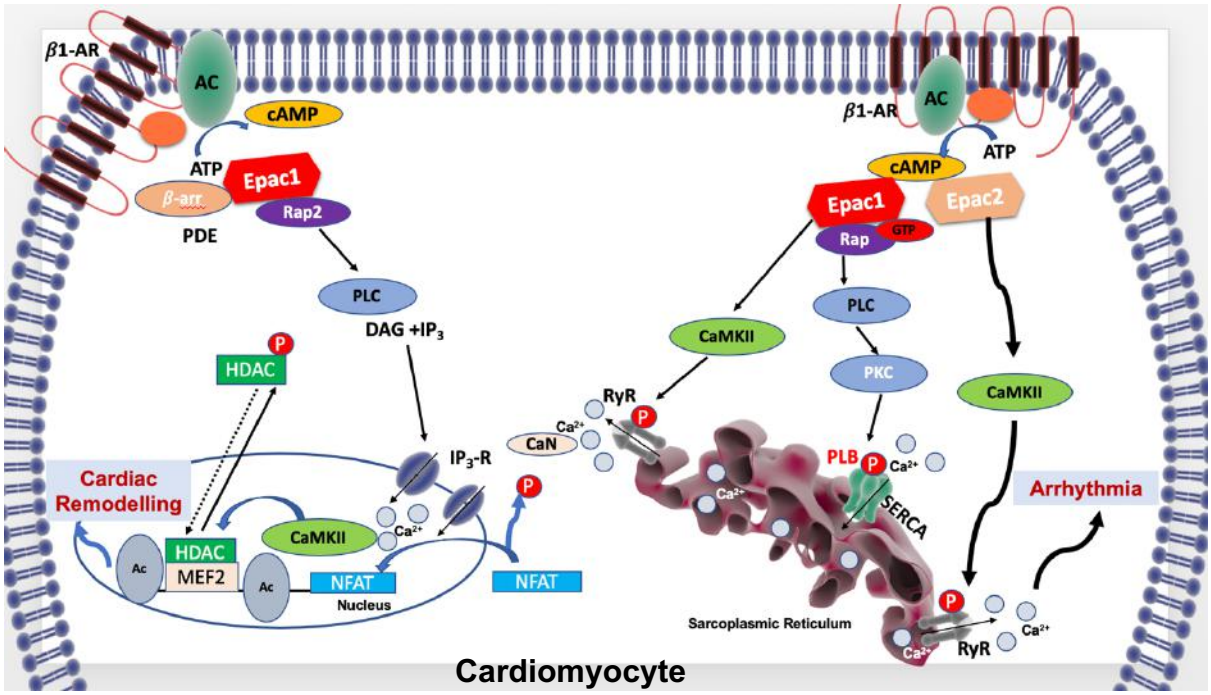

Figure 1. 7 An overview of Epac signalling and cardiac remodelling.

In cardiomyocytes, beta-arrestin (β-arr) and PDE regulate EPAC1 hypertrophic signalling, which also involves calcineurin (CaN) and nuclear factor of activated T-cells (NFAT). Eapc1-Rap2 pathway phosphorylates RyR via activation of CaMKII and PLCε / PKC ε, this results in Ca^{2+} leakage from the sarcoplasmic reticulum which may trigger arrhythmia. Further, Epac1 increases phosphorylation of PLB which inhibits sarcoplasmic reticulum Ca^{2+} ATPase (SERCA) activity and may contribute to the development of arrhythmia and heart failure. Adapted from: (Laudette *et al.*, 2018; Métrich *et al.*, 2010)

Several animal and human studies have investigated the role of Epac in cardiomyocytes, providing evidence that Epac plays a crucial role in modulating intracellular Ca^{2+} signalling (Cazorla *et al*., 2009; Domínguez-Rodríguez *et al.*, 2015; Kaur *et al.*, 2016; Morel *et al*., 2005; Oestreich *et al.*, 2009, 2007; Pereira *et al*., 2017, 2012; Ruiz-Hurtado *et al*., 2013, 2012). In cardiomyocytes, Epac is involved cardiac contraction by forming gap junctions and enhancing intracellular Ca^{2+} release by activating CaMKII (Pereira *et al*., 2007). A sustained Epac activation with its selective agonist CPT increases a spontaneous Ca^{2+} release as Ca^{2+} waves and extra Ca^{2+} transients, suggesting proarrhythmic effects (Figure 1.7) (Ruiz-Hurtado *et al*., 2012). Furthermore, CPT critically regulates action potential by reducing potassium current thus prolonging repolarizing in rat adult ventricle, which may explain why Epac is upregulated in conditions such as cardiac hypertrophy (Brette *et al*., 2013). Some studies have demonstrated that inhibition of both Epac and PKA downregulates the expression and function of the gap junction protein connexin 43 in rats with myocardial infarction, which prevented ventricular arrhythmias (Lee *et al*., 2013). Cardiac arrhythmias are associated with increased late sodium current (I_{NaL}), β-adrenergic receptor regulates I_{NaL} via PKA and CaMKII pathways, however, the mechanism is unclear. Recently, Yang and co-workers (2016) demonstrated that *in vivo* inhibition of Epac2-Rap1 in rats induced ventricular fibrillation followed by sudden death and the possible mechanism was through an increase in mitochondrial ROS and activation of I_{NaL} (Yang *et al*., 2016). Another study confirmed that β-adrenergic receptor stimulation regulates I_{NaL} via both PKA and CaMKII and suggest that ROS and NO may contribute to this effect (Hegyi *et al*., 2018). Pereira and colleagues (2017) proposed two possible pathways, the β-adrenergic- cAMP-Epac- PI3K-PKB-NOS1-CaMKII pathway to mediate Ca^{2+} leak and the β-adrenergic-cAMP-PKA–pathway which plays a role in inotropic and lusitropic effects through regulation of Ca^{2+} current and sarcoplasmic reticulum Ca^{2+} ATPase (Pereira *et al*., 2017). Thus, suggesting that studying these pathways could be a novel target against arrhythmias and heart failure (Pereira *et al*., 2017).

1.9 Epac, metabolic syndrome and cardiovascular disease

The evidence collected over the years indicates that Epac plays a critical role in integrating and transducing multiple signalling pathways in the cardiovascular system, including some reports suggesting detrimental effects, such as cardiac remodelling and arrythmias (Lee *et al*., 2013; Okumura *et al*., 2014; Pereira *et a*l., 2017; Yang *et al*., 2016). Several studies have been published on Epac1, Epac2 or Epac1/2 knockout mice (Table 1.2). The knockout mice models have revealed diverse functions of Epac in different organs. In the brain (hypothalamus), Epac1 deletion mice fed with a high-fat diet (HFD) was associated with an improved leptin signalling, reduced food intake and reduced adiposity (Yan *et al*., 2013). Interestingly, Kai and colleagues (2013) reported that Epac1 deficient mice developed pancreatic β-cell dysfunction and metabolic syndrome (Kai *et al*., 2013). Furthermore, Epac2 deletion in mice impaired hypothalamic leptin signalling (Hwang *et al*., 2017). In addition, Rap1 knockout mice presented with signs of metabolic syndrome and developed hepatic steatosis (Martínez *et al*., 2013).

In the cardiovascular system, Epac1 deletion was shown to be cardioprotective but not Epac2 deletion (Okumura *et a*l., 2014). However, Epac1 deletion was detrimental on infarct size in mice fed with a HFD; furthermore, the HFD “paradoxically reduced” infarct size in both HFD wild type and HFD Epac2 knockout mice (Edland *et al.*, 2016). In rats fed with a standard chow, a pharmacological activation of Epac1/2 with CPT did not affect infarct size. However, co-treatment with a PKA activator (6-Bnz) and CPT reduce the infarct size (Khaliulin *et al*., 2017). Clinically, dysfunctional epicardial adipose tissue (EAT) may promote maladaptive cardiac remodelling through Epac2 and ST2 (cardiac biomarker) expression, which inhibits an interleukin 33 (IL-33)-mediated cardioprotective mechanism (Vianello *et a*l., 2019).

Table 1.2: Epac1/2 in obesity, insulin signalling and cardiovascular disease

Epac isoform	Model	Organ	Proposed mechanism	Reference
Epac1	Mice: *in vivo* and *in vitro* (High-Fat Diet induced)	Brain: hypothalamus	- Epac1 induced leptin resistance. - HFD increased Rap1 expression after 4 weeks. - Epac1 blunted leptin signalling pathway (PKB-STAT3, mTOR-S6K, ERK, and AMPK)	(Fukuda *et al.*, 2011)
Epac 1	Rap1 knock out mice	Liver and visceral fat	- Accumulation of abdominal fat - Developed hepatic steatosis - High-fasting plasma levels of insulin - High glucose concentration - High cholesterol	(Martínez *et al.*, 2013)
Epac1	Epac1 knock out mice: *in vivo* study (HFD induced)	Brain: hypothalamus	- Reduced food intake - Reduced adiposity - Reduced plasma leptin - pSTAT3 was enhanced	(Yan *et al.*, 2013)
Epac1	Epac1 knock out mice: *in vivo* study (HFD induced)	Pancreas: β-cells	- Elevated plasma triglycerides - Severe diet-induced obesity - Developed insulin resistance - β-cells dysfunction - Reduced GLUT2 and PDX-1 expression	(Kai *et al.*, 2013)
Epac1/2	Epac1/ and Epac2 knockout mice	**Heart**	- Epac1 deletion protects the hearts from various stresses - Epac2 deletion was not protective	(Okumura *et al.*, 2014)
Epac1 Epac2	Epac1 and Epac2 knock out mice (HFD induced)	**Heart**	- HFD "paradoxically reduced" infarct size in both HFDwt and HFD Epac2 knockout - Epac1 deletion detrimental on infarct size	(Edland *et al.*, 2016)
Epac1/2	Rats (normal diet)	**Heart**	- Only co-treatment of PKA (6-Bnz) and Epac (CPT) led to infarct size reduction via PKC inhibition	(Khaliulin *et al.*, 2017)
Epac 2	Epac 2 knockout mice (HFD induced)	Brain: hypothalamus	- Impaired hypothalamic leptin signalling	(Hwang *et al.*, 2017)
Epac2	Clinical (patients)	**Heart:** epicardial adipose tissue (EAT)	- Dysfunctional EAT, Epac2 and ST2 expression inhibits IL-33 cardioprotective mechanism	(Vianello *et al.*, 2019)

Given the above, it is evident that Epac plays a critical role in different systems or organs as shown in Epac knockout experiments. However, some of the data are inconclusive and contradictory. In addition, Lochner and colleagues (1999) have demonstrated that an increase in tissue cAMP during preconditioning is cardioprotective against I/R injury (Lochner *et al*., 1999). PKA and Epac are the downstream signalling cascade targets of cAMP. Therefore, this warrants more investigation on the role of Epac in myocardial I/R, obesity and insulin resistance. Furthermore, it is relevant to investigate Epac's role on the RISK pathway, which is one of the best described cardioprotective pathways.

1.10 Problem statement and study aims

1.10.1 Problem statement

Despite intense research over decades on the prevalence, treatment, and management of CVD, it still remains the number one cause of death globally, and it affects both men and women. NCDs, particularly CVDs, are already among the top causes of death in South Africa (Nojilana *et al*., 2016). In 2010, NCDs accounted for 39% of total deaths in the country. More than a third (36%) of these deaths occurred before the age of 60 years. In 2010, the number of deaths due to NCDs was similar to the number from HIV/AIDS and tuberculosis (TB) combined (Nojilana *et al*., 2016). In 2006, with almost two-thirds of the patients enrolled in the Heart of Soweto study cohort presented with multiple cardiovascular risk factors such as hypertension and obesity (Pretorius *et al*., 2017; Tibazarwa *et al*., 2009).

Obesity could increase the risk of CAD and heart failure (Kenchaiah *et al*., 2002) and could worsen the sequelae of a myocardial infarction (Aronson *et al*., 2010; Clavijo *et al*., 2006). These adverse effects are consistent with experimental evidence of ischaemic intolerance and suppressed cardioprotection in hearts from obese, insulin-resistant animals (du Toit *et al.*, 2008, 2005; Essop *et al*., 2009; Huisamen *et al*., 2012; Maarman *et al*., 2012). Conversely, obesity with insulin resistance could decrease myocardial tolerance to I/R but the mechanisms for this decreased tolerance remains unclear (Donner *et al.*, 2012). Therefore, the strong association between obesity and CVDs stresses the necessity of elucidating the underlying molecular mechanisms

linking these pathologies. Thus, detailed knowledge of intracellular events at a molecular level is a prerequisite for the development of therapeutic regimens aimed at protection of the vascular system and the heart. One such candidate mechanism is the cAMP-Epac pathway.

1.10.2 Study aim, hypothesis and obejectives

1.10.2.1 Study aim

We aimed to investigate use a selective Epac agonist (CPT) and a newly discovered Epac1 selective antagonist (ESI-09) may provide a new path for the development of novel therapeutics for the treatment of CVDs.

1.10.2.2 Hypothesis:

We hypothesise that Epac activation with CPT is specifically involved in mediating cardioprotection during I/R injury and that Epac activation is an effective means of pre- and possible post- ischaemic treatment.

1.10.2.3 Objectives:

i. To elucidate the role of Epac in myocardial I/R of *ex vivo* hearts of a healthy rat model **(Chapter 2)**

ii. To elucidate the role of Epac in myocardial I/R of *ex vivo* hearts from a rat model of high-calorie diet-induced obesity **(Chapter 3)**

iii. To investigate the role of Epac signalling in *ex vivo* thoracic aortas from a rat model of high-calorie diet-induced obesity **(Chapter 4)**

iv. To investigate the role of Epac signalling in palmitic and oleic acid-induced endothelial dysfunction in rat aortic endothelial cells (RAECs) **(Chapter 5)**

Chapter Two

The role of Epac in myocardial I/R of *ex vivo* hearts of a healthy rat model

2.1 Introduction

β-adrenoceptors play a crucial role in the regulation of cardiac function in both normal and disease state (Port and Bristow, 2001). Stimulation of these receptors activates adenyl cyclase to form cAMP from ATP. It has been demonstrated that the *β*-adrenergic -cAMP signalling pathway is involved in several cardioprotective events including ischaemic preconditioning (Khaliulin *et al*., 2014, 2010; Lochner *et al*., 1999). The latter is short cycles of non-injurious I/R that protect the myocardium from subsequent long periods of ischaemia (Ferdinandy *et al*., 2014; Murry *et al*., 1986). A moderate pre-ischaemic stimulation of β-adrenoceptors before a sustained I/R has a cardioprotective affect (Lochner *et al*., 1999) while overstimulation of these receptors can have detrimental effects which may lead to heart failure (Port and Bristow, 2001). In heart failure, β-adrenoceptors are desensitized/downregulated due to hyperactivity of the sympathetic nervous system (de Lucia *et al*., 2018). Therefore, by targeting cAMP and its downstream effectors without stimulating the β-adrenoceptors could be an advantage in cardioprotection. However, cAMP via the PKA pathway did not yield a conclusive mechanism on cardioprotection, suggesting that an alternative cAMP effector might be involved (Makaula *et al*., 2005). Epac proteins are an additional class of cAMP effectors and the availability of pharmacological agents such as CPT (Epac selective agonist) and ESI-09 (Epac selective antagonist) has made it possible to discriminate between the role of Epac and PKA in cardioprotection against I/R injury. In this study we aimed to evaluate the role of Epac in myocardial I/R injury of a normal body weight rat model. To achieve this, Epac was activated with CPT or inhibited with ESI-09 respectively in *ex vivo* hearts using an isolated rat heart perfusion model. Cardiac functional recovery, infarct size and selected signalling pathways (using western blots) were measured as endpoints.

2.2 Methods and materials

2.2.1 General materials used

Cell Signaling Technologies (Beverly, MA, USA)

1. Total ERKp44/p42 (catalogue number: #9102)
2. Phopho-ERKp44/p42 (Thr^{202}/Tyr^{204}) (ERK1/2) (catalogue number: #9101)
3. Total PKB (catalogue number: #4691)
4. Phospho-PKB/ (Ser^{473}) (catalogue number: #4058)
5. Total CREB (catalogue number: #4820)
6. Phospho-CREB (Ser^{133}) (catalogue number: #9198)
7. Cleaved-caspase-3 (catalogue number: #9664)
8. Horseradish peroxidise-linked anti-rabbit IgG (catalogue number: #7074)

Bio-Rad Laboratories, USA

1. Enhanced chemiluminescence (ECL) detection reagent (catalogue number: #1705060)

Millipore (Billerica, MA, USA)

1. Polyvinylidene difluoride (PVDF) membrane (Immobilon™-P) (catalogue number: #IPVH00010)
2. Rap1 Activation Assay Kit (catalogue number: #17-321)

Sigma-Aldrich (St Louis, Mo, USA)

1. MEK-ERKp44/p42/ ERK1/2 inhibitor (PD98059) (catalogue number: #P215-5M
2. PKB kinase inhibitor (A6730-5mg) (catalogue number: #A6730)
3. 8-pCPT-2'-O-Me-cAMP (CPT): Epac agonist. (catalogue number: #C8988)
4.

Biolog Life Science Institute (Bremen, Germany)

1. 3- [5- (tert.-Butyl)isoxazol- 3- yl]- 2- [2- (3- chlorophenyl)hydrazono]- 3- oxopropanenitrile (ESI-09): Epac antagonist (catalogue number: #B133-05)

All other chemicals were of Analar grade and were purchased from Merck (including methanol, standard salts for solutions and buffers, and dimethyl sulfoxide (DMSO)).

2.2.2 Animals

The study was approved by the University of Stellenbosch animal ethics committee (SU-ACUD14-00020) appendix (Figure A. 6). Animals used were housed at the University of Stellenbosch Central Research Facility (Tygerberg Campus). The animals were treated in accordance with the South African National Standard (SANS) guidelines for animal care and usage. The rats had free access to food and water and house in a temperature of (22°C), the humidity of (40%) and a 12 hour light/dark cycle. The rats were fed standard rat laboratory chow. Male Wistar rats (6 weeks old) weighing between 250 to 300g were used in this study.

2.2.3 Rat Heart Perfusion Technique

The isolated working heart model was used, using the well-characterized perfusion technique (not electrically stimulated; preload 15 cm H_2O; afterload 100 cm H_2O) as described previously (Figure 2.1) (Lochner *et al*., 1999; Salie *et al*., 2019).

Rats were anaesthetized by lethal intraperitoneal injection of pentobarbital (160 mg/kg) for sacrifice. Immediately after removal, hearts were arrested with ice-cold (4°C) Krebs-Henseleit buffer (with composition in mmol/L: NaCl 119, KCl 4.74, $CaCl_2$ 1.25, $MgSO_4$ 0.6, Na_2SO_4 0.59, KH_2PO_4 1.79, $NaHCO_3$ 24.9, Glucose 10) (Salie *et al*., 2019). The hearts were immediately mounted onto an aortic cannula and perfused retrogradely with the Krebs-Henseleit buffer that was pre-warmed (37°C) and gassed (95% O_2, 5% CO_2) before and during the perfusion protocol. Retrograde perfusion was in a non-recirculating manner at a pressure of 100 cm H_2O for 30 minutes (stabilization period). During this time, the left atrium was cannulated to allow for working heart perfusion at the preload of 15 cm H_2O. After the stabilization period, the mode of perfusion was changed to a working heart mode for 10 minutes, the left ventricle ejecting against a hydrostatic pressure of 100 cm H_2O (afterload) (not electrically stimulated). The temperature was monitored and maintained at 37°C throughout the perfusion protocol.

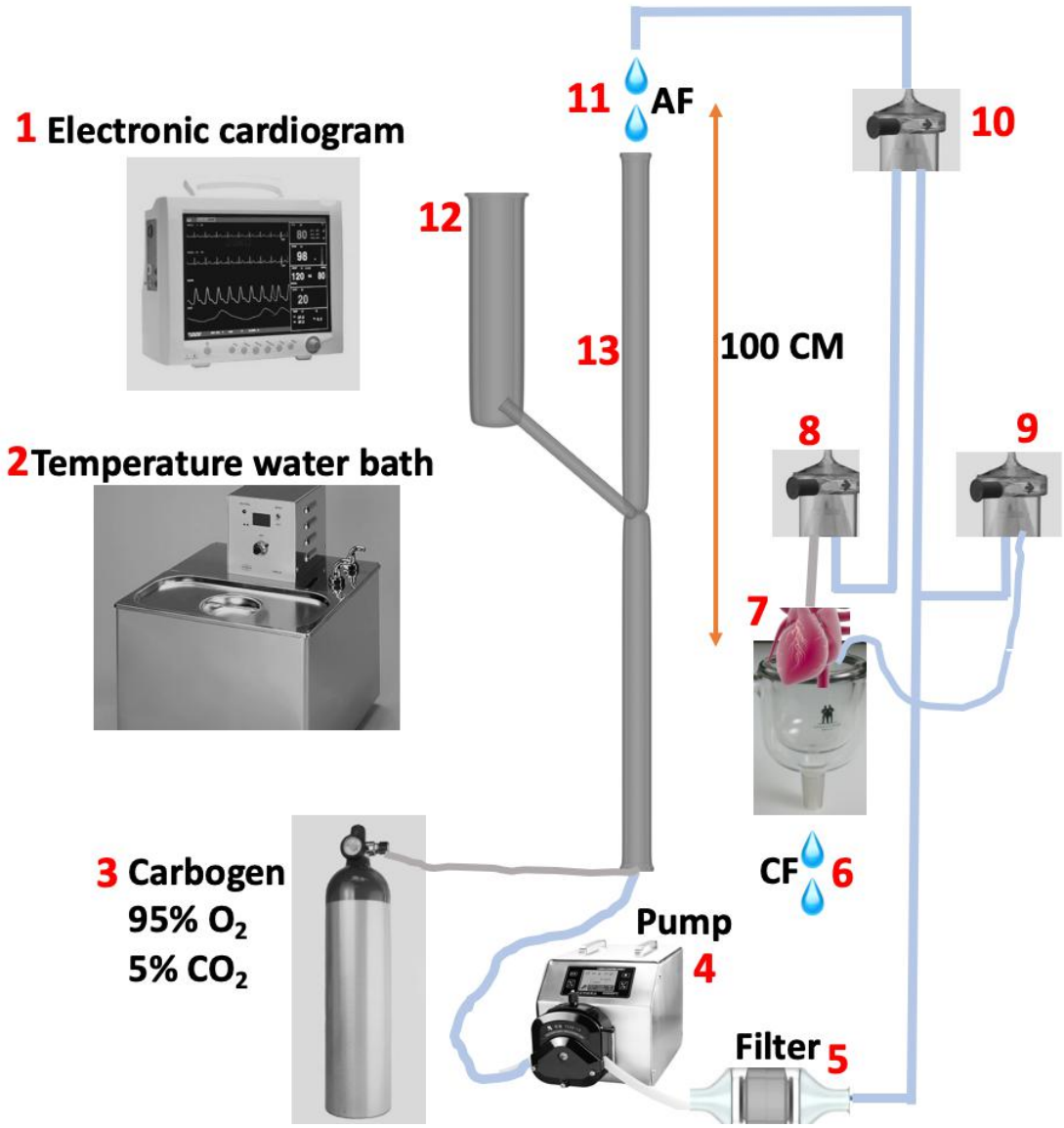

Figure 2. 1 A schematic overview of the perfusion circuit.

1. Electronic cardiogram
2. Temperature water bath
3. Carbogen tank
4. Perfusion pump
5. Filter
6. Coronary flow (CF)
7. Heart chamber with isolated heart

8., 9., 10., Bubble traps
11. Aortic flow (AF)
12. Reservoir
13. Heart heat exchanger

2.2.4 Regional ischemia

Thirty minutes stabilization was allowed before the induction of ischaemia. Regional myocardial ischaemia was induced by inserting silk suture around the left anterior descending (LAD) coronary artery. Thereafter, coronary artery occlusion was maintained for 35 minutes at a myocardial temperature of 36,5°C. The myocardial temperature was measured by inserting a temperature probe in the coronary sinus. After 35 minutes of regional ischaemia, the silk suture was released and the myocardium was reperfused for 65 minutes. Reperfusion included 10 minutes of retrograde perfusion, followed by 20 minutes of working heart perfusion and again by retrograde perfusion for another 30 minutes.

2.2.5 Experimental protocols

2.2.5 (a) Pre-treatment

The hearts were perfused with an Epac selective-agonist, 8-pCPT-2'-O-Me-cAMP (CPT, 2 µM) or novel Epac inhibitor, ESI-09 (5 µM) or beta-adrenergic agonist, isoproterenol (ISO, 0.1 µM). The concentrations of CPT (Vliem *et al*., 2008) and ESI-09 (Almahariq *et al*., 2012; Rehmann, 2013; Tsalkova *et al*., 2012) were obtained from the literature and for CPT dose-response see (Appendix A, Figure A. 2A).

Drug administration was through an aortic cannula and perfused retrogradely (at a pressure of 100 cm H_2O) 15 minutes before regional ischaemia (for protocol see Figure. 2.2).

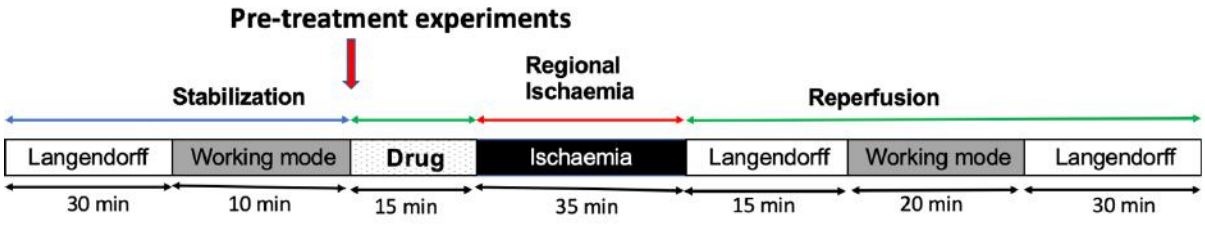

Figure 2. 2 The general experimental protocol for hearts pre-treated before I/R (see detailled protociols with results).

2.2.5 (b) Post-treatment

For post-treatment, drug administration was through an aortic cannula and perfused retrogradely in the first 10 minutes of reperfusion. The hearts were perfused with an Epac selective-agonist, 8-pCPT-2'-O-Me-cAMP (CPT, 2 µM) or novel Epac inhibitor, ESI-09 (5 µM) (Figure. 2.3). In order to determine the mechanism of cardioprotection by Epac on I/R injury, the involvement of the Reperfusion injury salvage kinase (RISK) pathway was investigated by co-treatment of CPT (2 µM) with a MEK-ERK inhibitor (PD98059, 10 µM), and a selective PKB inhibitor (A6730, 2.5 µM) respectively (Figure 2.3).

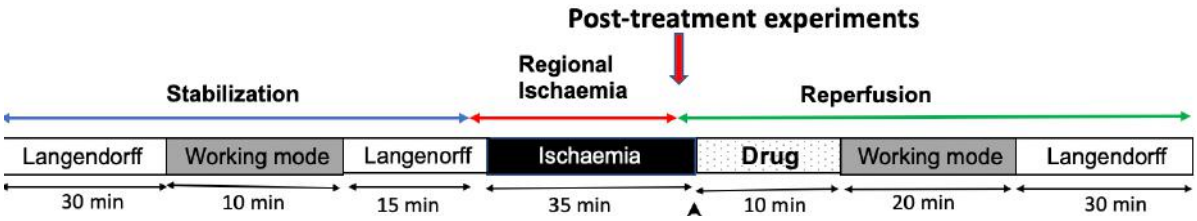

Figure 2. 3 The experimental protocol for hearts post-treated after I/R (see detailled protociols with results).

2.2.6 Assessment of cardiac function

Baseline measurements were taken 10 minutes into working mode, and included coronary flow (CF, ml/min), aortic flow (AF, ml/min), cardiac output (CO,-ml/min), heart rate (HR, beats/min), peak systolic pressure (PSP, mmHg) and total work performance (TW, mWatts). Left ventricular rate of work production (power) was calculated using the formula of Kannengiesser *et al*. (1979): Total work performance (TW) = 0002222 x PSP x CO.

Post-regional ischaemia cardiac function measurements were taken 20 minutes into working mode during reperfusion. Functional recovery was assessed as post-ischaemic CO and TW expressed as a percentage of pre-ischaemic values using the formula:

$$\text{Percentage recovery (\%)} = \frac{\text{Post-ischaemia measurement} \times 100}{\text{Pre-ischaemia (Baseline) measurement}}$$

2.2.7 Assessment of infarct size

After an hour of reperfusion, the coronary artery was re-occluded permanently, and ~1ml of a 0.25% Evans blue solution was infused via the aorta to outline viable tissues. Hearts were removed and frozen at -20°C and then sliced into 2 mm thick transverse sections. The latter were stained with 1% triphenyl tetrazolium chloride (TTC) in phosphate buffer, pH 7.4 for 10-15 minutes. TTC is used to differentiate between the metabolically active and inactive heart tissue. In healthy viable heart tissue, the TTC is enzymatically reduced to a deep red TPF (1,3,5-triphenylformazan) due to the activity of cardiac lactate dehydrogenases (enzymes important in cellular metabolism). In dead necrotic tissue (infarct), the enzymes are either denatured or degraded and therefore the heart tissue remains unreacted with a paler (white) colour (Figure 2.4). The TTC reaction was stopped by placing heart tissue sections in a 10% v/v formaldehyde solution to enhance the contrast between stained viable tissue and unstained necrotic tissue (Lochner *et al*., 2003). The sections were placed between two glass plates, scanned and saved in a tiff image format in a resolution of 1024 X 796. The images were then traced (Figure 2.4) and infract size (I/S) was determined using computerised planimetry (UTHSCSA Image Tool, University of Texas Health Science Centre at San Antonio, Texas, USA). The volume of infarcted tissue (I) and the risk zone or area at risk (R) were then calculated by multiplying each area with the slice thickness and calculating the sum of the products. The degree of occlusion is indicated as (R) R and was expressed as a percentage of the total viable area (VA+R) of the left ventricle. Infarct size was expressed as a percentage of the area at risk (I/R %) (Lochner *et al*., 2003).

Figure 2. 4 Illustration of infarct size determination

Blue: Non-risk / viable area (VA, stained with Evan's blue)

Deep red: Area at risk (R, healthy heart tissue in the risk zone, stained with TTC)

Pale (white): Infarcted area (I, Necrotic heart tissue in the risk zone)

2.2.8 Western blot measurements

After 10 minutes of reperfusion, the area at risk of the left ventricle was removed, snap-frozen in liquid nitrogen and stored at -80°C for subsequent biochemical analyses. For protein extraction, ~80mg of pulverised heart tissue was lysed in 800 µL lysis buffer containing: Triton X-100 1%, Tris-Hydro chloride (pH 7.5) 20 mM, Ethylene glycol tetra acetic acid (EGTA) 1 mM, Ethylene diamine tetra acetic acid (EDTA) 1 mM, Sodium chloride (NaCl) 150 mM, Beta-glycerophosphate 1 mM, Tetra-sodium-pyrophosphate 2.5 mM, Sodium fluoride (NaF) 50 nM, Sodium orthovanadate 1 mM, Leupeptin 10 µg/ml, Aprotinin 10 µg/ml, sodium dodecyl sulphate (SDS) 0.1%, phenylmethylsulfonyl fluoride (PMSF) 50 µg/ml. Stainless steel beads (1.6 mm) were added to the tissue lysate and then it was homogenised at 4ºC in a Bullet blender (Next Advance laboratory, NY, USA) at a speed of 8 for three one-minute cycles. The lysates were rested at 4ºC for 20 minutes and then centrifuged at 15,000 rpm (12074 x g) for 20 minutes at 4ºC. The Bradford protein assay was used to measure the concentration of the proteins (Bradford, 1976). For protein separation, an equal amount of lysate (60 µg per well) in Laemmli sample buffer (62.5 mM Tris-HCl (pH 6.8), 4% SDS, 10% glycerol, 0.03% Bromophenol blue and 5% mercaptoethanol) were separated by SDS-PAGE using 12% stain-free SDS-polyacrylamide gel. The stain-free gels were then photoactivated for immediate vitalisation of proteins in the gel using Bio-Rad Chemidoc-XRs imager (Bio-Rad Laboratories, USA). The Stain-free gel imaging technology utilizes a proprietary polyacrylamide gel chemistry to make proteins fluorescent directly in the gel allowing visualization of proteins at any stage of blotting, without staining the gel (BioRad Laboratories, 2019). The proteins were transferred to polyvinylidene fluoride (PVDF) membrane, blocked for an hour with 5% long life fat-free milk in Tris-buffered Saline-Tween (TBS-T: 20 mM Tris-HCl (pH 7.6), 137 mM NaCl, 0.1% Tween-20). PVDF membranes were then probed with the specific primary antibody in TBS-T by overnight shaking at 4ºC (1:1000 dilutions of phosphorylated or total primary antibodies: Total ERKp44/p42, phospho-ERKp44/p42 (Thr^{202}/Tyr^{204}), total PKB, and phospho-PKB/ (Ser^{473}), phospho-CREB (Ser^{133}), total-CREB, cleaved caspase-3 from Cell signalling. Membranes were washed with TBS-T and then

incubated with horseradish peroxidase-linked secondary antibody (Cell signalling, USA) at 1:4000 dilution for an hour at room temperature. The protein signal was enhanced with a chemiluminescent agent (Bio-Rad Laboratories, USA) and quantified using a Chemidoc-XRs imager and analysed with Image Lab 5 Software (Bio-Rad Laboratories, USA).

In addition, a Stain-Free technology was used for quality control and this approach offers a novel and unique quality control for data normalization in a standardized manner (Taylor and Posch, 2014). Briefly, the Stain-Free gels were activated with UV in Chemidoc-XRs imager and the proteins bands become visible and captured with a camera. After the proteins were transfer to the PVDF membranes, the blot (reference blot) is immediately imaged to verify the transfer of proteins for each lane. The image data is then analysed using Image lab software by selecting is a single band in each lane and stretched the band width to cover all volume peaks in a lane profile. The blot is then probed for a specific antibody and normalized using the reference blot images.

2.2.9 Epac/Rap1 activation assay (Pull-down assay)

Rap is a small GTPase that regulates molecular events by cycling an inactive GDP-bound form and an active GTP-bound form. The Rap1 assay is based on the differential affinity of Rap1 GTP-bound form and Rap1 GDP-bound form for Rap binding domain of Ral GDS. For determination of Epac activation, the downstream Rap1 activation assay was performed with a Rap1-activity Assay Kit (EMD Millipore Corp, MA, USA) according to the manufacturer's instructions. The Rap1 assay utilizes Ral GDS-RBD agarose beats to selectively isolate and pull down the activated GTP form of Rap1. Briefly, the left ventricle of the hearts was removed and snap-frozen after 15 min pre-treatment with CPT and ESI-09 during the perfusion protocol. The samples were homogenised in the provided Rap1 activation lysis buffer [Tris-HCl 100 mM, pH 7.4, NaCl 1 M, NP40 2%, $MgCl_2$ 5 mM and glycerol 10%] which was 1:1 diluted, prior to use, with 10% glycerol in deionized water and added 10 µg/ml aprotinin, 10 µg/ml leupeptin 25 mM, sodium fluoride and 1mM sodium orthovanadate. The heart lysates were by centrifugation for 10 minutes at 15,000 rpm and the Bradford

assay was used for protein determination. An equal amount of proteins was added in each tube and incubated with Ral- GDS-RBD agarose beads for 45 minutes at 4ºC. The beads were rinsed three times with ice-cold lysis buffer, resuspended in 40 µl of 2X Laemmli reducing sample buffer and 2 µl of 1 M dithiothreitol prior to boiling for 5 minutes. Then, the activated Rap1 GTP is detected by western blotting (as described in section 2.2.8) using the anti-Rap1 primary antibody.

2.2.10 Statistics

All data are expressed as mean ± standard error of the mean (SEM) and Graph Pad Prism™ 6 used for statistical analyses. Comparisons of groups were performed by ANOVA (one-way analysis of variance) followed by Bonferroni post-hoc test or student's t-tests (indicated in grey asterisk) where applicable. Significance was established at a p-value of <0.05.

2.3 Results

2.3.1 The effect of drugs (CPT and ESI-09) on cardiac function

The effect of the Epac agonist, CPT and different concentrations of the Epac antagonist, ESI-09 on cardiac function was investigated using the heart perfusion protocol as shown in Figure 2.5. The baseline function was measured after 30 minutes Langendorff and 10 minutes working mode and the recovery function was measured after 15 minutes drug treatment and 10 minutes working mode. NOTE: the hearts were not subjected to ischaemia.

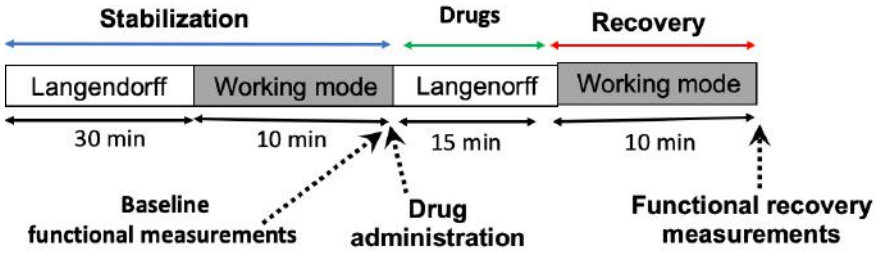

Figure 2. 5 Perfusion protocol for drug effect on cardiac function.

2.3.1 (a) Baseline cardiac function (before drug treatment)

Cardiac function was measured using the *ex vivo* working mode perfusion system. CF, AF, CO, HR, PSP and TW were measured before the hearts were perfused with either CPT 2 µM (see Appendix A, Figure A.2A) or different concentrations of ESI-09 [5 µM, 10 µM and 20 µM]. Baseline parameters were comparable since there were no significant differences in baseline values among the experimental groups (Table 2.1).

Table 2. 1 Baseline Cardiac function before treatment

	Control (n = 3)	CPT 2 µM 9 (n = 3)	ESI-09 5 µM (n = 3)	ESI-09 10 µM (n = 3)	ESI-09 20 µM (n = 3)
CF (ml/min)	16.3 ± 0.25	16.5 ± 0.5	14.3 ± 0.9	13.3 ± 1.3	16.7 ± 0.7
AF (ml/min	36.5 ± 1.7	41.3 ± 1.3	37.3 ± 0.7	39.1 ± 1.5	37.3 ± 0.7
CO (ml/min)	52.5 ± 1.7	58 ± 1.5	51.7 ± 1.4	51 ± 1.5	54 ± 1.2
PSP (mmHg)	91 ± 1.8	87.3 ± 1.3	87 ± 4.1	90.7 ± 2.9	88.7 ± 2.9
HR (bpm)	391 ± 44.1	351 ± 5.8	331 ± 43.1	340 ± 48.2	287 ± 34.1
TW (mWatts)	10.8 ± 0.4	11.2 ± 0.3	9.6 ± 0.3	10.2 ± 0.7	10.4 ± 0.7

All values are expressed as means ± SEM. Comparisons of groups were tested by ANOVA. n = 3 per group.

2.3.1 (b) Cardiac function after treatment

Hearts treated with 5 µM ESI-09 had significantly lower heart rates compared to the CPT treated hearts (5 µM ESI-09: 225.7 ± 18.9 vs. CPT: 324.3 ±. 6.2, P<0.05) (Figure 2.6A). The PSP of the hearts were not significantly affected by different drugs (Figure 2.6B). There were no significant difference between CPT and the control in cardiac function of CF, AF, CO, and TW (Figure 2.7A, B, C and D). Furthermore, hearts treated with Epac inhibitor (ESI-09) did not recover (Figure 2.7).

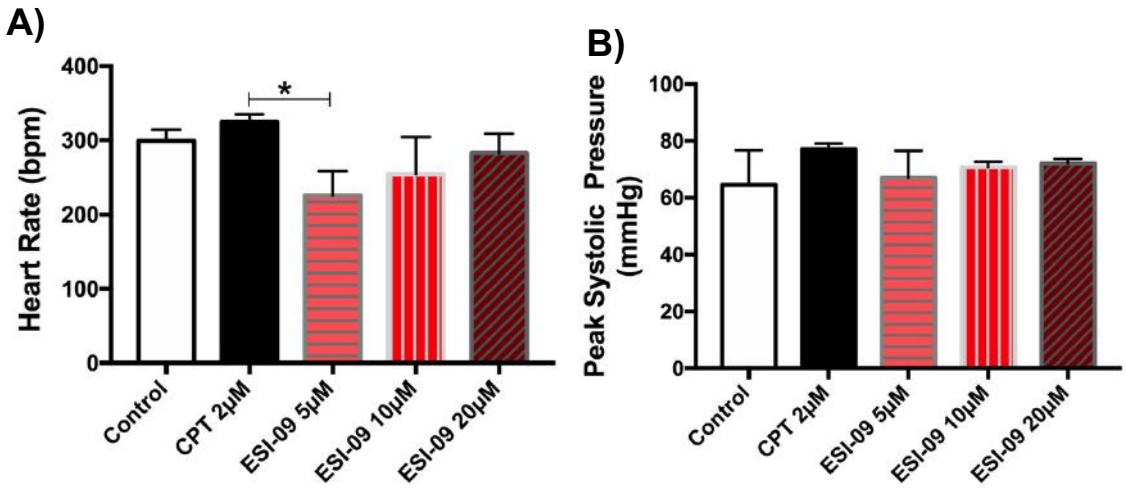

Figure 2. 6 The effect of drugs on cardiac function

A), Heart Rate (rpm, beat per minute), B), Peak Systolic Pressure of hearts treated with CPT [2 µM] and different ESI-09 [5 µM, 10 µM, and 20 µM] concentrations. All values are expressed as mean ± SEM. n = 3 per group. *P<0.05.

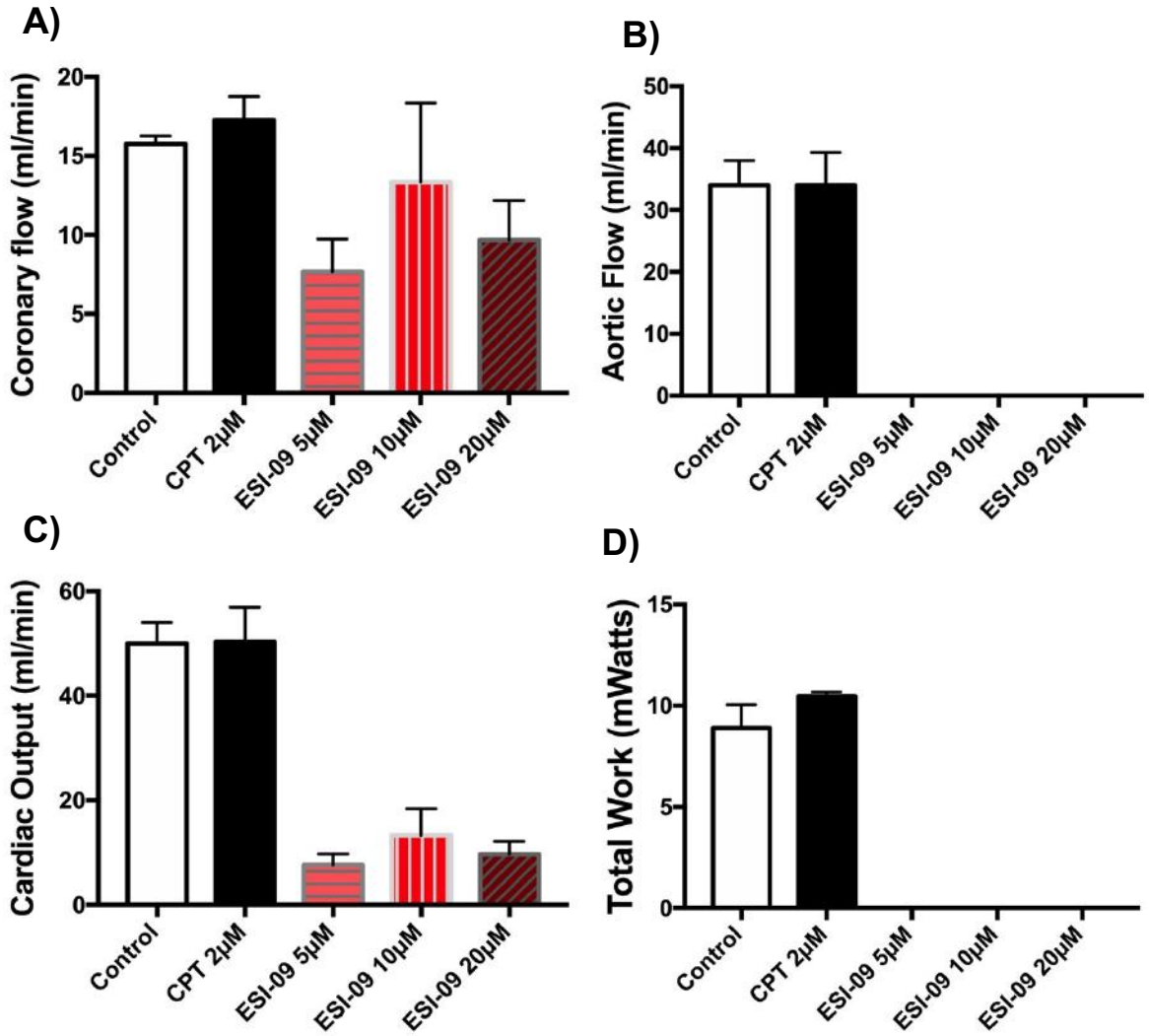

Figure 2. 7 The effect of drugs on cardiac function.

A) Coronary flow, B) Aortic Flow, C) Cardiac Output, D) Total Work performance of hearts treated with CPT and different ESI-09 concentrations. All values are expressed as mean ± SEM. n = 3 per group.

2.3.1 (C) Western blot measurements (activated Rap1)

Figure 2.8 represents Rap-GTP activation and Rap-GDP expression in hearts. CPT [2 μM] significantly increased percentage GTP-Rap1 compared to control (CPT: 74 ± 7.59% vs. control: 39.85 ± 0%, P<0.05) (Figure 2.8). Co-treatment of CPT [2 μM] + ESI-09 [20 μM] reduced the percentage GTP-Rap1 when compared to CPT treated hearts (ESI-09 [20 μM] + CPT [2 μM]: 43.94 ± 5.21% vs. CPT [2 μM]: 74 ± 7.59%, P<0.05) (Figure 2.8).

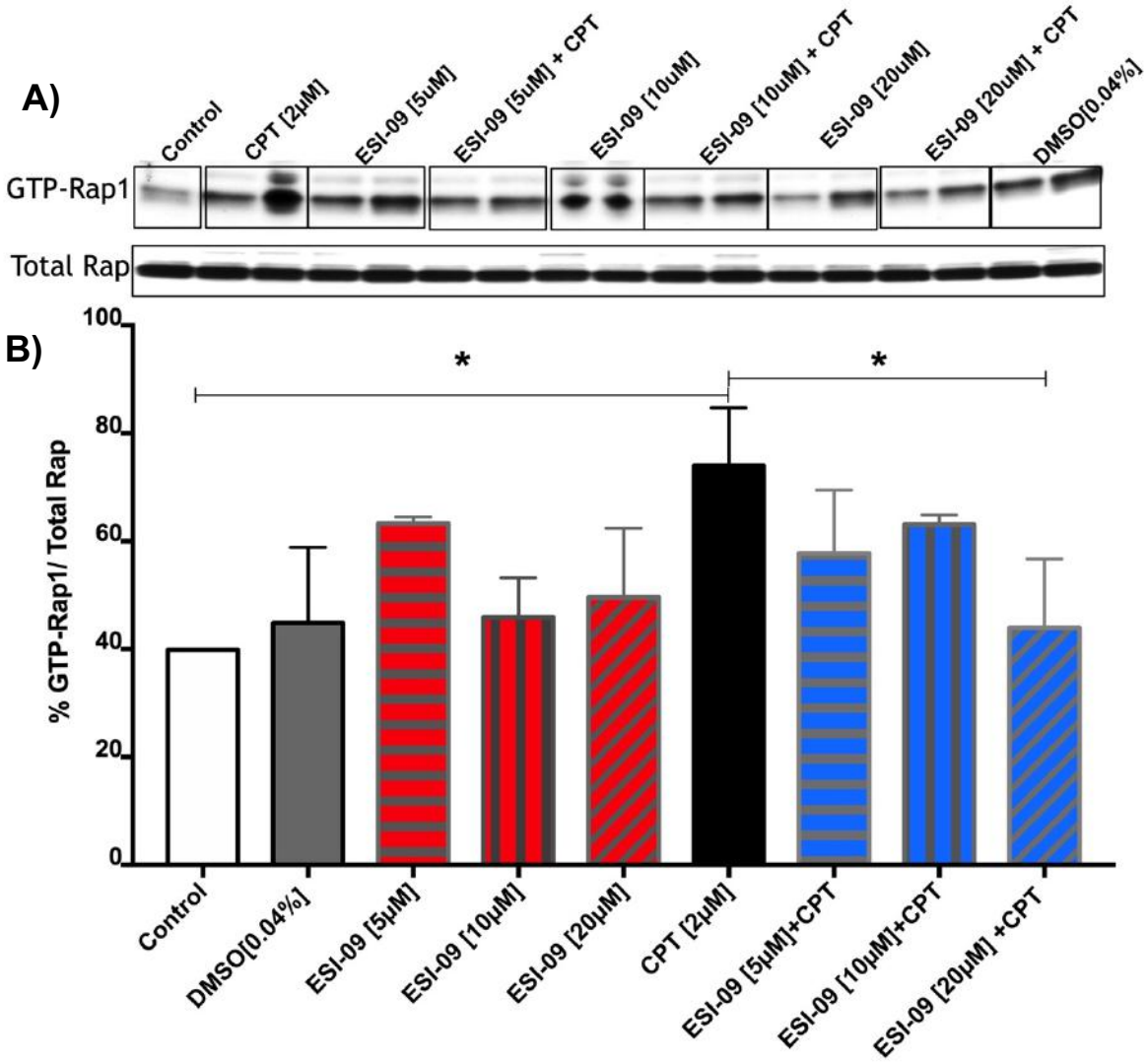

Figure 2. 8 Effect of Drugs on Rap1 Activation and expression.

(A) representative blots for activated GTP-rap1 and total Rap; (B), percentage of activated rap1. n= 2-4 per group. All values are expressed as mean ± SEM. *P<0.05.

2.3.2 Effect of drug pre-treatment on I/R: Cardiac function and Infarct size

The hearts were pre-treated with CPT [2 μM] (Epac agonist), ESI-09 [5 μM] (Epac antagonist) and ISO [0.1 μM] (beta-adrenergic agonist) (see protocol in Figure 2.9).

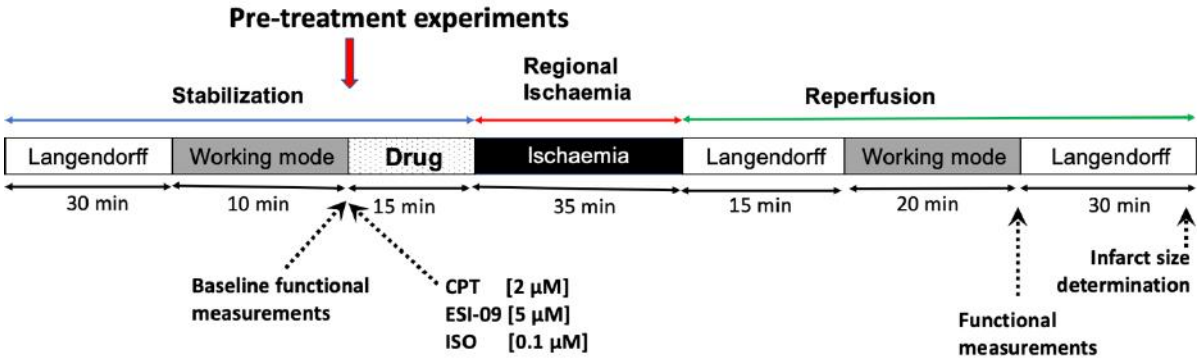

Figure 2. 9 Pre-treatment experimental protocol.

2.3.2 (a) Cardiac Function before and after ischaemia

Table 2.2 demonstrates cardiac function before and after regional ischaemia. Comparable baseline cardiac function was observed as there were no significant differences among the groups before ischaemia groups (Table 2.2).

There were no differences in post-ischaemic function in terms of CF, CO, PSP and HR among the treatment groups after 35 minutes of regional ischaemia and 65 minutes reperfusion (Table 2.2).

Epac inhibition with ESI-09 was detrimental on cardiac recovery post-I/R (Table 2.2). Co-treatment with CPT did not reverse the effects of ESI-09 (Table 2.2). Beta-adrenergic stimulation with ISO increased AF compared to control (ISO: 31.7 ± 1.9 vs. control: 19 ± 1.5, $P<0.01$). Co-treatment of ISO with ESI-09 could not reverse the deleterious effects of ESI-09 (Table 2.2).

Table 2. 2 Drug pre-treatment: Cardiac function before and after 35 min regional ischaemia and 35 min reperfusion.

	Control (n = 13)	CPT (n = 4)	ESI-09 (n = 3)	ESI-09+CPT (n = 3)	ISO (n = 3)	ISO+ESI-09 (n = 5)
Cardiac function before drug administration and ischaemia						
CF (ml/min)	10.8 ± 2.9	12 ± 1.2	14.6 ± 0.7	10.7 ± 1.3	13.3 ± 1.3	13.8 ± 1.03
AF (ml/min)	35.3 ± 0.7	38.7 ± 2.4	41.3 ± 1.33	42.1 ± 1.33	40.7 ± 0.7	39 ± 1.7
CO (ml/min)	47.3 ± 1.3	50.7 ± 1.3	56 ± 2.1	54.1 ± 2.2	54 ± 1.2	52.8 ± 2.4
PSP (mmHg)	79.7 ± 4.4	86.3 ± 0.1	94 ± 0.1	86.3 ± 1.7	97.3 ± 8.9	84.8 ± 0.1
HR (bpm)	360 ± 28.8	296 ± 26.6	311 ± 28.5	329 ± 27.3	268 ± 21.5	364 ± 40.6
TW (mWatts)	9.8 ± 0.4	9.6 ± 0.3	11.7 ± 0.5	10.8 ± 0.8	10.2 ± 0.4	10.5 ± 0.6
Cardiac function after ischaemia						
CF (ml/min)	11 ± 1.1	10.2 ± 1.5	11.1 ± 1.5	10 ± 2.5	14.3 ± 1.8	13 ± 1.47
AF (ml/min)	19 ± 1.5	24.1 ± 6.3	0	0	31.7 ± 1.9*	0
CO (ml/min)	30 ± 2.5	35.5 ± 6.5	11.1 ± 1.5	12.7 ± 4.3	45.67 ± 3.8	13.2 ± 1.5
PSP (mmHg)	77 ± 3.1	78 ± 2.6	67 ± 5.5	76.7 ± 2.3	88.3 ± 5.6	71 ± 0.4
HR (bpm)	336 ± 18.3	297 ± 44.5	183 ± 23.9	245 ± 61.4	304 ± 18.77	146 ± 21.5
TW mWatts)	3.2 ± 0.8	5.8 ± 0.8	0	0	8.3 ± 1.7	0

All values are expressed as mean ± SEM. Comparisons of groups were tested by ANOVA. n = 3-13 per group. *p < 0.05 vs Control. . **("zero", the hearts did not recover post I/R).**

2.3.2 (b) Recovery of cardiac function

ISO pre-treated hearts had a significant improvement in the percentage recovery of CO compared to control hearts (ISO: 84.4 ± 4.6 % vs. control: 46.5 ± 5.5%, P<0.05) (Figure 2.10A). The percentage recovery of TW between CPT pre-treated hearts and the control hearts was not significantly different. However, the beta-adrenergic agonist ISO significantly improved the percentage recovery of TW compared to the control hearts (ISO: 82.1 ± 19.3 % vs. control: 31.5 ± 7.8 %, P<0.05) (Figure 2.10B). Epac inhibition with ESI-09 [5 µM] was detrimental to the percentage recovery post I/R (Figure 2.10A and B).

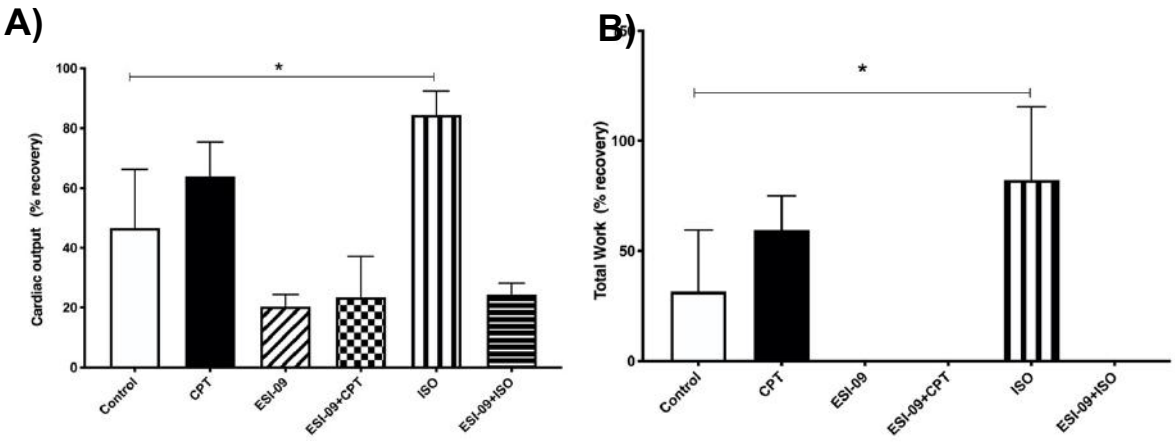

Figure 2. 10 Cardiac output and Total work of hearts after 35 min regional ischaemia and 30 min reperfusion, pre-treated with CPT [2 µM], ESI-09 [5 µM] and ISO [0.1 µM] 15 min before ischaemia.

(A) Cardiac output, percentage recovery; (B) Total work, percentage recovery. All values are expressed as mean ± SEM. n = 3-8 per group. *P<0.05.

2.3.2 (c) Infarct size

Epac activation with CPT before ischaemia significantly reduced infarct size compared to control hearts (CPT: 8.2 ± 1.7% vs. control: 23.7 ± 2.9%, P<0.01) (Figure 2.11A). Furthermore, beta-adrenergic stimulation with ISO also reduced infarct size compared to control hearts (ISO: 6.1 ± 2.2% vs. control: 23.7 ± 2.9%, P<0.01) (Figure 2.11A).

With regard to the effect of ESI-09: Firstly, ESI-09 did not affect the percentage infarct size compared to control. Secondly, the protection by CPT and ISO was lost/reversed when co-treated with ESI-09, because ESI-09+CPT and ESI-09+ISO were not significantly different compared to control. Thirdly, ESI-09 significantly increased the percentage of total area at risk compared to control (ESI-09: 65.75 ± 4.1% vs. Control: 47.9 ± 1.1%, P<0.001; ESI-09+CPT: 62.9 ± 3.8% vs. control: 47.9 ± 1.1%, P<0.01) (Figure 2.11B). This could be due to the fact that the hearts were unable to perfuse the Evans blue dye for viable tissue since ESI-09 impaired the cardiac function (Figure 2.10). It is essential that the total area at risk should be the same/comparable among the groups and that an average of 50% is recommended (Ytrehus *et al.*, 1994).

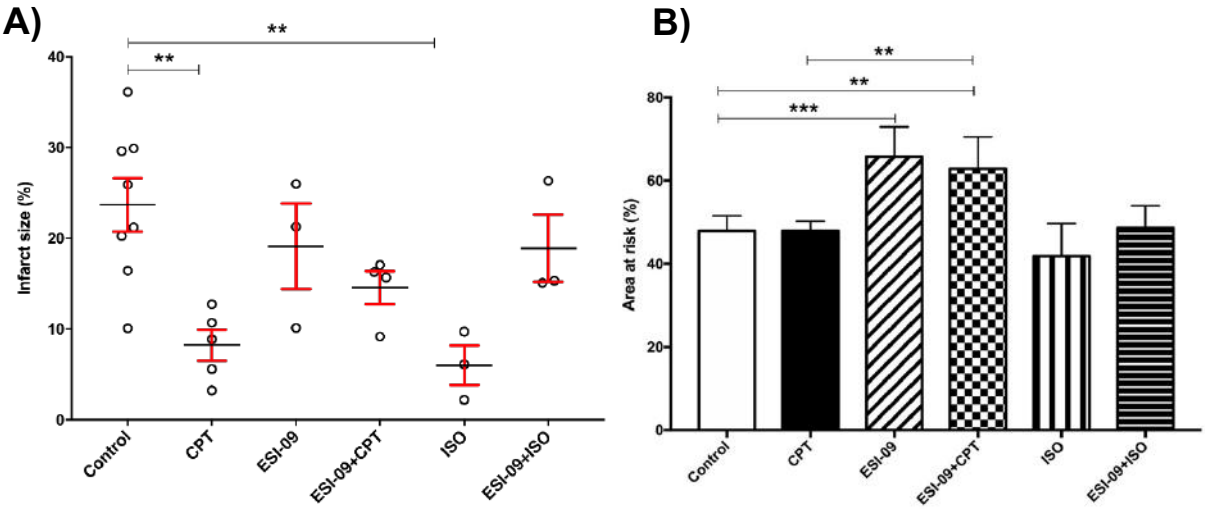

Figure 2. 11 Infarct size and Area at risk of hearts after 35 min regional ischaemia and 60 min reperfusion, pre-treated with CPT [2 µM], ESI-09 [5 µM] and [ISO 0.1 µM] 15 min before ischaemia.

(A), Infarct size, percentage of the area at risk; (B), Area at risk, percentage of the left ventricle. All values are expressed as mean ± SEM. n = 3-8 per group. *P<0.05, ***P<0.001, ****P<0.0001.

2.3.3 Effect of drug Post-treatment on I/R: cardiac function, infarct size and signalling pathways

The hearts were post-treated with CPT [2 μM] (Epac agonist) and ESI-09 [5 μM] (Epac antagonist) (see protocol in Figure 2.12).

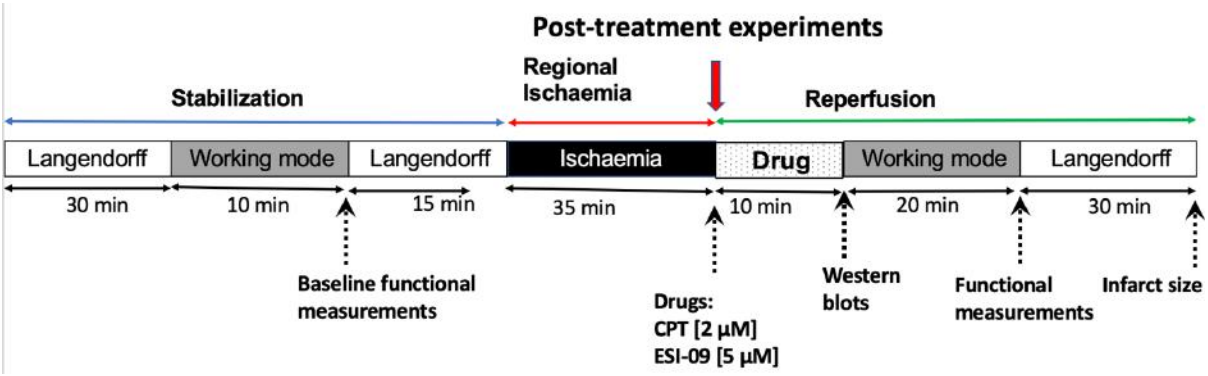

Figure 2. 12 Post-treatment experimental protocol.

2.3.3 (a) Cardiac Function before and after ischaemia (see protocol in Figure 2.12).

Comparable baseline cardiac function was observed as there were no significant differences among the groups before ischaemia (Table 2.3). There were no differences in post-ischaemic function in terms of CF, AF, CO, PSP, HR and TW among the treatment groups after 35 minutes of regional ischaemia and 30 minutes reperfusion (Table 2.3). Post-treatment with Epac inhibitor ESI-09 was detrimental on cardiac recovery post-I/R (Table 2.3).

Table 2. 3 Drug post-treatment: Cardiac function before and after 35 min regional ischaemia and 30 min reperfusion.

	DMSO 0.01% (n = 8)	CPT (n = 6)	ESI-09 (n = 5)	CPT+ESI-09 (n = 7)
Cardiac function before ischaemia				
CF (ml/min)	13.4 ± 0.8	14.8 ± 0.8	15.2 ± 1.0	12.4 ± 1.2
AF (ml/min)	38.5 ± 1.1	37.4 ± 1.2	38.4 ± 0.7	37.6 ± 1.2
CO (ml/min)	51.9 ± 1.5	52.2 + 1.6	53.6 ± 1.4	50.0 ± 2.3
PSP (mmHg)	80.5 ± 1.4	83. 4 ± 1.0	86.6 ± 2.5	87.6 ± 2.8
HR (bpm)	313 ± 15.8	315 ± 9.6	385 ± 40.3	256 ± 4.33
TW (mWatts)	9.1 ± 0.3	9.9 ± 0.3	8.3 ± 1.8	9.8 ± 0.7
Cardiac function after ischaemia				
CF (ml/min)	12.5 ± 0.7	15.4 ± 1.5	12.2 ± 1.4	13.6 ± 1.2
AF (ml/min)	13 ± 2.3	18.8 ± 0.8	0	0
CO (ml/min)	25.5 ± 2.5	34.2 ±1.2	12.2 ± 1.4	15.2 ± 2.4
PSP (mmHg)	72.3 ± 1.5	77.1 ± 1.1	66.4 ± 2.2	75.8 ± 3.9
HR (bpm)	367 ± 16.2	330 ± 49.9	258 ± 23.5	279 ± 22.5
TW (mWatts)	4.5 ± 0.5	6.1 ± 0.2	0	0

All values are expressed as mean ± SEM. Comparisons of groups were tested by ANOVA. n = 5-8 per group. **("zero", the hearts did not recover post I/R).**

2.3.3 (b) Recovery of cardiac function

Epac activation with CPT during reperfusion did not change the percentage recovery of CO and TW compared to the vehicle control (DMSO 0.01%) (Figure 2.13A and B). However, in our pilot study (PhD proposal) post-treatment with CPT significantly improved total work performance (TW %) compared to normal control (without the vehicle DMSO) (see Appendix A, Figure A.3). Post-treatment with Epac inhibitor ESI-09 was detrimental on percentage recovery of CO and TW (Figure 13A and B).

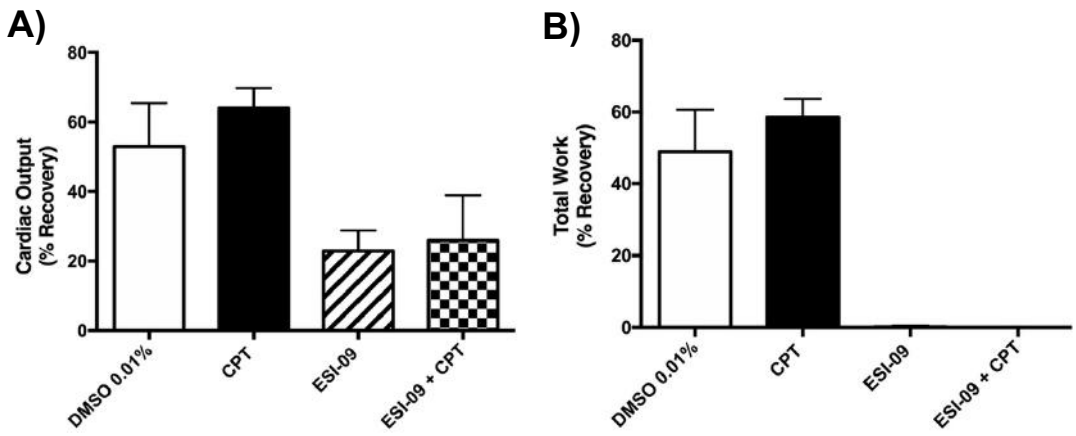

Figure 2. 13 Cardiac output and Total work of hearts, after 35 min regional ischaemia and 30 min reperfusion, post-treated with an Epac activator [CPT 2 µM] and Epac inhibitor [ESI-09 5 µM] in the first 10 minutes reperfusion.

(A), Cardiac output, percentage recovery; (B), Total work, percentage recovery. All values are expressed as mean ± SEM. n = 5-8 per group.

2.3.3 (c) Infarct size

Epac activation with CPT at the onset of reperfusion, significantly reduced infarct size compared to vehicle-control hearts (CPT: 11.6 ± 2.4% vs. DSMO: 23.8 ± 1.2%, P<0.05) (Figure 2.14A). Interestingly, hearts post-treated with ESI-09 had no significant effect on the infarct size (Figure 2.14A), but (as seen before with pre-treatment, Figure 2.11B) significantly increased the area at risk compared to the vehicle-controls (ESI-09: 66.7 ± 2.5% vs DMSO: 47.0 ± 1.3%, P<0.05) (Figure 2.14B). However, the combination of ESI-09 with CPT did not reverse the small infarct size (Figure 2.14A) and the area at risk (Figure 2.14B) was not significantly increased as seen with pre-treatment (Figure 2.11B).

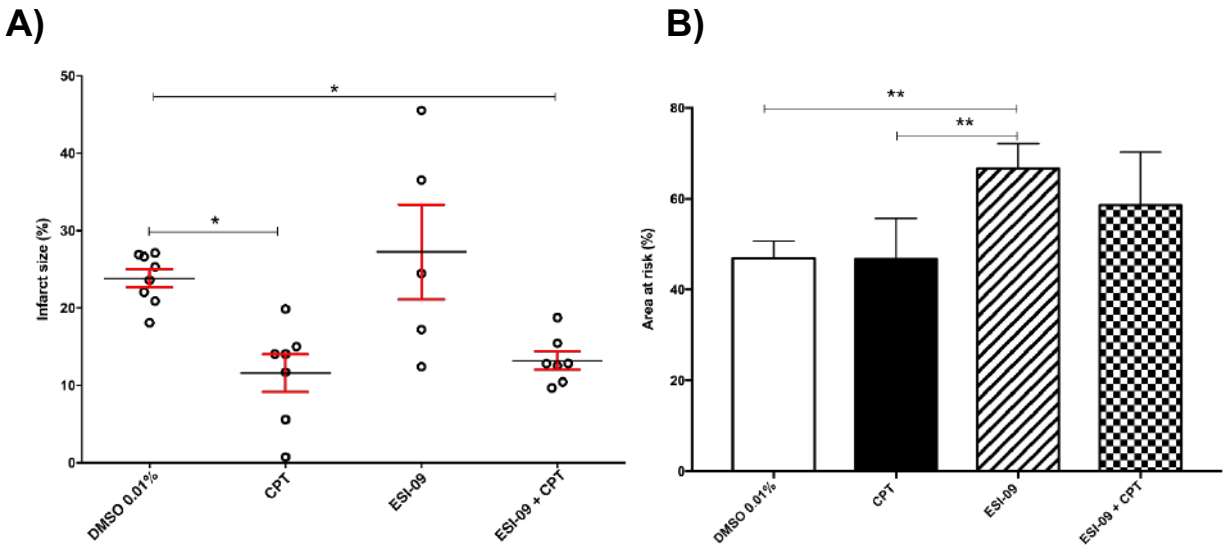

Figure 2. 14 Infarct size and Area at risk of hearts after 35 min regional ischaemia and 60 min reperfusion, post-treated with an Epac activator [CPT 2 µM] and Epac inhibitor [ESI-09 5 µM] in the first 10 minutes reperfusion.

(A), Infarct size, percentage of the area at risk; (B), Area at risk, percentage of the left ventricle. All values are expressed as mean ± SEM. n= 5-8 per group. *P<0.05, **P<0.01.

2.3.3 (d) Signaling Pathways (protein phosphorylation and expression during reperfusion)

There were no differences in PKB phosphorylation among the groups (Figure 2.15B). ESI-09 post-treatment increased total PKB expression compared to the vehicle control (ESI-09: 1.6 ± 0.1 vs. DMSO: 1.0 ± 0.1, P<0.05) (Figure 2.15C). However, co-treatment of ESI-09 with CPT significantly reduced the phospho: total PKB ratio compared to vehicle-control (ESI-09+CPT: 0.2 ± 0.1 vs. DMSO: 1.02 ± 0.2, P<0.01) (Figure 2.15D).

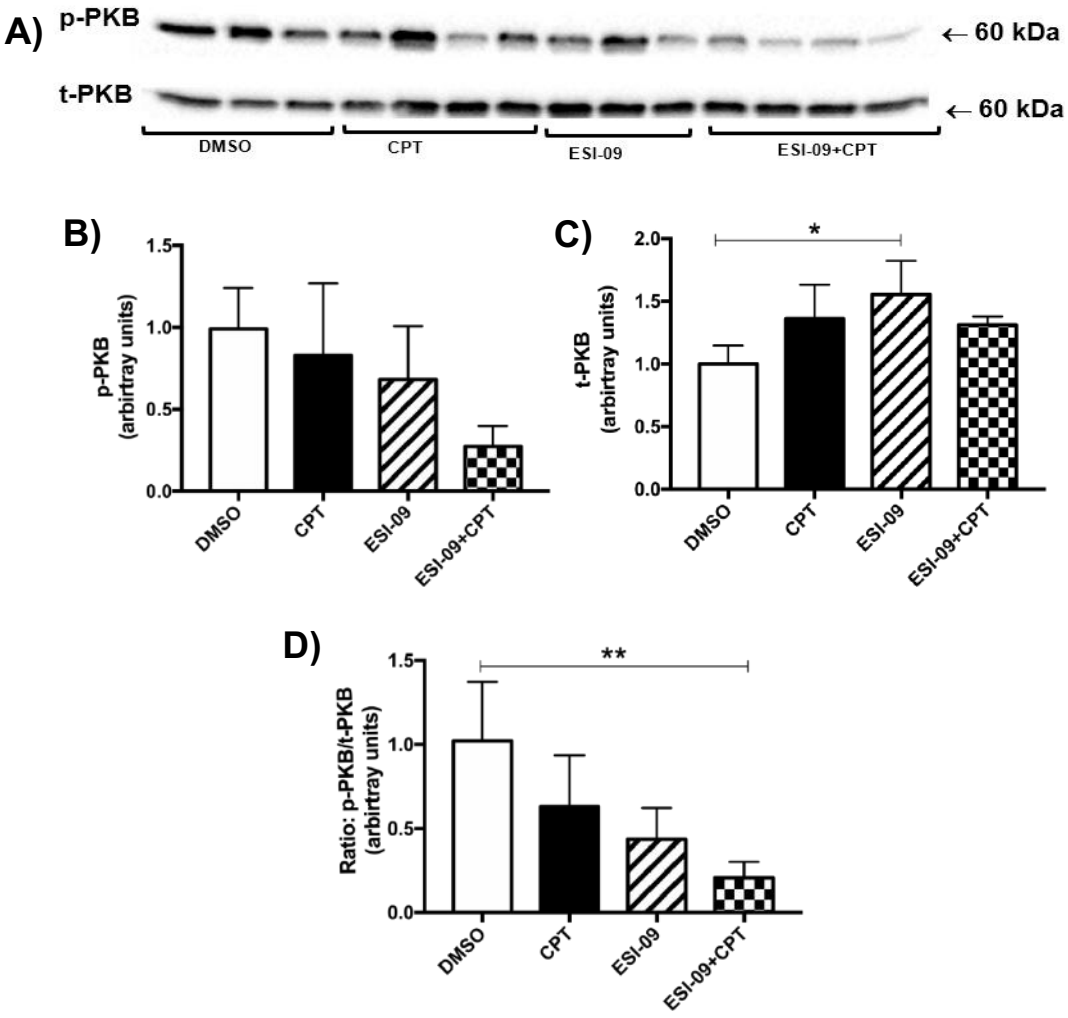

Figure 2. 15 PKB phosphorylation and expression in hearts after 35 min regional ischaemia and 10 min reperfusion, post-treated with an Epac activator [CPT 2 µM] and Epac inhibitor [ESI-09 5 µM] in the first 10 minutes reperfusion.

(A), representative Western blots for phosphorylated and total PKB; (B), phosphorylated PKB levels; (C), total PKB levels; (D), phospho/total ratio for PKB. n = 3-4 per group. All values are expressed as mean ± SEM.* P<0.05, **P<0.01.

Epac activation with CPT post-ischaemia had no effect on ERK1/2 phosphorylation, total expression or phospho: total ERK1/2 ratio compared to DMSO (Figure 12.16 B, C, and D).

Epac inhibition with ESI-09 at reperfusion caused a significant reduction in ERK1/2 phosphorylation compared to CPT treated hearts (ESI-09: 0.7 ± 0.11 vs. CPT: 1.0 ± 0.1, $P<0.001$; ESI-09+CPT: 0.5 ± 0.03 vs. CPT: 1.0 ± 0.1, $P<0.05$) (Figure 2.16B). Furthermore, the phospho: total ERK1/2 ratio was also reduced by ESI-09 compared to CPT treated hearts (ESI-09: 0.6 ± 0.1 vs. CPT: 1.2 ± 0.2, $P<0.01$; ESI-09+CPT: 0.5 ± 0.03 vs. CPT: 1.2 ± 0.2, $P<0.01$) (Figure 2.16D). The total ERK1/2 expression remained unchanged among the groups (Figure 2.16C).

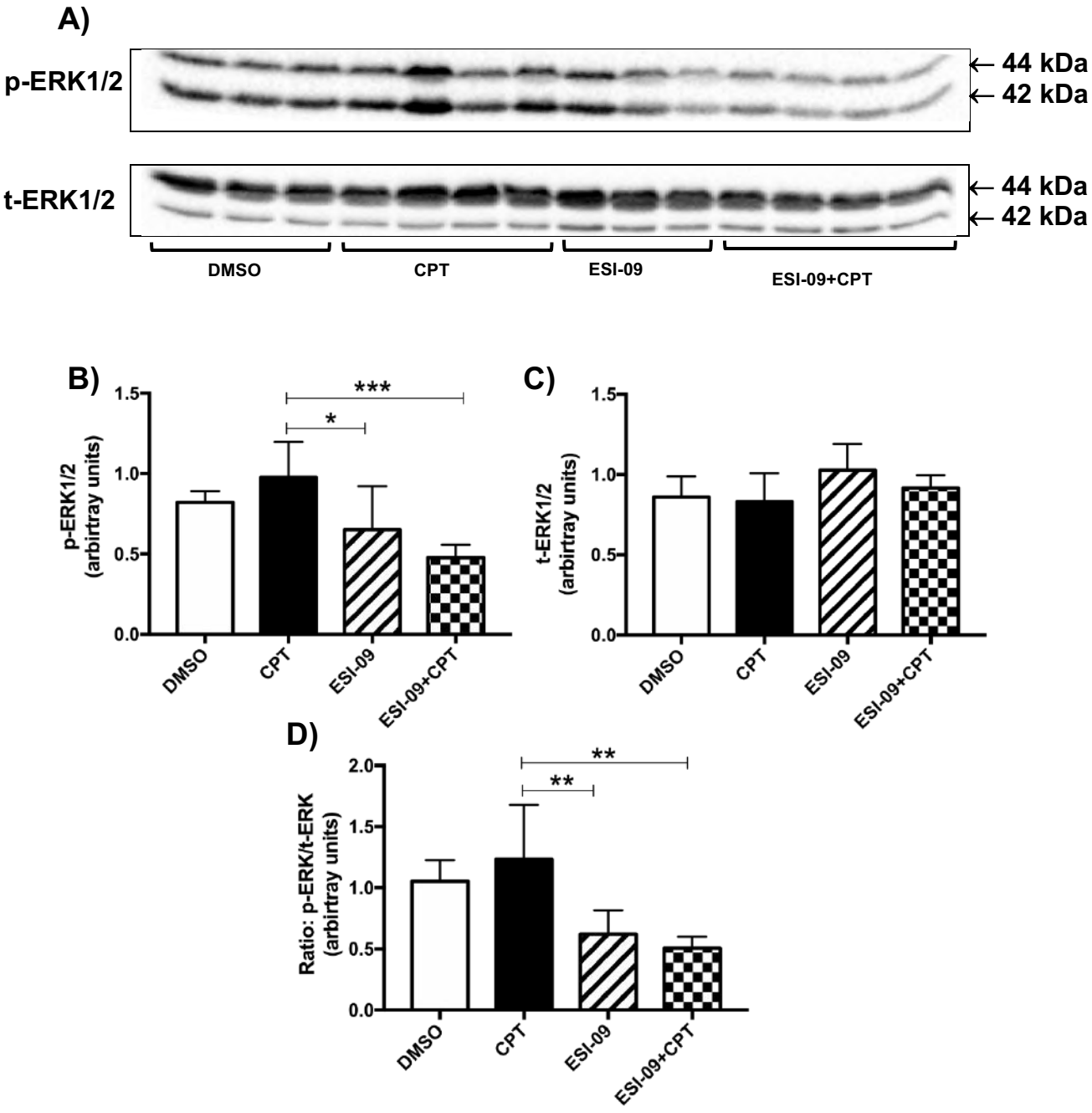

Figure 2. 16 ERK1/2 phosphorylation and expression in hearts after 35 min regional ischaemia and 10 min reperfusion, post-treated with an Epac activator [CPT 2 μM] and Epac inhibitor [ESI-09 5 μM] in the first 10 minutes reperfusion.

(A), representative Western blots for phosphorylated and total ERK1/2; (B), phosphorylated ERK1/2 levels; (C), total ERK1/2 levels; (D), phospho/total ratio for ERK1/2. n = 3-4 per group. All values are expressed as mean ± SEM. *P<0.05, **P<0.01, ***P<0.001.

There were no significant differences in CREB phosphorylation, CREB total expression and phospho: total CREB ratio among the treatment groups (Figure 2.17B, C and D).

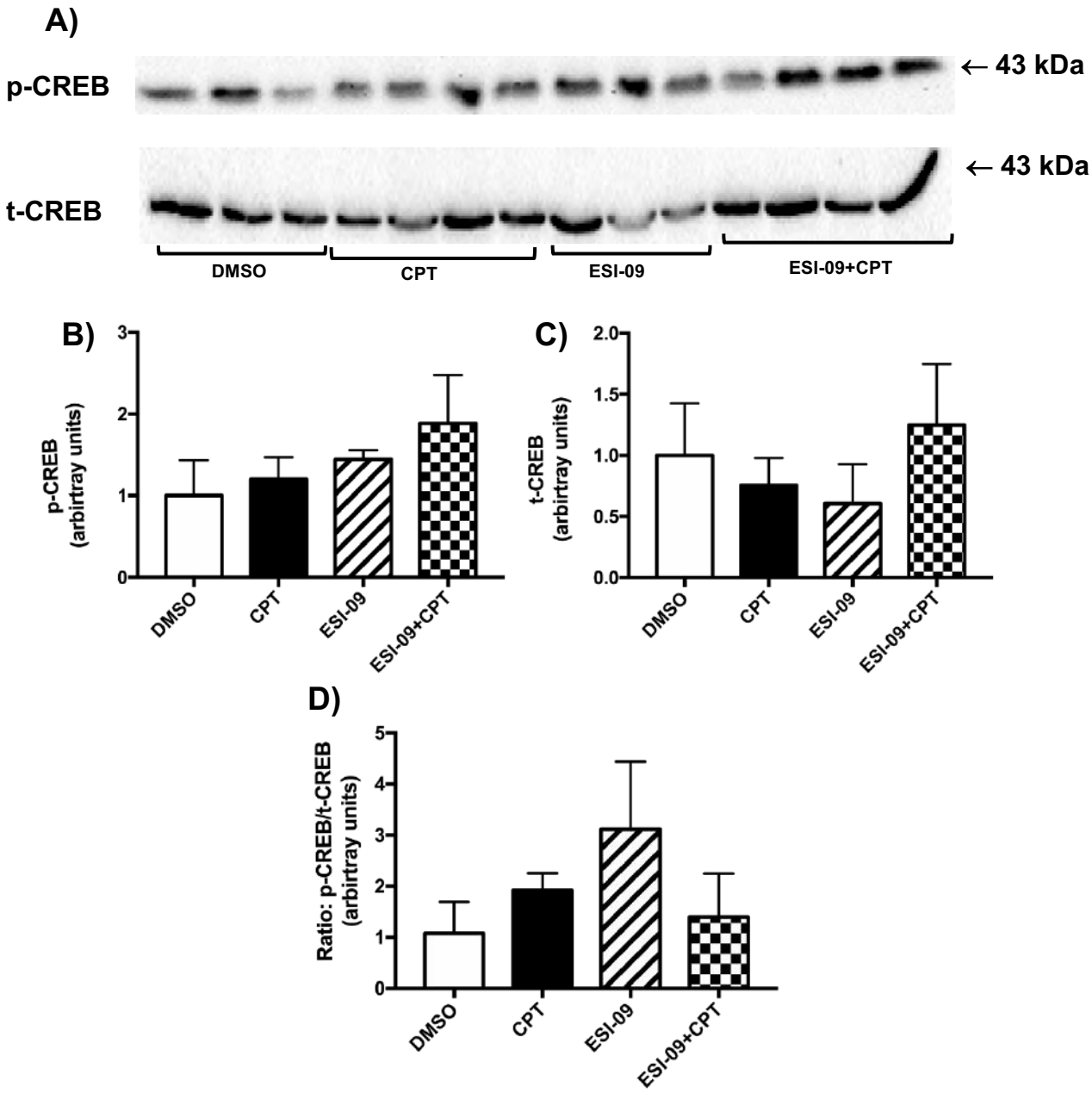

Figure 2. 17 CREB phosphorylation and expression in hearts after 35 min regional ischaemia and 10 min reperfusion, post-treated with an Epac activator [CPT 2 µM] and Epac inhibitor [ESI-09 5 µM] in the first 10 minutes reperfusion.

(A), representative Western blots for phosphorylated and total CREB; (B), phosphorylated CREB levels; (C), total CREB levels; (D), phospho/total ratio for CREB. n = 3-4 per group. All values are expressed as mean ± SEM.

Epac activation with CPT did not affect cleaved caspase-3 expression when compared to DMSO vehicle controls (Figure 2.18B). However, hearts post-treated with ESI-09 showed a significant increase in cleaved caspase-3 expression compared to DMSO control hearts (ESI-09: 3.2 ± 0.7 vs. DMSO: 1.7 ± 0.04, P<0.05) (Figure 2.18B).

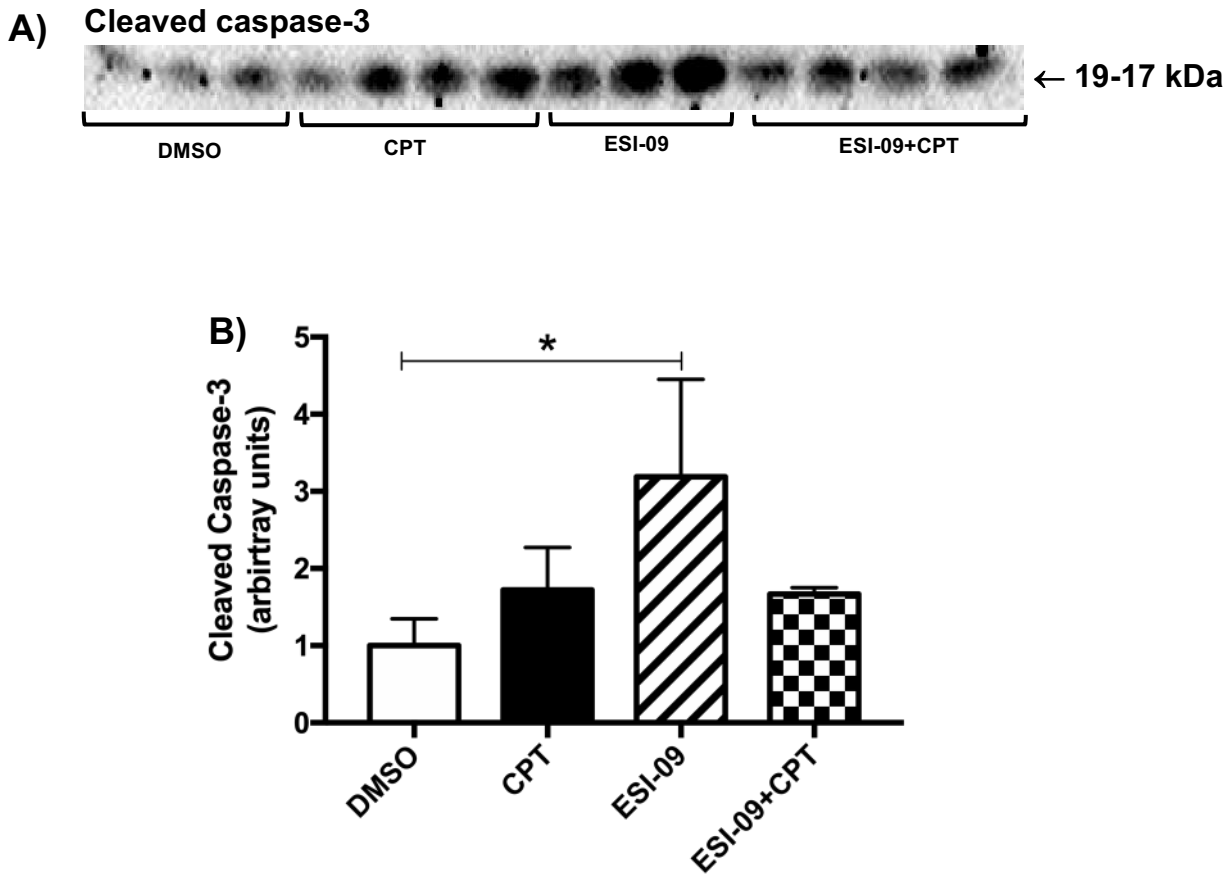

Figure 2. 18 Cleaved Caspase-3 expression in hearts after 35 min regional ischaemia and 10 min reperfusion, post-treated with an Epac activator [CPT 2 µM] and Epac inhibitor [ESI-09 5 µM] in the first 10 minutes reperfusion.

(A), representative Western blots for cleaved Caspase-3; (B), cleaved Caspase-3 levels. n = 3-4 per group. All values are expressed as mean ± SEM. *P<0.05.

2.3.4 Possible mechanism of protection: Epac stimulation and the Reperfusion Injury Salvage Kinase (RISK) pathway

In order to determine the mechanism of cardioprotection by Epac on I/R injury, the involvement of the Reperfusion injury salvage kinase (RISK) pathway was investigated by post-treatment of CPT (2 μM) with a MEK-ERK inhibitor (PD98059, 10 μM), or a selective PKB inhibitor (A6730, 2.5 μM) respectively (Figure 2.19).

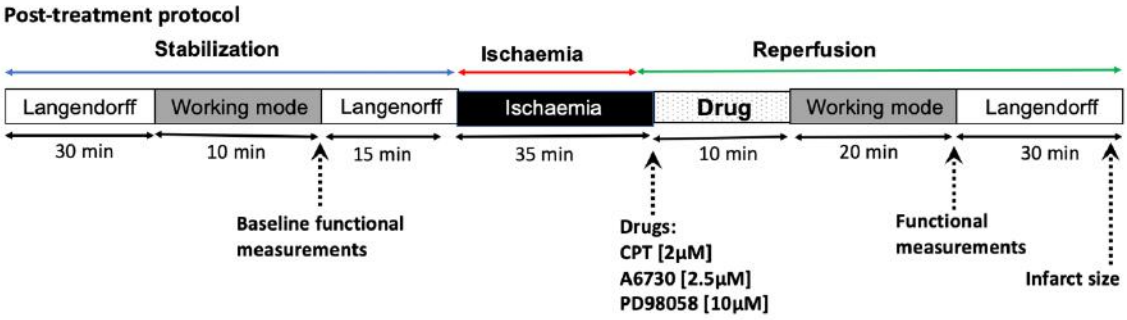

Figure 2. 19 Post-treatment protocol

2.3.4 (a) Cardiac Function before and after ischaemia

Comparable baseline cardiac function was observed as there were no significant differences among the groups before ischaemia (Table 2.4). There were also no differences in post-ischaemic function in terms of CF, PSP, HR among the post-treatment groups after 35 minutes of regional ischaemia and 30 minutes reperfusion (Table 2.4). Post-treatment with CPT had no significant effect on the post-ischaemic function of AF, CO and TW compared to DMSO-vehicle control. PKB inhibition with A6730 reduced the post-ischaemic function of AF ($P<0.01$ vs. DMSO; $P<0.01$ vs. CPT), CO ($P<0.001$ vs. DMSO; $P<0.0001$ vs. CPT) and TW ($P<0.01$ vs. DMSO; $P<0.0001$ vs. CPT) compared to CPT and DMSO treated hearts (Table 2.4). Furthermore, co-treatment of CPT and A6730 did not reverse the detrimental effects of A6730 on the recovery of AF, CO and TW. Furthermore, ERK1/2 inhibition with PD98058 significantly reduced the recovery CO compared to CPT ($P<0.05$ vs. CPT) (Table 2.4). The co-treatment of CPT with PD98058 did not reverse the effect of PD98058 on the recovery of CO ($P<0.05$ vs. CPT) (Table 2.4).

Table 2. 4 Cardiac function of the different post-treated groups before and after 35 min regional ischaemia and 30 min reperfusion.

	DMSO 0.01% (n = 8)	CPT (n = 7)	A6730 (n = 8)	A6730+CPT (n = 4)	PD98058 (n = 8)	PD98058+CPT (n = 6)
Cardiac function before ischaemia						
CF (ml/min)	13.4 ± 0.8	12.5 ± 0.8	12.6 ± 0.5	12.9 ± 0.9	13.4 ± 0.6	12.9 ± 0.1
AF (ml/min)	38.5 ± 1.1	39.6 ± 1.1	40.4 ± 1.2	38.3 ± 0.8	38.8 ± 1.5	40.1 ± 1.2
CO (ml/min)	51.7 ± 1.2	52.1 ± 1.6	52.9 ± 1.9	51.2 ± 1.7	52.2 ± 1.9	53.1 ± 1.3
PSP (mmHg)	80.5 ± 1.4	82.9 ± 1.2	83.4 ± 1.8	81.0 ± 1.3	83.9 ± 1.9	82.8 ± 1.8
HR (bpm)	313 ±1 5.8	310 ± 6.1	321 ± 15.9	320 ± 8.4	319 ± 11.4	325 ± 11.9
TW (mWatts)	9.3 ± 0.3	9.6 ± 0.3	9.8 ± 0.4	9.1 ± 0.4	9.7 ± 0.4	9.7 ± 0.3
Cardiac function after ischaemia						
CF (ml/min)	12.5 ± 0.7	14.9 ± 0.7	11.1 ± 1.3	12.7 ± 1.4	11.3 ± 0.7	11.8 ± 0.9
AF (ml/min)	13.1 ± 2.3	15.1 ± 3.6	1.8 ± 1.4*†	0.9 ± 0.9*†	6.1 ± 2.5	8.3 ± 2.1
CO (ml/min)	26.9 ± 2.4	30.1 ± 3.8	12.9 ± 2.1*†	13.6 ± 2.0*†	17.6 ± 2.8†	17.38 ± 2.4†
PSP (mmHg)	72.3 ± 1.5	72.3 ± 1.2	61.3 ± 7.8	64.9 ± 2.3	72.1 ± 2.5	72.5 ± 1.4
HR (bpm)	366 ± 16.2	341 ± 12.8	302 ± 57.9	313 ± 18.9	340 ± 17.9	353 ± 14.1
TW (mWatts)	4.1 ± 0.5	5.2 ± 0.7	1.1 ± 0.4*†	0.7 ± 0.5*†	2.4 ± 0.7	2.9 ± 0.5

All values are expressed as mean ± SEM. Comparisons of groups were tested by ANOVA. n = 4-9 per group. *$p < 0.05$ vs DMSO, †$p < 0.05$ CPT.

2.3.4 (b) Recovery of cardiac function

There were no differences in the percentage recovery of CO and TW between the CPT treated hearts and DMSO control hearts (Figure 2.20A and B). PKB inhibition significantly reduced the percentage recovery of CO and TW compared to DMSO vehicle control (CO: A6730: 25.7. ± 4.9 % vs. DMSO: 52.96 ± 4.7 % P<0.01) and (TW: A6730: 9.9 ± 4.1 % vs. DMSO: 44.9 ± 5.1%, P<0.01) (Figure 2.20A and B). Co-treatment of CPT with A6730 also significantly decreased the percentage recovery of CO and TW compared the CPT treated hearts (CO: A6730+CPT: 29.44 ± 4.6 % vs CPT: 55.9 ± 6.7 %, P<0.05) and (TW: A6730+CPT: 6.89 ± 4.8 % vs. CPT: 42.2 ± 9.84 %, P<0.01) (Figure 2.20A). ERK1/2 inhibition with PD98058 had no significant effect on both CO and TW percentage recovery (Figure 2.20B and C).

9.9 ± 4.1

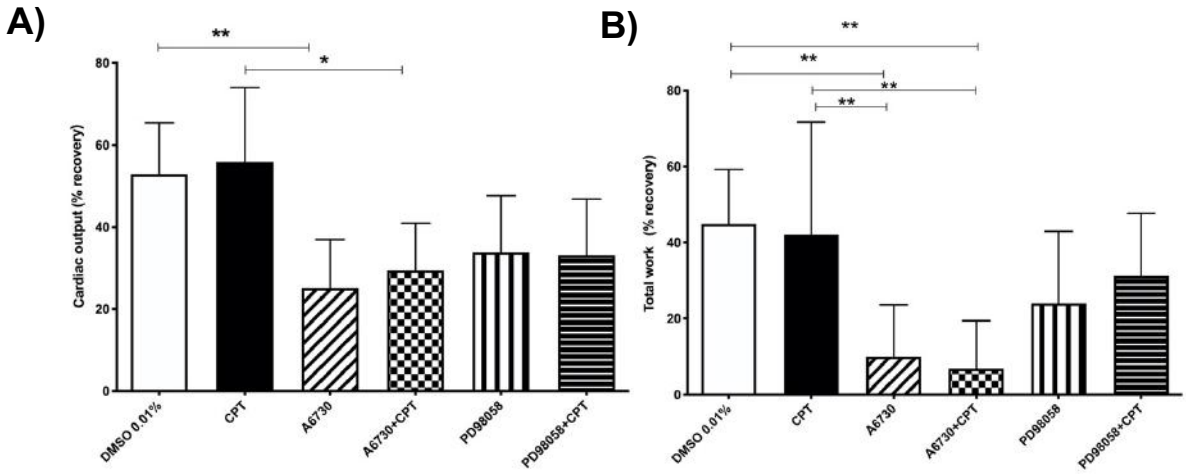

Figure 2. 20 Cardiac output and Total work of hearts after 35 min regional ischaemia and 30 min reperfusion, post-treated with an Epac activator [CPT 2 µM], PKB inhibitor [A6730 2,5 µM] and MEK-ERK inhibitor [PD98058 10 µM] in the first 10 minutes reperfusion.

(A), Cardiac output, percentage recovery; (B), Total work, percentage recovery. All values are mean ± SEM. n= 4-9 per group. *P<0.05, **P<0.01.

2.3.4 (c) Infarct size

Epac activation with CPT post-ischaemia significantly reduced infarct size compared to vehicle controls (CPT: 11.2 ± 1.6% vs. DMSO: 24.8 ± 1.1%, P<0.0001) (Figure 2.21A). A significant increase in infarct size was noted in hearts treated with A6730 compared to DMSO-controls (A6730: 31.4 ± 1.4% vs. DMSO: 24.8 ± 1.1%, P<0.05) (Figure 2.21A). However, the co-treatment of CPT with PKB inhibitor, A6730 reversed the effects of both CPT and A6730, resulting in no significant difference when compared to the DMSO-controls. Co-treatment of CPT with ERK1/2 inhibitor PD098058 significantly increased the infarct size when compared to hearts treated with CPT alone (PD98058+CPT: 28.1 ± 4.8% vs. CPT: 11.2 ± 1.6%, P<0.05) (Figure 2.21A). There were no differences in the total area at risk (Figure 2.21B).

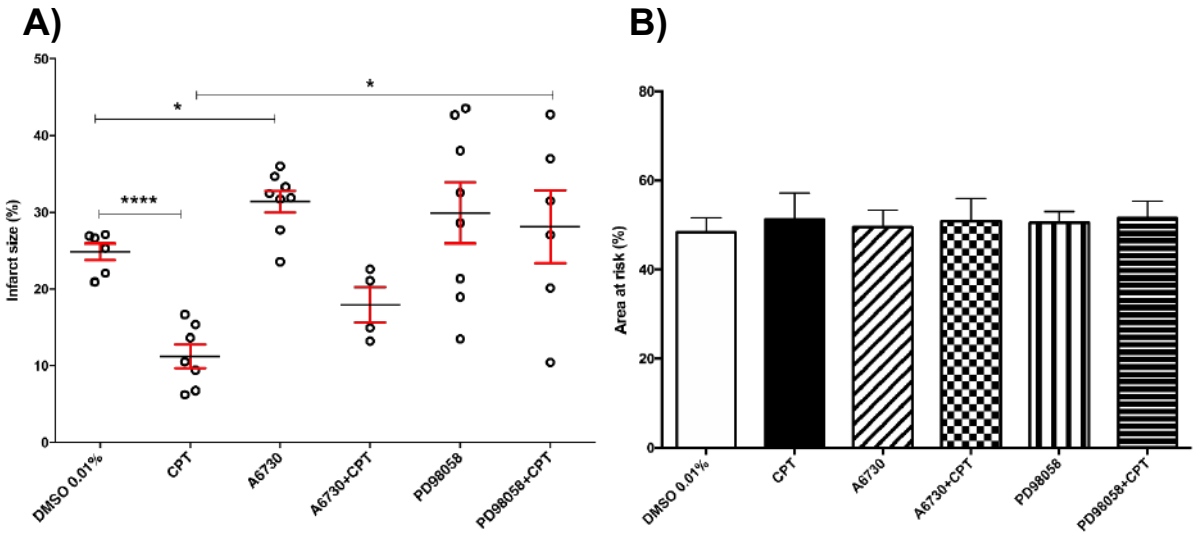

Figure 2. 21 Infarct size and Area at risk of hearts after 35 min regional ischaemia and 60 min reperfusion, post-treated with an Epac activator [CPT 2 μM], PKB inhibitor [A6730 2,5 μM] and MEK-ERK inhibitor [PD98058 10 μM] in the first 10 minutes reperfusion.

(A), Infarct size, percentage of area at risk; (B), Area at risk, percentage of the left ventricle. All values are expressed as mean ± SEM. n = 6-8 per group. *P<0.05, ****P<0.0001.

2.4 Discussion

The availability of a selective Epac agonist (CPT) and antagonist (ESI-09) made it possible to evaluate the involvement of Epac in the setting of beta-adrenergic induced cardioprotection. Therefore, in this preliminary study, we evaluated the specific role of Epac on myocardial I/R injury in a normal body weight rat model. Our results indicated that Epac stimulation pre- or post-ischaemia improved myocardial damage (Infarct size). In addition, treatment, but not post-treatment, with CPT also improved functional recovery. Furthermore, pharmacological inhibition of the RISK pathway suggested partial involvement of ERK1/2 and PKB in CPT-induced cardioprotection (Infarct size).

2.4.1 Effect of selective drug treatment on cardiac function of healthy rat hearts

In the current study, Rap1 activation was significantly higher in hearts pre-treated with CPT [2 μM] compared to untreated hearts (Figure 2.8). Co-treatment with an Epac inhibitor ESI-09 [20 μM] significantly reduced Rap1 activation compared to CPT. We also found that ESI-09 had detrimental effects on cardiac function (Figure 2.7), but peak systolic pressure was not affected (Figure 2.6). Even though ESI-09 is a specific inhibitor for Epac 1 and 2 (Chen *et al*., 2013; Zhu *et al*., 2015), it was previously reported to have general protein denaturing properties, suggesting that ESI-09 “inhibitory” properties might originate from its protein destabilizing effect (Rehmann, 2013). This raised a concern that ESI-09 may not act exclusively on Epac (Rehmann, 2013). However, other studies have demonstrated that ESI-09 inhibits Epac functions *in vitro* (Almahariq *et al*., 2012) and *in vivo* (Gong *et al*., 2013). Zhu and co-workers (2017) have also demonstrated that ESI-09 acts as a competitive inhibitor for Epac at a concentration below 20 μM, but that non-specific binding or protein denaturing are a concern at higher concentrations (Zhu *et al.*, 2015). In the present study, we decided to use the lower concentration of ESI-09 [5 μM] even though the CPT-induced Rap1 activation was significantly reduced with ESI-09 co-treatment at a concentration of 20 μM (Figure 2.8). This was mainly due to the detrimental effects of ESI-09 [20 μM] on cardiac function (Figure 2.6 and 2.7). This further also proves the importance of Epac in normal cardiac function. In support of our decision on the ESI-09 concentration of 5

μM other studies have used concentrations of ESI-09 as low as 1 μM (Khaliulin *et al*., 2017).

2.4.2 The contribution of Epac activation in beta-adrenergic induced cardioprotection against I/R: Pre-treatment study

We investigated the effects of pre-treatment with isoproterenol (ISO 0.1 μM) (a beta-agonist) in comparison to CPT 2 μM (Epac agonist) on cardiac function and infarct size in hearts subjected to I/R injury. After I/R, it was evident that pre-treatment with ISO protected the hearts against I/R injury. ISO significantly reduced myocardial damage (infarct size) (Figure 2.11) and improved the percentage recovery of cardiac output and total work performance (Figure 2.10). These results confirmed the initial studies (Lochner *et al*., 1999), which demonstrated that pharmacological preconditioning with ISO/Forskolin protected hearts from I/R injury through cAMP elevation (Lochner *et al*., 1999; Marais *et al*., 2001). The latter and resultant PKA activation during preconditioning was considered a prerequisite for cardioprotection (Lochner *et al*., 1999). However, reducing PKA activity in Forskolin-preconditioned hearts with H89 (non-specific PKA inhibitor) did not abolish cardioprotection but rather promoted it (Makaula *et al*., 2005). Thus, suggesting the involvement of an alternative, PKA-independent, pathway in cAMP-induced cardioprotection. It was discovered that cAMP downstream effects were not only via PKA but Epac proteins as well (Bos, 2006; De Rooij *et al*., 1998; Kawasaki *et al.*, 1998). In addition, we have shown that direct activation of Epac proteins before I/R is cardioprotective.

Pre-treatment with CPT (2 μM) (Epac agonist) improved the percentage cardiac output recovery (Figure 2.10). Furthermore, in similar studies performed previously, Epac activation with CPT (10 μM) increased cardiac pump function (Khaliulin *et al.*, 2017; Surinkaew *et al*., 2019), however, preconditioning with CPT (1 μM) had no effect on cardiac function after I/R injury (Duquesnes *et al.*, 2010). CPT has been reported to exert positive inotropic effects (increase contractility) and positive lusitropy (increased relaxation rate) (Ruiz-Hurtado *et al*., 2012). Positive inotropic agents are associated with increased cardiac output (Amin and Maleki, 2012). However, sustained activation

of Epac proteins with CPT may exert negative effects such as proarrhythmic effects and cardiac hypertrophy (Brette *et al.*, 2013; Ruiz-Hurtado *et al*., 2012).

The reduced myocardial damage (infarct size) (Figure 2.11) in the current study suggested that the [2 μM] CPT protection was Epac mediated. However, in a recent study, Epac activation with CPT [10 μM] did not protect the *ex-vivo* isolated rat hearts from I/R injury but simultaneous activation of Epac and PKA protected the hearts against I/R injury (Khaliulin *et al*., 2017).

2.4.3 The role of Epac stimulation in cardioprotection against I/R injury: Post-treatment study

We investigated the effects of post-treatment with an Epac agonist (CPT) on cardiac function and infarct size in hearts subjected to I/R injury. Post-treatment with 2 μM CPT reduced myocardial infarction by approximately 48% compared to untreated hearts (Figure 2.14). Similar findings were reported in mice were Epac activation with CPT improved cardiac function, left atrial fibrosis and reduced infarct size post-myocardial infarction (Surinkaew *et al.*, 2019). However, Epac stimulation at reperfusion did not affect cardiac functional recovery compared to untreated hearts (Figure 2.13). In animal models, smaller infarct size after I/R injury is considered as the point reference or more reliable in cardioprotection and this not always associated with an improvement in cardiac functional/mechanical recovery (Cohen *et al*., 1999; Jenkins *et al*., 1995; Lochner *et al*., 2003; Salie *et al*., 2011). Clinically, infarct size is directly associated with mortality (heart failure and death) (Lønborg *et al*., 2010; McAlindon *et al*., 2015). Therefore, our findings suggest that Epac stimulation, during early reperfusion is cardioprotective.

Furthermore, activation of the RISK pathway plays a central role in cardioprotection (Baxter *et al.*, 2001; Yellon and Baxter, 1999). Epac mediated activation of the RISK pathway, selective inhibition of the RISK pathway with A6730 (PKB inhibitor) and PD98050 (MEK-ERK1/2 inhibitor) suggested the involvement of the RISK pathway based on the infarct size findings (Figure 2.21). However, in the current study, the

cardioprotective mechanism is not clear, as the western blot data indicated that CPT/Epac stimulation could not activate the ERK 1/2 or PKB (RISK pathway) (Figure 2.15, Figure 2.16). We also found that co-treatment of CPT and ESI-09 reduced the phosphorylation of both ERK1/2 and PKB compared to untreated hearts. Therefore even though CPT's effect on the RISK pathway was inconclusive, Epac inhibition with 5 μM ESI-09 negatively affected the RISK pathway. This might explain the detrimental effects of ESI-09. In addition, we also found that ESI-09 significantly increased the pro-apoptotic caspase-3 versus untreated hearts (Figure. 2.18). Caspase-3 overexpression is associated with an increase in infarct size and a reduced cardiac function (Condorelli *et al*., 2001; Mocanu *et al*., 2000; Teringova and Tousek, 2017)

Our findings further proposed that post-treatment with CPT activates Epac independent of PKA-CREB. This was confirmed by the fact that CREB phosphorylation and expression was not affected by CPT treatment (Fig. 2.17) and therefore excluding the involvement of the PKA-CREB pathway. In conclusion, both pre- and post-ischaemic acute Epac stimulation with CPT (2 μM) protected the hearts against I/R injury (Surinkaew *et al*., 2019) via Epac-PKB and ERK1/2 pathway while Epac inhibition with ESI-09 was detrimental to cardiac function.

Chapter Three

The role of Epac in myocardial I/R of *ex vivo* hearts from a rat model of high-calorie diet-induced obesity

3.1 Introduction

Obesity could increase the risk of coronary artery disease (CAD) and heart failure (Clark, 2003), and worsen outcomes from myocardial infarction (Aronson *et a*l., 2010; Clavijo *et al*., 2006). Previous studies have demonstrated that myocardial injury (infarction) at reperfusion is mediated by the opening of mitochondrial permeability transition pore (mPTP) (Hausenloy and Yellon, 2007). Inhibition of mPTP via the Reperfusion injury salvage kinase (RISK) (ERK1/2 and PKB) pathway provides cardioprotection against I/R injury by preventing ROS accumulation and Ca^{2+} overload (Hausenloy and Yellon, 2007; Xia *et al*., 2016). In our preliminary studies, we have shown that cAMP is involved in mediating cardioprotection via the cAMP-Epac-PKB pathway (see Chapter 2, section 2.1).

Knockout animal models have revealed diverse functions of Epac in different organs. In the brain, Epac1 deletion is associated with improved leptin sensitivity in mice fed high-fat diet (Yan *et al*., 2013) and Epac2 is associated with impaired leptin sensitivity (Hwang *et al*., 2017). Interestingly, Epac1 deletion is associated with the development of the metabolic syndrome followed by pancreatic β-cell dysfunction (Kai *et al*., 2013). Furthermore, studies with Rap1 knockout mice also showed metabolic syndrome characteristics and developed hepatic steatosis (Martínez *et al*., 2013). *In vitro* studies have revealed that Epac contributes to cardiac remodelling and arrhythmias (Lee *et al*., 2013; Okumura *et a*l., 2014; Pereira *et al*., 2017; Yang *et al*., 2016).

In the heart, Epac1 deletion has cardioprotective against isoproterenol- and ageing-induced cardiomyopathy (Okumura *et al*., 2014). In knockout mice fed with a high-fat diet (HFD), Epac1 deletion increased infarct size, but HFD reduced infarct size in Epac2 knockout mice (Edland *et al*., 2016). In rats fed with a normal laboratory chow, pharmacological activation of Epac1/2 with CPT had no effect on infarct size.

However, co-treatment with a PKA activator (6-Bnz) and CPT reduced the infarct size (Khaliulin *et al*., 2017). Therefore, in the current study, we aimed to investigate the role of Epac in myocardial I/R, obesity and insulin resistance. Furthermore, we aimed to elucidate the mechanisms involved in Epac-induced cardioprotection by evaluation of the following: RISK pathway, nitric oxide signalling, calcium signalling, apoptotic signalling and autophagy.

3.2 Methods

3.2.1 General materials used

Cell Signaling Technologies (Beverly, MA, USA): Antibodies

1. Total ERKp44/p42 (catalogue number: #9102)
2. Phospho-ERKp44/p42 (Thr^{202}/Tyr^{204}) (catalogue number: #9101)
3. Total PKB (catalogue number: #4691)
4. Phospho-PKB (Ser^{473}) (catalogue number: #4058)
5. Total AMPKα (catalogue number: #5832)
6. Phospho-AMPKα (Thr^{172}) (catalogue number: #2535)
7. Total CaMKII (pan) (catalogue number: #4436)
8. Phospho-CaMKII (Thr^{286}) (catalogue number: #12716)
9. Calcineurin (pan) (catalogue number: #2614)
10. cleaved-Caspase-3 (catalogue number: #9664)
11. Total eNOS (catalogue number: #9572)
12. Phospho-eNOS (Ser^{1177}) (catalogue number: #9571)
13. Total GSK3β (catalogue number: #9315)
14. Phospho- GSK3β (^{Ser9}) (catalogue number: #9336)
15. Total DRP1 (catalogue number: #8570)
16. Phospho-DRP1 (Ser^{616}) (catalogue number: #3455)
17. Total ULK1 (catalogue number: #8054)
18. Phospho-ULK1 (Ser^{555}) (catalogue number: #5869)
19. Cleaved PARP (catalogue number: #5625)

Santa Cruz Biotechnology (Dallas, TX, USA): Antibodies

1. Nitrotyrosine (catalogue number: #39B6)

3.2.2 Animal and ethical approval

The study was approved by the University of Stellenbosch animal ethics committee (SU-ACUD14-00020). Animals used were housed at the University of Stellenbosch Central Research Facility (Tygerberg Campus). The animals were treated in accordance with the South African National Standard (SANS) guidelines for animal care and usage. The rats had free access to food and water and house in a temperature of (22°C), the humidity of (40%) and a 12 hour light/dark cycle. Male Wistar rats weighing (180-200 g) were fed either a control diet (CD), of standard laboratory rat chow or a high-calorie diet (HC), of rat chow supplemented with sucrose and Holsum cooking fat, for 16 weeks (Table 3.1).

Table 3. 1 Macronutrient content of experimental diets

Macronutrient	(CD) Control Diet	(HC) High-calorie diet
Fat (g/100g)	4.8	11.5
Cholesterol (mg/100g)	3.0	13
Sugar (g/100g)	6.6	24.4
Carbohydrate (%)	34.6	42
Protein (%)	17	8.3
Total kj/100g	1272	1354

3.2.3 Rat Heart Perfusion Technique

The isolated working heart model was used, using the well-characterized perfusion technique as described previously (Lochner *et al*., 1999; Salie *et al.*, 2019). The detailed description of the heart perfusion protocol is in **Chapter 2, Section 2.2.3.**

3.2.4 Experimental protocol

Hearts were stabilized for 55 minutes followed by 35 minutes of regional ischaemia (see section 2.2.4) and 60 minutes reperfusion. Drug administration was through an aortic cannula and perfused retrogradely in the first 10 minutes of reperfusion (post-treatment). The hearts were perfused with an Epac selective-agonist, 8-pCPT-2'-O-Me-cAMP (CPT, 2 μM) or novel Epac inhibitor, ESI-09 (5 μM) (Figure 3.1). In order to

investigate the mechanism of Epac-induced cardioprotection on ischaemia-reperfusion injury, the involvement of RISK pathway was investigated by co-treatment of CPT (2 μM) with a MEK-ERK inhibitor (PD98059, 10 μM), and a selective PKB inhibitor (A6730, 2,5 μM) respectively (Figure 3.1).

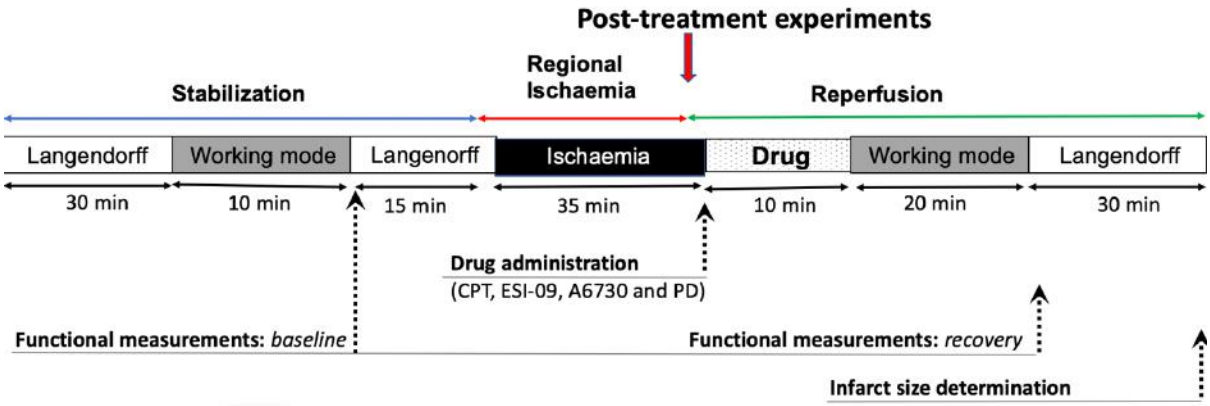

Figure 3. 1 Heart perfusion protocol for cardiac function and infarct size determination.

DMSO 0.01%: vehicle control, **CPT:** Epac agonist (2 μM), **ESI-09:** Epac antagonist (5 μM), **A6730:** selective PKB inhibitor (2,5 μM) and **PD98059**: MEK-ERK inhibitor (10 μM).

3.2.5 Assessment of cardiac function

Cardiac function was assessed and described in Chapter 2, section 2.2.6. Briefly, baseline measurements were taken 10 minutes into working mode during stabilization (Figure 3.1) and that included coronary flow (CF) (ml/min), aortic output (AO) (ml/min), cardiac output (CO) (ml/min), heart rate (HR) (bpm), peak systolic pressure (PSP) (mmHg) and total work performance (TW) (mWatts). Post-regional ischaemia cardiac function measurements were taken 20 minutes into working mode during reperfusion. Functional recovery was assessed as post-ischaemic CO and TW expressed as a percentage of pre-ischaemic values.

3.2.6 Assessment of infarct size

After an hour of reperfusion, the coronary artery was re-occluded permanently, and ~1ml of a 0.25% Evans blue solution was infused via the aorta to outline viable tissues (see Chapter 2, Section 2.2.7 for detailed description). Briefly, the heart was sectioned and stained with 1% w/v triphenyl tetrazolium chloride in phosphate buffer (pH 7.4) and then fixed in 10% v/v formaldehyde solution. The volume of infarcted tissue (I) and the area at risk (R) were determined using computerised planimetry (UTHSCSA Image Tool, University of Texas Health Science Centre at San Antonio, Texas). The infarct size was expressed as a percentage of the area at risk (I/R %) as described by Lochner *et al* (2003).

3.2.7 Western blot measurements

After 10 minutes of reperfusion (Figure 3.2) the left ventricle was removed and snap-frozen in liquid nitrogen and stored at -80°C for Western blot analysis as previously described in Chapter 2, section 2.2.8, to assess the degree of phosphorylation and total expression of pro-survival kinases: Total ERKp44/p42 (1:1000), phospho-ERKp44/p42 (Thr-^{202}/Tyr-^{204}) (1:1000), total PKB (1:1000), and phospho-PKB (Ser^{473}) (1:1000); metabolic signalling: total AMPKα (1:1000) and phospho-AMPKα (Thr^{172}) (1:1000); calcium signalling: total CaMKIIβ (1:1000), phospho-CaMKII (Thr^{286}) (1:1000) and Pan-Calcineurin (1:1000); oxidative stress: Nitrotyrosine (1:1000); apoptotic signalling: cleaved-PARP(1:1000) and cleaved-Caspase-3 (1:1000); nitric oxide signalling: total eNOS (1:1000 with SignalBoost™ immunoreaction Enhancer Kit) and phospho-eNOS (Ser^{1177}) (1:1000 with SignalBoost™ immunoreaction Enhancer Kit); glycogen synthase kinase-3 (GSK3) signalling: total GSK3β (1:1000) and phospho- GSK3β (Ser^{9}) (1:1000); autophagy: total (Dynamin-related protein 1) DRP1 (1:1000) and phospho-DRP1 (Ser^{616}) (1:1000) and total (Unc-51 like autophagy activating kinase 1) ULK1 (1:1000) and Phospho-ULK1 (Ser^{555}) (1:1000). All primary antibodies were purchased from Cell Signaling Technology, United States.

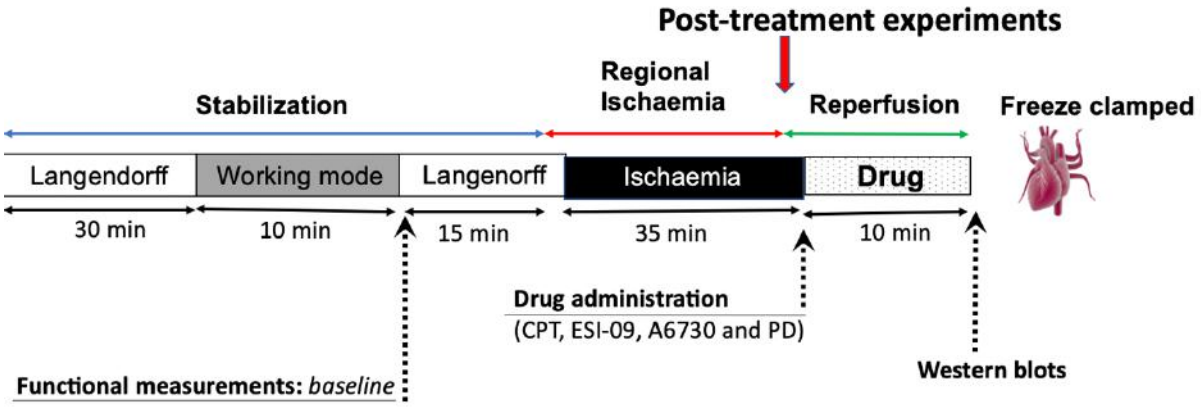

Figure 3. 2 Heart perfusion protocol for western blot determination.

DMSO 0.01%: vehicle control, **CPT:** Epac agonist (2 μM), **ESI-09:** Epac antagonist (5 μM), **A6730:** selective PKB inhibitor (2,5 μM) and **PD98059**: MEK-ERK inhibitor (10 μM).

3.2.8 Statistics

All data are expressed as mean ± standard error of the mean (SEM) and Graph Pad Prism™ 6 used for statistical analyses. Comparisons of groups were performed by ANOVA (one-way) followed by Bonferroni's post-test or student's t-tests (indicated in grey asterisk) where applicable. Significance was established at a p-value of <0.05.

3.3 Results

3.3.1 Body weight, heart weight, glucose level and HOMA-IR after 16 weeks feeding

This study was part of a much larger cohort of rats. The food consumption, water intake, oral glucose tolerance test (OGTT) and homeostatic model for insulin resistance (HOMA-IR) were assessed by Dr Sybrand Smith as part of his PhD study (2018) (see supplementary Appendix A Table A.1 and Figure A.1). In summary: after 16 weeks of feeding the HC group had elevated non-fasting blood glucose levels (HC: 7.78 ± 0.14 vs. CD: 6.88 ± 0.11, $P<0.001$, N= 63-65 per group) (Table A.1), increase in HOMA-IR index (HC: 3.5 ± 0.34 vs. CD: 2.2 ± 0.3, $P < 0.05$, N = 4) (Figure A.1C) and developed insulin resistance (according to OGTT measurements) (Figure A.1A).

In addition, the HC group had a significant increase in body weight (HC: 388.5 ± 6.99 g vs CD: 354.8 ± 6.33 g, $P<0.001$) and intraperitoneal fat percentage (HC: 6.38 ± 0.22 % vs CD: 3.87 ± 0.17 %, $P<0.0001$) (Figure 3.3A, B and C) compared to the CD group. However, there were no significant changes in heart weight or heart weight/body weight ratio or heart weight/tibia length ratio (Figure 3.3 D, E and F).

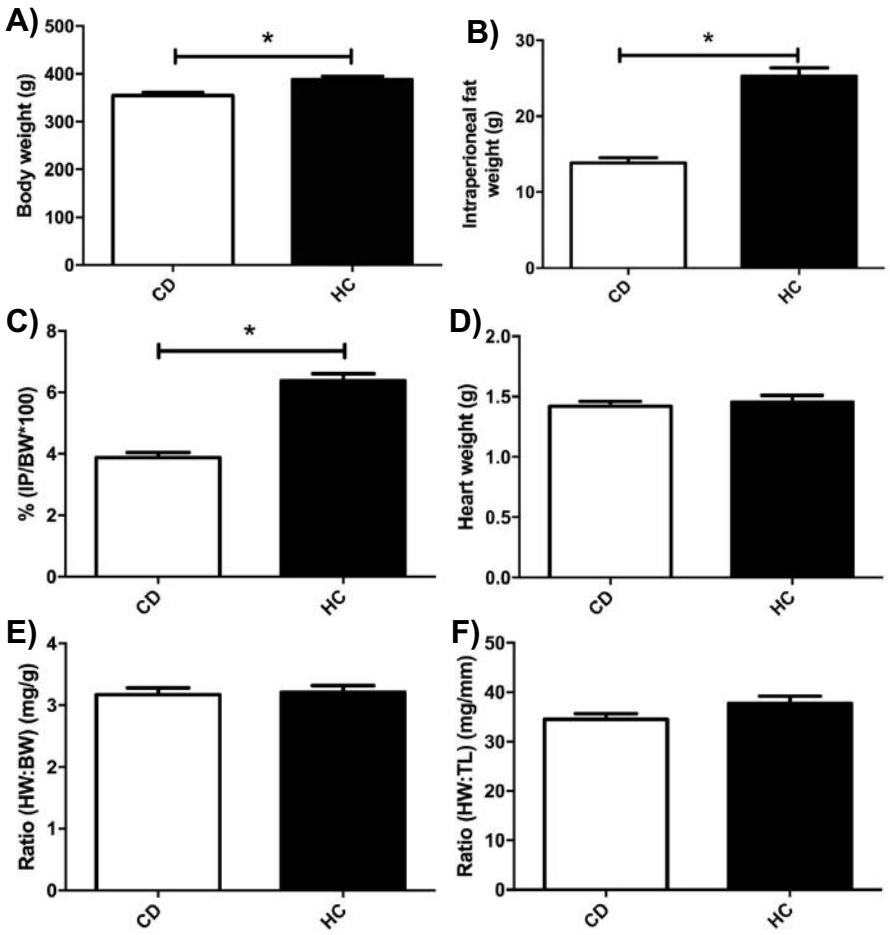

Figure 3. 3 Body weights (BW) and intraperitoneal fat (IP) percentage in control diet (CD) and high calorie diet (HC).

(A), Body weight (BW) at (16 weeks); (B), intraperitoneal fat; (C), % intraperitoneal fat/body weight; (D), Heart weight (HW); (E), Ratio (heart weight/body weight); (F), Ratio (heart weight/tibia length). All values are expressed as mean ± SEM. *$p < 0.05$. n = 34-38 per group.

3.3.2 Baseline cardiac function (pre-ischaemic)

The cardiac function was determined on the *ex vivo* working heart perfusion system. Haemodynamics such as coronary flow (CF), aortic output (AO), cardiac output (CO), heart rate (HR), peak systolic pressure (PSP) and total work performance (TW) were measured before the hearts were subjected to 35 minutes regional ischaemia (Table 3.2). There were no significant differences between the baseline, pre-ischaemic haemodynamics of the hearts from the HC and the CD groups.

3.3.3 Cardiac function of the different post-treated groups after 35 min regional ischaemia and 30 min reperfusion (post-ischaemic)

There were no significant differences post-ischaemia in CF, AO, CO, HR, PSP, and TW between hearts of vehicle-controls from the control diet (CD+DMSO 0.01%) and the high-calorie diet (HC+DMSO 0.01%) groups (Table 3.3).

Cardiac function: CD hearts with treatment

Hearts treated with CPT during reperfusion showed a significant increase in AO (ml/min: CD+CPT: 14.60 ± 2.40 vs. CD+DMSO: 4.29 ± 1.87) and CO (ml/min: CD+CPT: 28.80 ± 2.56 vs. CD+DMSO: 19.86 ± 2.58) compared to DMSO group ($P<0.05$) (Table 3.3) However, these changes did not affect the cardiac output percentage recovery (Figure 3.4A) as well as total work percentage recovery (Figure 3.5A). Also, CF, HR, PSP and TW did not differ among the groups.

Epac inhibition with its antagonist ESI-09 was detrimental on cardiac recovery of CF, AO, CO, HR, PSP and TW (Table 3.3) (Figure 3.4, 3.5). Furthermore, co-treatment of CPT with its antagonist ESI-09 did not reverse the detrimental effects of Epac inhibition on cardiac function.

In addition, we investigated the effect of co-treatment of hearts with CPT and the PKB (A6730) inhibitor or MEK-ERK (PD98059) inhibitor on cardiac function. The hearts treated with A6730 had a poor recovery of CF, AO, CO and PSP only when compared to the DMSO group ($P<0.05$) (Table 3.3). Co-treatment of CPT with A6730 did not prevent the damaging effects of the PKB inhibitor on cardiac function (Table 3.3). The percentage recovery of CO was significantly lower in the A6730 (24.64 ± 3.17 %) and the A6730+CPT (21.16 ± 2.02 %) groups compared to both CPT (58.12 ± 4.14 %) and DMSO (41.28 ± 4.68 %) groups ($P<0.05$) (Figure 3.4A). PKB inhibition also reduced the TW percentage recovery compared to CPT: CD+A6730+CPT: 13.48 ± 3.7 % vs. CD+CPT: 49.71 ± 6.1 %, $P<0.05$) and DMSO (CD+A6730: 12.32 ± 4.6 % vs. CD+DMSO: 38.55 ± 3.91 %, $P<0.05$; CD+A6730+CPT: 13.48 ± 3.7 % vs. CD+DMSO: 38.55 ± 3.91 %, $P<0.05$) groups (Figure 3.5A).

MEK-ERK inhibition with PD98059 (10μM) had no significant effect on the cardiac recovery of CF, AO, CO, HR, PSP and TW compare to the DMSO control hearts (Table 3.3). The co-treatment of PD98059 with CPT showed a significant reduction in post-ischaemic AO and CO compared to CPT treated hearts ($p<0.05$)(Table 3.3). The percentage recovery of CO (CD+PD98059+CPT: 29.95 ± 6.29 % vs. CD+CPT: 58.12 ± 4.14 %, $P<0.05$) (Figure 3.4A).

Cardiac function: HC hearts with treatment

Hearts from the HC group treated with an Epac agonist CPT showed a significant post-ischaemic improvement in TW (Table 3.3). However, the percentage TW recovery did not change compared to the DMSO group (Figure 3.5B). Furthermore, there were no changes in the recovery of CF, AO, CO, HR and PSP among the groups (Table 3.3).

The HC hearts treated with ESI-09 also did not recover after post I/R (Table 3.3). Furthermore, co-treatment of CPT with its antagonist ESI-09 did not improve the detrimental effects of Epac inhibition (Table 3.3).

The PKB inhibitor A6730 showed no significant effect on the cardiac function of the hearts from HC diet rats, however, A6730 significantly reduced PSP with or without the Epac activator, CPT (Table3.3).

ERK1/2 inhibition (PD98059) in hearts from the HC diet rats showed no significant changes in CF, AO, CO, HR, PSP and TW compare to both DMSO and the Epac activator CPT (Table 3.3).

Table 3. 2 Baseline cardiac function (before ischaemia or drug treatment)

	Treatment groups	CF ml/min	AO ml/min	CO ml/min	HR bpm	PSP mmHg	TW mWatts
Control diet	**CD+DMSO**	13.40 ± 0.58	34.71 ± 1.79	48.10 ± 2.01	282.9 ± 11.82	87.53 ± 1.10	9.49 ± 0.31
	CD+CPT	15.25 ± 0.67	34.25 ± 2.49	49.50 ± 2.605	278.4 ± 7.34	88.65 ± 1.39	10.11 ± 0.44
	CD+ESI-09	10.17 ± 1.55	29.92 ± 2.85	41.75 ± 2.91	267.2 ± 30.43	85.20 ± 1.39	8.81 ± 0.22
	CD+ESI-09+CPT	10.17 ± 2.32	31.67 ± 3.48	41.83 ± 4.08	258 ± 13.71	87.60 ± 1.75	8.71 ± 0.74
	CD+A6730	12.33 ± 1.59	33.33 ± 2.17	45.67 ± 2.94	329.8 ± 20.25	85.60 ±1.75	8.74 ± 0.70
	CD+A6730+CPT	10.36 ± 0.28	29.43 ± 2.57	39.79 ± 2.37	289.4 ± 20.69	86.57 ± 1.89	7.56 ± 0.46
	CD+PD98059	15.51 ± 4.11	32.01 ± 1.37	47.50 ± 4.29	294.8 ± 12.4	86.50 ± 1.77	9.05 ± 0.86
	CD+PD98058+CPT	11.83 ± 0.98	34.33 ± 3.40	46.17 ± 4.28	308.4 ± 9.48	88.33 ± 2.70	9.88 ± 0.79
High calorie diet	**HC+DMSO**	14.01 ± 0.76	29.78 ± 4.07	43.78 ± 4.22	316.9 ± 15.97	88.86 ± 2.01	9.39 ± 0.57
	HC+CPT	12.29 ± 0.71	38.29 ± 2.16	50.57 ± 2.53	272.1 ± 9.26	88.25 ± 0.79	9.26 ± 0.45
	HC+ESI-09	11.25 ± 1.06	28.67 ± 3.32	39.92 ± 4.28	277.7 ± 24.56	83.50 ± 1.52	7.92 ± 0.87
	HC+ESI-09 CPT	12.01 ± 0.67	29.08 ± 1.93	41.08 ± 2.35	294 ± 15.97	84.8 ± 1.319	8.39 ± 0.38
	HC+A6730	13.61 ± 1.94	30.20 ± 2.29	43.60 ± 4.17	322.8 ± 25.09	85.01 ± 2.45	9.52 ± 0.91
	HC+A6730+CPT	12.21 ± 1.20	28.80 ± 3.61	41.01 ± 4.54	307.2 ± 25.1	84.80 ± 2.84	8.49 ± 1.02
	HC+PD98059	11.91 ± 0.78	29.2 ± 1.74	41.30 ± 2.42	302.4 ± 10.99	84.25 ± 0.85	7.73 ± 0.46
	HC+PD98059+CPT	11.36 ± 1.17	32.21 ± 3.15	43.57 ± 3.96	282.8 ± 17.37	87.29 ± 2.38	8.39 ± 0.93

All values are expressed as mean ± SEM. Comparisons of groups were tested by ANOVA. n = 5-7 per group.

DMSO: 0.01%
CD: control diet
HC: high calorie diet
CPT: Epac agonist (2 μM)
ESI-09: Epac antagonist (5 μM)
A6730: selective PKB inhibitor (2,5 μM)
PD98059: MEK-ERK inhibitor (10 μM)

Table 3. 3 Cardiac function of the different post-treatment groups after 35 min regional ischaemia and 60 min reperfusion

	Treatment groups	CF mL/min	AO ml/min	CO ml/min	HR Beat/min	PSP mmHg	WT mWatts
Control diet	**CD+DMSO**	15.57 ± 1.09	4.29 ± 1.87	19.86 ± 2.58	272.8 ± 43.98	78.75 ± 1.15	2.92 ± 0.57
	CD+CPT	14.20 ± 1.02	14.60 ± 2.40*	28.80 ± 2.56*	230.8 ± 42.05	78.2 ± 1.62	3.73 ± 0.8
	CD+ESI-09	3.83 ± 1.72	0	3.83 ± 1.72	0	0	0
	CD+ESI-09+CPT	3.50 ± 2.2	0	3.50 ± 2.25	0	0	0
	CD+A6730	11.25 ± 1.25	0	11.25 ± 1.25	204.3 ± 69.02	60.25 ± 2.25*	1.02 ± 0.35
	CD+A6730+CPT	8.50 ± 0.29*†	0	8.50 ± 0.29†	218.9 ± 80.76	70 ± 4.49*†	0.84 ± 0.28†
	CD+PD98059	13.08 ± 1.88	4.08 ± 1.69	17.17 ± 3.41	349.3 ± 23.9	77.33 ± 0.95	2.91 ± 0.61
	CD+PD98058+ CPT	10.83 ± 1.38	3.01 ± 2.62†	13.83 ± 3.90†	324.8 ± 70.89	76.2 ± 0.9695	2.01 ± 0.81
High calorie diet	**HC+DMSO**	13.02 ± 1.53	5.33 ± 5.33	18.33 ± 5.04	206.5 ± 47.76	77.33 ± 0.75	1.18 ± 0.65
	HC+CPT	15.01 ± 1.05	8.57 ± 2.72	23.57 ± 3.42	267.1 ± 35.94	78.23 ± 0.98	4.13 ± 0.64‡
	HC+ESI-09	9.08 ± 0.78	0	9.08 ± 0.78	0	0	0
	HC+ESI-09 + CPT	6.25 ± 1.42	0	6.25 ± 1.42	0	0	0
	HC+A6730	12.75 ± 1.97	0	12.75 ± 1.97	257.3 ± 96.43	68.33 ± 6.12‡	1.37 ± 0.56
	HC+A6730+CPT	17.01 ± 1.53	0	17.01 ± 1.53	278.0 ± 105.6	66.67 ± 7.36‡§	1.887 ± 0.70§
	HC+PD98059	11.90 ± 0.95	6.60 ± 3.6	18.50 ± 3.92	353.6 ± 23.72	78.6 ± 1.47	3.18 ± 0.73
	HC+PD98059+CPT	13.02 ± 1.36	6.93 ± 2.48	19.93 ± 2.65	255.0 ± 69.23	77.6 ± 1.54	3.73 ± 0.62

All values are expressed as mean ± SEM. Comparisons of groups were tested by ANOVA. *p < 0.05 vs CD+DMSO, †p < 0.05 vs CD+CPT, ‡p < 0.05 vs. HC+DMSO, §p < 0.05 vs HC+CPT. n = 5-7 per group. **("zero", the hearts did not recover post I/R).**

DMSO: 0.01%
CD: control diet
HC: high calorie diet
CPT: Epac agonist (2 μM)
ESI-09: Epac antagonist (5 μM)
A6730: selective PKB inhibitor (2.5 μM)
PD98059: MEK-ERK inhibitor (10 μM)

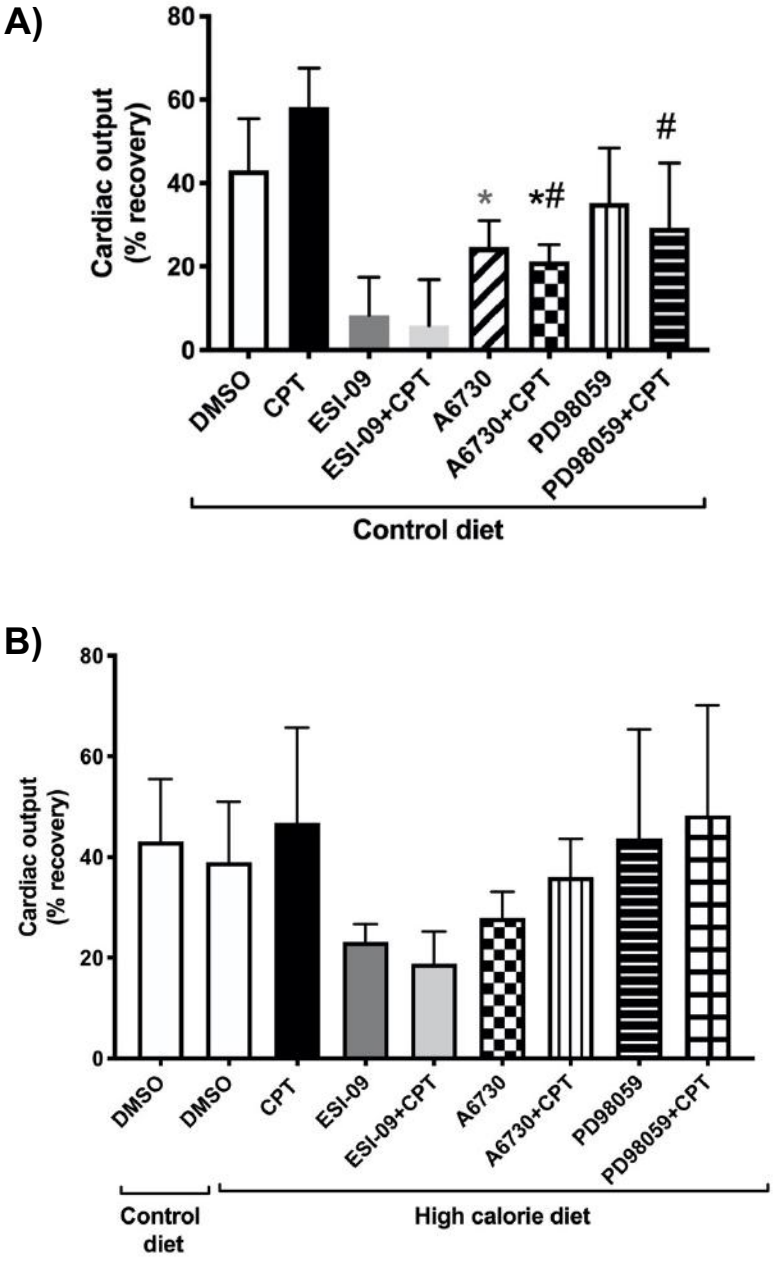

Figure 3. 4 Post-ischaemic cardiac output (% recovery) of treated groups after 35 min regional ischaemia and 60 min reperfusion.

(A), cardiac output percentage recovery in CD; (B), cardiac output percentage recovery in HC. All values are expressed as mean ± SEM. *p < 0.05 vs CD+DMSO, #p < 0.05 vs CD+CPT. n = 5-7 per group.

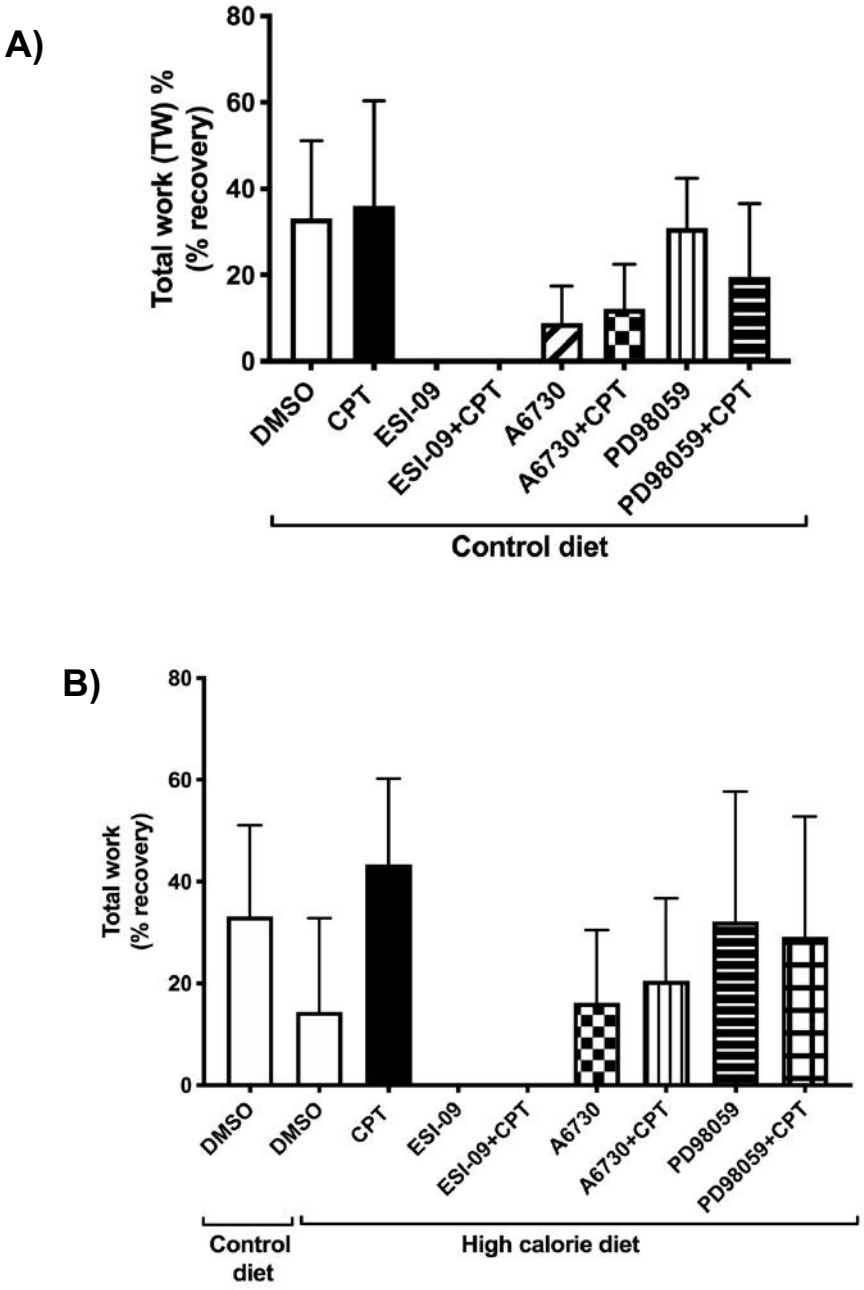

Figure 3. 5 Post-ischaemic total work (% recovery) of treated groups after 35 min regional ischaemia and 60 min reperfusion.

(A), cardiac output percentage recovery in CD; (B), cardiac output percentage recovery in HC. All values are expressed as mean ± SEM. n = 5-7 per group.

3.3.4 Infarct size in the different post-treated groups after 35 min regional ischaemia and 60 min reperfusion.

There were no significant differences in infarct size or the area at risk between CD and HC hearts (Figure 3.6A and 3.6B).

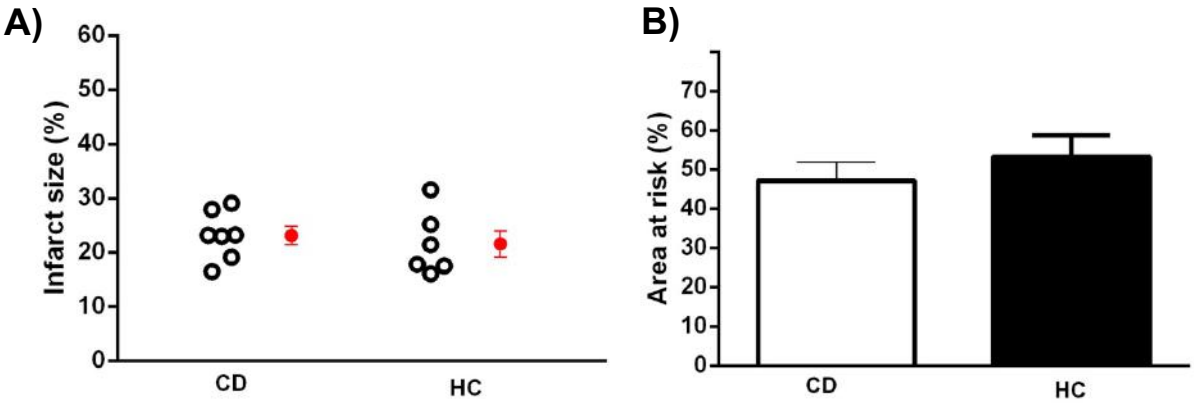

Figure 3. 6 The effect of diet on infarct size after 35 min regional ischaemia and 60 min reperfusion.

(A), Infarct size (%); (B), Area at risk (%). All values are expressed as mean ± SEM. n = 6-7 per group.

Infarct size: CD hearts with treatment

CPT post-treated hearts exhibited a significant reduction in infarct size compared to the DMSO control group (CD+CPT: 12.95 ± 2.13 % vs. CD+DMSO: 23.15 ± 1.46 %, P<0.01) (Figure 3.7A). However, Epac inhibition with ESI-09 did affect the CPT protection as would have been expected. The reason for this was that the hearts treated with ESI-09 (5 μM) for 10 minutes at reperfusion went into contracture in the first 5 minutes of treatment and followed by a loss cardiac function (Table 3.3). The fact that the hearts could not perfuse hampered the infusion of Evan's blue dye for the staining of viable tissue. This resulted in a significant increase in the total area at risk in ESI-09 treated hearts (CD+ESI-09: 59.78 ± 3.28 % vs. CD+DMSO: 47.17 ± 1.67 %, P<0.01); and ESI-09+CPT treated hearts (CD+ESI-09+CPT: 66.4 ± 2.02 % vs. CD+DMSO: 47.17 ± 1.67 %, P<0.0001); (CD+ESI-09+CPT: 66.4 ± 2.02 % vs. CD+CPT: 53.97 ± 1.61 %, P<0.01) (Figure 3.7B).

The mechanisms of protection were also investigated through the inhibition of the RISK signalling cascades in the first 10 minutes of reperfusion. Inhibition of both PKB

and ERK1/2 had a detrimental effect on the infarct size in CD hearts (CD+A6730: 43.55 ± 5.75 % vs. CD+DMSO: 24.1 ± 1.27 %, P<0.01) (Figure 3.8A); (CD+PD98058: 36.33 ± 2.946 % vs. CD+DMSO: 24.1 ± 1.27 %, P<0.05) (Figure 3.9A). In addition, CPT protection was abolished by both PKB and ERK1/2 inhibitors in CD hearts (CD+A6730+CPT: 21.81 ± 2.13 % vs. CD+CPT: 12.95 ± 2.13 %, P<0.05) (Figure 3.8A); (CD+PD98058+CPT: 26.51 ± 3.97 % vs. CD+CPT: 12.95 ± 2.13 %, P<0.01) (Figure 3.9A). In addition, the percentage of the area at risk did not differ in all treatment groups.

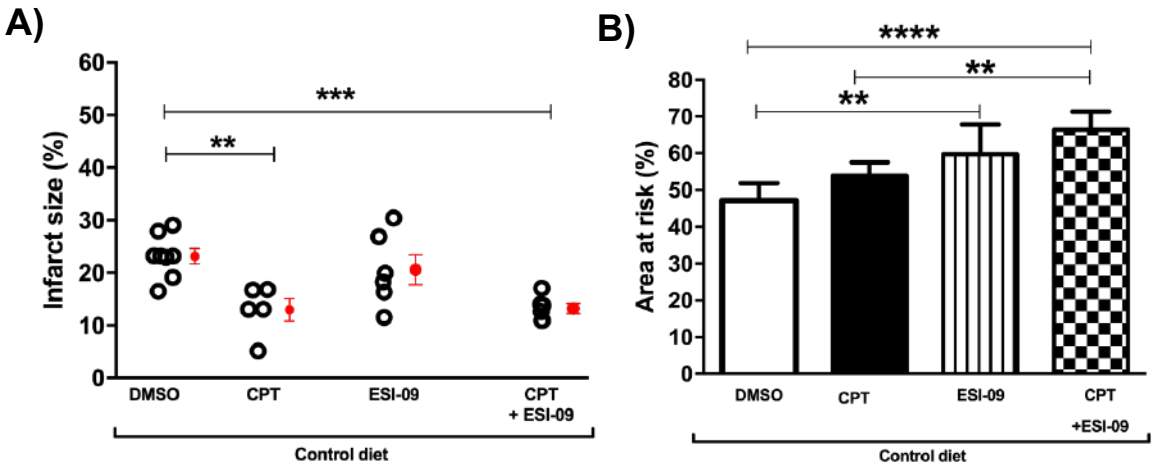

Figure 3. 7 Infarct size of hearts from Control Diet animals.

The effects of Epac agonist, CPT, and antagonist, ESI-09, administered in the first 10 minutes of reperfusion, on infarct size after 35 minutes regional ischaemia and 60 min reperfusion. (A), Infarct size (%); (B), Area at risk (%). All values are expressed as mean ± SEM. **P < 0.01, ***P < 0.001, ****P < 0.0001. n = 5 -7 per group.

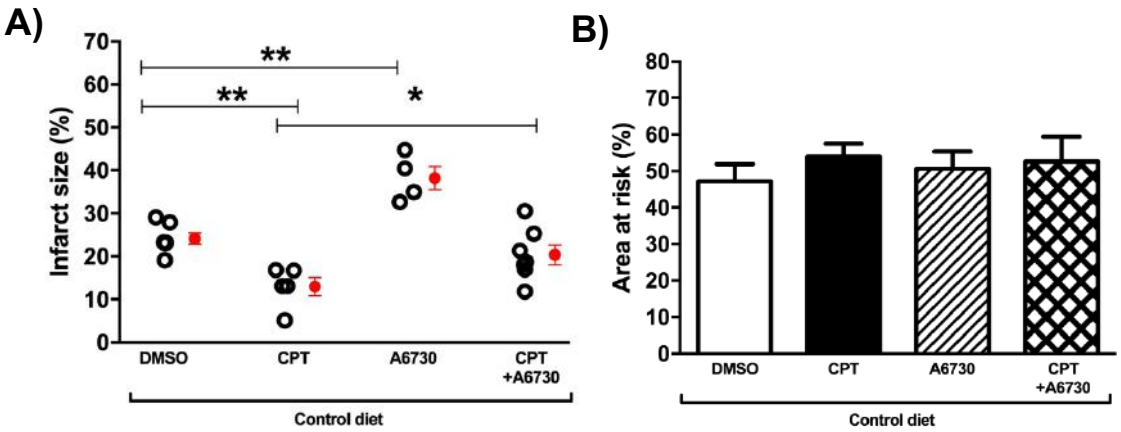

Figure 3. 8 Infarct size of hearts from Control Diet animals.

Effects of PKB (A6730) inhibition on Epac stimulation (CPT) in the first 10 min of reperfusion, on infarct size after 35 min regional ischaemia and 60 min reperfusion. (A), Infarct size (%); (B), Area at risk (%). All values are expressed as mean ± SEM. *P < 0.05, **P < 0.01. n = 4 – 6 per group.

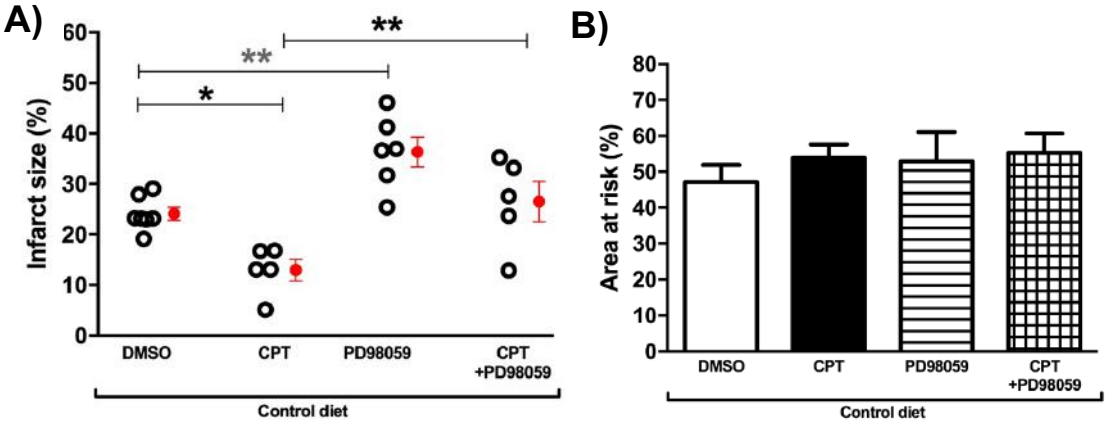

Figure 3. 9 Infarct size of hearts from Control Diet animals.

Effects of MEK-ERK (PD98059) inhibition on Epac stimulation (CPT) in the first 10 min of, on infarct size after 35 min regional ischaemia and 60 min reperfusion. (A), Infarct size (%); (B), Area at risk (%). All values are expressed as mean ± SEM. *P < 0.05, **P < 0.01. n = 5 – 7 per group.

Infarct size: hearts from HC animals with treatment

Epac activation with CPT after regional ischaemia significantly reduced infarct size in the HC group. (HC+DMSO: 25.49 ± 4.39 % vs. HC+CPT: 13.56 ± 2.21 %, P<0.05) (Figure 3.10A). Similarly to the CD group, the post treatment with Epac inhibitor ESI-09 did not affect the CPT protection. In fact, the HC hearts also showed a significant increase in area at risk (HC+ESI-09: 69.85 ± 2.91 % vs. HC+DMSO: 53.31± 2.05 %, P<0.001; HC+ESI-09+CPT: 66.31 ± 3.24 % vs. HC+DMSO: 53.31 ± 2.05 %,P<0.01; HC+ESI-09+CPT: 66.31 ± 3.24 % vs. HC+CPT: 50.59 ± 1.85 %, P< 0.01) (Figure 3.10B).

CPT protection was abolished by post-treatment with the PKB inhibitor in the HC hearts (Infarct size: HC+A6730+CPT: 26.65 ± 1.43 % vs. HC+CPT: 13.56 ± 2.21 %, P<0.01) (Figure 3.11A). There were no significant differences in the area at risk (Figure 3.11B). Furthermore, post-treatment with the ERK1/2 inhibitor (PD98058) did not affect CPT protection in HC hearts (Figure 3.12A). The % area at risk was the same among the groups (Figure 3.12B).

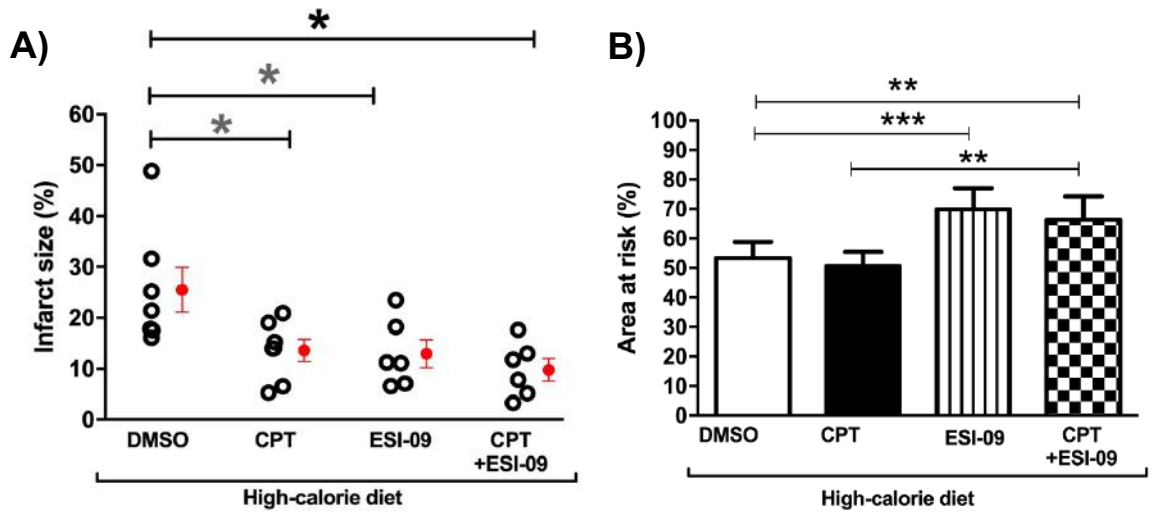

Figure 3. 10 Infarct size of hearts from High-calorie Diet animals.

The effects of Epac agonist, CPT, and antagonist, ESI-09, administered in the first 10 minutes of reperfusion, on infarct size after 35 min regional ischaemia and 60 min reperfusion. (A), Infarct size (%); (B), Area at risk (%). All values are expressed as mean ± SEM. *P < 0.05, **P < 0.01, ***P < 0.001. n = 5 -7 per group.

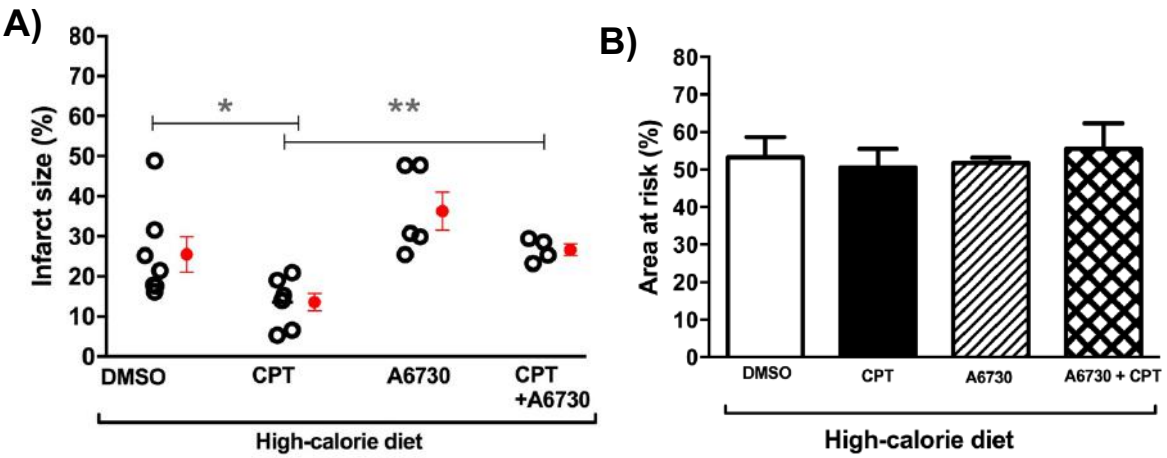

Figure 3. 11 Infarct size of hearts from High-calorie Diet animals.

Effects of PKB (A6730) inhibition on Epac stimulation (CPT) in the first 10 min of reperfusion, on infarct size after 35 min regional ischaemia and 60 min reperfusion. (A), Infarct size (%); (B), Area at risk (%). All values are expressed as mean ± SEM. *P < 0.05, **P < 0.01. n = 4 – 7per group.

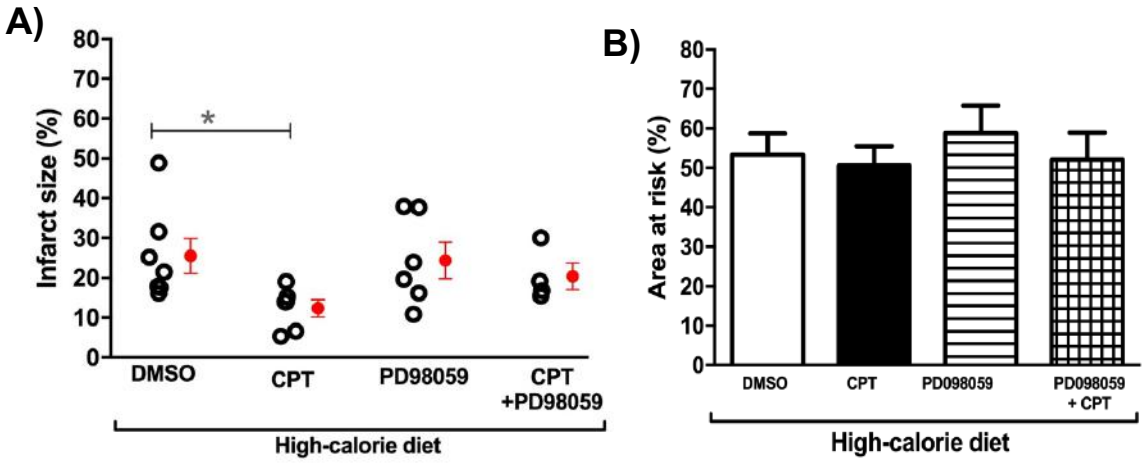

Figure 3. 12 Infarct size of hearts from High-calorie Diet animals.

Effects of MEK-ERK (PD98059) inhibition on Epac stimulation (CPT) in the first 10 min of reperfusion, on infarct size after 35 min regional ischaemia and 60 min reperfusion. (A), Infarct size (%); (B), Area at risk (%). All values are expressed as mean ± SEM. *P < 0.05. n = 5 – 6 per group.

3.3.5 Cardiac Signal Transduction after treatment with CPT (Epac agonist), ESI-09 (Epac antagonist), A6730 (PKB antagonist) and PD98058 (ERK1/2 antagonist).

Protein expression and phosphorylation in the left ventricle tissue were measured by Western blot analysis after 35 min regional ischaemia and subsequent exposure to different treatment in the first 10 minutes of reperfusion.

3.3.5.1 PKB phosphorylation and expression

In CD hearts

There were no significant differences in PKB phosphorylation between CPT treated hearts and DMSO control hearts (Figure 3.13B). PKB inhibition with A6730 significantly reduced PKB phosphorylation compared to DMSO control (CD+A6730: 0.33 ± 0.08 vs. CD+DMSO: 1 ± 0.21, $P<0.05$) (Figure 3.13B). A significant decrease in PKB phosphorylation was also observed in CPT co-treatment with A6730 compared to CPT treatment (CD+A6730+CPT: 0.46 ± 0.08 vs. CD+CPT: 1.11 ± 0.22, $P<0.05$) (Figure 3.13B). In addition, when phosphorylated PKB was expressed as a ratio of total PKB, the CPT co-treatment with PKB inhibitor A6730 remained decreased compared to CPT treated hearts (CD+A6730+CPT: 0.48 ± 0.08 vs. CD+CPT: 1.18 ± 0.23, $P<0.05$) (Figure 3.13 D). Total PKB expression showed no significant changes between different treatment groups.

In figure 3.14 Epac inhibition with ESI-09 resulted in decreased PKB phosphorylation, and phospho:total PKB ratio compared to DMSO control, even though the reduction was not significant. (CD+ESI-09: 0.1605 ± 0.05 vs. CD+DMSO: 1 ± 0.31, $P=0.052$; CD+ESI-09+CPT: 0.24 ± 0.01 vs. CD+DMSO: 1 ± 0.31, $P=0.07$) (Figure 3.14 B). This same trend was also noted in phospho:total PKB ratio (Figure 3.14 D).

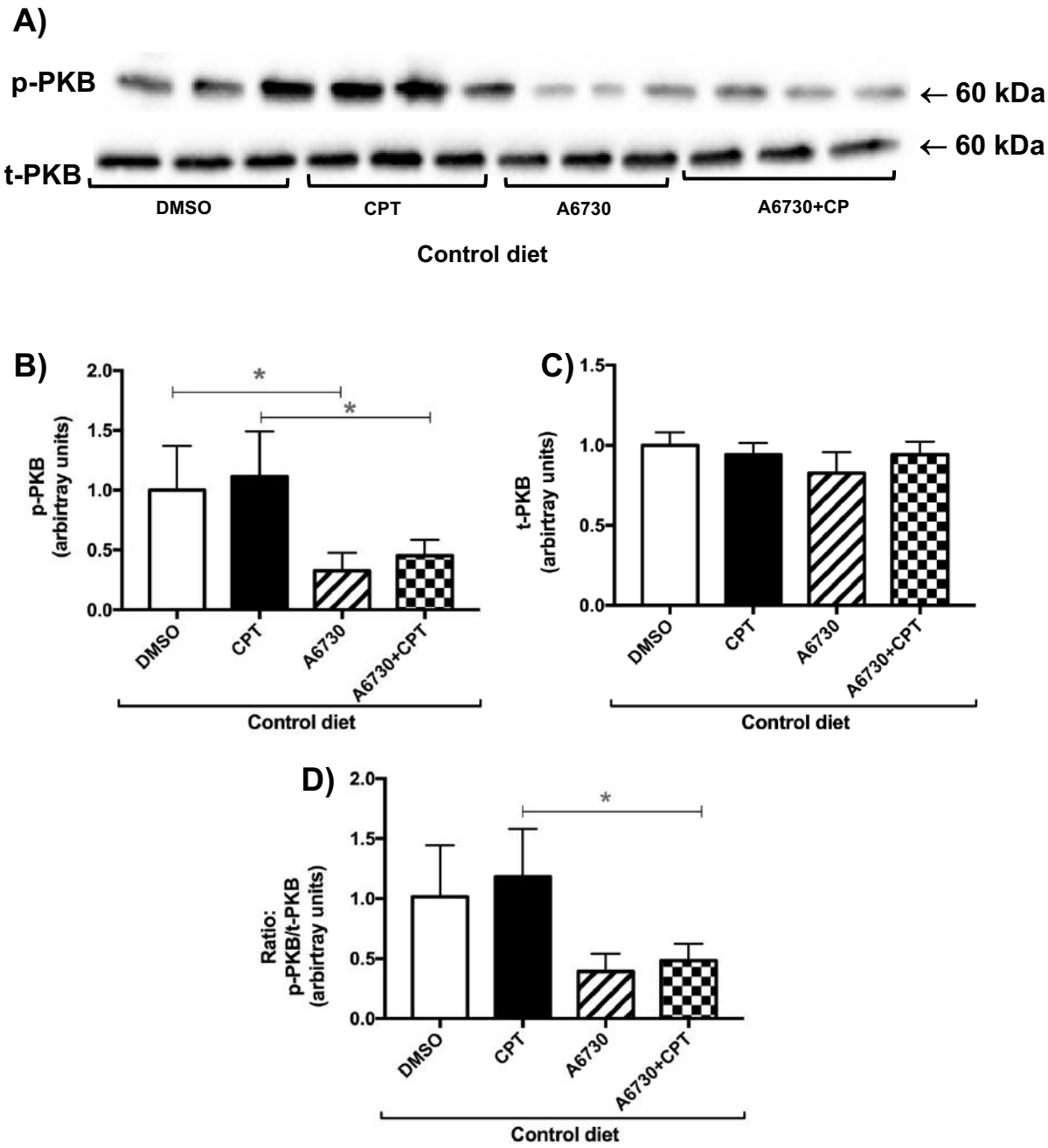

Figure 3. 13 PKB phosphorylation and expression in hearts from the CD group post-treated with an Epac activator (CPT) and PKB inhibitor (A6730) in the first 10 minutes reperfusion.

(A), representative Western blots for phosphorylated and total PKB; (B), phosphorylated PKB levels; (C), total PKB levels; (D), phospho/total ratio for PKB. n= 3 per group. All values are expressed as mean ± SEM.* P<0.05.

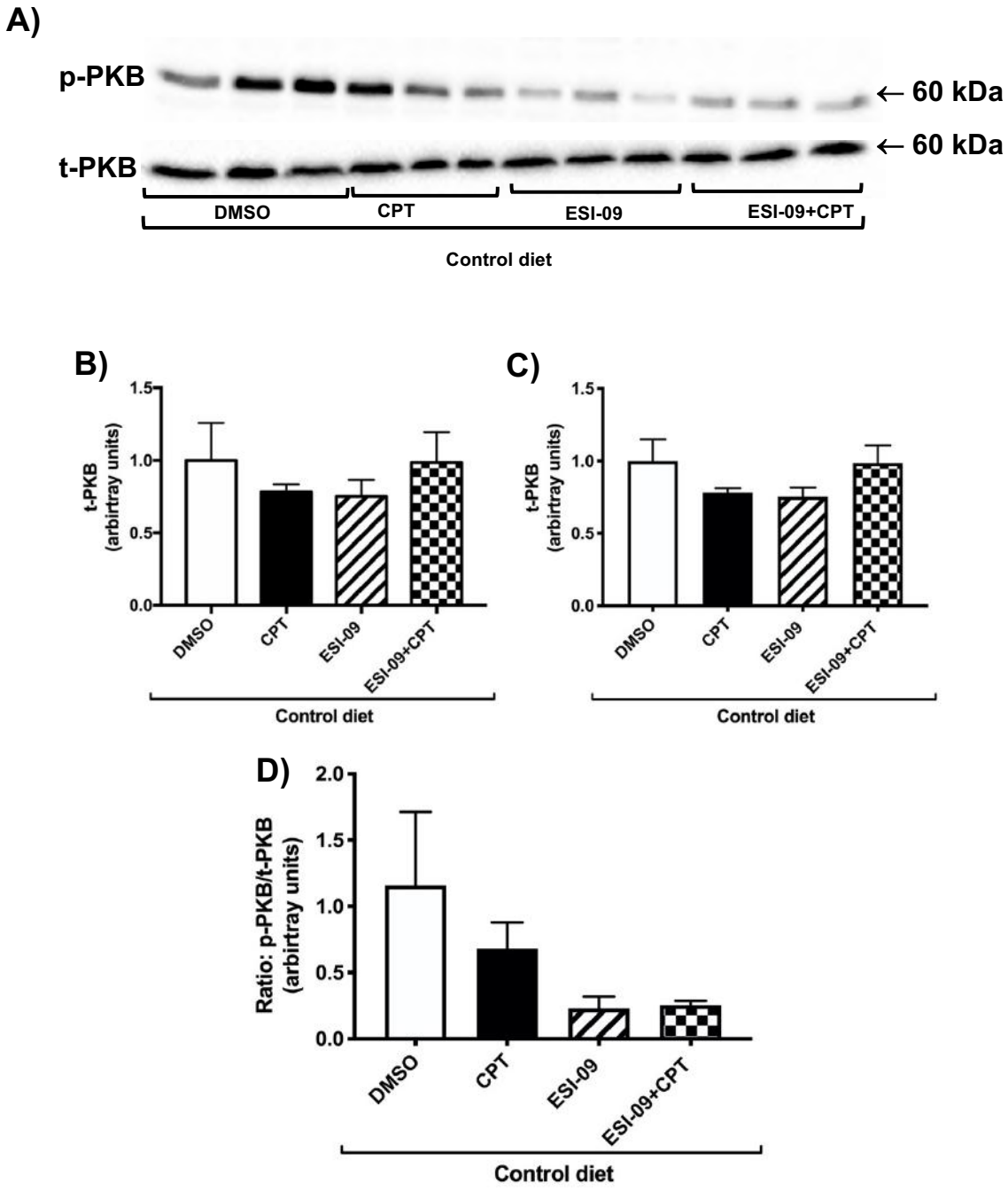

Figure 3. 14 PKB phosphorylation and expression in hearts from the CD group post-treated with an Epac activator (CPT, 2 μM) and Epac inhibitor (ESI-09, 5 μM) in the first 10 minutes reperfusion.

(A), representative Western blots for phosphorylated and total PKB; (B), phosphorylated PKB levels; (C), total PKB levels; (D), phospho/total ratio for PKB. n = 3 per group. All values are expressed as mean ± SEM.

In HC hearts

The HC hearts showed a significant increase in both phosphorylated PKB (HC+DMSO: 2.79 ± 0.12 vs. CD+DMSO: 1 ± 0.21, P<0.01) (Figure 3.15B) and phospho:total PKB ratio (Ratio: HC+DMSO: 3.69 ± 0.37 vs. CD+DMSO: 1.07 ± 0.39, P<0.05) (Figure 3.15D) compared to the hearts in CD group.

PKB phosphorylation did not differ between CPT treated hearts and DMSO controls in the HC group. PKB inhibition in hearts from HC with A6730 led to a significant reduction in phosphorylated PKB compared to DMSO control hearts (HC+A6730: 0.79 ± 0.21 vs. HC+DMSO: 2.79 ± 0.12 ,P<0.01) (Figure 3.15B). In addition, PKB phosphorylation was also significantly decreased in hearts co-treated with CPT and A6730 compared to CPT treated hearts (HC+A6730+CPT: 1.13 ± 0.55 vs. HC+CPT: 3.3 2 ± 0.64, P<0.05) (Figure 3.15B.) There were no changes observed in total PKB expression among the groups, therefore the phospho:total PKB ratio reflected the same changes as seen in PKB phosphorylation. For example, the phospho: total PKB ratio was decreased by A6730 in both CPT treated (HC+A6730+CPT: 1.27 ± 0.62 vs. HC+CPT: 4.08 ± 0.76, P<0.05) (Figure 3.15D) and DMSO control hearts (HC+A6730: 1.29 ± 0.51 vs. HC+DMSO: 3.699 ± 0.37, P<0.05) (Figure 3.15D).

Epac inhibition with ESI-09 in HC hearts had no significant effect on PKB phosphorylation, total PKB expression or the phospho: total PKB ratio (Figure 3.16).

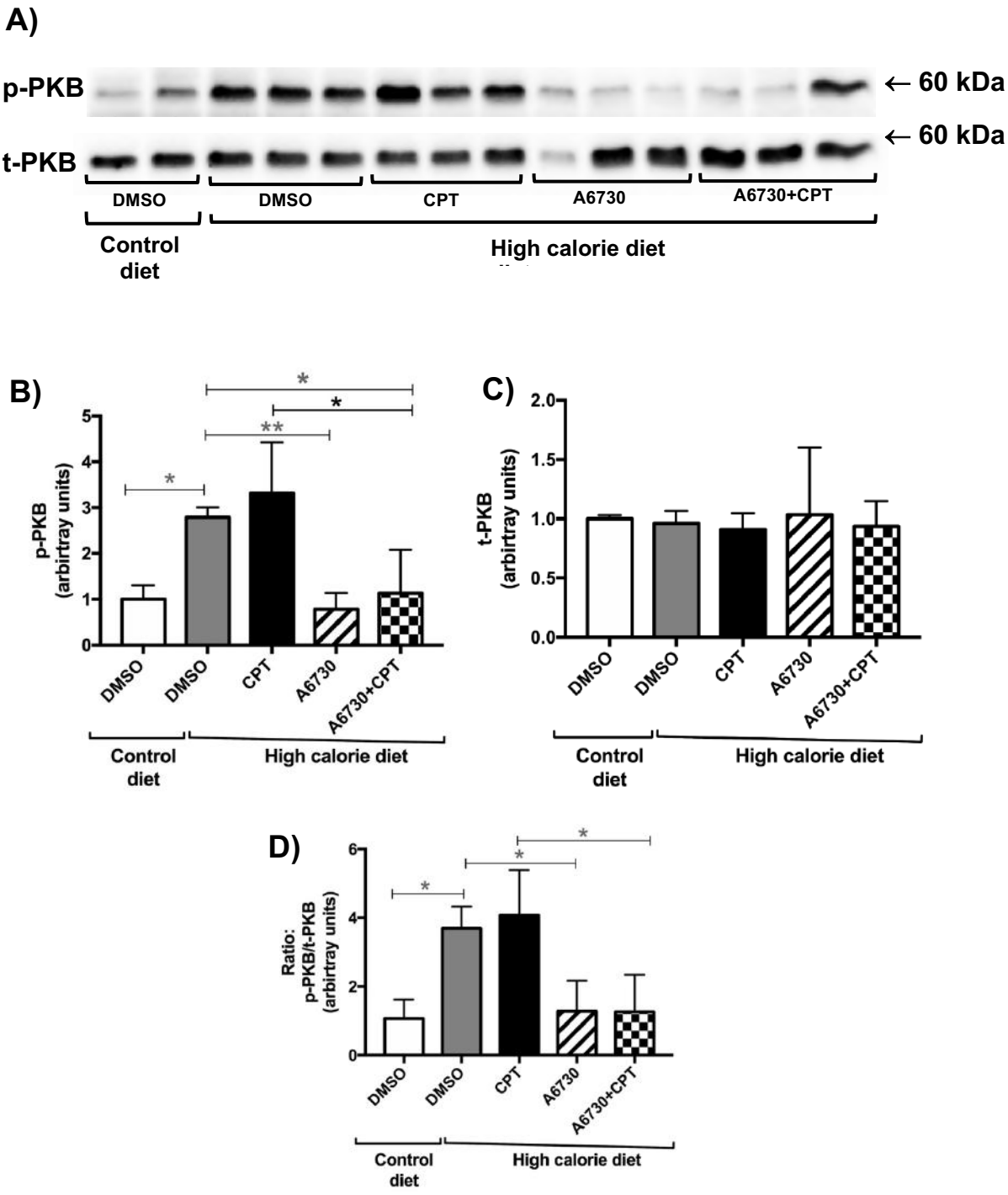

Figure 3. 15 PKB phosphorylation and expression in hearts from the HC group post-treated with an Epac activator (CPT) and PKB inhibitor (A6730) in the first 10 minutes reperfusion.

(A), representative Western blots for phosphorylated and total PKB; (B), phosphorylated PKB levels; (C), total PKB levels; (D), phospho/total ratio for PKB. n = 2-3 per group. All values are expressed as mean ± SEM.* P<0.05,** P<0.01.

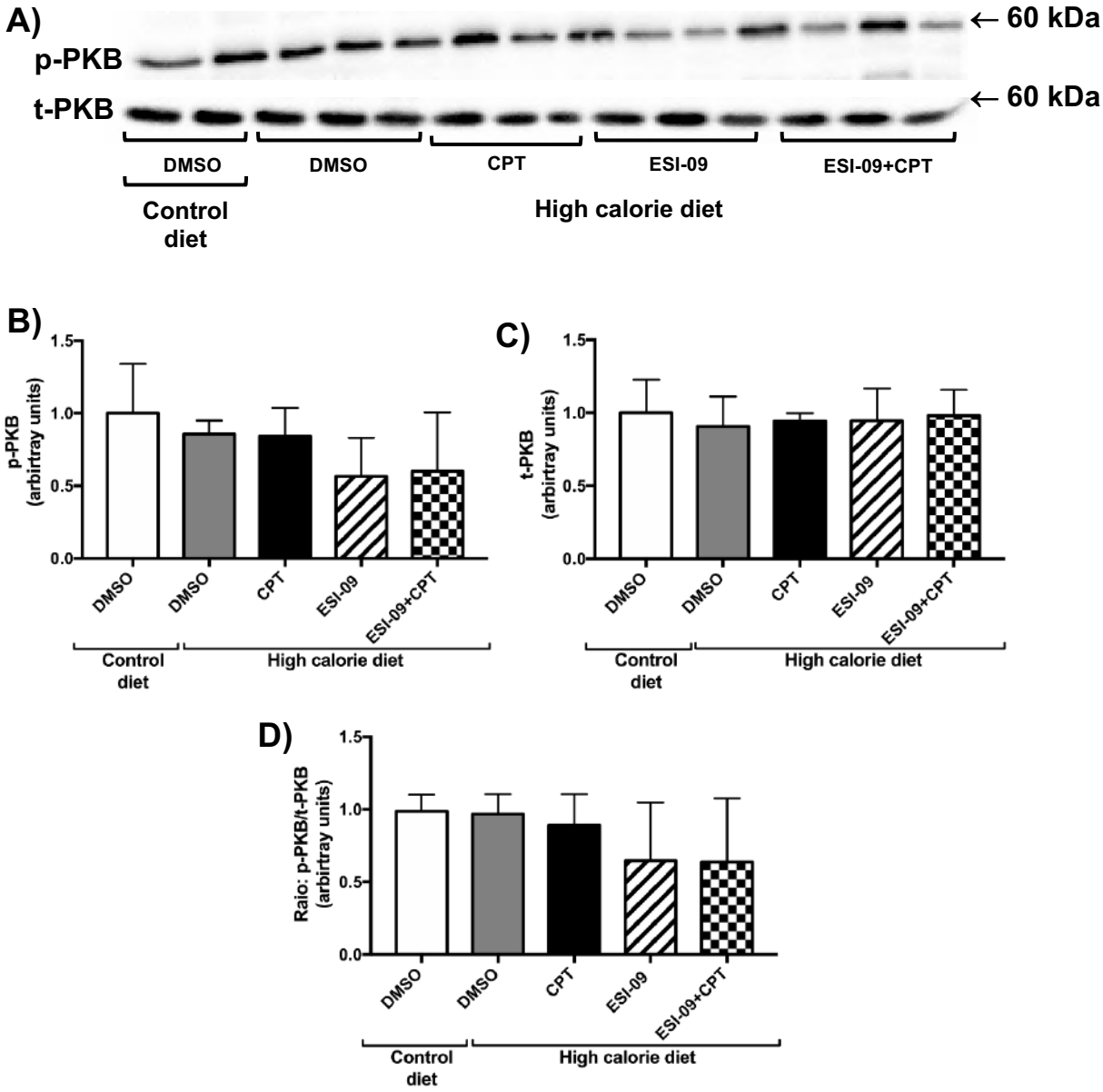

Figure 3. 16 PKB phosphorylation and expression in hearts from the HC group post-treated with an Epac activator (CPT, 2 μM) and Epac inhibitor (ESI-09, 5 μM) in the first 10 minutes reperfusion.

(A), representative Western blots for phosphorylated and total PKB; (B), phosphorylated PKB levels; (C), total PKB levels; (D), phospho/total ratio for PKB. n =2- 3 per group. All values are expressed as mean ± SEM.

3.3.5.2 ERK1/2 phosphorylation and expression

In CD hearts

In CD hearts, Epac activation with CPT decreased ERK1/2 phosphorylation compared to DMSO controls. However, this decrease was not significant in Figure 3.17, but statistically significant in Figure 3.18B (pERK1/2: CD+CPT: 0.58 ± 0.09 vs. CD+DMSO: 1 ± 0.08, $P<0.05$). MEK-ERK inhibition with PD98058 in CD hearts did not significantly affect ERK1/2 phosphorylation, ERK1/2 total expression nor phospho: total ERK1/2 ratio (Figure 3.17).

However, following Epac inhibition with ESI-09, ERK1/2 phosphorylation and phospho:total ERK1/2 ratio were significantly reduced compared to DMSO control (p-ERK1/2: CD+ESI-09: 0.3 ± 0.08 vs. CD+DMSO: 1 ± 0.08, $P<0.01$, Figure 3.18B); (p-ERK1/2:t-ERK1/2 ratio: CD+ESI-09: 0.41 ± 0.05 vs. CD+DMSO: 1.02 ± 0.16, $P<0.05$, Figure 3.18D). The total ERK1/2 expression remained the same in all treatment groups (Figure 3.18C).

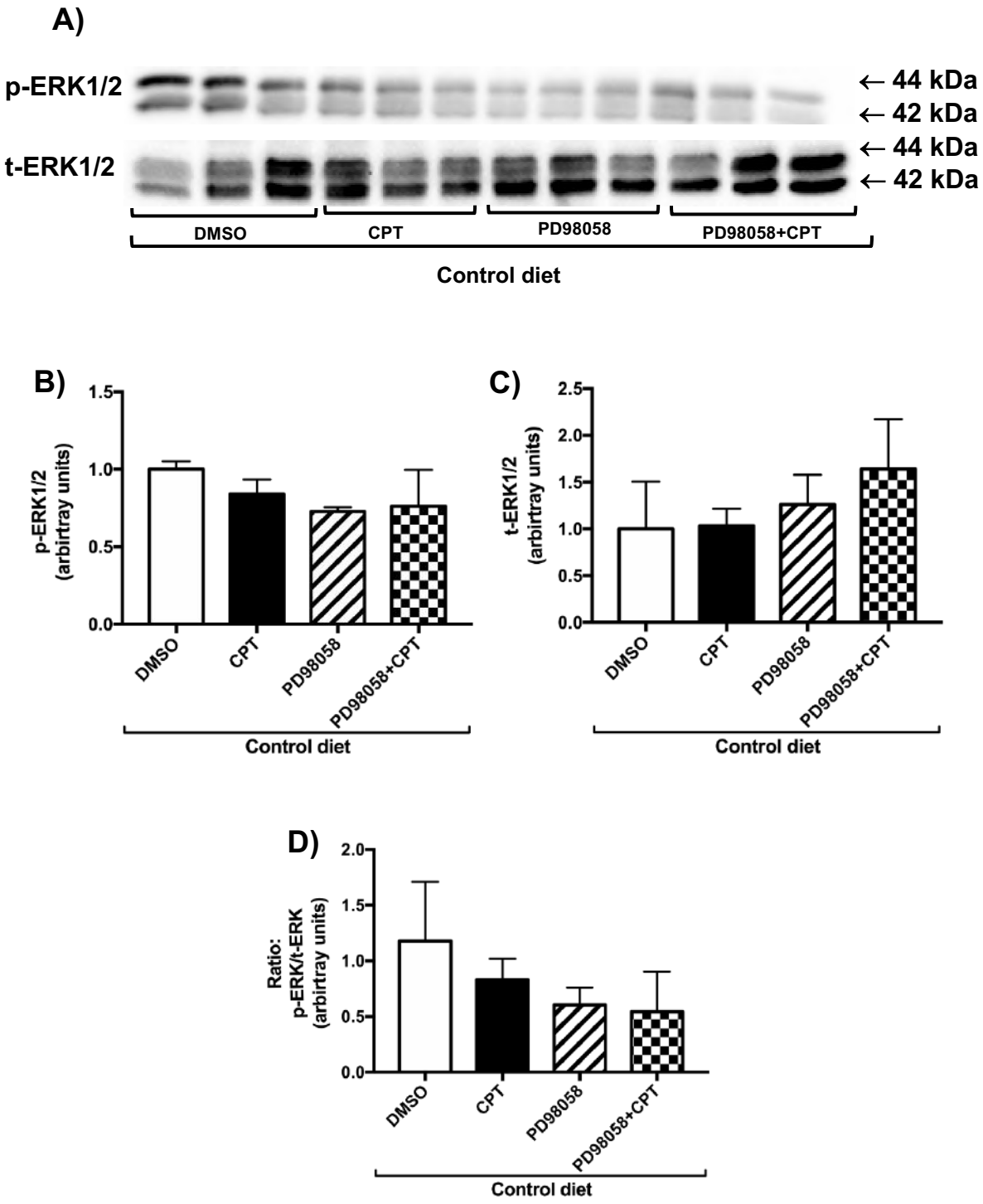

Figure 3. 17 ERK1/2 phosphorylation and expression in hearts from the CD group post-treated with an Epac activator (CPT) and ERK1/2 inhibitor (PD98058) in the first 10 minutes reperfusion.

(A), representative Western blots for phosphorylated and total ERK1/2; (B), phosphorylated ERK1/2 levels; (C), total ERK1/2 levels; (D), phospho/total ratio for ERK1/2. n = 3 per group All values are expressed as mean ± SEM.

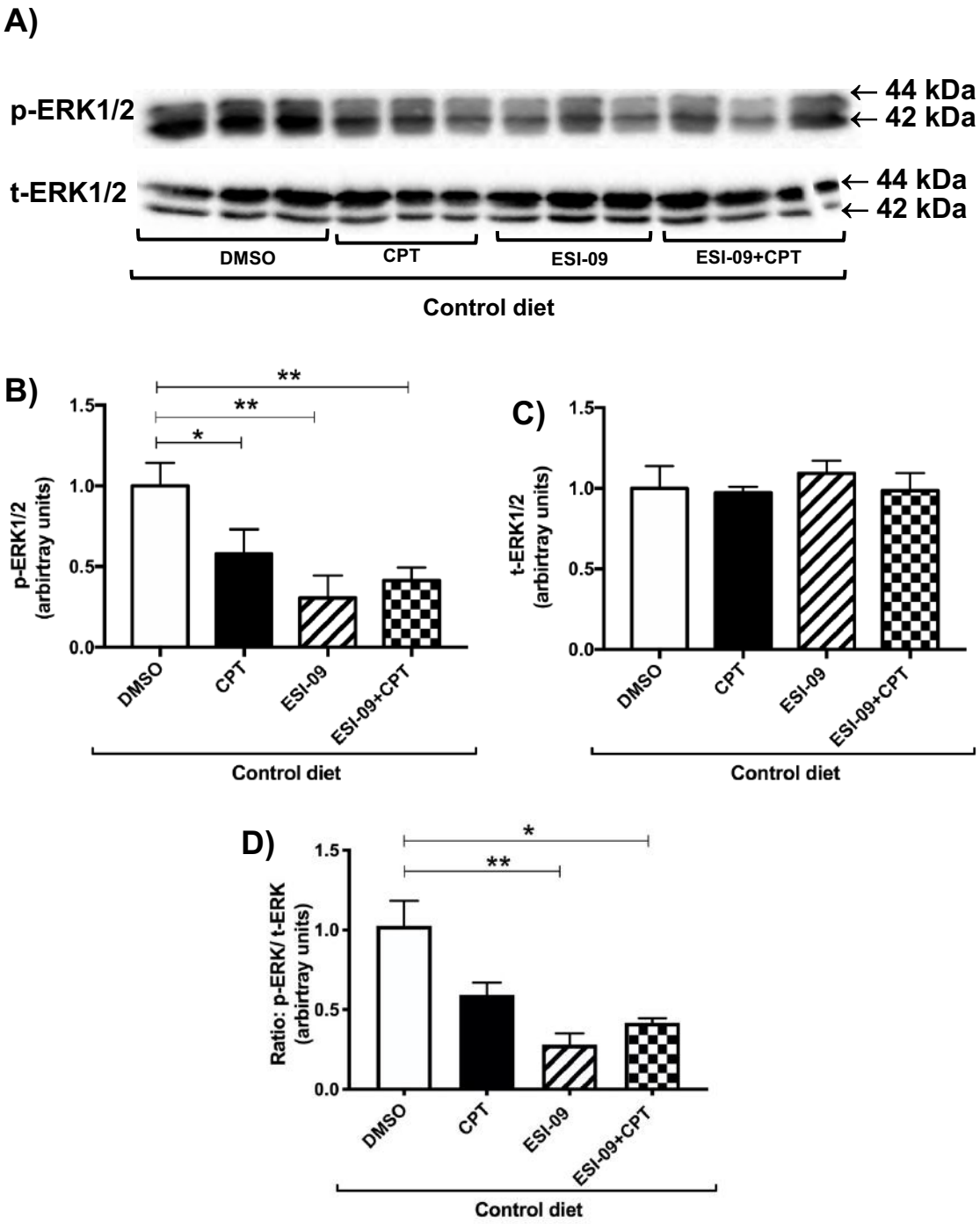

Figure 3. 18 ERK1/2 phosphorylation and expression in hearts from the CD group post-treated with an Epac activator (CPT, 2 μM) and Epac inhibitor (ESI-09, 5 μM) in the first 10 minutes reperfusion.

(A), representative Western blots for phosphorylated and total ERK1/2; (B), phosphorylated ERK1/2 levels; (C), total ERK1/2 levels; (D), phospho/total ratio for ERK1/2. n = 3 per group. All values are expressed as mean ± SEM. *P<0.05, **P<0.01.

In HC hearts

The HC hearts showed a decrease in both phosphorylated ERK1/2 and phospho:total ERK1/2 ratio compared to the hearts in the CD group, although not significant (Figure 3.19B,D). The CPT treated hearts had an elevation in phospho-ERK1/2 and phospho: total ERK1/2 compared to DMSO controls, but this was not significant. (Figure 3.19B, D). In addition, MEK-ERK1/2 inhibition with PD98058 showed no significant difference in total ERK1/2 expression in all treatment groups (Figure 3.19C).

Epac inhibition with ESI-09 showed a significant reduction both phospho-ERK1/2 and phospho:total ERK1/2 ratio compared to DMSO control hearts (pERK1/2: HC+ESI-09: 0.79± 0.02 vs. HC+DMSO: 1.304 ± 0.18, $P<0.05$, Figure 3.20B) (p-ERK1/2/t-ERK1/2: HC+ESI-09: 0.58 ± 0.05 vs. HC+DMSO: 1.09 ± 0.15, $P<0.05$, Figure 3.20D). Total ERK1/2 expression did not differ between any of the treatment groups.

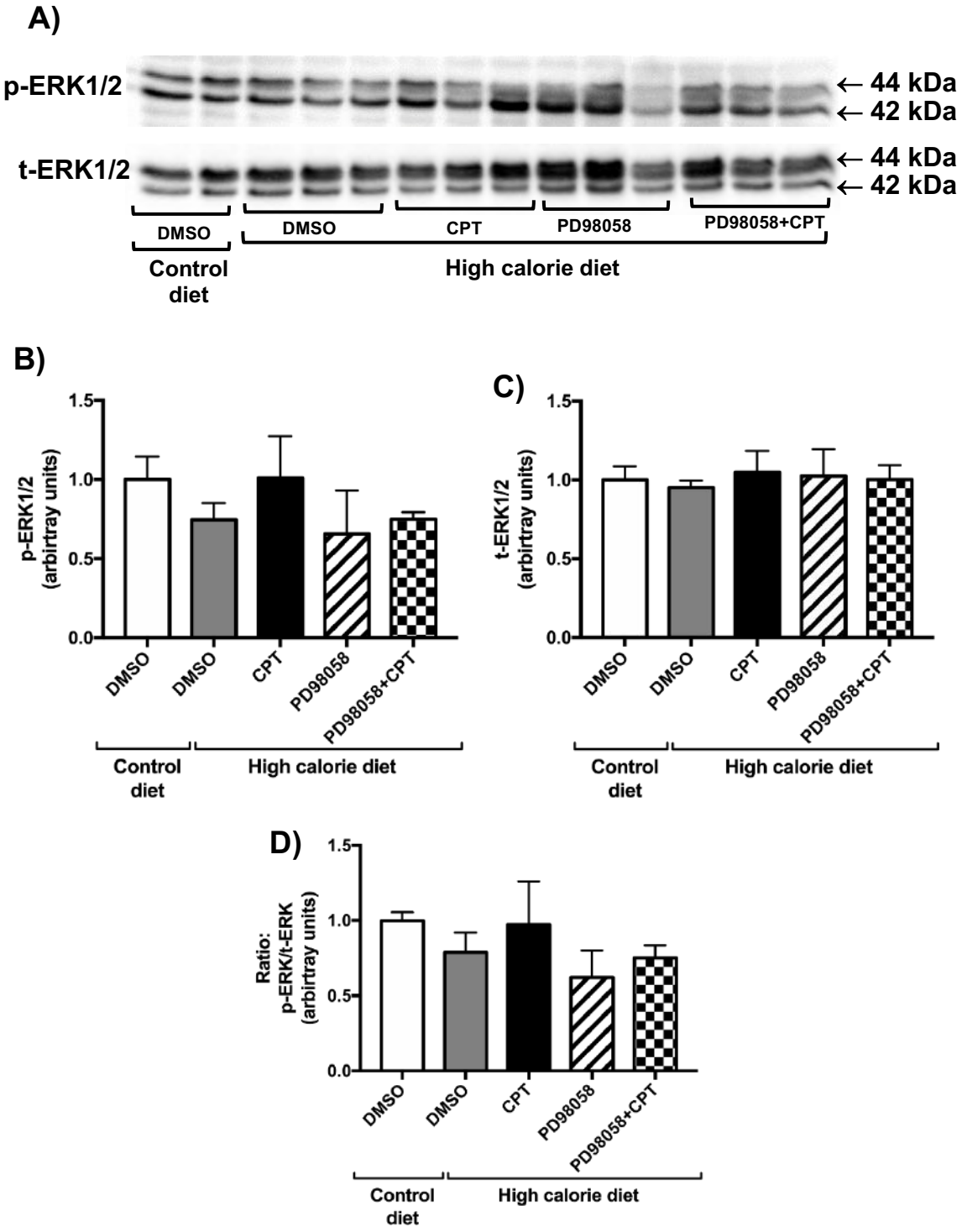

Figure 3. 19 ERK1/2 phosphorylation and expression in hearts from the HC group post-treated with an Epac activator (CPT) and ERK1/2 inhibitor (PD98058) in the first 10 minutes reperfusion.

(A), representative Western blots for phosphorylated and total ERK1/2; (B), phosphorylated ERK1/2 levels; (C), total ERK1/2 levels; (D), phospho/total ratio for ERK1/2. n =2- 3 per group. All values are expressed as mean ± SEM.

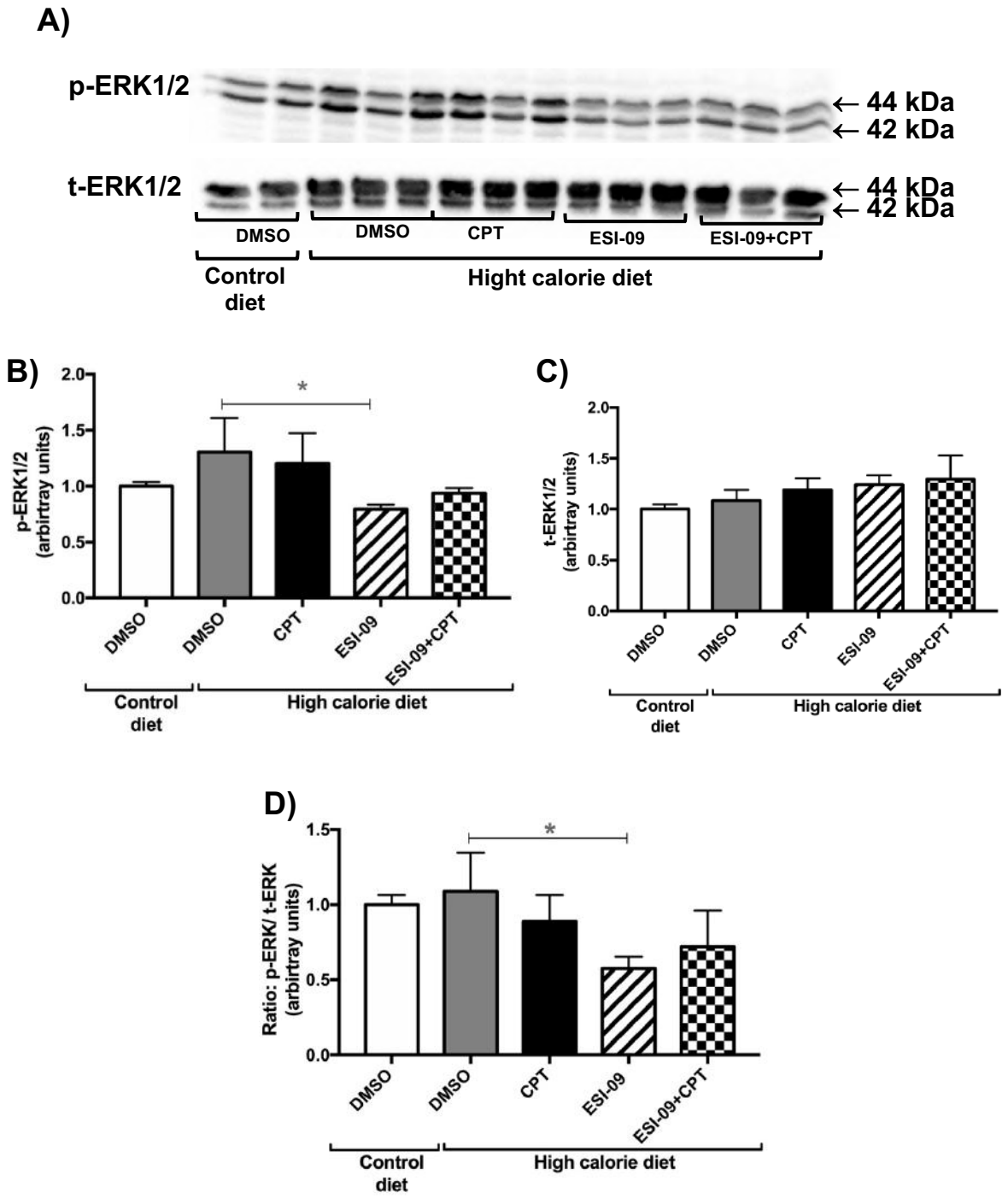

Figure 3. 20 ERK1/2 phosphorylation and expression in hearts from the HC group post-treated with an Epac activator (CPT, 2 μM) and Epac inhibitor (ESI-09, 5 μM) in the first 10 minutes reperfusion.

(A), representative Western blots for phosphorylated and total ERK1/2; (B), phosphorylated ERK1/2 levels; (C), total ERK1/2 levels; (D), phospho/total ratio for ERK1/2. n = 2-3 per group. All values are expressed as mean ± SEM.

3.3.5.3 GSK3β expression and activation

In CD hearts

Hearts treated with ESI-09 had a reduced phospho-GSK3β expression compared to the DMSO control hearts (p-GSK3β: CD+ESI-09: 0.21 ± 0.03 vs. CD+DMSO: 1 ± 0.28, P<0.05) (Figure 3.21). Epac activation with CPT could not reverse the reduced phospho-GSK3β cause by ESI-09 in hearts co-treated with CPT and ESI-09 when compared to the DMSO control (CD+ESI-09+CPT: 0.19 ± 0.02 vs. CD+DMSO: 1 ± 0.28, P<0.05) (Figure 3.21B). An elevation in phospho-GSK3β and phospho: total GSK3β levels was also noted in CPT treated hearts compared to the CPT hearts co-treated with an Epac inhibitor (p-GSK3β: CD+CPT: 0.59 ± 0.09 vs. CD+ESI-09+CPT: 0.19 ± 0.02, P<0.05, Figure 3.21B) (p/t-GSK3β ratio: CD+CPT: 0.58 ± 0.08 vs. CD+ESI-09+CPT: 0.16 ± 0.03, P<0.01, Figure 3.21D). There were no significant changes in total GSK3β expression in any of the treatment groups (Figure 3.21C).

In HC hearts

Even though there were indications of a decrease in phospho-GSK3β in hearts of HC compared to CD, and increased phospho-GSK3β in hearts of HC treated with CPT compared to HC controls, these changes were not significant (Figure 3.22B).

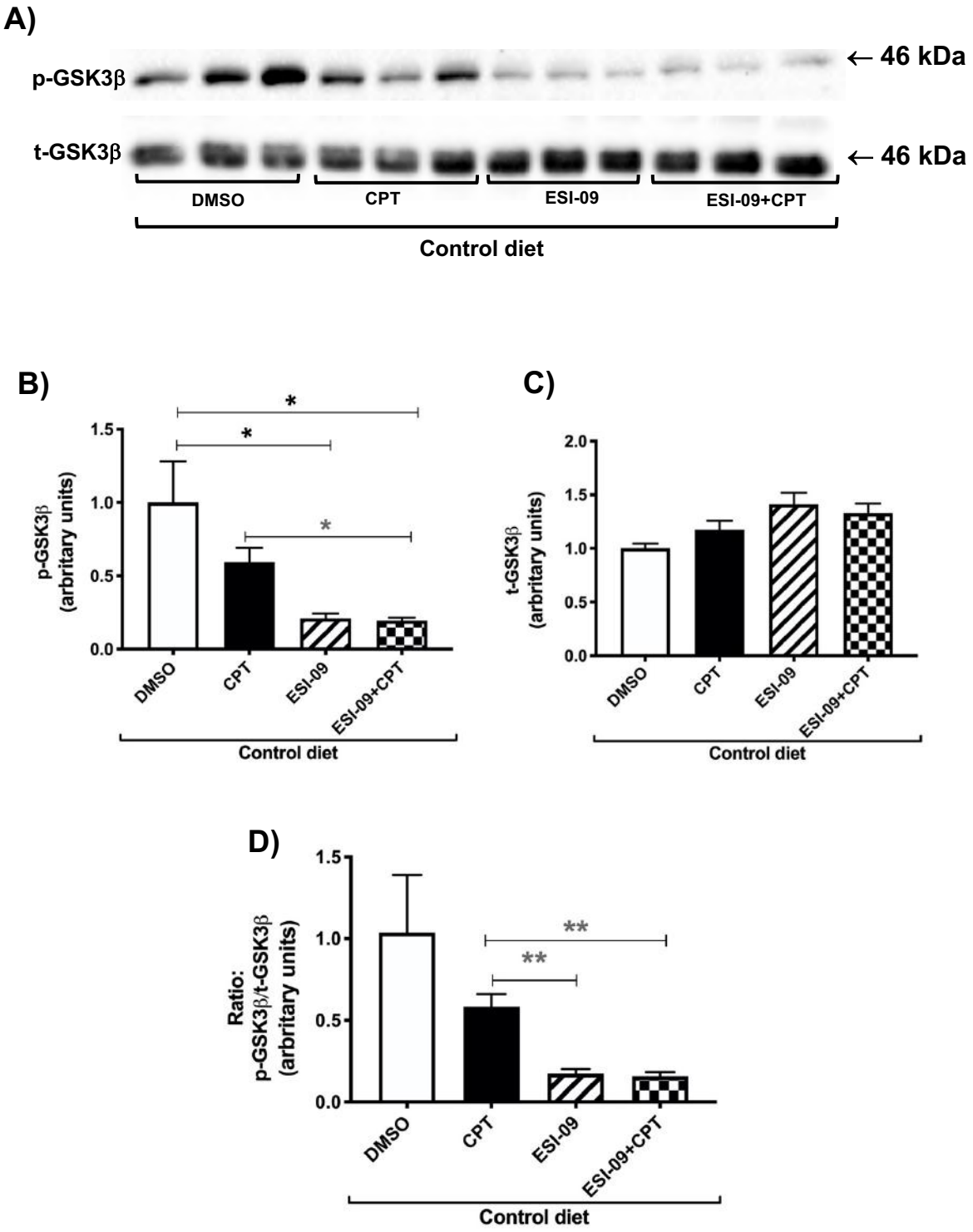

Figure 3. 21 GSK3β phosphorylation and expression in hearts from the CD group post-treated with an Epac activator (CPT, 2 μM) and Epac inhibitor (ESI-09, 5 μM) in the first 10 minutes reperfusion.

(A), representative Western blots for phosphorylated and total GSK3β; (B), phosphorylated levels; (C), total GSK3β levels; (D), phospho/total ratio for GSK3β. n = 3 per group. All values are expressed as mean ± SEM.*P<0.05,**P<0.01.

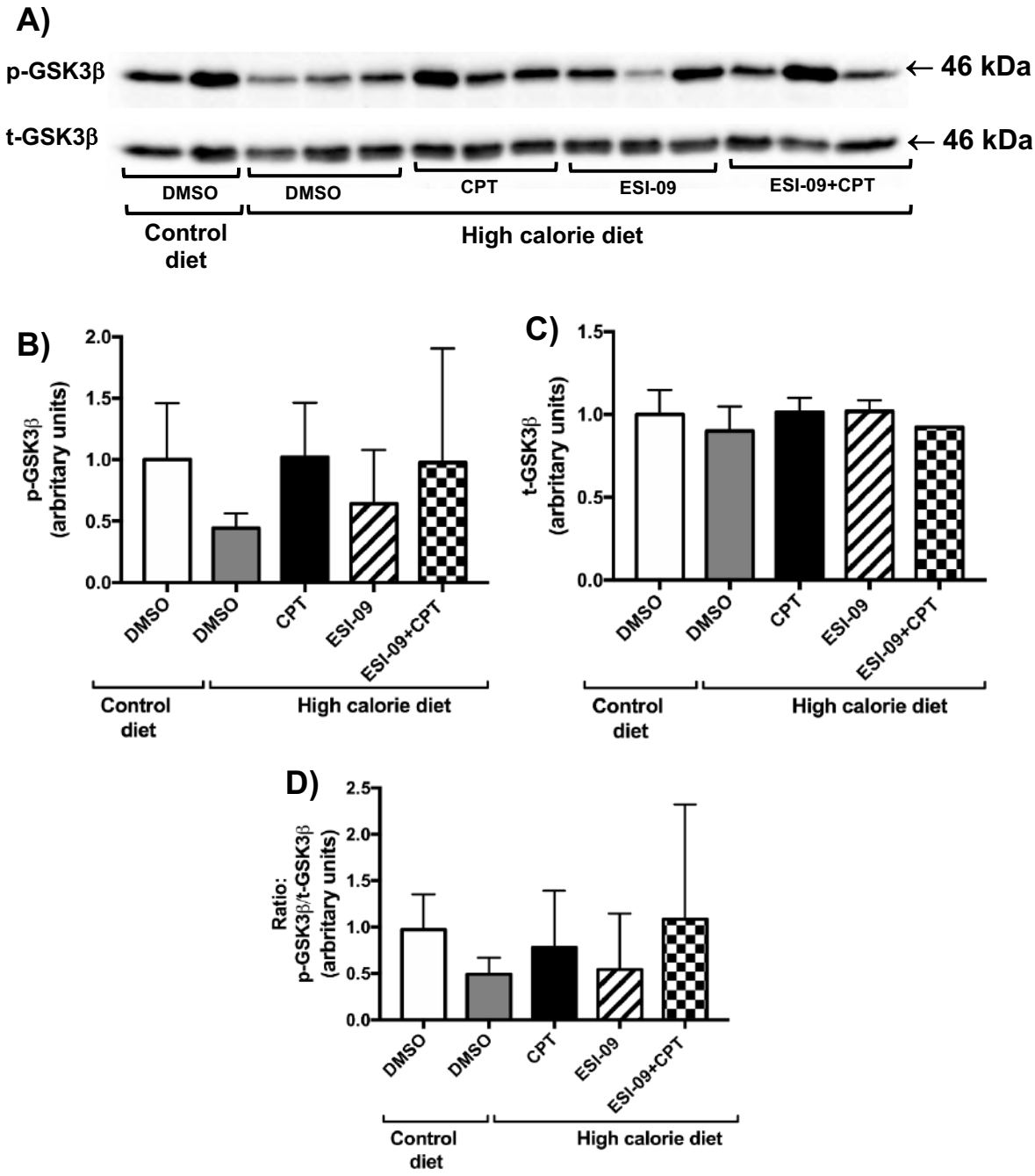

Figure 3. 22 GSK3β phosphorylation and expression in hearts from the HD group post-treated with an Epac activator (CPT, 2 μM) and Epac inhibitor (ESI-09, 5 μM) in the first 10 minutes reperfusion.

(A), representative Western blots for phosphorylated and total GSK3β; (B), phosphorylated GSK3β levels; (C), total GSK3β levels; (D), phospho/total ratio for GSK3β. n = 2-3 per group. All values are expressed as mean ± SEM.

3.3.5.4 Total CaMKII expression and activation

In CD hearts

Epac activation with CPT in the CD hearts showed no significant increase in phospho-CaMKII or phospho: total CaMKII in any of the treatment groups (Figure 3.23). In addition, the decrease following ESI-09 treatment was also not significant.

In HC hearts

In HC DMSO control hearts, the decrease in phospho-CaMKII, total CaMKII expression and phospho: total CaMKII versus CD DMSO controls was not significant (Figure 3.22). However, Epac activation with CPT significantly increased CaMKII phosphorylation and phospho: total CaMKII ratio compared to HC DMSO control (p-CaMKII: HC+CPT: 1.21 ± 0.17 vs. HC+DMSO: 0.59 ± 0.11, $P<0.05$, Figure 3.24B) (p-CaMKII/t-CaMKII: HC+CPT: 1.47 ± 0.17 vs. HC+DMSO: 0.76 ± 0.19, $P<0.05$, Figure 3.24D). Furthermore, co-treatment of CPT with the Epac inhibitor (ESI-09) showed reduced (borderline significant, $P=0.05$) phospho-CaMKII levels compared to hearts treated with CPT alone (Figure 3.24B). On the other hand, the phospho:total CaMKII ratio was significantly decreased in ESI-09 and CPT co-treated hearts versus hearts treated with CPT alone (HC+ESI-09+CPT: 0.52 ± 0.07 vs. HC+CPT: 1.47 ± 0.17, $P<0.01$) (Figure 3.24D). The total CaMKII expression was not altered among the treatments groups (Figure 3.24C).

3.3.5.5 Calcineurin total expression

Epac activation with CPT did not significantly increase calcineurin in CD hearts (Figure 3.25B)

The HC DMSO hearts showed a significant increase in total calcineurin expression compared to CD DMSO hearts (HC+DMSO: 1.61 ± 0.08 vs. CD+DMSO: 1 ± 0.01, $P<0.01$) (Figure 3.25D). However, there were no differences in total calcineurin expression between different treatment groups in HC treated hearts.

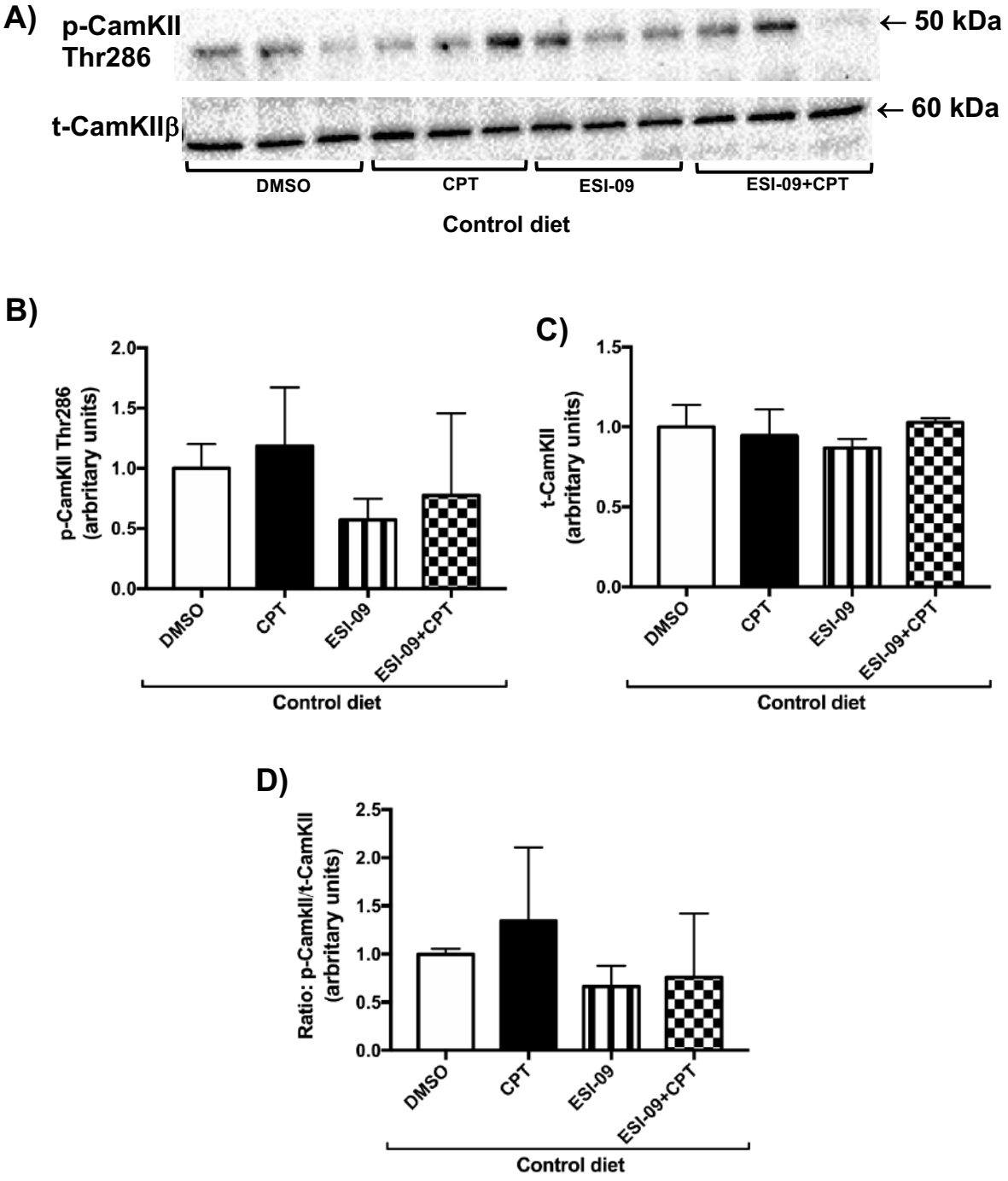

Figure 3. 23 CaMKII phosphorylation and expression in hearts from the CD group post-treated with an Epac activator (CPT, 2 μM) and Epac inhibitor (ESI-09, 5 μM)in the first 10 minutes reperfusion.

(A), representative Western blots for phosphorylated and total CaMKII; (B), phosphorylated CaMKII levels; (C), total CaMKII levels; (D), phospho/total ratio for CaMKII. n = 3 per group. All values are expressed as mean ± SEM.

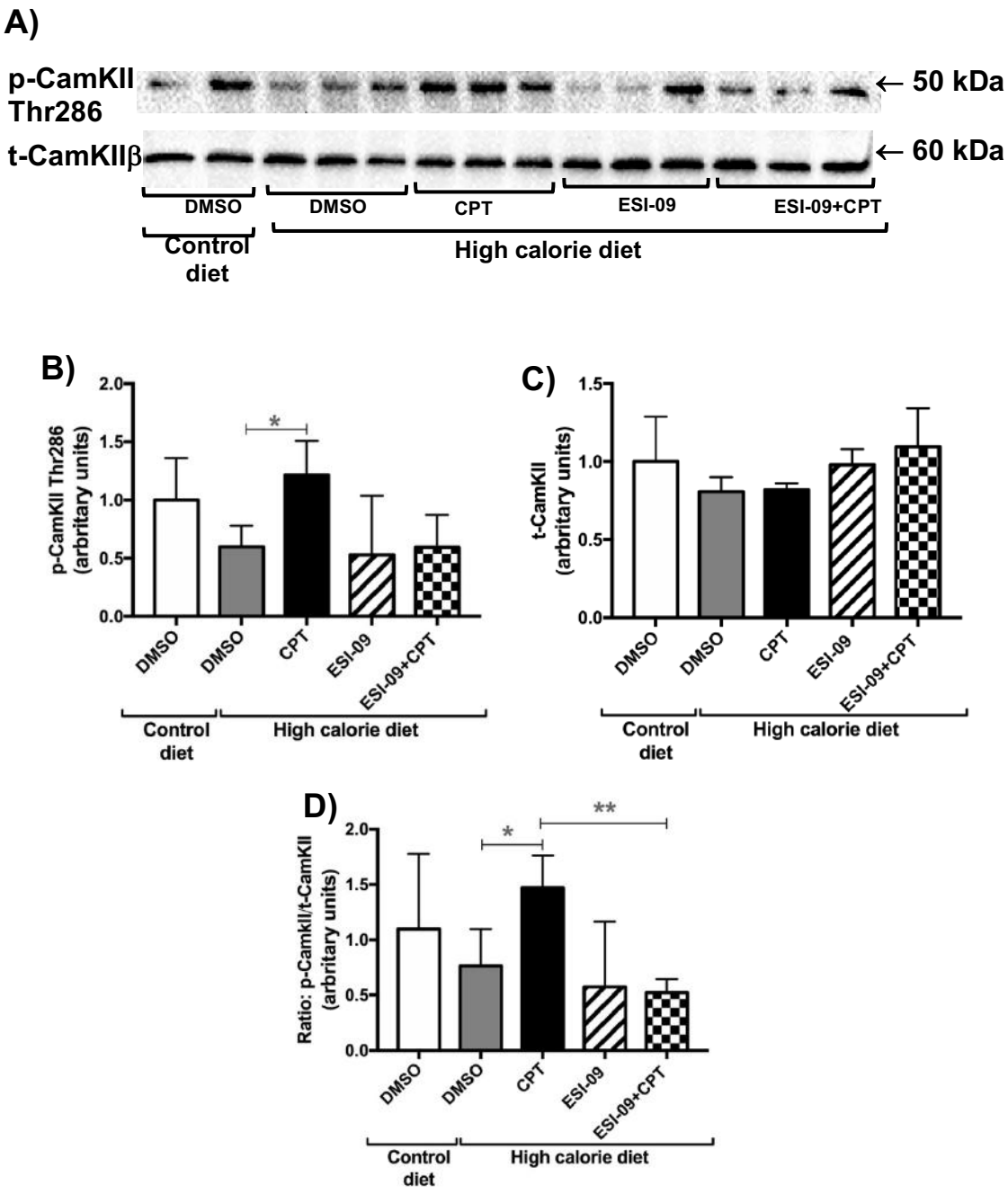

Figure 3. 24 CaMKII phosphorylation and expression in hearts from the HC group post-treated with an Epac activator (CPT, 2 μM) and Epac inhibitor (ESI-09, 5 μM) in the first 10 minutes reperfusion.

(A), representative Western blots for phosphorylated and total CaMKII; (B), phosphorylated CaMKII levels; (C), total CaMKII levels; (D), phospho/total ratio for CaMKII. n = 2-3 per group. All values are expressed as mean ± SEM.*P<0.05, **P<0.01.

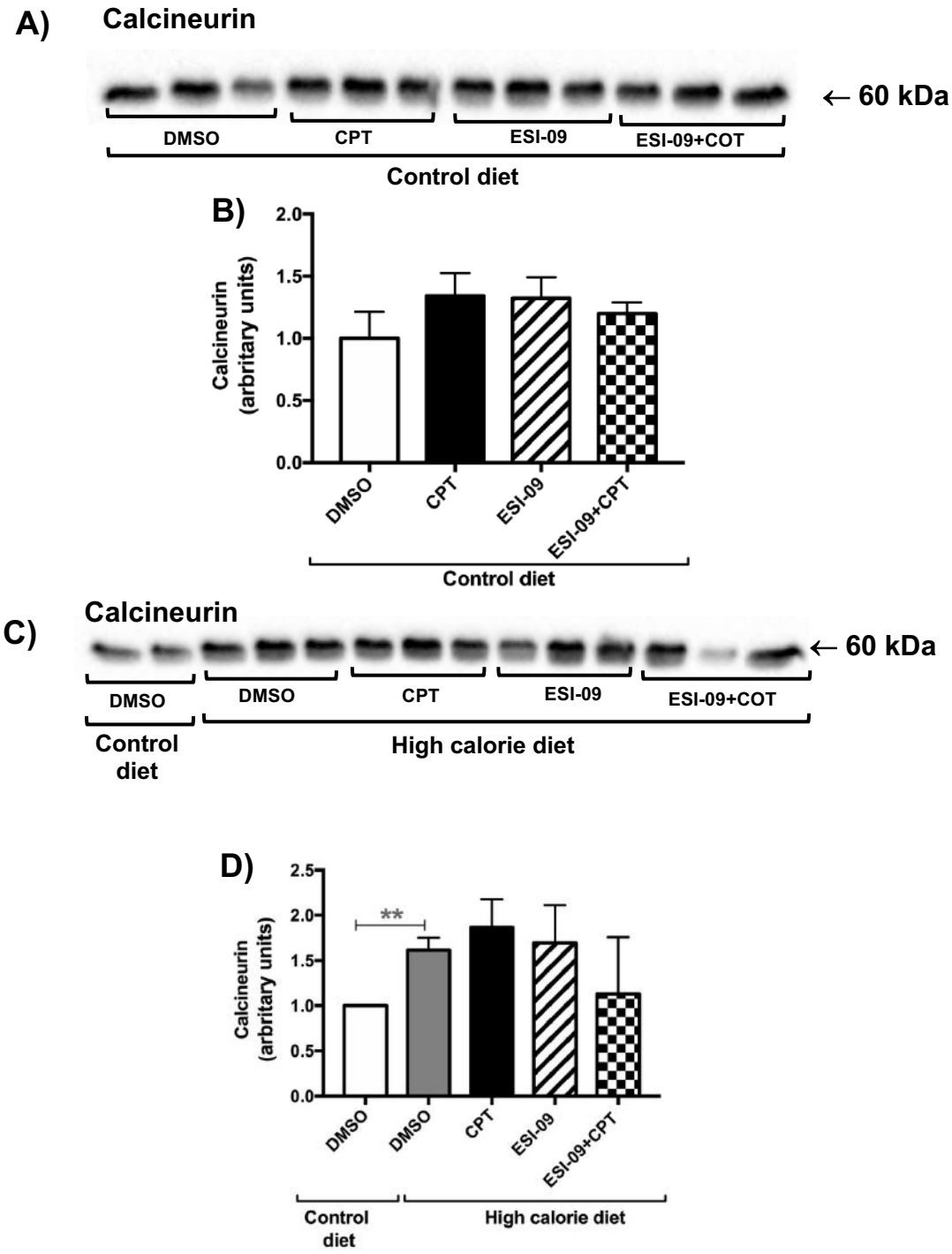

Figure 3. 25 **Calcineurin expression in hearts from the CD and HC groups post-treated with an Epac activator (CPT, 2 μM) and Epac inhibitor (ESI-09, 5 μM) in the first 10 minutes reperfusion**.

(A), representative Western blots for CD total calcineurin; (B), CD total calcineurin levels; (C), representative Western blots for HC total calcineurin; (D), HC total calcineurin level. n = 2-3 per group. All values are expressed as mean ± SEM.**P<0.01.

3.3.5.6 Cleaved PARP expression

In CD hearts, both CPT and ESI-09 treated hearts showed a significant increase in cleaved PARP expression as compared to DMSO control (CD+CPT: 2.26 ± 0.38 vs. CD+DMSO: 1 ± 0.17, P<0.05; CD+ESI-09: 3.78 ± 0.60 vs. CD+DMSO: 1 ± 0.17, P<0.05) (Figure 3.26B).

Furthermore, the HC hearts also showed an elevation in cleaved PARP expression compared to CD DMSO controls (HC+DMSO: 1.381 ± 0.03 vs. CD+DMSO: 1 ± 0.00, P<0.01) (Figure 3.26D).

3.3.5.7 Cleaved Caspase-3 expression

Despite the fact that there were indications of an increase in cleaved caspase-3 expression in hearts of HC compared to CD, as well as an increased cleaved caspase-3 expression in hearts of HC treated with CPT compared to HC controls, these changes were not significant (Figure 3.27D).

3.3.5.8 Nitrotyrosine total expression

There were no significant differences in nitrotyrosine expression between the CD DMSO and the HC DMSO groups. Neither Epac activation nor inhibition caused significant changes in any of the treatment groups (Figure 3.28B and D).

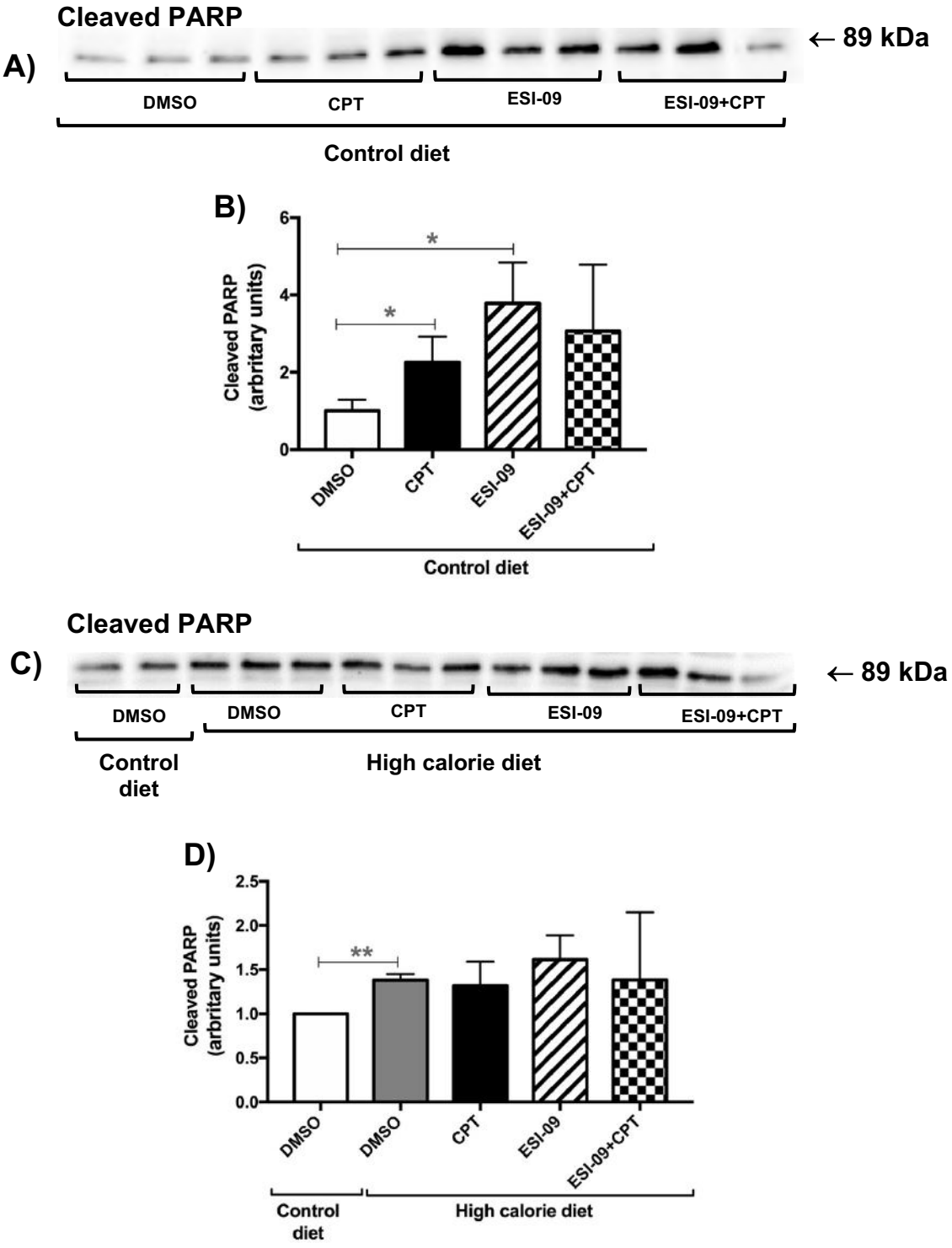

Figure 3. 26 Cleaved PARP expression in hearts from the CD and HC groups post-treated with an Epac activator (CPT, 2 μM) and Epac inhibitor (ESI-09, 5 μM) in the first 10 minutes reperfusion.

(A), representative Western blots for CD total cleaved PARP; (B), CD total cleaved PARP levels; (C), representative Western blots for HC total cleaved PARP; (D), HC total cleaved PARP level. n = 2-3 per group. All values are expressed as mean ± SEM.*P<0.05; **P<0.01.

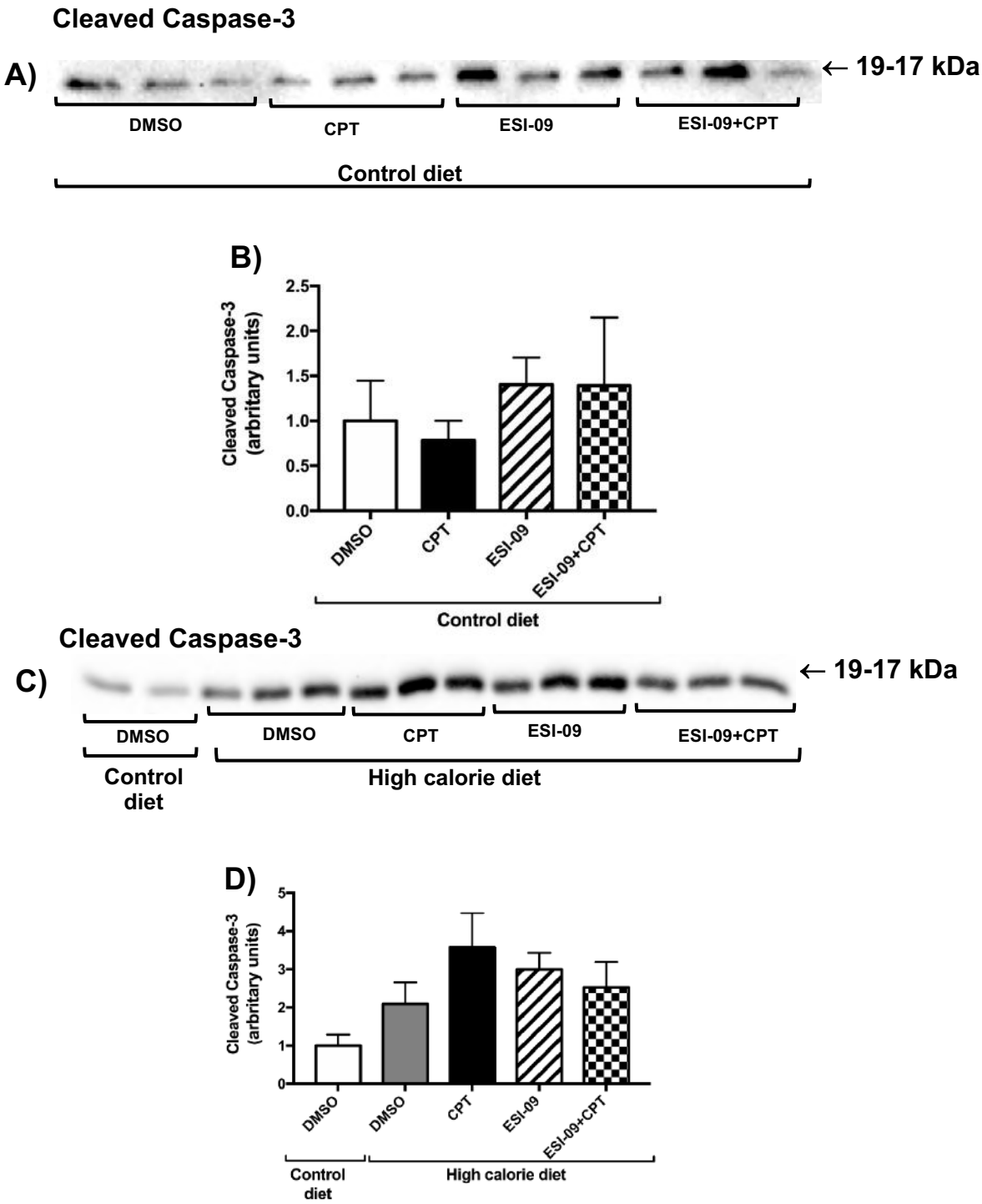

Figure 3. 27 Cleaved Caspase-3 expression in hearts from the CD and HC groups post-treated with an Epac activator (CPT, 2 μM) and Epac inhibitor (ESI-09, 5 μM) in the first 10 minutes reperfusion.

(A), representative Western blots for CD total cleaved Caspase-3; (B), CD total cleaved Caspase-3 levels; (C), representative Western blots for HC total cleaved Caspase-3; (D), HC total cleaved Caspase-3 level. n = 2-3 per group. All values are expressed as mean ± SEM.

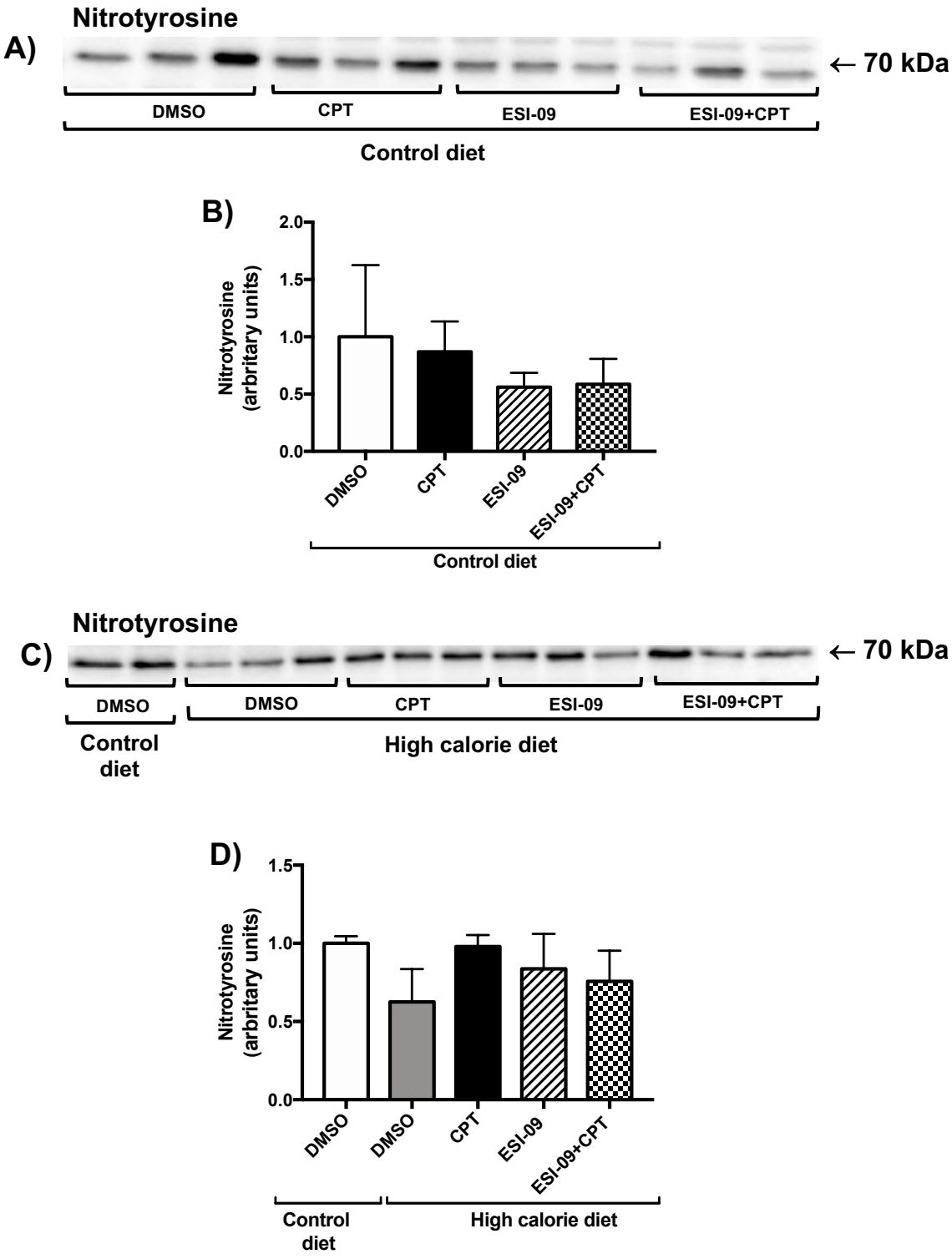

Figure 3. 28 Nitrotyrosine expression in hearts from the CD and HC groups post-treated with an Epac activator (CPT, 2 μM) and Epac inhibitor (ESI-09, 5 μM) in the first 10 minutes reperfusion.

(A), representative Western blots for CD Nitrotyrosine; (B), CD total Nitrotyrosine levels; (C), representative Western blots for HC total Nitrotyrosine; (D), HC total Nitrotyrosine level. n = 2-3 per group. All values are expressed as mean ± SEM.

3.3.5.9 AMPK phosphorylation and expression

In CD hearts

The CD hearts showed no significant differences in phospho-AMPK, total AMPK or phospho: total AMPK ratio in any of the treatment groups (Figure 3.29). However, the co-treatment with ESI-09 and CPT demonstrated borderline significant increases in phospho-AMPK and phospho:total AMPK ratios as compared to CD DMSO control (p-AMPK: CD+ESI-09+CPT: 0.85 ± 0.11 vs. CD+DMSO: 0.39 ± 0.06, P=0.050, Figure 3.29B) (p-AMPK/t-AMPK: CD+ESI-09+CPT: 0.97 ± 0.12 vs. CD+DMSO: 0.45 ± 0.07, P=0.05, Figure 3.29D).

In HC hearts

Epac activation with CPT showed no changes in phospho-AMPK, total AMPK expression or phospho: total AMPK ratio as compared to HC DMSO control. However, hearts treated with ESI-09 demonstrated significant increases in phospho-AMPK level and phospho: total AMPK ratio compared to HC DMSO control hearts (p-AMPK: HC+ESI-09: 3.74 ± 0.63 vs. HC+DMSO: 0.54 ± 0.09, P<0.05, Figure 3.30B) (p-AMPK/t-AMPK: HC+ESI-09: 5.43 ± 0.91 vs. HC+DMSO: 0.79 ± 0.13, P<0.05, Figure 3.30D). In addition, phospho-AMPK and phospho: total AMPK ratio remained elevated in hearts treated with the combination of CPT and ESI-09 compared to HC DMSO control hearts (p-AMPK: HC+ESI-09+CPT: 3.33 ± 0.25 vs. HC+DMSO: 0.54 ± 0.09, P<0.01, Figure 3.30B) (p-AMPK/t-AMPK: HC+ESI-09+CPT: 4.835 ± 0.36 vs. HC+DMSO: 0.79 ± 0.13), P<0.01, Figure 3.30D). There were no changes in total AMPK expression in any of the treatment groups.

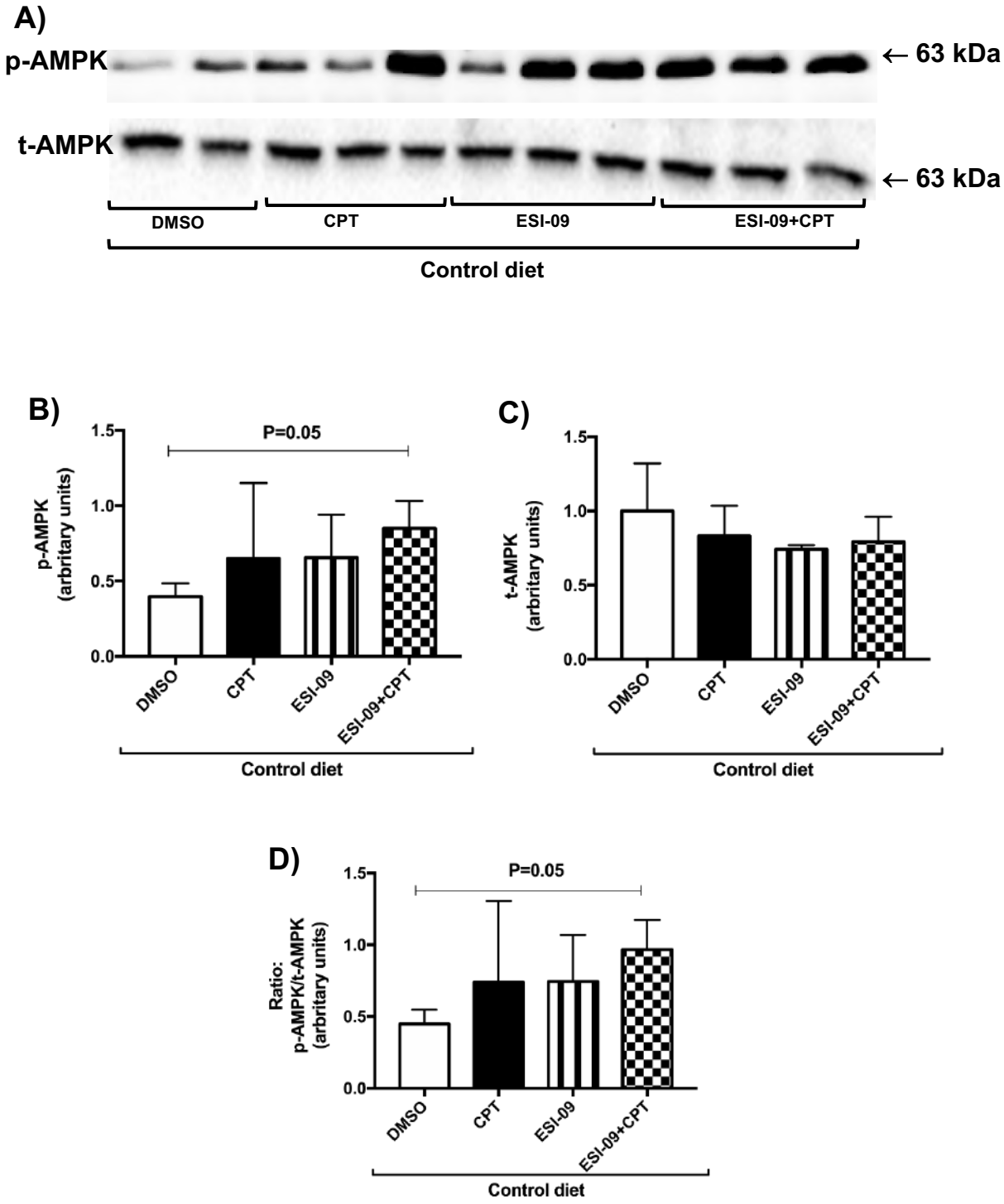

Figure 3. 29 AMPK phosphorylation and expression in hearts from the CD group post-treated with an Epac activator (CPT, 2 μM) and Epac inhibitor (ESI-09, 5 μM) in the first 10 minutes reperfusion.

(A), representative Western blots for phosphorylated and total AMPK; (B), phosphorylated AMPK levels; (C), total AMPK levels; (D), phospho/total ratio for AMPK. n = 2-3 per group. All values are expressed as mean ± SEM.

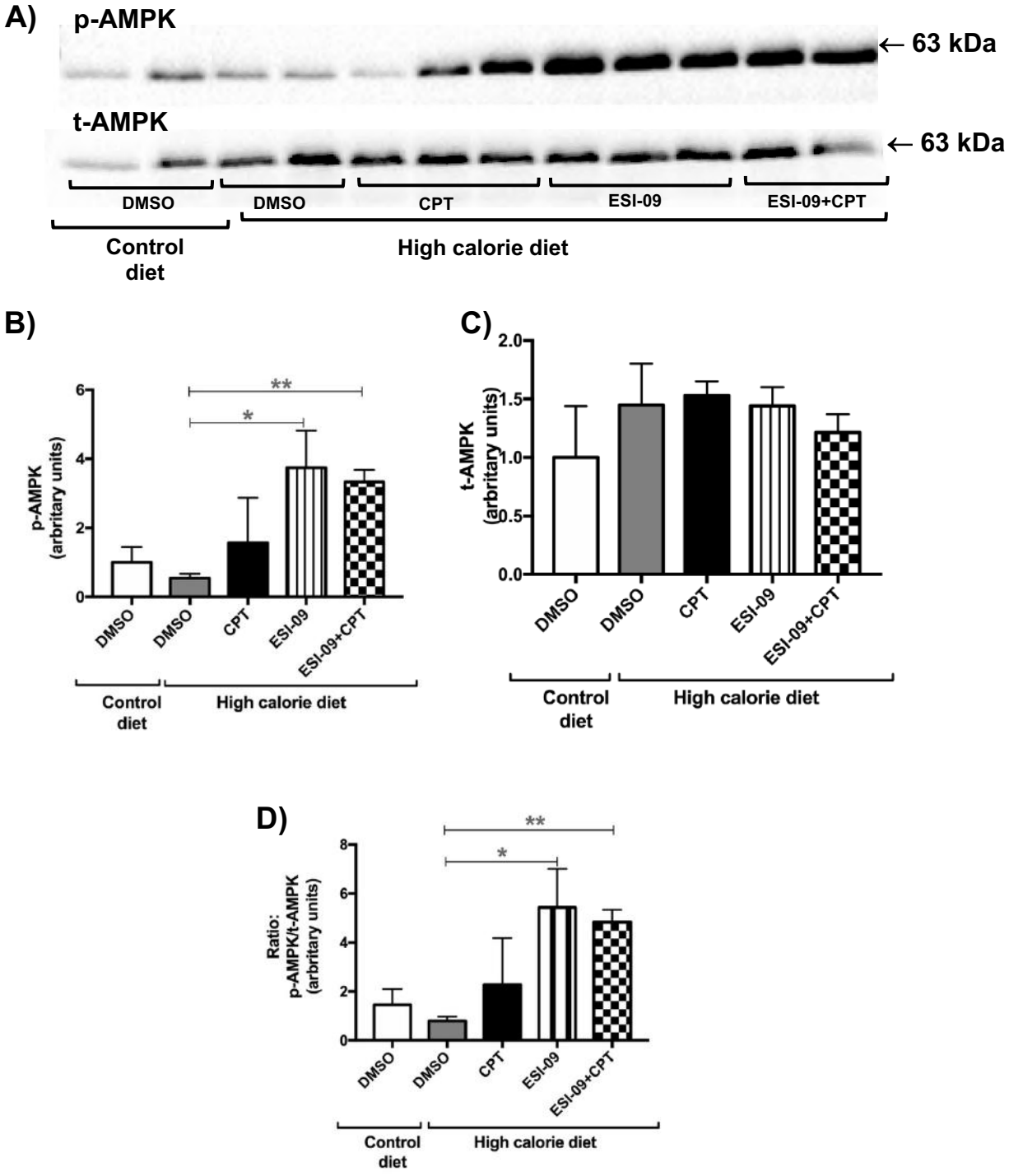

Figure 3. 30 AMPK phosphorylation and expression in hearts from the HC group post-treated with an Epac activator (CPT, 2 μM) and Epac inhibitor (ESI-09, 5 μM) in the first 10 minutes reperfusion.

(A), representative Western blots for phosphorylated and total AMPK; (B), phosphorylated AMPK levels; (C), total AMPK levels; (D), phospho/total ratio for AMPK. n = 2- 3 per group. All values are expressed as mean ± SEM.*P<0.05; **P<0.01.

3.3.5.10 eNOS phosphorylation and expression

Treatment of the hearts from the CD animals had no significant effect on phospho-eNOS, total eNOS expression or phospho: total eNOS ratio (Figure 3.31).

In HC hearts

The HC hearts showed an increase in phospho-eNOS as compared to CD hearts (HC+DMSO: 1.57 ± 0.03 vs. CD+DMSO: 1 ± 0.12, $P<0.05$) (Figure 3.32B). Hearts treated with CPT had a reduced phospho-eNOS compared to the DMSO control hearts (HC+CPT: 0.58 ± 0.04 vs. HC+DMSO: 1.57 ± 0.03, $P<0.0001$) (Figure 3.32B). Epac inhibition with ESI-09 and co-treatment with CPT also exerted a reduced effect on phospho-eNOS levels compared to DMSO control (HC+ESI-09: 0.61 ± 0.10 vs. HC+DMSO: 1.57 ± 0.03 $P<0.001$; HC+ESI-09+CPT: 0.35 ± 0.09 vs. HC+DMSO: 1.57 ± 0.03, $P<0.001$) (Figure 3.32B).

The phospho:total eNOS ratio was also reduced in CPT, ESI-09 and ESI-09+CPT treated hearts compared to DMSO control (HC+CPT: 0.31 ± 0.03 vs. HC+DMSO: 1.22 ± 0.18, $P<0.01$; HC+ESI-09: 0.42 ± 0.09 vs. HC+DMSO: 1.22 ± 0.18, $P<0.05$; HC+ESI-09+CPT: 0.24 ± 0.09 vs. HC+DMSO: 1.22 ± 0.18, $P<0.01$) (Figure 3.32D).

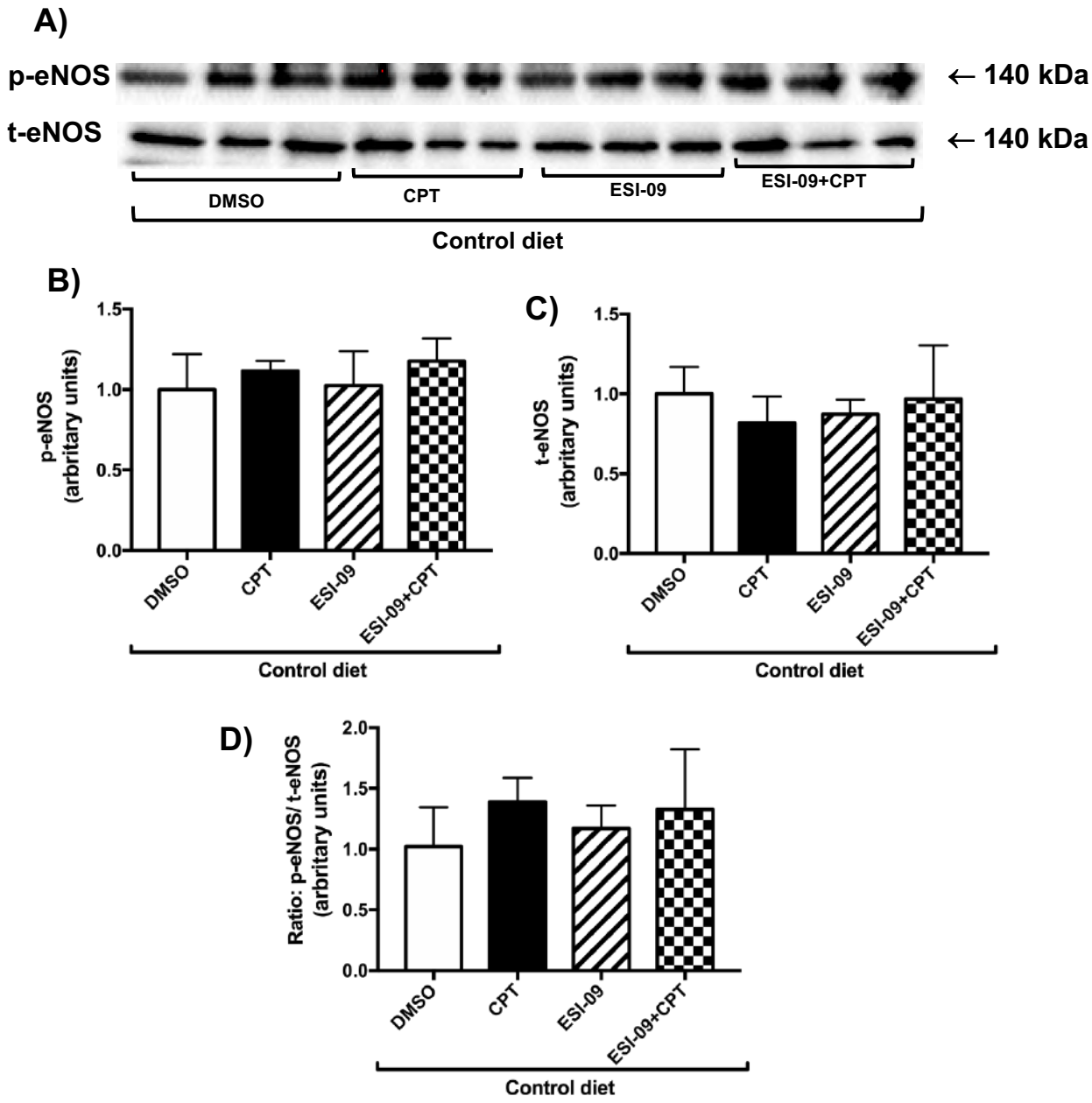

Figure 3. 31 eNOS phosphorylation and expression in hearts from the CD group post-treated with an Epac activator (CPT, 2 μM) and Epac inhibitor (ESI-09, 5 μM) in the first 10 minutes reperfusion.

(A), representative Western blots for phosphorylated and total eNOS; (B), phosphorylated eNOS levels; (C), total eNOS levels; (D), phospho/total ratio for eNOS. n = 3 per group. All values are expressed as mean ± SEM.

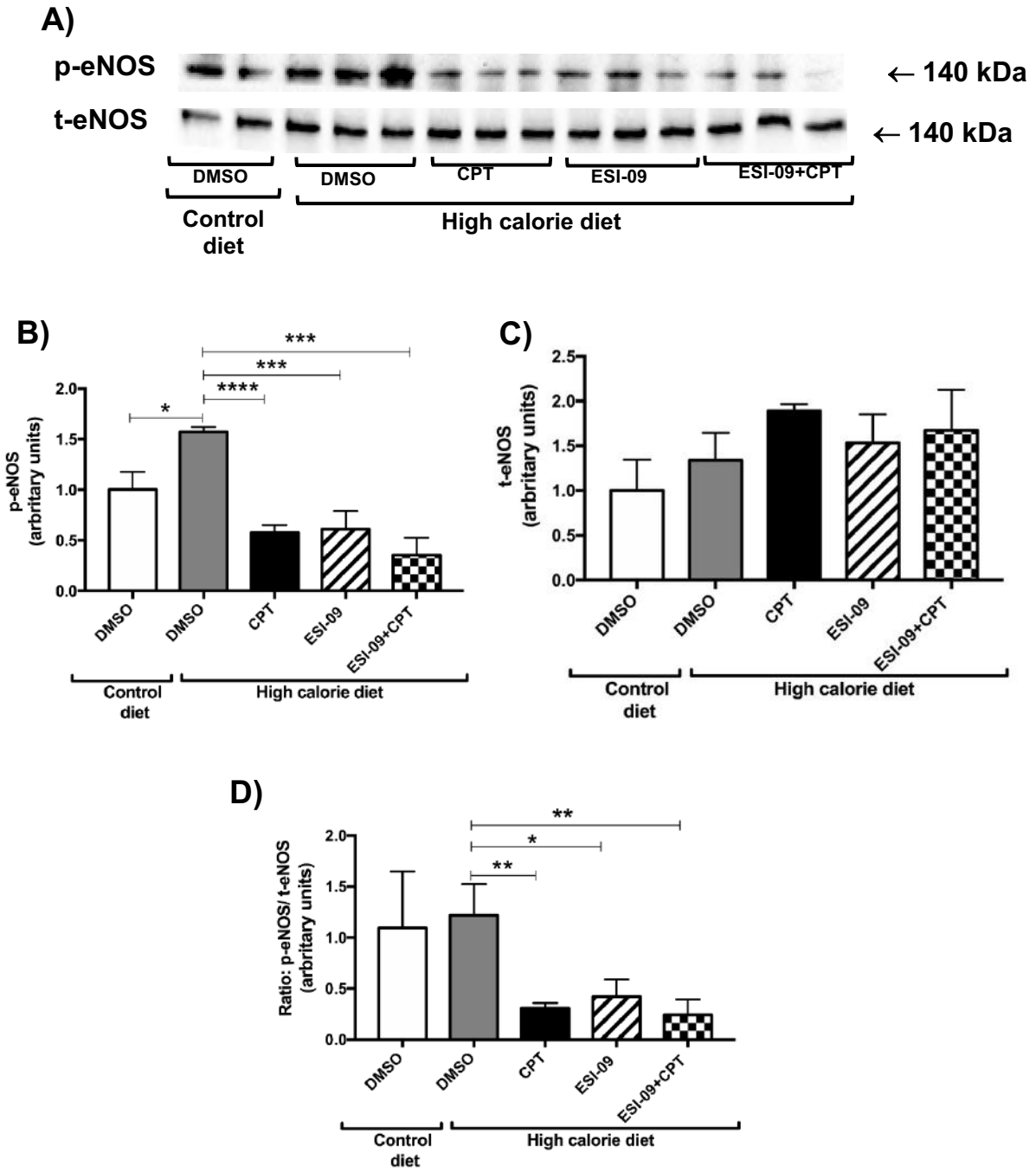

Figure 3. 32 eNOS phosphorylation and expression in hearts from the HC group post-treated with an Epac activator (CPT, 2 μM) and Epac inhibitor (ESI-09, 5 μM) in the first 10 minutes reperfusion.

(A), representative Western blots for phosphorylated and total eNOS; (B), phosphorylated eNOS levels; (C), total eNOS levels; (D), phospho/total ratio for eNOS. n = 3 per group. All values are expressed as mean ± SEM. *P<0.05, **P<0.01,***<0.001,****P<0.0001.

3.3.5.11 DRP1 phosphorylation and expression

Treatment of the hearts from the CD group had no significant effect on phospho-DRP1, total DRP1 expression or phospho: total DRP1 ratio (Figure 3.33).

In HC hearts

In HC hearts, ESI-09 treatment showed an increase in phospho-DRP1 as well as phospho: total DRP1 ratio compared to HC DMSO control hearts, although the increase was not significant (Figure 3.34B and D). There were no changes in total DRP1 expression in all treatment groups (Figure 3.34C).

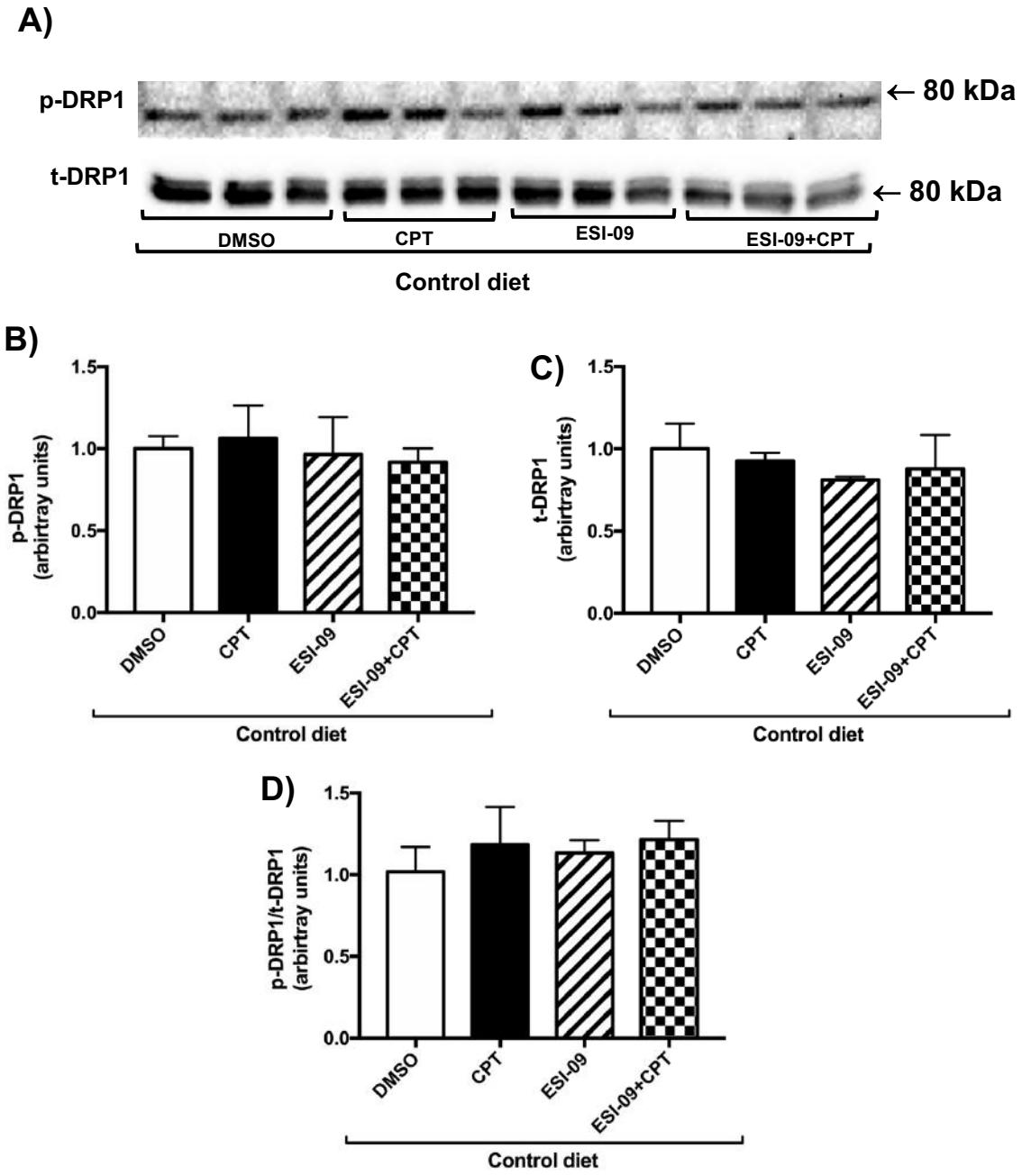

Figure 3. 33 DRP1 phosphorylation and expression in hearts from the CD group post-treated with an Epac activator (CPT, 2 μM) and Epac inhibitor (ESI-09, 5 μM) in the first 10 minutes reperfusion.

(A), representative Western blots for phosphorylated and total DRP1; (B), phosphorylated DRP1 levels; (C), total DRP1 levels; (D), phospho/total ratio for DRP1. n = 3 per group. All values are expressed as mean ± SEM.

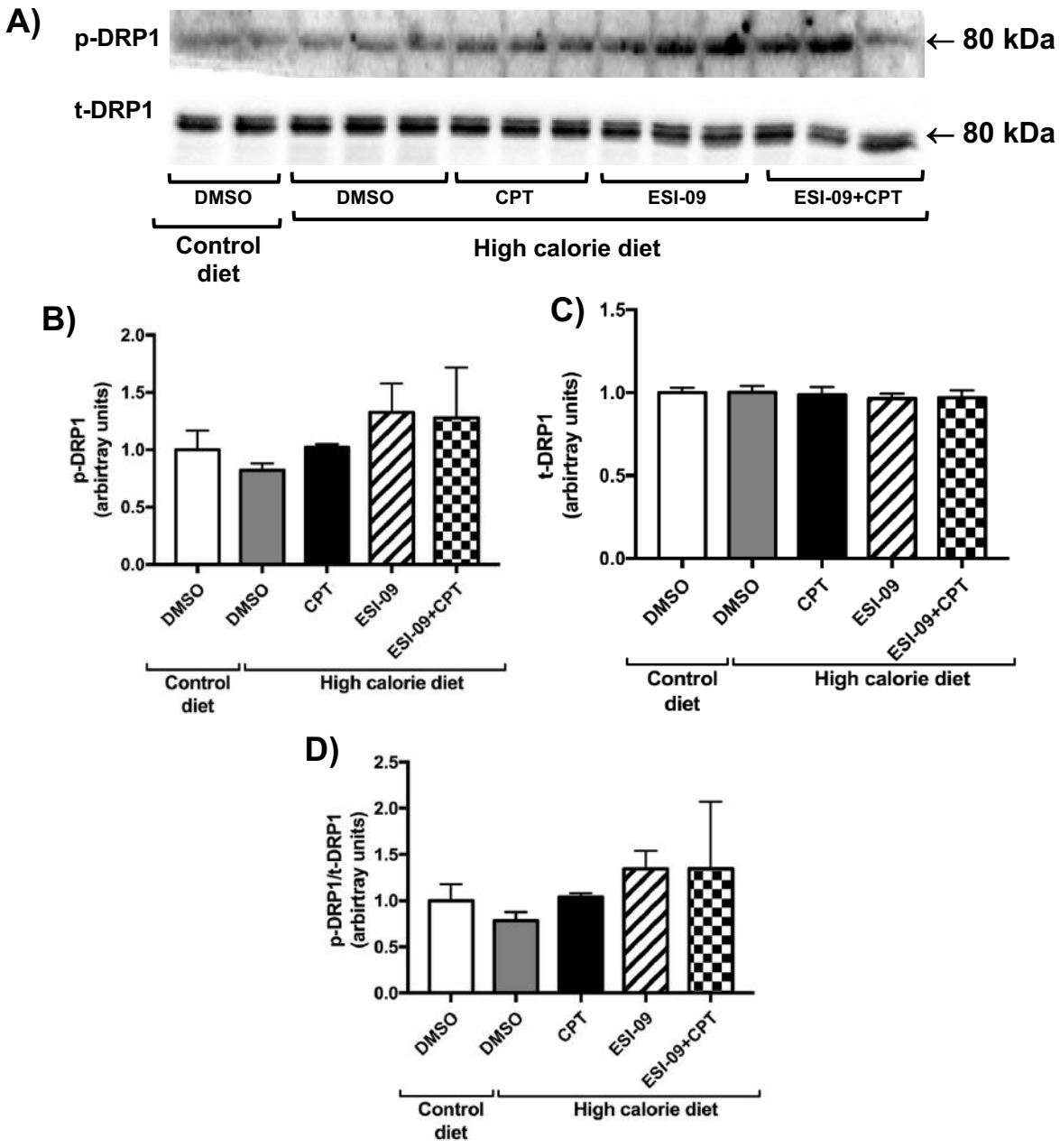

Figure 3. 34 DRP1 phosphorylation and expression in hearts from the HC group post-treated with an Epac activator (CPT, 2 μM) and Epac inhibitor (ESI-09, 5 μM) in the first 10 minutes reperfusion.

(A), representative Western blots for phosphorylated and total DRP1; (B), phosphorylated DRP1 levels; (C), total DRP1 levels; (D), phospho/total ratio for DRP1. n = 2-3 per group. All values are expressed as mean ± SEM.

3.3.5.12 ULK1 phosphorylation and expression

In CD hearts

CPT treated hearts had reduced phospho-ULK1 compared to DMSO control hearts (CD+CPT: 0.78 ± 0.02 vs. CD+DMSO: 1 ± 0.04, P<0.01) (Figure 3.35B). Co-treatment with ESI-09 increased phospho-ULK1 compare to CPT treated hearts (CD+ESI-09+CPT: 1.07 ± 0.04 vs. CD+CPT: 0.78 ± 0.02, P<0.01) (Figure 3.35B). There were no significant differences in total ULK1 in any of the treatment groups (Figure 3.35C).

In HC hearts

Treatment of the hearts from the HC group had no significant effect on phospho-ULK1, total ULK1 expression or phospho: total ULK1 ratio (Figure 3.36).

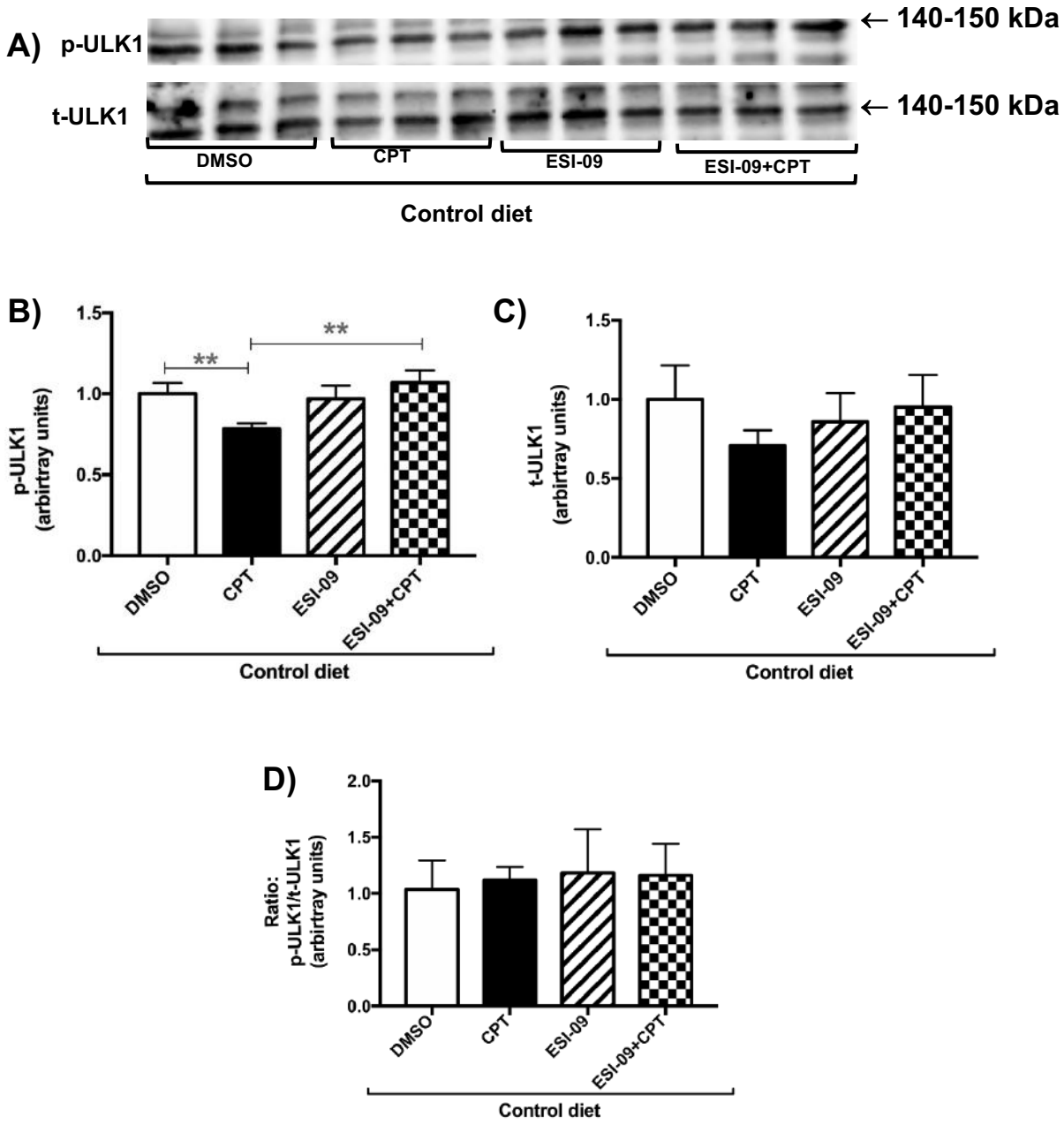

Figure 3. 35 ULK1 phosphorylation and expression in hearts from the CD group post-treated with an Epac activator (CPT, 2 μM) and Epac inhibitor (ESI-09, 5 μM) in the first 10 minutes reperfusion.

(A), representative Western blots for phosphorylated and total ULK1; (B), phosphorylated ULK1 levels; (C), total ULK1 levels; (D), phospho/total ratio for ULK1. n = 3 per group. All values are expressed as mean ± SEM. **P<0.01.

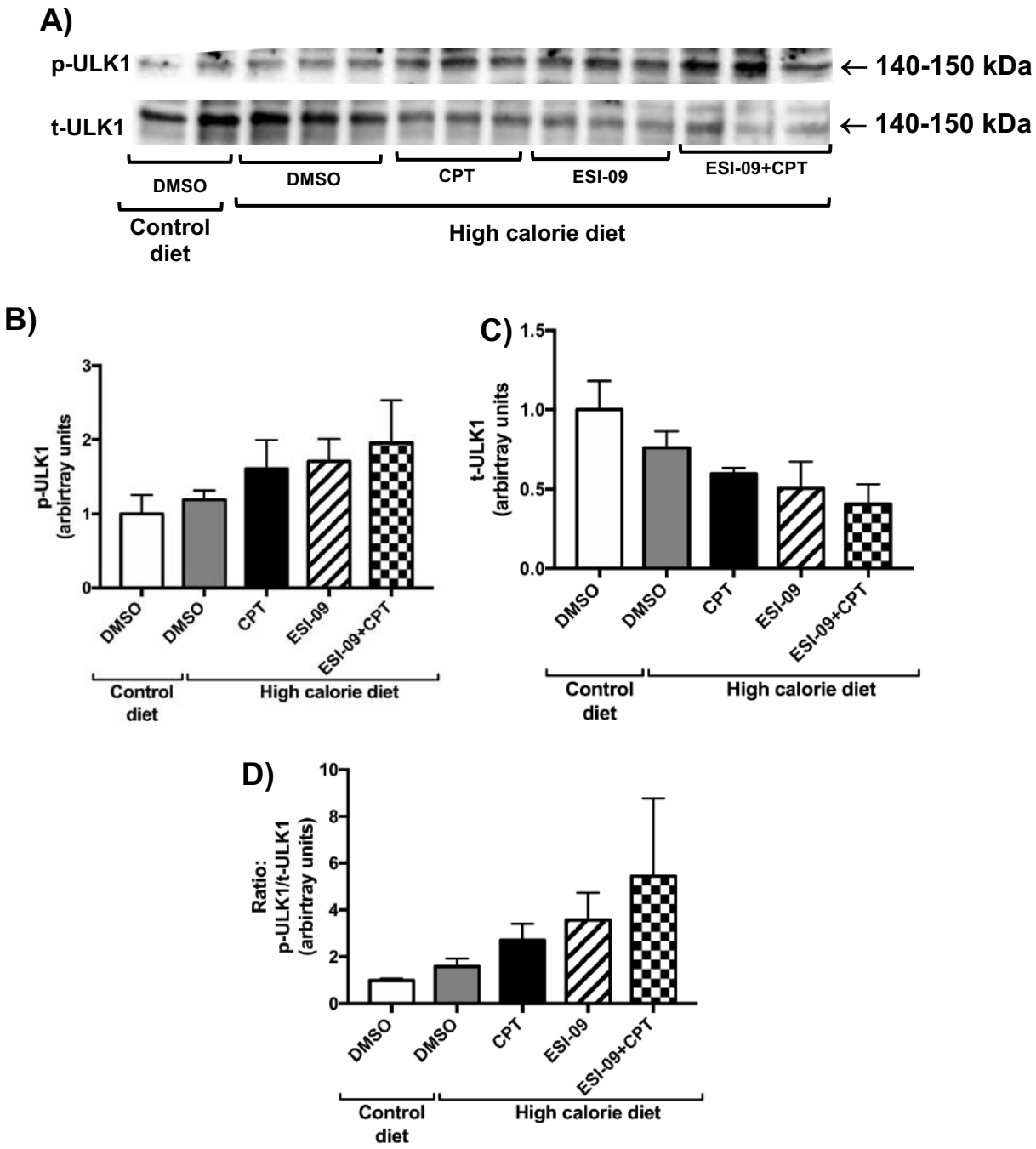

Figure 3. 36 ULK1 phosphorylation and expression in hearts from the HC group post-treated with an Epac activator (CPT, 2 μM) and Epac inhibitor (ESI-09, 5 μM) in the first 10 minutes reperfusion.

(A), representative Western blots for phosphorylated and total ULK1; (B), phosphorylated ULK1 levels; (C), total ULK1 levels; (D), phospho/total ratio for ULK1. n = 3 per group. All values are expressed as mean ± SEM.

3.4 Discussion

In this study, we aimed to elucidate the mechanisms involved in Epac-induced cardioprotection by evaluation of the following cellular pathways and processes: the RISK pathway, nitric oxide signalling, calcium signalling, apoptotic signalling and autophagy. Therefore, we have established a pre-diabetic model with rats on a HC diet for 16 weeks. These rats had increased body weight, increased intraperitoneal fat, elevated non-fasting glucose concentration and increased HOMA-IR index. However, the HC diet had no detrimental effects on post ischaemic cardiac function and infarct size. The HC diet effects were associated with activated cardioprotective proteins PKB (Figure 3.15) and eNOS, but also increased Calcineurin and cleaved PARP.

We have demonstrated that Epac activation, with a selective agonist, CPT (2μM), at reperfusion protected the hearts against I/R injury, independent of the diet. The CPT-mediated protection, based on post ischaemic recovery of cardiac function and infarct size, was partially mediated by PKB and ERK (Figure 3.9) in the CD group, but mainly by PKB in the HC group.

Interestingly, CPT activated CaMKII in the HC group but not eNOS and therefore this needs further elucidation. Epac inhibitor (ESI-09, 5 μM) was detrimental to cardiac function and was associated with decreased phosphorylated ERK1/2 in both diets, decreased phosphorylated GSK-3β in CD, increased phosphorylated AMPK in both diets, increased PARP cleavage in CD and increased autophagy (phosphorylated ULK-1) in CD.

3.4.1 The effect of diet on I/R

In the current study, Wistar rats fed a HC had a significant increase in body weight and intraperitoneal fat which may be an indication of overweight/obesity. This was associated with an elevation in non-fasting glucose concentration and insulin resistance (HOMA-IR index) after 16 weeks on diet. These data confirm the insulin resistant, pre-diabetic model from previous findings by Salie and colleagues (Salie *et al*., 2014). In the clinical setting, obesity is a risk factor for hypertension, dyslipidemia,

insulin resistance and diabetes, which may all increase the risk of myocardial infarction and eventually heart failure (Martí, 2016; Pi-Sunyer, 2009; Ritchie and Connell, 2007).

We found that, even though the HC rats developed metabolic disturbances, the baseline cardiac function was comparable to the CD group (Table 3.2). The infarct size was also the same as the CD group after I/R injury. However, our research indicated that the post-ischaemic cardiac function was affected by HC diet as shown by a decrease in percentage recovery of TW compared to CD group (Figure 3.5B). In contrast, Salie and co-workers (2014) have demonstrated that a high-fat diet protects the hearts against I/R injury in non-preconditioned hearts (Salie *et al*., 2014). Similar to our work, Thim and co-workers (2006) also showed that Sprague–Dawley rats fed moderate high-fat diets for 13 weeks developed metabolic disturbances (similar to metabolic syndrome), but the infarct size did not change after the hearts were exposed to I/R (Thim *et al*., 2006). The explanation for these findings in our study might be due to the fact that the rats did not develop diabetes. Therefore, HC feeding in rats mimics the prediabetic condition and it has been reported that up to 70% of prediabetic patients eventually develop diabetes, which increases the chances of developing cardiovascular disease (Rahmati-Najarkolaei *et al*., 2017). Another explanation might be the type of fat we used to induce obesity. Holsum, used in our HC, is a solid vegetable oil made from palm oil which contains palmitic acid as the main saturated fat. It has been reported that palmitic acid from palm oil has the same effect on the lipid profile as oleic acid (a monosaturated fat) (Odia, 2015). Furthermore, palm oil contains powerful antioxidants including oleic and linoleic acids, and vitamin E tocotrienols which may be cardioprotective (Chong and Ng, 1991; Odia, 2015). In most studies, animal fat (lard) is used to induce the insulin resistance, diabetes and to mimic metabolic syndrome (Briaud *et al*., 2002; Gustafson *et al*., 2002; Haluzik *et al*., 2004; Yaspelkis *et al*., 2001). Hence, in our study, despite the lack of animal fat, the rats on the HC presented with early signs of metabolic disturbances.

The HC model in our study also demonstrated a significant rise in phosphorylated PKB. Insulin activation of PKB, a pro-survival kinase has been reported to be cardioprotective against I/R injury by preventing mPTP opening (Davidson *et al*., 2006; Matsui *et al*., 2001). Our findings suggest that the HC diet did not impair the insulin-dependent activation of PKB even though the animals had signs of insulin resistance.

However, it has been shown that high-fat induced hyperinsulinemia and high plasma FFAs improved cardiac metabolism in spite of peripheral insulin resistance (Gupte *et al*., 2013). Insulin resistance in peripheral tissues (skeletal muscle, liver and adipose tissue) is believed to be the factor behind impaired glucose homeostasis and diabetes (Kahn *et al*., 2006). The heart is an insulin-sensitive organ and the impairment of insulin PI3K-PKB-eNOS-NO pathway may affect cardiovascular performance and could eventually lead to heart failure (Mangmool *et al*., 2017).

Surprisingly, we found that the hearts from the HC group had an increase in phosphorylated eNOS which could be cardioprotective when compared to the CD group. In models of obesity and insulin resistance, phosphorylation of eNOS (downstream of PKB) is downregulated (HuisamenB *et al.*, 2011; Wensley *et al*., 2013). However, it has also been demonstrated that high carbohydrate-induced obesity improved PKB and eNOS indicating cardioprotection in insulin resultant rats (Donner *et al*., 2013).

Furthermore, a study by Donner and co-workers (2012), demonstrated that obesity improves myocardial tolerance to I/R through activation of PKB, eNOS, ERK1/2 and phosho-inhibition of GSK3β in insulin-sensitive Wistar rats (Donner *et al*., 2012). The phospho-inhibition of GSK3β at Ser^{9} is known to protect the heart through inhibition of mPTP opening (Fullmer *et al*., 2013; Tsang *et a*l., 2005; Yu and Cui, 2016). We found that phosphorylated PKB in HC hearts was not associated with phospho-inhibited GSK3β which was not consistent with the previous finding (Donner *et al*., 2012). It has previously demonstrated that GSK3β inhibition is not essential IPreC and IPosC in mice (Nishino *et al.*, 2008).

MEK-ERK 1/2 is part of the RISK pathway and the downregulation of ERK1/2 leads to Ca^{2+} overload which could contribute to cell death by inducing cardiomyocyte hypercontracture and mPTP opening (Hausenloy *et al*., 2009). ERK1/2 has been reported to participate cardioprotection of IPreC, IPosC and pharmacological postconditioning against I/R injury (Chen *et al*., 2008; Tai *et al*., 2012). In the current study, the HC diet had no detrimental effects on ERK1/2. In most studies, diabetes, rather than a non-diabetes inducing high-fat diet, seems to be the main factor that

contributes to downregulation of ERK1/2 (Kim *et al*., 2010; Lambert *et al*., 2014; Tai *et al*., 2012).

Interestingly, we found that the HC hearts had an increase in calcineurin compared to controls. Calcineurin is a calcium-calmodulin-activated, serine/threonine protein phosphatase that responds to elevated intracellular Ca^{2+} (Crabtree, 1999; Klee *et al*., 1998). Calcineurin is known for its role in hypertrophy (Wilkins and Molkentin, 2002) and also known to trigger apoptosis or mediate pro-apoptotic effects in cardiomyocytes (Wang *et al*., 2011). A study by He and co-workers (2014) suggests that activated calcineurin induces apoptosis by suppressing AMPK/mTOR-dependent autophagy is a mechanism that protects cardiomyocytes against oxidative stress (He *et al*., 2014). It is still not clear whether calcineurin is protective or anti-protective in the heart. Furthermore, it has been reported to be cardioprotective in a muscle lim protein (MLP) knock-out mice (Heineke *et al*., 2010). We also observed that the HC diet had no effects on nitrotyrosine, a marker for oxidative stress (Ahsan, 2013). Others have shown high-fat increases the expression of nitrotyrosine and alter myocardial oxidative stress and function after I/R injury (Liu and Lloyd, 2013).

Even though we did not see changes in nitrotyrosine, the apoptotic proteins poly (ADP-ribose) polymerases (cleaved-PARP) and cleaved -caspase-3 were higher (but not significant) in these hearts versus the CD group**.** This might be attributed to the palmitic acid which is the major saturated fatty acid in our HC diet. Palmitate has been demonstrated to induce apoptosis by increasing the activity of caspase-3 and PARP in cardiomyocytes (Wei *et al*., 2013). Although PARP is involved in routine DNA repair processes, its activation is an indicator of cellular stress (Chaitanya *et al*., 2010).

3.4.2 The role of Epac and the RISK pathway on cardiac function and infarct size

Epac-Rap has a broad spectrum of effects in cardiac pathophysiology including cardiac hypertrophy, arrhythmias and heart failure (Morel *et al*., 2005; Okumura *et al*., 2014; Pereira *et al*., 2017). However, little is known about Epac's cardioprotective

effects. In the current study, we have found that an acute administration of an Epac selective agonist CPT (2 μM) in the first 10 minutes of reperfusion significantly improved post ischaemic cardiac function (Table 3.3) and reduced infarct size (Figure 3.9 and 3.10) in both HC and CD groups. These findings suggests that Epac-mediated protection was independent of the HC diet and resultant increased body weight.

On the other hand, we observed that the selective inhibition of Epac with ESI-9 (5 μM) did not affect infarct size, instead it enlarged the area risk (as explained in chapter 2, section 2.4). In addition, ESI-09 had a detrimental effect on cardiac function in both HC and CD groups. This emphasizes the important role of Epac in normal cardiac physiology.

The current study focused on ischaemic post-treatment with CPT as a potential clinical relevant model of cardioprotection. Our findings showed that post-treatment with CPT improved post-ischaemic total work performance of the heats in the HC group, as well as aortic flow and cardiac output recovery in the CD group. In contrast, others who also used a similar model of I/R injury found that pre-treatment with CPT (1 μM) for 10 minutes had no effect on post-ischaemic cardiac functional recovery (Duquesnes *et al*., 2010). Another recent study by Khaliulin and co-workers (2017) demonstrated that pre-treatment with CPT (10 μM) alone had no effect on haemodynamic functional recovery but co-treatment with a PKA activator yielded a significant haemodynamic functional recovery (Khaliulin *et al.*, 2017). Therefore our post-treatment model was more effective since a low concentration of CPT could elicit protection. The protection was likely to be PKA independent as it was previously shown that CPT has a low affinity for PKA (Enserink *et al*., 2002; Poppe *et al*., 2008) and therefore, treating hearts with CPT did not alter PKA activity (Khaliulin *et al.,* 2017). Furthermore, Mangmool *et al*. (2015) reported that Epac has a crucial role in glucagon-like peptide-1 receptor (GLP-1R)- mediated inhibition of oxidative stress and apoptosis in neonatal cardiomyocytes (Mangmool *et al.*, 2015). Edland and co-workers (2016) have reported that Epac1 is required in HFD cardioprotection which may explain the so-called “obesity paradox” (Edland *et al.*, 2016). Therefore, when we pharmacologically activated Epac with CPT in the first 10 minutes of reperfusion it elicited cardioprotection against I/R injury. In cardioprotection, time is an important factor especially during early reperfusion to prevent ROS production. In this regard, we

further investigated the mechanism of Epac-induced protection by studying the pro-apoptotic cascades and the RISK pathway, after activation with CPT at reperfusion.

We defined the role of the RISK pathway in CPT-induced cardioprotection using PKB (A6730) and MEK-ERK1/2 (PD98058) inhibitors, respectively. In the HC group, ERK inhibition did not affect CPT protection. However, the PKB antagonist A6730 abolished CPT induced functional recovery in HC hearts. PKB is a key player in the modulation of myocardial contractility and intracellular Ca^{2+} handling (Cittadini *et al*., 2006; Condorelli *et al*., 2002). Furthermore, Epac activation with CPT (10 μM) enhances phosphorylation of PKB at Ser^{473} suggesting its contribution to Ca^{2+} spark via NOS (Pereira *et al*., 2017). Therefore, the findings suggest that Epac activation with CPT enhances myocardial contractility and could be partially medicated via PKB. We also found that CPT reduced infarct size in the HC group and co-treatment of CPT and A6730 abolished the protection. We speculate that the post-treatment with CPT enhanced activation of the survival kinase PKB in that first 10 minutes of reperfusion and prevented the opening of the mPTP which led to the reduced infarct size.

3.4.3 Mechanism of cardioprotection: signalling pathways

We showed that Post-treatment with CPT in the HC group increased phosphorylated PKB compared to CD DMSO control group but not HC DMSO control (Figure 3.15). This effect was abolished by a PKB inhibitor A6730. Furthermore, CPT administration had no significant effect on the MEK-ERK1/2 signalling cascades. However, Epac inhibition with ESI-09 significantly reduced ERK1/2 phosphorylation, but had no effect on PKB. It has been shown that IPosC is cardioprotective against I/R injury through activation of PI3K-PKB and its downstream targets eNOS and GSK3β (but not ERK1/2) (Zhu *et al*., 2006). The PI3K-PKB-eNOS-NO signalling pathway is also known to be cardioprotective (Zhang and Casadei, 2012). We demonstrated that Epac activation with CPT significantly decreased phosphorylated eNOS in the HC group. However, we also found that the HC diet alone significantly increased phosphorylated eNOS compared to hearts from the CD control group. Therefore, the western blot results do not confirm or explain the reduction of infarct size caused by CPT. An

alternative pathway needs to be investigated e.g. connexins (Schulz *et al*., 2007) or the survivor activating factor enhancement (SAFE) pathway (Lecour, 2009).

Interestingly, we found that CPT significantly increased CaMKII (Thr^{286}) phosphorylation which was reversed by ESI-09. It has been demonstrated that oxidative stress and I/R injury downregulate the anti-apoptotic isoforms of CaMKII - delta B and upregulate the pro-apoptotic isoform of CaMKII-delta C (Little *et al*., 2009; Peng *et al*., 2010). Sarcoplasmic reticulum Ca^{2+} leakage is associated with CaMKII-dependent phosphorylation of RyR2 in heart failure myocytes, thus leading to arrhythmias and contractile dysfunction (Ai *et al*., 2005). Oxidative stress increases Ca^{2+} leaks causing mitochondrial Ca^{2+} overload that leads to a release of caspase cofactors and apoptosis (Pinton *et al*., 2008). In this regard, it has been shown that Epac activation with CPT increases Ca^{2+} sparks via CaMKII activation in cardiomyocytes (Pereira *et al*., 2007). Therefore, the phosphorylation of CaMKII at Thr^{286} by CPT (2 µM) had no detriment effects, instead, it was cardioprotective as shown by the reduced infarct size in HC hearts in this study.

Epac inhibition with ESI-09 significantly increased AMPK phosphorylation in the current study. AMPK is a stress-activated kinase that responds to intercellular stress such as glucose deprivation, hypoxia, oxidative stress and ATP depletion (Nagata *et al*., 2003). We demonstrated that the hearts treated with ESI-09 (5 µM) went into contracture in the first 5 minutes of treatment, followed by a loss in cardiac function (Table 3.3). Therefore, we can speculate that an increase in AMPK was due to cellular stress caused by ESI-09 and resulted in poor cardiac perfusion. On the other hand, AMPK activation in early reperfusion was shown to be cardioprotective by reducing infarct size (Paiva *et al*., 2011, 2010). Even though we found that the ESI-09 treated hearts also had a reduction in infarct size, this was rather due to a significant increase in the area at risk than a true decrease in necrotic tissue. ESI-09 was previously reported to have general protein denaturing properties, suggesting that ESI-09's "inhibitory" properties originate from its protein destabilizing effect (Rehmann, 2013). This raised a concern that ESI-09 may not act exclusively on Epac (Rehmann, 2013). Studies have demonstrated that ESI-09 synergistically suppresses pancreatic cancer cell proliferation and survival (Wang *et al*., 2017). Interestingly, we found that both CPT

and ESI-09 increased the apoptotic marker, cleaved PARP in the control group. The reason for this is unclear and needs to be investigated further. In the HC group, on the other hand, we found that ESI-09 had no effect on apoptosis markers, cleaved caspase-3 and PARP, nor on the oxidative stress maker, nitrotyrosine.

3.4.4 The role of Epac in autophagy

Epac has been reported to promote cardiac remodelling and ventricular hypertrophy (Métrich *et al*., 2008; Morel *et al*., 2005; Schwede *et al*., 2015). Emerging evidence suggests that cardiac autophagy is upregulated in cardiac remodelling to reverse ventricular hypertrophy by increasing protein degradation (Gottlieb and Mentzer, 2013). In our study, Epac inhibition with ESI-09 increased (though not significantly) phospho-dynamin-related protein 1 (DRP1 Ser^{616}) in the HC group. DRP1 is upregulated in excessive mitochondrial fusion which contributes to cell death during I/R injury (Ong *et al*., 2010). Excessive mitochondrial fusion causes mitochondrial fragmentation, ATP depletion, ROS accumulation and a release of apoptotic cofactors (Hu *et al*., 2017; Park *et al*., 2018). In contrast, some studies indicate that inhibition of DRP1 reduces mitochondrial damage and myocardial injury (Disatnik *et al*., 2013; Lin *et al*., 2017). Recently Huang and colleagues (2018) showed that inhibition of the ERK-DPR1 pathway reduces insulin-like growth factor receptor II (IGF-IIR)-mediated mitochondrial dysfunction during heart failure (Huang *et al*., 2018). IGF-IIR has been demonstrated to promote activation of JNK-mediated Bcl-2 phosphorylation to promote ULK1/Beclin 1-dependent autophagosome formation (Huang *et al.,* 2018). In our study Epac activation with CPT reduced phospho ULK1 at (Ser^{555}) and co-treatment with ESI-09 increased its phosphorylation in the CD group. In the HC group, however, CPT and ESI-09 had no effect on phosphorylation or expression of ULK1. Collectively, this suggests that an association exists between Epac and autophagy. This needs further investigation and the use of autophagy inhibitors might provide a better understanding.

Chapter Four

The role of Epac signalling in *ex vivo* thoracic aortas from a rat model of high-calorie diet-induced obesity

4.1 Introduction

The vascular endothelium modulates vascular function and homeostasis, and serves as the structural barrier between blood vessels and surrounding tissues (Tousoulis *et al*., 2011). Furthermore, vascular endothelial cells are the primary targets for a range of harmful metabolic stimuli associated with cardiovascular risk factors, including obesity and insulin resistance (Bakker *et al*., 2000; Heusch *et al*., 2014; Steinberg *et al*., 1994). Such stimuli can cause both vascular smooth muscle cells and vascular endothelial cells to undergo phenotypic changes resulting in the development of cells with a proliferative and migratory phenotype that can contribute to endothelial dysfunction (Lezoualc'H *et al*., 2016). Prolonged exposure of the endothelium to potentially noxious stimuli such as inflammation, high circulating free fatty acids, increased levels of oxidised low-density lipoproteins (LDL_{ox}) and hyperglycaemia can be associated with obesity-induced endothelial dysfunction (Deanfield *et al*., 2007).

Endothelial dysfunction is characterised by reduced nitric oxide (NO) bioavailability resulting in an increase in oxidative stress in the endothelium and this results in a phenotype characterized by impaired endothelium vasodilation and a proinflammatory and prothrombic status (Rogier van der Velde *et al*., 2015). The endothelium mainly secretes mediators such as NO to maintain homoeostasis (Tousoulis *et al*., 2011). NO is a soluble gas synthesised from the amino acid L-arginine in endothelial cells by the nitric oxide synthase (NOS) (Behrendt and Ganz, 2002; Palmer *et al*., 1988). Endothelial NOS (eNOS) is one of the three distinct isoforms of NOS and is constitutively expressed. eNOS is referred to as a Ca^{2+}- calmodulin-dependent enzyme even though it can also be activated in a Ca^{2+}-independent manner (Behrendt and Ganz, 2002; Förstermann and Kleinert, 1995). Shear stress (forces exerted on the vascular wall by blood flow) is the main trigger of NO production under physiological conditions. Other triggers include acetylcholine (ACh), serotonin, thrombin and bradykinin (Behrendt and Ganz, 2002).

cAMP is one of the well-known second messenger signalling molecules which mediates a wide range of vascular processes, including endothelial barrier function and vasodilation (Patterson *et al*., 2000; Roberts and Dart, 2014).

Impaired cGMP and cAMP-mediated vasorelaxation in the smooth muscle cells was associated with reduced endothelium-derived NO production in rats with chronic heart failure (Nasa *et al.*, 1996). Epac proteins (downstream effectors of cAMP) are a family of guanine nucleotide exchange factors (GEFs) for the small GTPases, Rap1(Epac1) and Rap2 (Epac2) (De Rooij *et al*., 2000; Kawasaki *et a*l., 1998). Current studies have provided evidence on the role of Epac in the vasculature using healthy animal model (Cuíñas e*t al*., 2016; García-Morales *et al.*, 2017, 2014; Lakshmikanthan *et al.*, 2014). However, based on our knowledge there are no studies on rat models that show a link or a role for Epac in obesity/high-calorie induced endothelium dysfunction. Therefore, the aim of this chapter was to elucidate a putative role Epac signalling in *ex vivo* thoracic aortas of a rat model of high calorie diet-induced obesity.

4.2 Materials and methods

4.2.1 General materials used

Cell Signaling Technologies (Beverly, MA, USA): antibodies

1. Total ERKp44/p42 (catalogue number: #9102)
2. Phospho-ERKp44/p42 (Thr^{202}/Tyr^{204}) (catalogue number: #9101)
3. Total PKB (catalogue number: #4691)
4. Phospho-PKB (Ser^{473}) (catalogue number: #4058)
5. Total CREB (catalogue number: #4820)
6. Phospho-CREB (Ser^{133}) (catalogue number: #9198)
7. Total eNOS (catalogue number: #9572)
8. Phospho-eNOS (Ser^{1177}) (catalogue number: #9571)

Sigma-Aldrich (St Louis, Mo, USA)

1. 8-pCPT-2'-O-Me-cAMP (CPT): Epac agonist. (catalogue number: #C8988)
2. Isoproterenol hydrochloride (ISO): (catalogue number: #I6504)
3. N(ω)-nitro-L-arginine methyl ester (L-NAME) (catalogue number: #N5751)
4. Phenylephrine (PE) (catalogue number: #P6126)
5. Acetylcholine (ACh) (catalogue number: #A6625)

Biolog Life Science Institute (Bremen, Germany)

2. 3- [5- (tert.-Butyl)isoxazol- 3- yl]- 2- [2- (3- chlorophenyl)hydrazono]- 3- oxopropanenitrile (ESI-09): Epac antagonist (catalogue number: #B133-05)

Millipore (Billerica, MA, USA)

1. Signal Boost™ Immunoreaction Enhancer Kit (catalogue number: #4072070)
2. Anti-Rap1 antibody (catalogue number #07-916)

All other chemicals were of Analar grade and were purchased from Merck (including methanol, standard salts for solutions and buffers, and dimethyl sulfoxide (DMSO)).

4.2.2 Assessment of vascular reactivity

Male Wistar rats were obtained from the University of Stellenbosch Central Research Facility (Tygerberg Campus) and the study was approved by the University of Stellenbosch ethics committee (SU-ACUD14-00020). The animals were housed as described in Chapter 3, Section 3.2.2. After 16 weeks on the different diets (as described in Chapter3, Section 3.2.2, Table 3.1), rats were anaesthetized by lethal intraperitoneal injection of pentobarbital (160 mg/kg) for sacrifice. The chest cavity was opened by incision. The thoracic aorta was carefully excised and placed in ice-cold Krebs Henseleit buffer (mmol/L: NaCl 119, KCl 4.74, $CaCl_2$ 1.25, $MgSO_4$ 0.6, Na_2SO_4 0.59, KH_2PO_4 1.79, $NaHCO_3$ 24.9, Glucose 10). Excess perivascular fat (PVAT) and connective tissue were removed. Aortas were cut into 3 - 5 mm ring segments, mounted onto 2 steel hooks and suspended horizontally in a 25 ml organ bath (AD Instruments, Bella Vista, New South Wales, Australia) containing oxygenated (95% O_2, 5% CO_2) Krebs-Henseleit buffer at 37°C. Aortic ring tension was recorded with an isometric force transducer (TRI202PAD, Panlab, lCornellà, BCN, Spain) and data analysed with AD LabChart 7 software (Dunedin, New Zealand). The isometric tension measurement followed a modified protocol of a previously described technique (Privett *et al*., 2004).

Briefly, aorta rings were equilibrated at a resting tension of 1.5 g for at least 30 minutes, during which the Krebs buffer was replaced every 10 minutes with pre-warmed Krebs buffer. After stabilization, the isometric contraction was induced with 100 nM phenylephrine (PE), followed by 10 µM acetylcholine (ACh)-induced relaxation to confirm the presence of functional endothelium.

For the assessment of vascular reactivity, aortic ring function was evaluated by pre-contraction with cumulative PE: 100 nM-1 µM, followed by cumulative ACh induced relaxation (30 nM-10 µM) (Fig. 4.1). Preceding this cumulative contraction-relaxation responses, aortas were stabilized for 30 minutes and pre-incubated for 15 min with either a beta-adrenergic agonist, isoproterenol (ISO, 0.1µM) or Epac selective-agonist, 8-pCPT-2'-O-Me-cAMP (CPT, 2 µM) or novel Epac inhibitor, ESI-09 (5 µM) or NOS inhibitor N(ω)-nitro-L-arginine methyl ester (L-NAME, 100 µM), respectively.

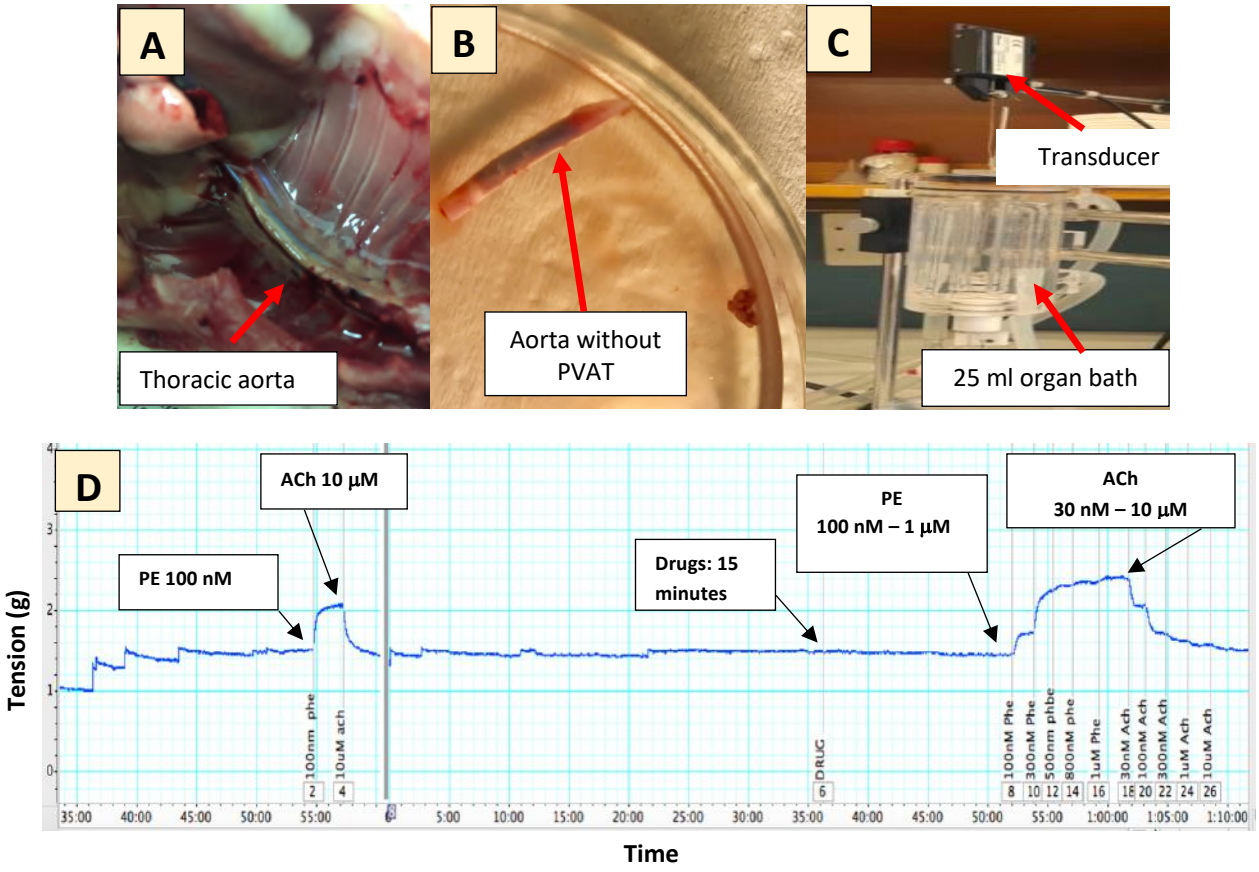

Figure 4. 1 Vascular reactivity experimental protocol.

(A) Wistar rat thoracic aorta, (B) aorta without PVAT, (C) 25 ml organ bath used for isometric tension studies, (D) isometric tension chart (AD LabChart 7 software).

4.2.3 Western blot measurements

Rat thoracic aortas were excised and PVAT and connective tissue were removed, and incubated into an organ bath containing 25 ml Krebs-Henseleit buffer solution completely submerge for 30 minutes stabilization followed by 15 minutes treatment with the following drugs (beta-adrenergic agonist, isoproterenol (ISO, 0.1 µM) or Epac selective-agonist, 8-pCPT-2'-O-Me-cAMP (CPT, 2 µM) or novel Epac inhibitor, ESI-09 (5 µM), respectively). Thereafter, the aortas were snap-frozen in liquid nitrogen and stored at -80°C. Frozen aortic tissues were pulverized, and 2-3 aortas were pooled per sample for each experimental group. Aortic tissues were then lysed in homogenization buffer, the composition of the lysis buffer in mM: 20 Tris-HCl, 1 EGTA, 1 EDTA, 150 NaCl, 1 β-glycerophosphate, 2,5 tetra-sodium-pyrophosphate, 1 Na_3VO_4, along with 50 µg/ml PMSF, 10 µg/ml leupeptin, 10 µg/ml aprotinin, 1% Triton

X-100, 0.1% sodium dodecyl sulphate (SDS). A Bradford protein assay was used to measure the concentration of the proteins. For protein separation, an equal amount of lysate (15 μg per well) was separated by SDS-PAGE using 4-15% Criterion™ TGX™ precast gradient gels (Bio-Rad Laboratories, USA). The proteins were transferred to polyvinylidene fluoride (PVDF) membrane, blocked for an hour with 5% long life fat-free milk in Tris-buffered Saline (TBS) containing 0.1% Tween-20. PVDF membranes were then probed with a specific primary antibody in TBS-tween by overnight shaking at 4°C (dilutions of primary antibodies: phosphorylated (p) -ERK, Total (t)-ERK, p-PKB, t-PKB, p-CREB, t-CREB, p-AMPK, t-AMPK p-eNOS, t-eNOS (from Cell signalling, USA) at 1:1000 dilution; for p-eNOS and t-eNOS signal boost (from Millipore, USA) at 1:1000 dilution was used. Membranes were washed and then incubated with horseradish peroxidase-linked secondary antibody (Cell signalling, USA) at 1:4000 dilution for an hour at room temperature. The protein signal was enhanced with a chemiluminescent agent (Bio-Rad Laboratories, USA) and quantified using a Chemidoc-XRs imager and analysed with Image Lab™ 5 Software (Bio-Rad Laboratories, USA).

4.2.4 Statistical analysis

All data are expressed as mean ± standard error of the mean (SEM) and Graph Pad Prism™ 6 used for statistical analyses. Comparisons of groups were performed by one-way ANOVA followed by Bonferroni's post-test or student's t-tests (indicated in grey asterisk) where applicable. Significance was established at a p-value of <0.05.

Vascular reactivity data (E_{max}, maximal tension and R_{max}, maximal relaxation) were analysed by two-way ANOVA followed by Bonferroni's post-test. The EC_{50} (the drug concentration inducing 50% of the maximal response), was determined by nonlinear regression model analysis following the log X (dose) vs. response transformation of the percentage relaxation or tension. Significance was established at a p-value of <0.05.

4.3 Results

4.3.1 Biometric data

Body weights, intraperitoneal fat percentage, glucose and insulin are described in chapter 3, section 3.3.1.

4.3.2 The effect of diet and NOS inhibition on aortic function

Aortas from HC fed rats showed no significant difference in vascular reactivity compared to the CD-fed rats (Fig.4.2A and Fig.4.2B). To assess the NO contribution to endothelium-dependent contraction and relaxation, aortic rings were pre-incubated with a nitric oxide synthase (NOS) inhibitor L-NAME (100 μM) for 30 minutes. PE induced a maximal contraction response (E_{max}) in absence of NO which was significantly higher compared to control rings in both diet groups: CD + L-NAME versus CD (E_{max}: CD + L- NAME: 1.85 ± 0.19 g vs. CD: 0.90 ± 0.09 g, $P<0.05$) (Table 1 and Fig. 4.2A), HC+L-NAME versus HC group (E_{max}: HC+L-NAME: 1.98 ± 0.18 g vs. HC: 0.78 ± 0.07 g, $P<0.05$) (Table 4.1 and Fig. 4.2A).

The maximal relaxation (R_{max}), as induced by Ach, was similar in aortas from both CD and HC groups. Pre-treatment with L-NAME significantly attenuated the ACh-induced relaxation, thereby confirming NOS-dependence in both diet groups. (R_{max}: CD+L-NAME: 8.59 ± 1.72 % vs. CD: 90.70 ± 3.18 %, $P<0.05$; HC+L-NAME: 6.35 ± 1.54 % vs. HC: 87.89 ± 3.47 %, $P<0.05$) (Table 4.1 and Fig. 4.2B).

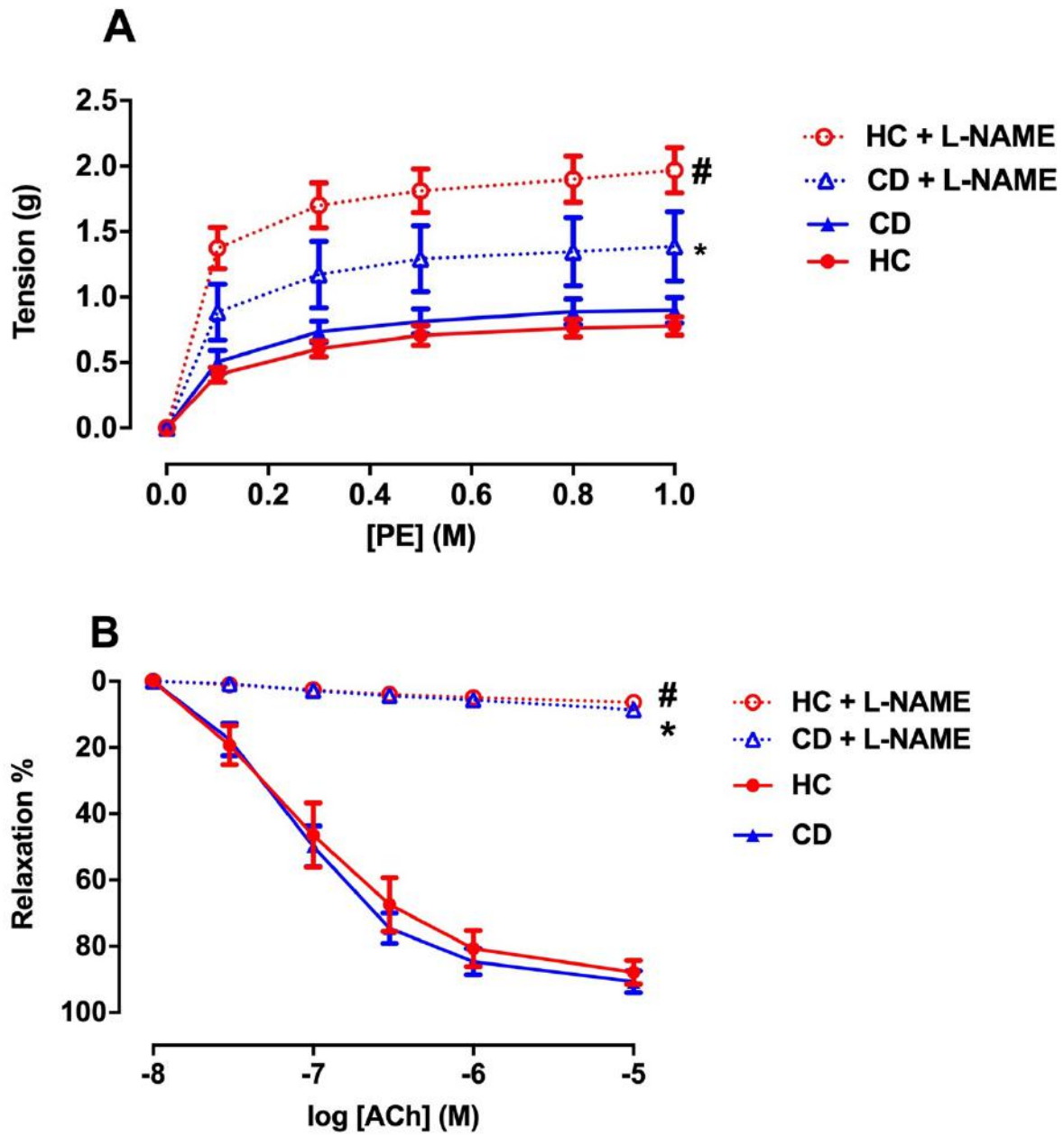

Figure 4. 2 The effect of diet and L-NAME on aortic function.

Aortic rings from rats fed a CD or HC for 16 weeks. (A), aortic tension (g) after phenylephrine (PE) induced contraction in absence or presence of L-NAME; (B), aortic relaxation (percentage) induced by Acetylcholine (ACh) in absence and presence of L-NAME. Data are expressed as mean ± SEM. Two-way ANOVA p-vales: *$p < 0.05$ CD+L-NAME vs CD, $^{\#}p < 0.05$ HC+L-NAME vs HC,. n = 4 per group.

CD: Control diet

HC: high calorie diet

L-NAME: NOS inhibitor (100 μM)

Table 4. 1 The effect of diet and L-NAME on the sensitivity (-LogEC$_{50}$) and maximal effect (E$_{max}$ of PE-induced contraction and R$_{max}$ of Ach -induced relaxation).

Phenylephrine induced contraction			Acetylcholine induced relaxation		
Experimental group (n = 4)	**E$_{max}$ Tension (g)**	**(-LogEC$_{50}$)**	**Experimental group (n = 4)**	**R$_{max}$ (% relaxation)**	**(-LogEC$_{50}$)**
CD	0.9 ± 0.09	0.83 ± 0.96	CD	90.70 ± 3.18	7.07 ± 0.08
HC	0.78 ± 0.07	0.74 ± 0.68	HC	87.89 ± 3.47	7.04 ± 0.13
CD+L-NAME	1.36 ± 0.32*	0.89 ± 2.18	CD+L-NAME	8.59 ± 1.72*	6.50 ± 0.26
HC+L-NAME	1.98 ± 0.18†	0.75 ± 1.14	HC+L-NAME	6.35 ± 1.54†	6.77 ± 0.29

All values are expressed as mean ± SEM. *p < 0.05 vs CD, †p < 0.05 vs HC. n = 4 per group.

CD: Control diet

HC: high calorie diet

L-NAME: NOS inhibitor (100 μM)

4.3.3 Role of Epac in beta-adrenergic stimulation on aortic function

To test the involvement of Epac in beta-adrenergic stimulation on aortic function, aorta rings were pre-incubated with isoproterenol (ISO) (0.1 µM), a beta-adrenergic receptor agonist and Epac was inhibited with a selective inhibitor, ESI-09 (5 µM) prior to PE induced vasocontraction and ACh induced vasorelaxation.

Aorta rings from CD

Pre-incubation of the rat aorta rings from CD animals for 15 min with ISO (0.1 µM) caused a significant increase in PE-induced vasocontraction compared to DMSO vehicle control (E_{max}: CD+ISO: 1.57 ± 0.11 g vs. CD+DMSO: 1.24 ± 0.11 g, $P<0.05$) (Table 4.2 and Fig. 4.3A). Co-incubation with ESI-09 partially reduced the pro-contractile effect of both ISO (E_{max}: CD+ISO+ESI-06: 1.46 ± 0.11 g vs. CD+ISO: 1.57 ± 0.11 g, not significant, ns) (Table 4.2 and Fig. 4.3A) as well as with the vehicle (E_{max}: CD+ESI-06: 1.09 ± 0.14 g vs CD+DMSO: 1.24 ± 0.11 g, ns). There were no significant differences observed in ACh-induced vasorelaxation among the groups (Fig. 4.3B).

Aorta rings from HC

Pre-incubation of the rat aorta rings from HC with ISO had no significant effect in PE induced contraction in HC groups (Fig. 4.4A).

However, ISO (0.1 µM) significantly improved vasorelaxation induced by ACh at the following concentrations: 30 nM (HC+ISO: 40.03 ± 5.36 % vs. HC+DMSO: 17.09 ± 3.40 %, $p<0.05$); 100 nM (HC+ISO: 71.21 ± 5.83 % vs. HC+DMSO: 45.68 ± 6.66 %, $p<0.05$); 1 µM (HC+ISO: 85.21 ± 6.39 % vs. HC+DMSO: 63.21 ± 6.62 %, $p<0.05$) (Fig. 4.4B).

Furthermore, ISO (0.1 µM) was able to effectively improve relaxation of the aortas compared to HC+DMSO aortas (-$LogEC_{50}$: HC+ISO: 7.45 ± 0.09 vs. HC+DMSO: 7.07 ± 0.12, $p<0.05$ (Table 4.2). Co-incubation of ISO (0.1 µM) with ESI-09 partially reduced the pro-relaxant effect of ISO compared to vehicle (-$LogEC_{50}$: HC+ISO+ESI-09: 7.29 ± 0.13 vs HC+DMSO: 7.07 ± 0.12, not significant)(Table 4.2).

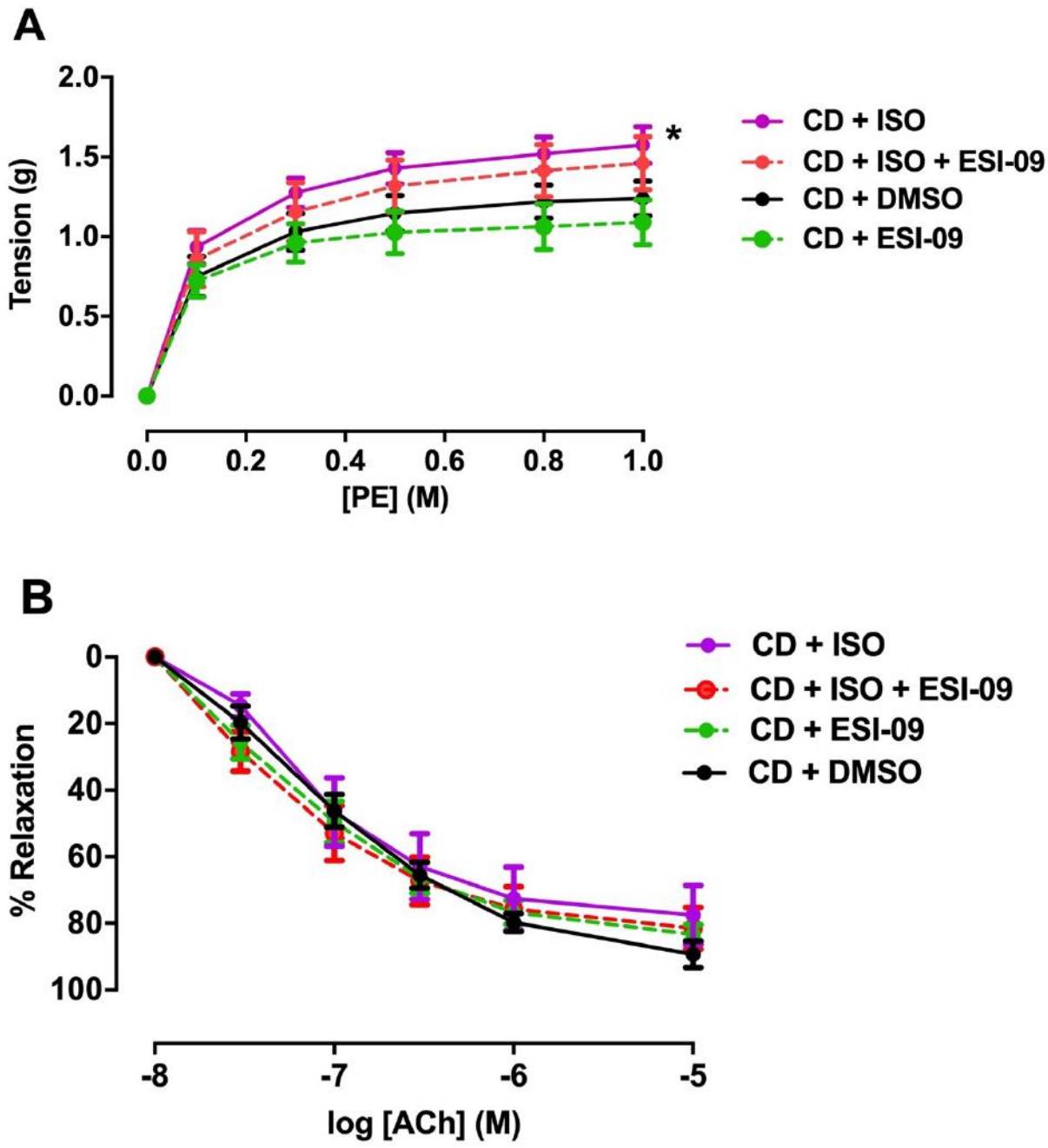

Figure 4. 3 Role of Epac in beta-adrenergic stimulation of aortic function in CD groups.

(A), Phenylephrine (PE) induced endothelium contraction (aortic tension) and (B), Acetylcholine (Ach) induced relaxation (aortic percentage relaxation) on rat aortas fed a CD for 16 weeks. All values are expressed as mean ± SEM. Two-way ANOVA p-vales: *$p < 0.05$ CD+ISO vs CD+DMSO. n = 6-10 per group.

CD: control diet

ISO: beta-adrenergic agonist (0.1 μM)

ESI-05: Epac antagonist (5 μM)

DMSO: vehicle control (0.01%)

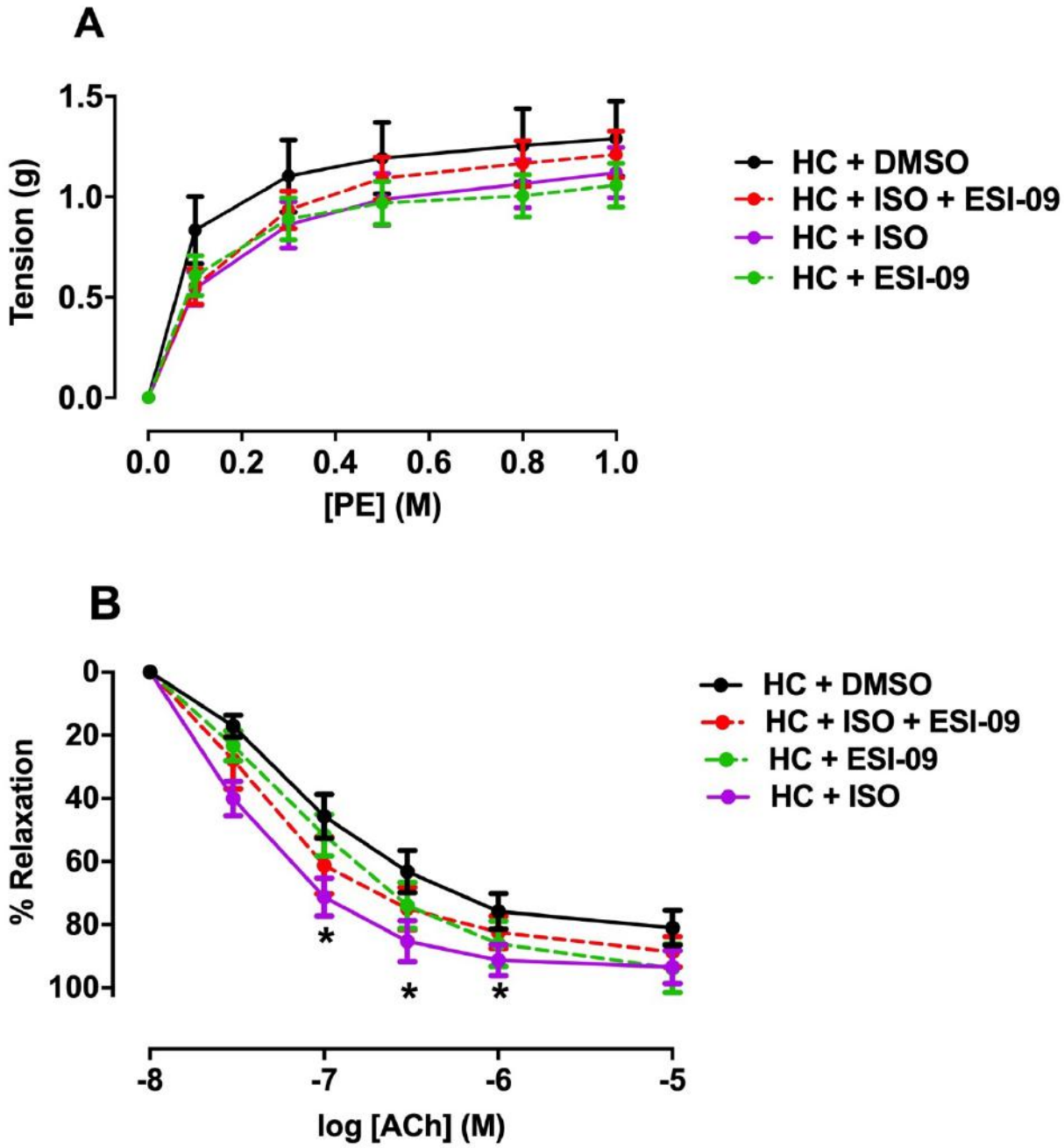

Figure 4. 4 Role of Epac in beta-adrenergic stimulation of aortic function in HC groups.

(A), Phenylephrine (PE) induced endothelium contraction (aortic tension) and (B), Acetylcholine (Ach) induced relaxation (aortic percentage relaxation) on rat aortas fed a HC for 16 weeks. All values are expressed as mean ± SEM. Two-way ANOVA p-vales: *p < 0.05 HC+ISO vs HC+DMSO. n = 6-10 per group.

HC: high calorie diet

ISO: beta-adrenergic agonist (0.1μM)

ESI-05: Epac antagonist (5μM)

DMSO: vehicle control (0.01%)

4.3.4 The effect of Epac on aortic function

To assess the effect of Epac manipulation on PE-induced vasocontraction and ACh-induced vasorelaxation, the aortic rings were pre-incubated for 15 min with CPT, a selective Epac agonist or ESI-09, a specific Epac antagonist prior aortic tension studies.

Aorta rings from CD

Pre-incubation of the rat aorta rings with CPT (2 μM) for 15 min had no significant effect on PE-induced dependent contraction (Fig. 4.5A).

However, the CPT (2 μM) treated aortas showed a significant improvement in ACh-induced vasorelaxation versus the untreated aortas at the following ACh concentrations: 30 nM (CD+CPT: 49.57 ± 10.25 % vs. CD+DMSO: 19.69 ± 4.86 %, $p<0.05$); 100 nM (CD+CPT: 73.60 ± 4.47 % vs. CD+DMSO: 46.19 ± 6.62 %, $p<0.05$) (Fig. 4.5B).

Furthermore, Epac activation with its agonist CPT (2 μM) was able to significantly improve the sensitivity in CD+CPT aortas compared to CD+DMSO aortas ($-LogEC_{50}$: CD+CPT: 7.60 ± 0.14 vs. CD+DMSO: 7.01 ± 0.08, $P<0.05$)(Table 4.2 and Fig. 4.5B). In addition, co-incubation of CPT (2 μM) with its antagonist ESI-09 (5 μM) significantly reduced the sensitivity compared to CPT ($-LogEC_{50}$: CD+CPT+ESI-09: 7.29 ± 0.06 vs. CD+CPT: 7.60 ± 0.14, $P<0.05$)(Table 4.2 and Fig. 4.5B). These findings confirm that the CPT effects were mediated by Epac.

Aorta rings from HC

CPT (2 μM) significantly decreased the maximal contractile response (E_{max}) response of the aorta rings to PE in HC (E_{max}: HC+CPT: 1.02 ± 0.11 g vs, HC+DMSO: 1.29 ± 0.19 g, P<0.05) (Fig. 4.6A).

CPT (2 μM) treated HC aortas significantly increased ACh-induced vascular relaxation as compared to the untreated HC+DMSO aortas at the following ACh concentrations: 100 nM (HC+CPT: 69.23 ± 5.95 % vs. HC+DMSO: 45.68 ± 6.97 %, P<0.01) 300 nM (HC+CPT: 84.87 ± 4.25 % vs. HC+DMSO: 63.21 ± 6.62 %, P<0.05 (Fig. 4.6B). Epac activation with CPT (2 μM) was able to significantly improve the sensitivity of HC aortas to ACh-induced vasorelaxation (-$LogEC_{50}$: HC+CPT: 7.34 ± 0.08 vs. HC+DMSO: 7.07 ± 0.12, p<0.05 (Table 4.2 and Fig. 4.6B) which was reduced by the ESI-09 (5 μM) (-$LogEC_{50}$: HC+CPT+ESI-09: 7.11 ± 0.07 vs. HC+CPT: 7.34 ± 0.08, P<0.05 (Table 4.2 and Fig. 4.6B). There were, however, no significant differences in the maximal vasorelaxation response (R_{max}) values (Table 4.2 and Fig. 4.6B).

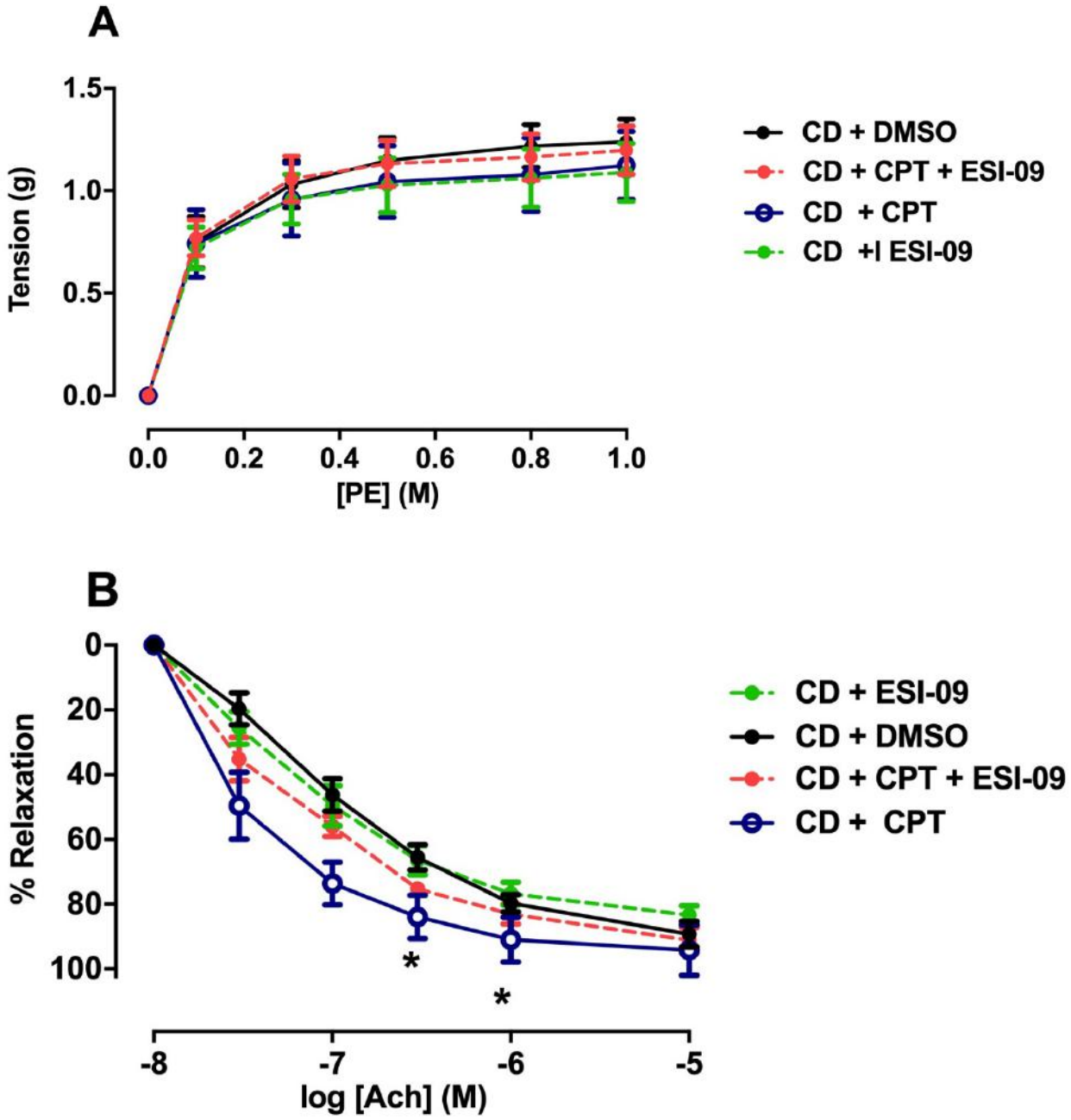

Figure 4. 5 The effect of Epac on aortic function in CD groups.

(A), Phenylephrine (PE) induced endothelium contraction (aortic tension) and (B), Acetylcholine (Ach) induced relaxation (aortic percentage relaxation) on rat aortas fed a CD for 16 weeks. All values are expressed as mean ± SEM. Two-way ANOVA p-vales: *p < 0.05 CD+CPT vs CD+DMSO. n = 6-10 per group.

CD: control diet

CPT: Epac agonist (2 μM)

ESI-09: Epac antagonist (5 μM)

DMSO: vehicle control (0.01%)

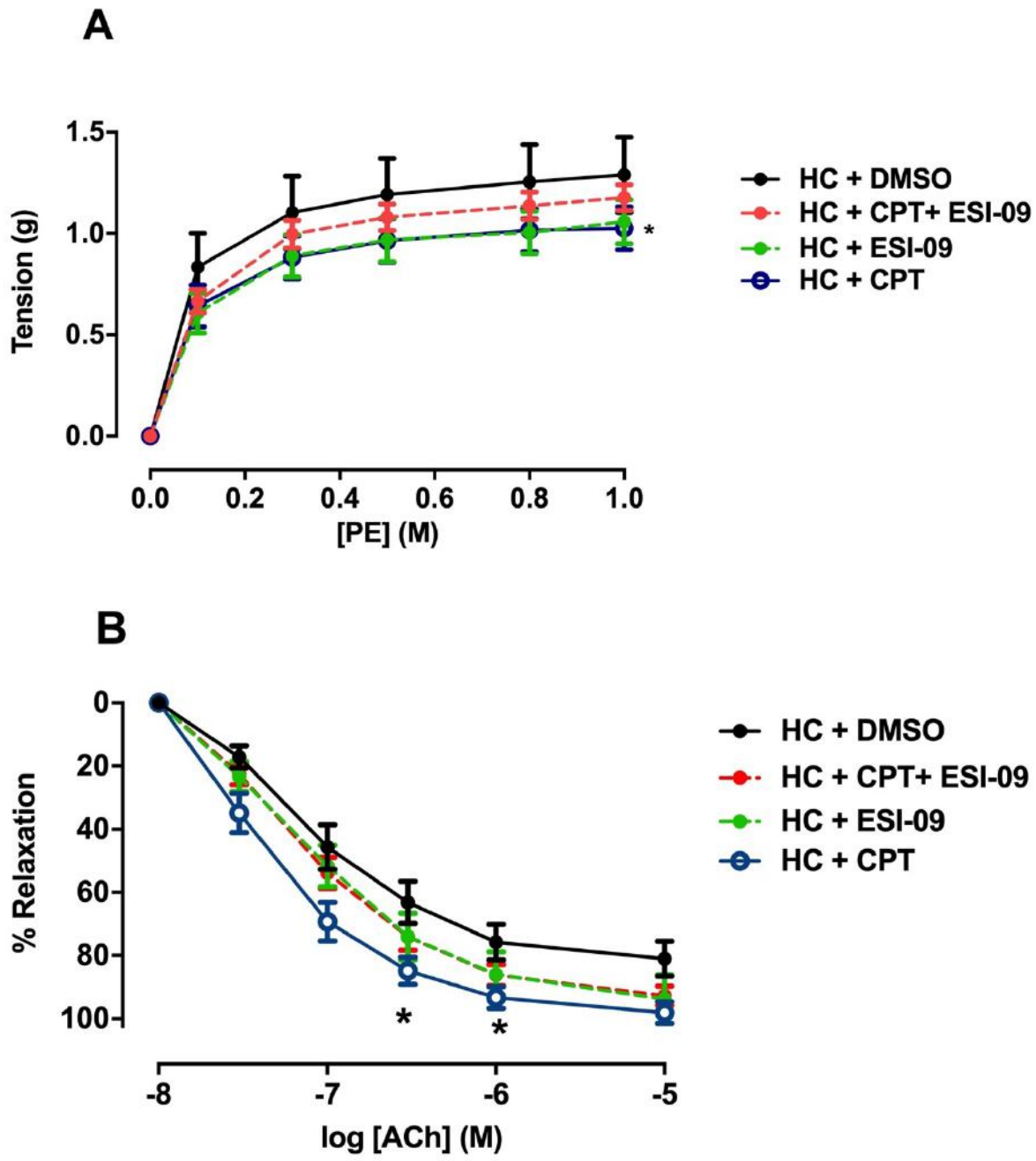

Figure 4. 6 The effect of Epac on aortic function in HC groups.

(A), Phenylephrine (PE) induced endothelium contraction (aortic tension) and (B), Acetylcholine (Ach) induced relaxation (aortic percentage relaxation) on rat aortas fed a HC for 16 weeks. All values are expressed as mean ± SEM. Two-way ANOVA p-vales: *p < 0.05 HC+CPT vs HC+DMSO. n = 6-10 per group.

HC: high calorie diet

CPT: Epac agonist (2μM)

ESI-09: Eapc antagonist (5μM)

DMSO: vehicle control (0.01%

4.3.5 The role of NOS on CPT-induced vasorelaxation

We further investigated whether direct Epac activation could independently induce vasorelaxation. The isolated aortic rings were pre-contracted with PE and then cumulative concentrations of only the specific Epac activator, CPT (2 – 10 μM) were directly administered to the aortas. In addition, to determine the influence of NOS on CPT-induced relaxation, aortas were pre-incubated with L-NAME (100 μM) for 30 minutes. The CPT induced relaxation was significantly attenuated by L-NAME in CD but not in HC aortas (R_{max} :CD+L-NAME: 5.28 ± 0.76 % vs. CD: 10.96 ± 1.97 %, P< 0.05) (Table 4.3 and Fig. 4.7). Furthermore, the CD+CPT and HC+CPT aortas showed greater relaxation compared to baseline controls (R_{max} : CD: 3.11 ± 0.06% vs. CD+CPT: 10.96 ± 1.97, P < 0.05; HC: 3.15 ± 0.74% vs. HC+CPT: 7.27 ± 1.91%, P < 0.05). This suggests that CPT-induced vasorelaxation is mediated by NOS in CD aortas.

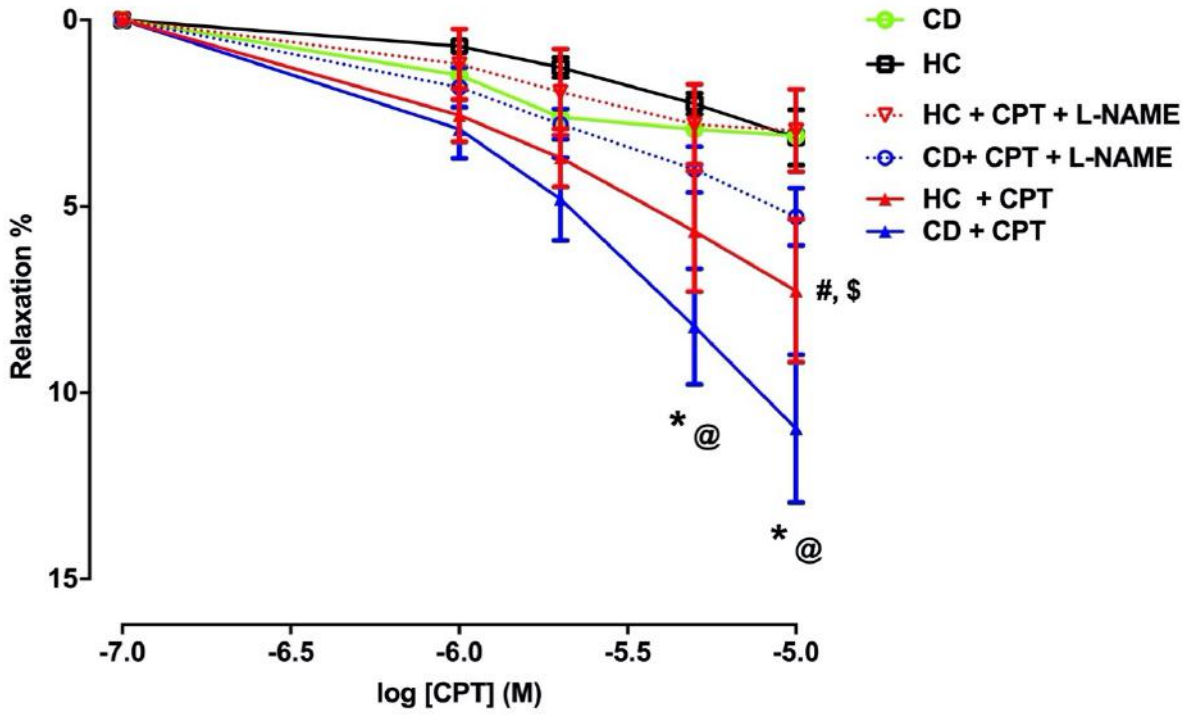

Figure 4. 7 CPT induced aortic relaxation in both CD and HC groups in absence or presence of L-NAME.

All values are expressed as mean ± SEM**.** Two-way ANOVA p-vales: $^{*}p < 0.05$ vs. CD L-NAME, $^{@}p < 0.05$ vs. CD, $^{\#}p < 0.05$ vs. HC+CPT+L-NAME, $^{\$}p < 0.05$ vs. HC. n = 3-4 per group.

Table 4. 2 The effect of Epac manipulation on the sensitivity (-LogEC$_{50}$) and the maximal effect (E$_{max}$ of PE-induced contraction and R$_{max}$ of Ach - induced relaxation).

Phenylephrine induced contraction			Acetylcholine induced relaxation		
Experimental group	**E$_{max}$ Tension (g)**	**(-LogEC$_{50}$)**	**Experimental group**	**R$_{max}$ (% relaxation)**	**(-LogEC$_{50}$)**
CD+DMSO	1,24 ± 0,11	0,87 ± 0,97	CD+DMSO	89,29 ± 3,87	7,01 ± 0,08
CD+CPT	1,13 ± 0,17	0,87 ± 1,97	CD+CPT	94,17 ± 7,62	7,60 ± 0,14*
CD+ESI-09	1,09 ± 0,14	1,21 ± 2,41	CD+ESI-09	83,32 ± 2,77	7,18 ± 0,09
CD+ESI-09 + CPT	1,19 ± 0,12	1,42 ± 2,48	CD+ESI-09 + CPT	91,09 ± 3,77	7,29 ± 0,06†
CD+ISO	1,57 ± 0,11*	0,72 ± 0,62	CD+ISO	77,55 ± 8,80	7,11 ± 0,18
CD+ESI-09 + ISO	1,46 ± 0,17	0,60 ± 1,02	CD+ESI-09 + ISO	81,49 ± 6,23	7,28 ± 0,14
HC+DMSO	1,29 ± 0,187	0,92 ± 1,79	HC+DMSO	81,02 ± 5,44	7,07 ± 0,12
HC+CPT	1,03 ± 0,11	1,06 ± 1,46	HC+CPT	98,11 ± 3,37	7,34 ± 0,08‡
HC+ESI-09	1,06 ± 0,11	1,14 ± 1,45	HC+ESI-09	93,80 ± 7,59	7,09 ± 0,12
HC+ESI-09 + CPT	1,18 ± 0,06	1,20 ± 0,88	HC+ESI-09 + CPT	92,77 ± 3,00	7,11 ± 0,07§
HC+ISO	1,12 ± 0,13	0,78 ± 0,80	HC+ISO	93,44 ± 5,18	7,45 ± 0,09‡
HC+ESI-09 + ISO	1,21 ± 0,12	0,92 ± 0,72	HC+ESI-09 + ISO	88,56 ± 4,66	7,29 ± 0,13

All values are mean ± SEM. n = 6-10 per group.*p < 0.05 vs CD+DMSO, †p < 0.05 vs CD+CPT, ‡p < 0.05 vs. HC+DMSO, §p < 0.05 vs HC+CPT.

CD: control diet **CPT:** Epac agonist (2 μM)

HC: high calorie diet **ESI-09:** Epac antagonist (5 μM)

ISO: beta-adrenergic agonist (0.1 μM) **DMSO:** vehicle control (0.01%

Table 4. 3 Direct effect of CPT on maximal response (R_{max}) and sensitivity ($-LogEC_{50}$) values to CPT, with and without L-NAME in both diet groups.

CPT induced relaxation		
Experimental group	**R_{max} (% relaxation)**	**($-LogEC_{50}$)**
CD *(baseline)*	3.11 ± 0.06	6.1 ± 0.12
CD+CPT	10.96 ± 1.97*@	5.38 ± 0.31
CD+CPT+L-NAME	5.28 ± 0.7	5.59 ± 0.24
HC *(baseline)*	3.15 ± 0.74	5.26 ± 0.34
HC+CPT	7.27 ± 1.91#$	5.58 ± 0.39
HC+CPT+L-NAME	2.97 ± 1.10	5.82 ± 0.64

Aortic percentage relaxation by CPT in absence and presence of L-NAME on thoracic aorta rings fed a CD and HC for 16 weeks. Maximal response and EC_{50} are expressed as mean ± SEM. $^{*}p < 0.05$ vs. CD+CPT+L-NAME, $^{@}p < 0.05$ vs. CD, $^{\#}p < 0.05$ vs. HC+CPT+L-NAME, $^{\$}p < 0.05$ vs. HC. n = 3-4 per group.

HC: high calorie diet

L-NAME: NOS inhibitor (100 μM)

CPT: Epac agonist (2-10 μM)

4.3.6 Western blot results

4.3.6.1 Rap-GDP expression

There were no significant differences in aortic Rap expression between the CD DMSO and the HC DMSO groups. Neither Epac activation nor inhibition caused significant changes in any of the treatment groups (Figure 4.8C and D).

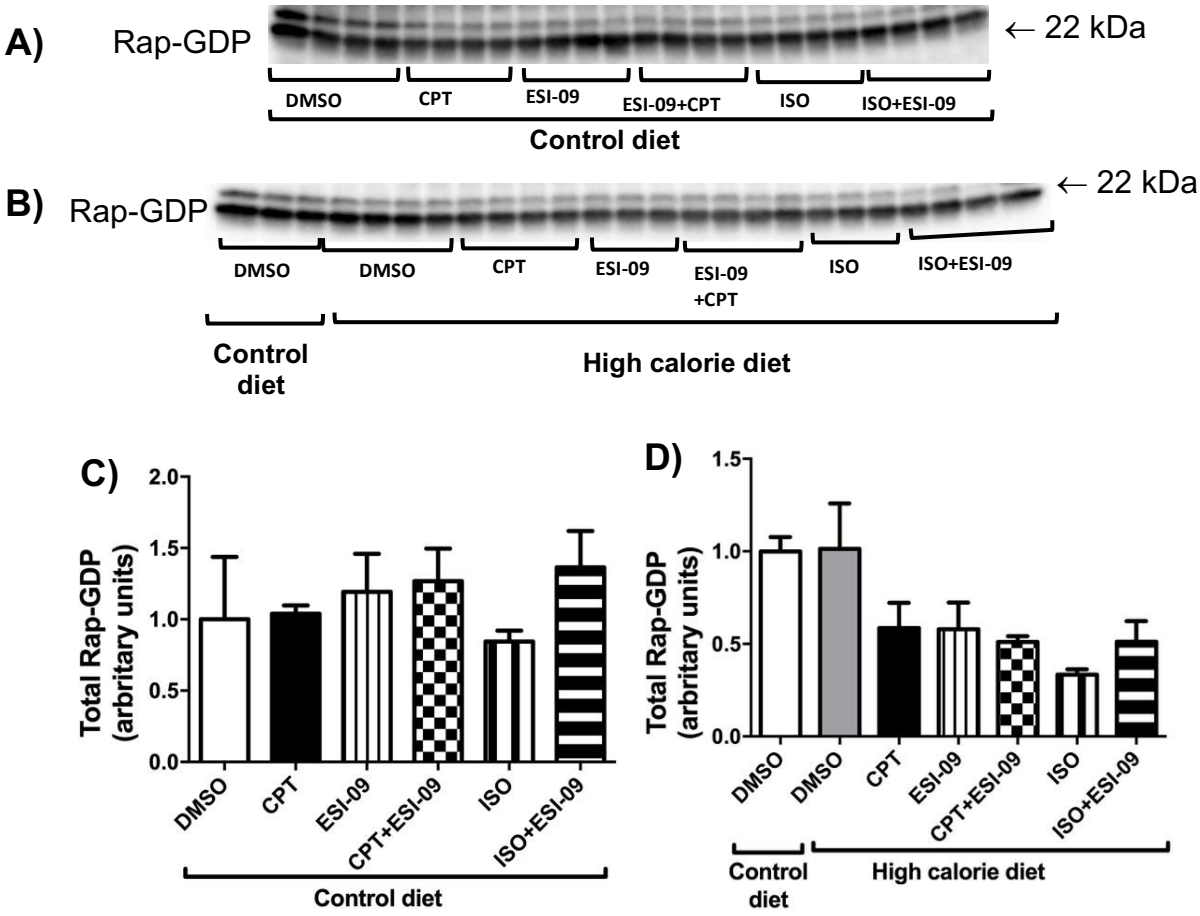

Figure 4. 8 Aortic Rap-GDP expression in CD and HC groups exposed to different treatments.

(A), representative western blots for total Rap-GDP in CD groups; (B) representative western blots for total Rap-GDP in HC groups, (C) total Rap-GDP in CD groups (D), total Rap-GDP in HC groups. All values are expressed as mean ± SEM. n = 3-4 per group.

4.3.6.2 PKB phosphorylation and expression

In CD groups, ESI-09 reduced phosphorylated PKB compared to DMSO (ESI-09: 0.69 ± 0.06 vs. DMSO: 1 ± 0.04, P<0.01; ESI-09+CPT: 0.72 ± 0.02 vs. DMSO: 1 ± 0.04, P<0.01) (Figure 4.9B). ISO significantly reduced phosphorylated PKB compared to DMSO (ISO: 0.62 ± 0.08 vs. DMSO: 1 ± 0.04, P<0.01) (Figure 4.9B). There were no differences in total PKB and phospho:total PKB ratio among the treatment groups.

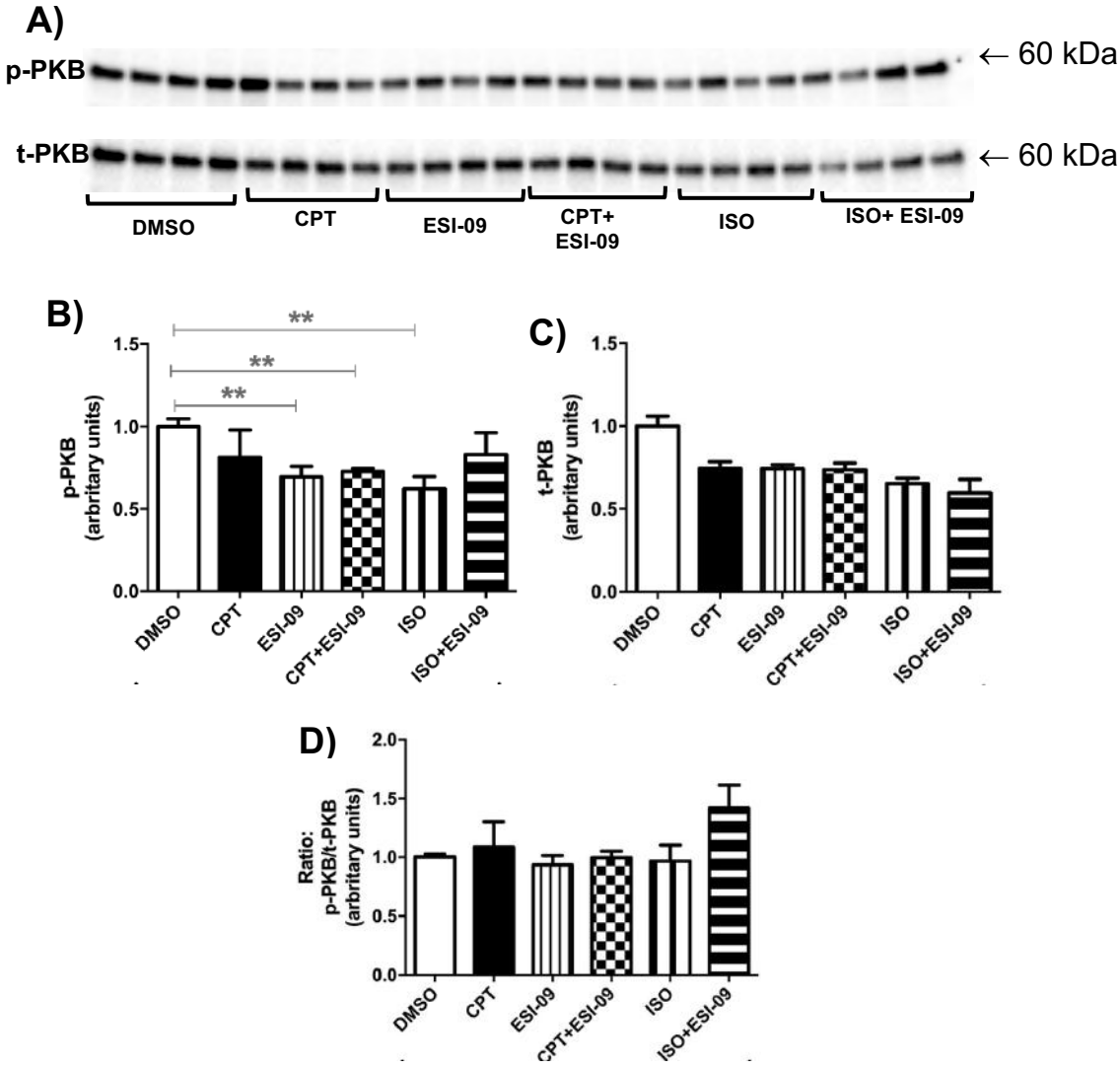

Figure 4. 9 Aortic PKB phosphorylation and expression in CD groups exposed to different treatments.

(A), representative western blots for total PKB and phosphorylated PKB; (B), phosphorylated PKB; (C), total PKB; (D), phospho/total ratio for PKB in rat thoracic aortas. All values are expressed as mean ± SEM. n = 4 per group.**P<0.01.

In HC groups, there were no differences in phosphorylated PKB, total PKB and phospho: total PKB ratio between CD DMSO and HC DMSO (Figure 4.10B, C and D). ESI-09 reduced phosphorylated PKB (ESI-09+CPT:0.69 ± 0.02 vs. DMSO: 0.8 ± 0.04, P<0.05) (Figure 4.10B). ISO significantly increased phospho: total PKB ratio compared to DMSO (ISO: 1.34 ± 0.05 vs. DMSO: 1.02 ± 0.1, P<0.001) (Figure 4.10D). There were no differences in total PKB expression.

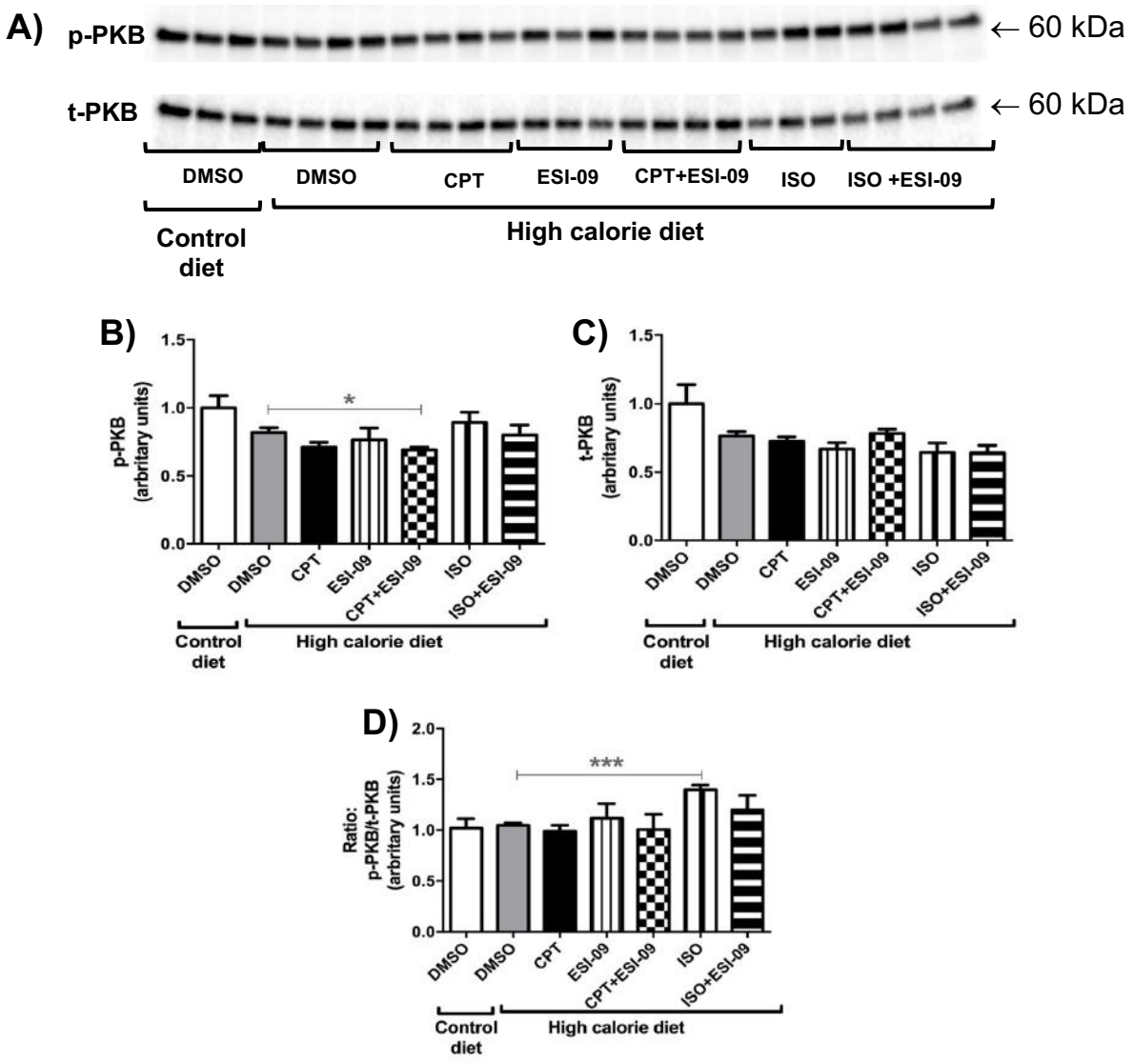

Figure 4. 10 Aortic PKB phosphorylation and expression in HC groups exposed to different treatments.

(A), representative western blots for total PKB and phosphorylated PKB; (B), phosphorylated PKB; (C), total PKB; (D), phospho/total ratio for PKB. All values are expressed as mean ± SEM. n = 3-4 per group. *P < 0.05, ***P<0.001.

4.3.6.3 eNOS phosphorylation and expression

Figure 4.11 demonstrates phosphorylated eNOS, total eNOS and phospho: total eNOS ratio for aortas from CD groups. There were no significant differences among the groups.

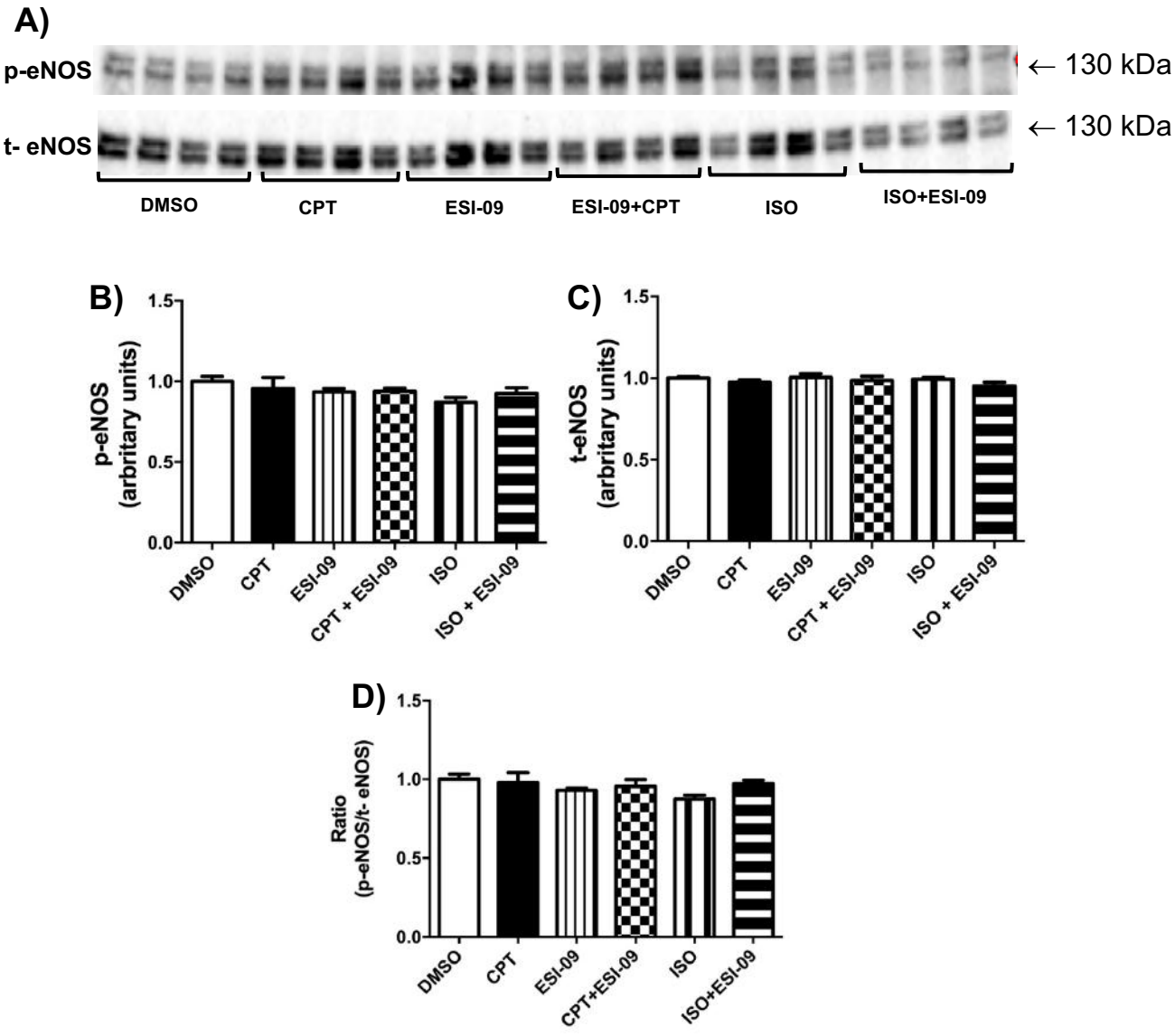

Figure 4. 11 Aortic eNOS phosphorylation and expression in CD groups exposed to different treatments.

(A), representative Western blots for phosphorylated and total eNOS; (B), phosphorylated eNOS levels; (C), total eNOS levels; (D), phospho/total ratio for eNOS. All values are expressed as mean ± SEM. n = 3-4 per group.

In HC groups, ESI-09 inhibition in aortas co-treated with ISO resulted in reduced eNOS phosphorylation (ESI-09+ISO: 0.88 ± 0.11 vs. ISO: 1.59 ± 0.23, P<0.05, Figure 4.12B) and phospho: total eNOS ratio (ESI-09+ISO: 1.01 ± 0.08 vs. ISO: 1.5 ± 0.16, P<0.05, Figure 4.12D) compared to ISO treated aortas. There were no differences in total eNOS.

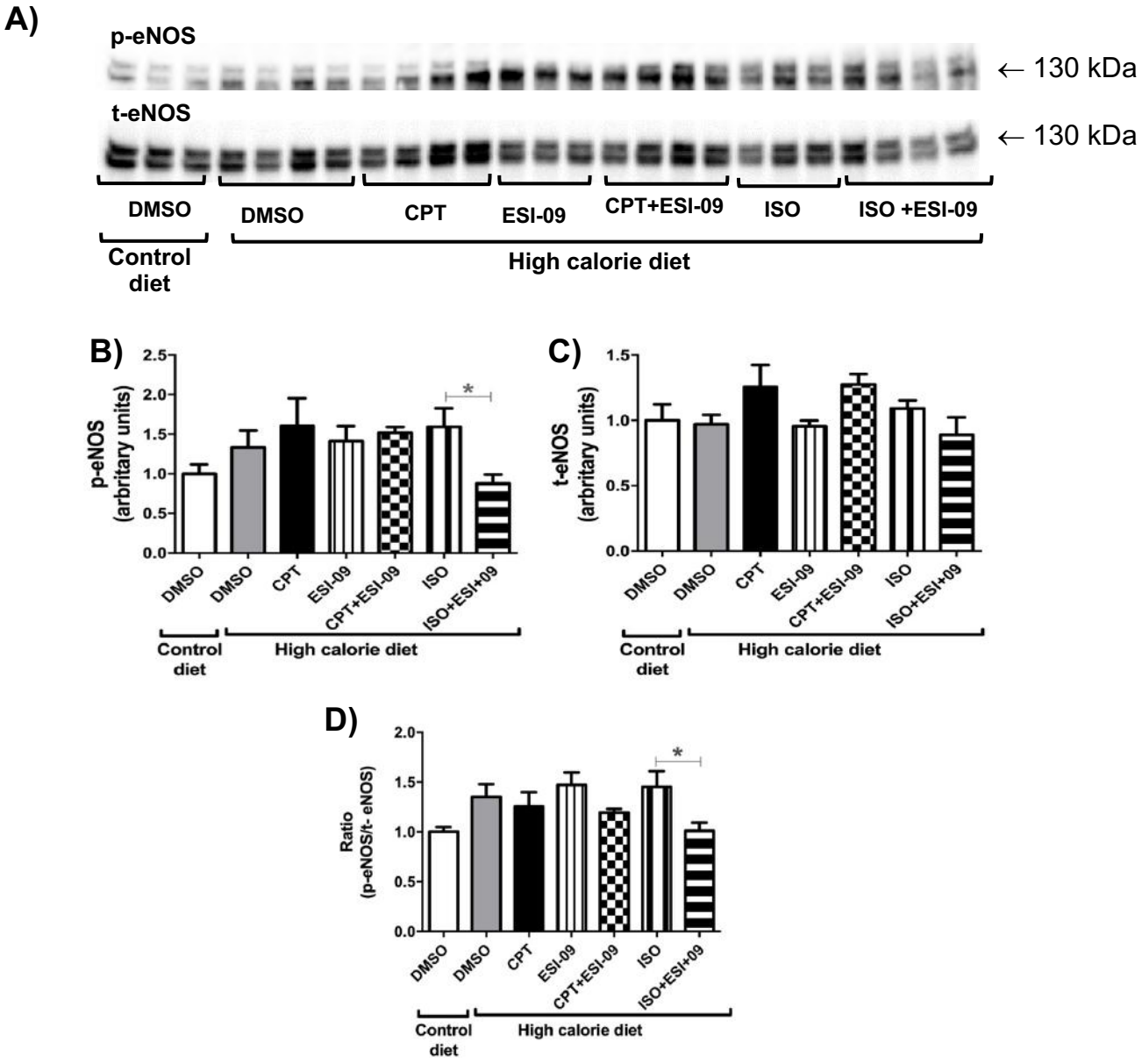

Figure 4. 12 Aortic eNOS phosphorylation and expression in HC groups exposed to different treatments.

(A), representative western blots for total eNOS and phosphorylated and total eNOS; (B), phosphorylated eNOS; (C), total eNOS; (D), phospho/total ratio for eNOS in rat thoracic aortas (without perivascular fat). All values are expressed as mean ± SEM. n = 3-4 per group.* P<0.05.

4.3.6.4 ERK1/2 phosphorylation and expression

Figure 4.13 demonstrates phosphorylated ERK1/2, total ERK1/2 and phospho: total ERK1/2 ratio for aortas from CD groups. There were no significant differences among the groups.

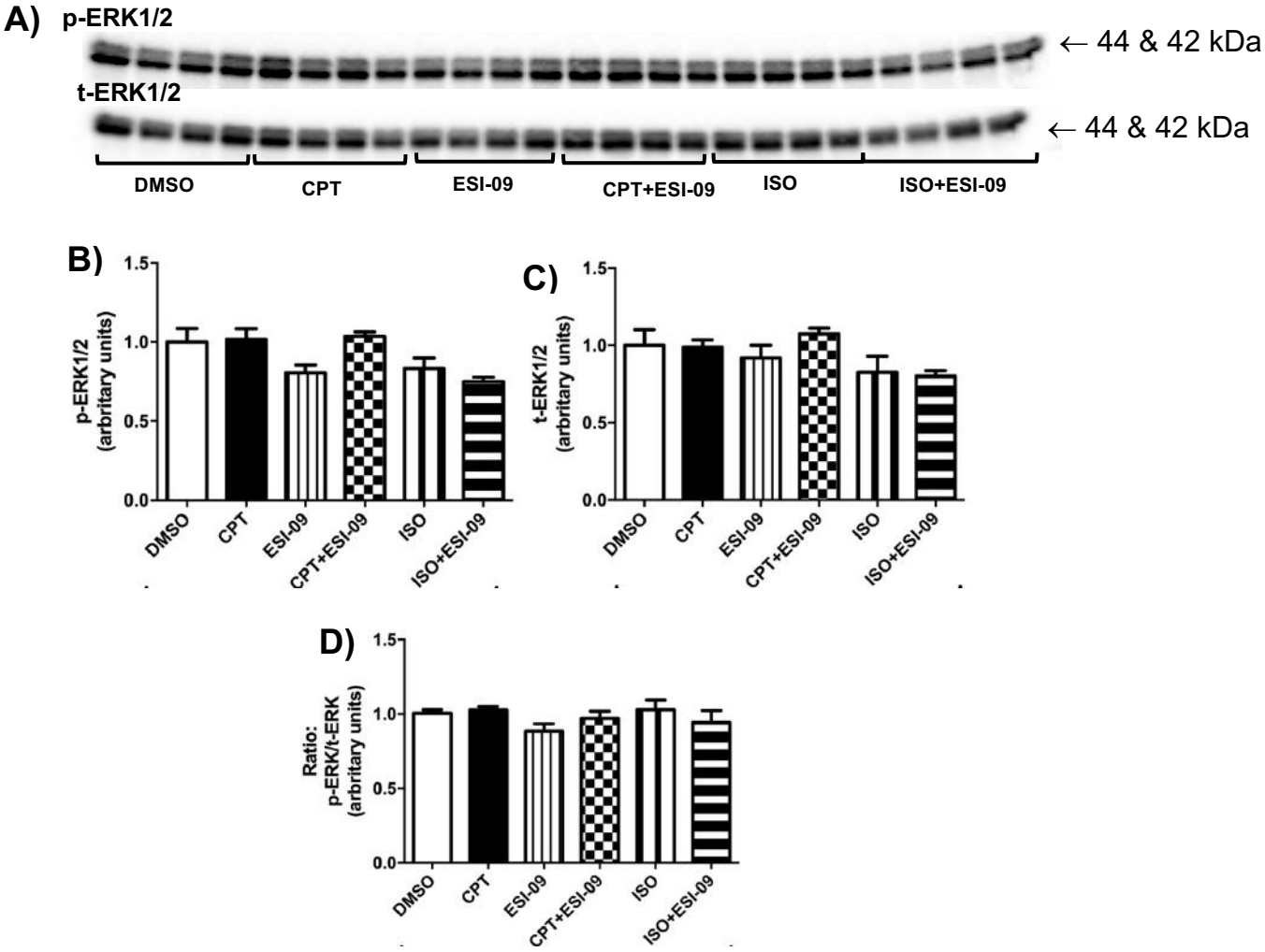

Figure 4. 13 Aortic ERK phosphorylation and expression in CD groups exposed to different treatments.

(A), representative western blots for total ERK1/2 and phosphorylated ERK1/2; (B), phosphorylated ERK1/2; (C), total ERK1/2; (D), phospho/total ratio for ERK1/2 in rat thoracic aortas (without perivascular fat). All values are expressed as mean ± SEM. n = 3-4 per group.

In HC aortas, ISO reduced total ERK1/2 expression (ISO: 0.62 ± 0.05 vs. DMSO:1 ± 0.05, P<0.01, Figure 4.14C) and significantly increased phospho: total ERK1/2 ratio (ISO: 1.08 ± 0.06 vs. DMSO: 0.85 ± 0.02, P<0.05, Figure 4.14D).

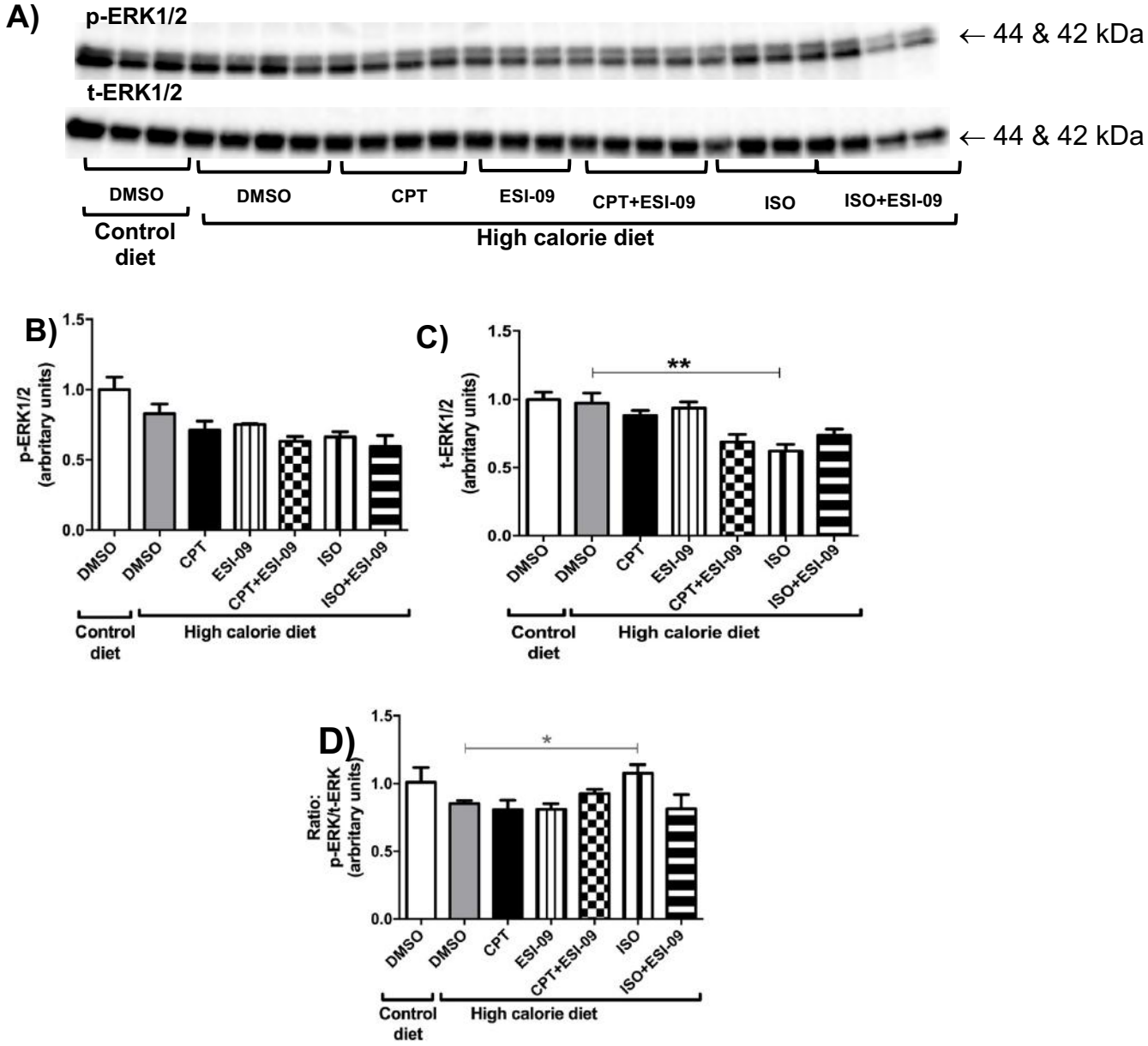

Figure 4. 14 Aortic ERK phosphorylation and expression in HC groups exposed to different treatments.

(A), representative western blots for total ERK1/2 and phosphorylated ERK1/2; (B), phosphorylated ERK1/2; (C), total ERK1/2; (D), phospho/total ratio for ERK1/2 in rat thoracic aortas (without perivascular fat). All values are expressed as mean ± SEM. n = 3-4 per group. *P<0.05,**P<0.01.

4.3.6.5 AMPK phosphorylation and expression

In CD groups, ESI-09 inhibition increased AMPK phosphorylation (ESI-09: 2.77 ± 0.03 vs. DMSO: 1 ± 0.27, P<0.05, Figure 4.15B) and phospho: total AMPK ratio (ESI-09: 3.78 ± 0.86 vs. DMSO: 0.97 ± 0.18, P<0.05, Figure 4.15D.

CPT and ISO could not reverse the effects of ESI-09 on phosphorylated AMPK (CPT+ESI-09: 2.61 ± 0.63 vs. DMSO: 1 ± 0.27, P<0.05; ISO+ESI-09: 2.1 ± 0.54 vs. DMSO: 1 ± 0.27,P<0.05, Figure 4.15B) and phospho: total AMPK ratio (CPT+ESI-09: 5.18 ± 0.59 vs. DMSO: 0.97 ± 0.18, P<0.001; ISO+ESI-09: 4.52 ± 1.01 vs. DMSO: 0.97 ± 0.18, P<0.05, Figure 4.15D). There were differences in total AMPK expression among the groups.

In HC groups, there were no differences in phosphorylated AMPK, total AMPK and phospho: total AMPK ratio between CD DMSO and HC DMSO. ESI-09 significantly increased AMPK phosphorylation compared to HC DMSO (ESI-09: 2.51 ± 0.35 vs. DMSO: 0.91 ± 0.11, P<0.05, Figure 4.16B).

Epac inhibition increased phospho: total AMPK ratio (ESI-09: 4.12 ± 0.96 vs. DMSO: 1.38 ± 0.26 , P<0.05, Figure 4.16D), which was reversed by CPT (CPT+ESI-09: 3.01 ± 1.03 vs. DMSO: 1.38 ± 0.26, ns), but not by ISO (ISO+ESI: 4.33 ± 0.81 vs. DMSO: 1.02 ± 38, P<0.05, Figure 4.16D). There were no differences in total AMPK expression among the groups.

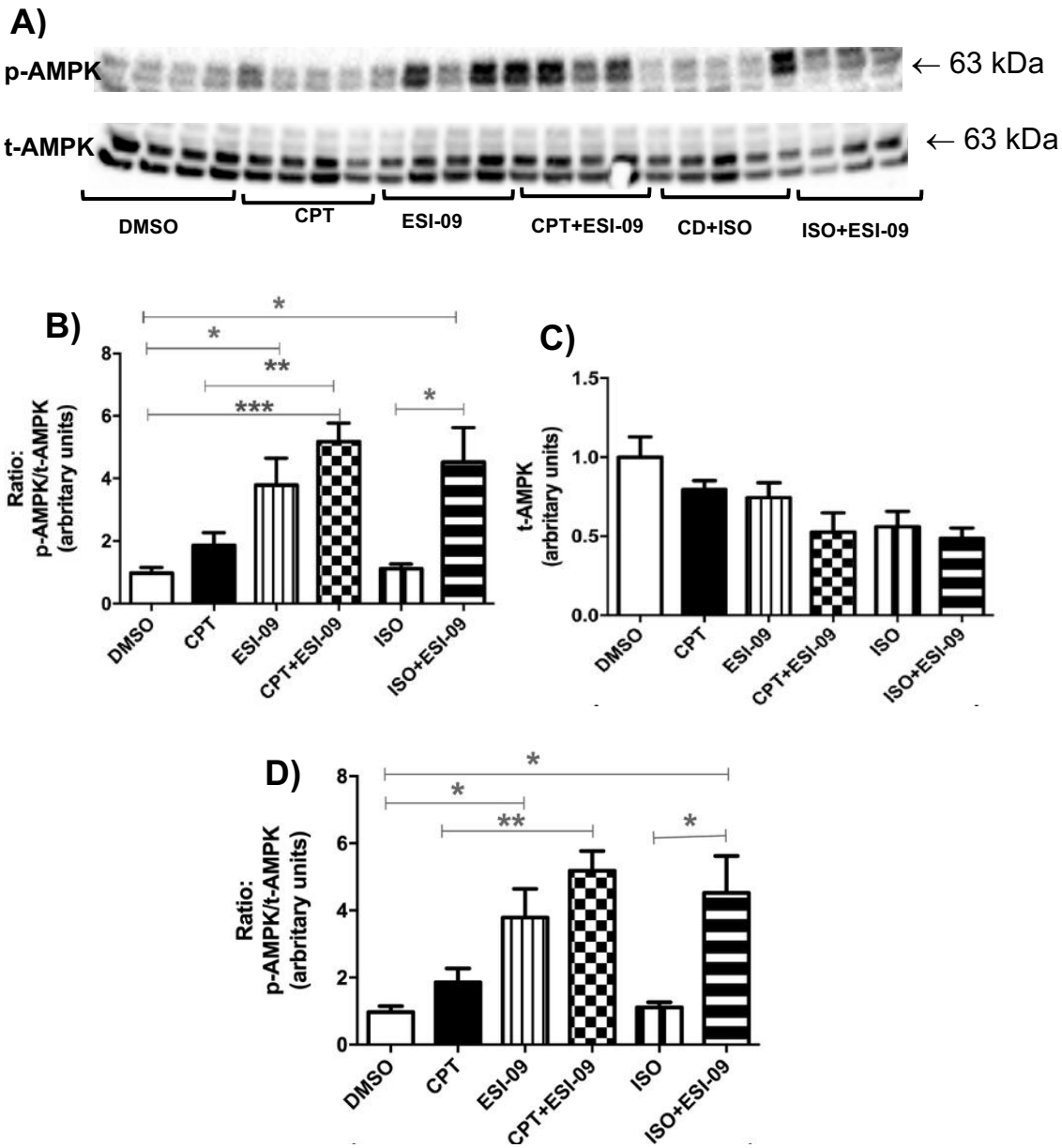

Figure 4. 15 Aortic AMPK phosphorylation and expression in CD groups exposed to different treatments.

(A), representative western blots for total AMPK and phosphorylated AMPK; (B), phosphorylated AMPK; (C), total AMPK; (D), phospho/total ratio for AMPK in rat thoracic aortas (without perivascular fat). All values are expressed as mean ± SEM. n = 4 per group. *P < 0.05, **P<0.01.

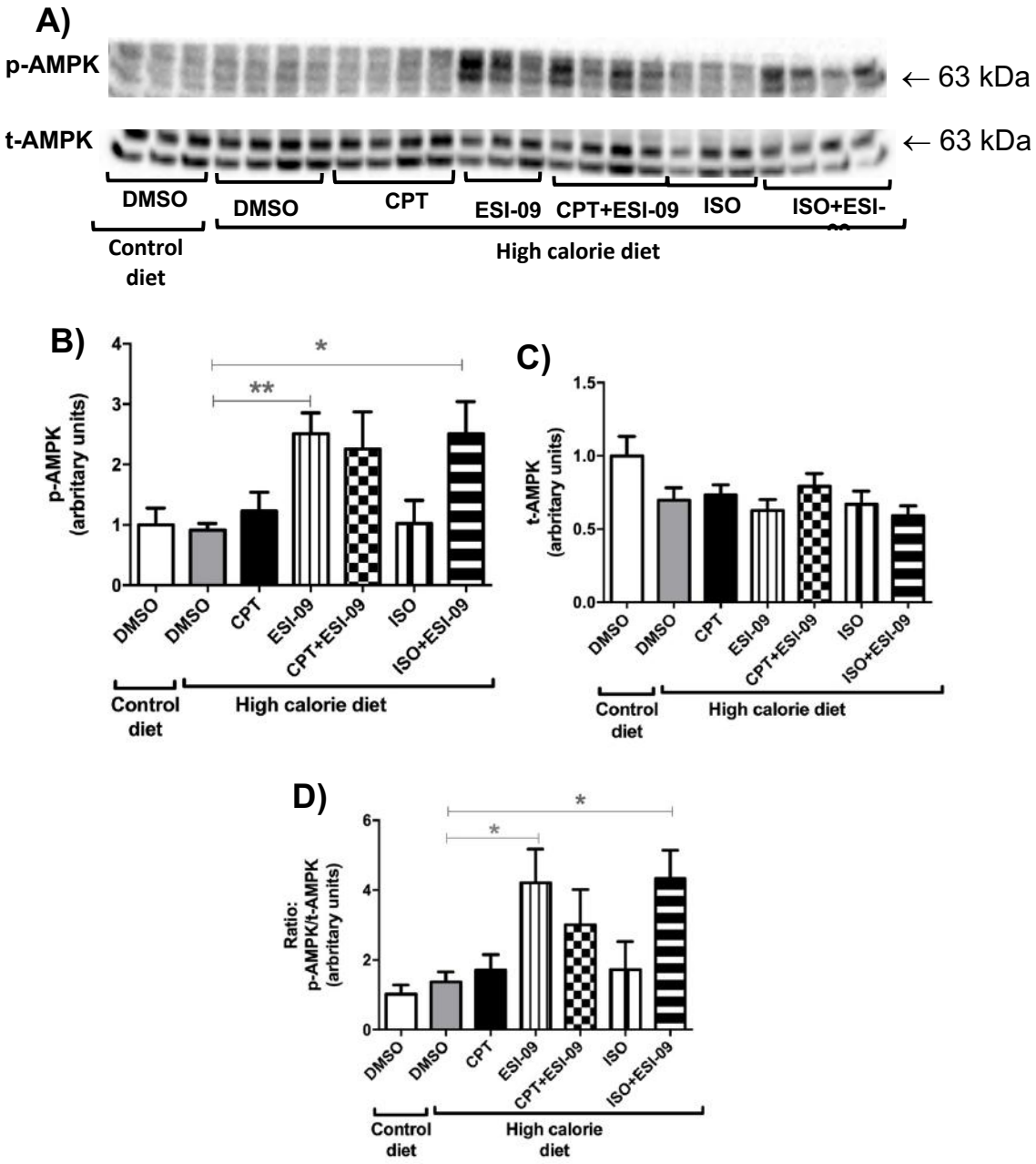

Figure 4. 16 Aortic AMPK phosphorylation and expression in HC groups exposed to different treatments

(A), representative western blots for total AMPK and phosphorylated AMPK; (B), phosphorylated AMPK; (C), total AMPK; (D), phospho/total ratio for AMPK in rat thoracic aortas (without perivascular fat). All values are expressed as mean ± SEM. n = 3-4 per group. *P < 0.05, **P<0.01

4.3.6.6 CREB phosphorylation and expression

Figure 4.17 represents CREB phosphorylation, total CREB and phospho: total CREB ratio in aortas from the CD group. ISO increased phospho:total CREB ration compared DMSO (ISO: 2.11 ± 0.33 vs. DMSO: 0.98 ± 0.15, P<0.05, Figure 4.17D). Epac inhibition reverse the effect of ISO (ISO+ESI-09: 1.11 ± 0.22 vs. DMSO: 0.98 ± 0.15, ns, Figure 4.17D). There were no significant differences in total CREB expression among the groups.

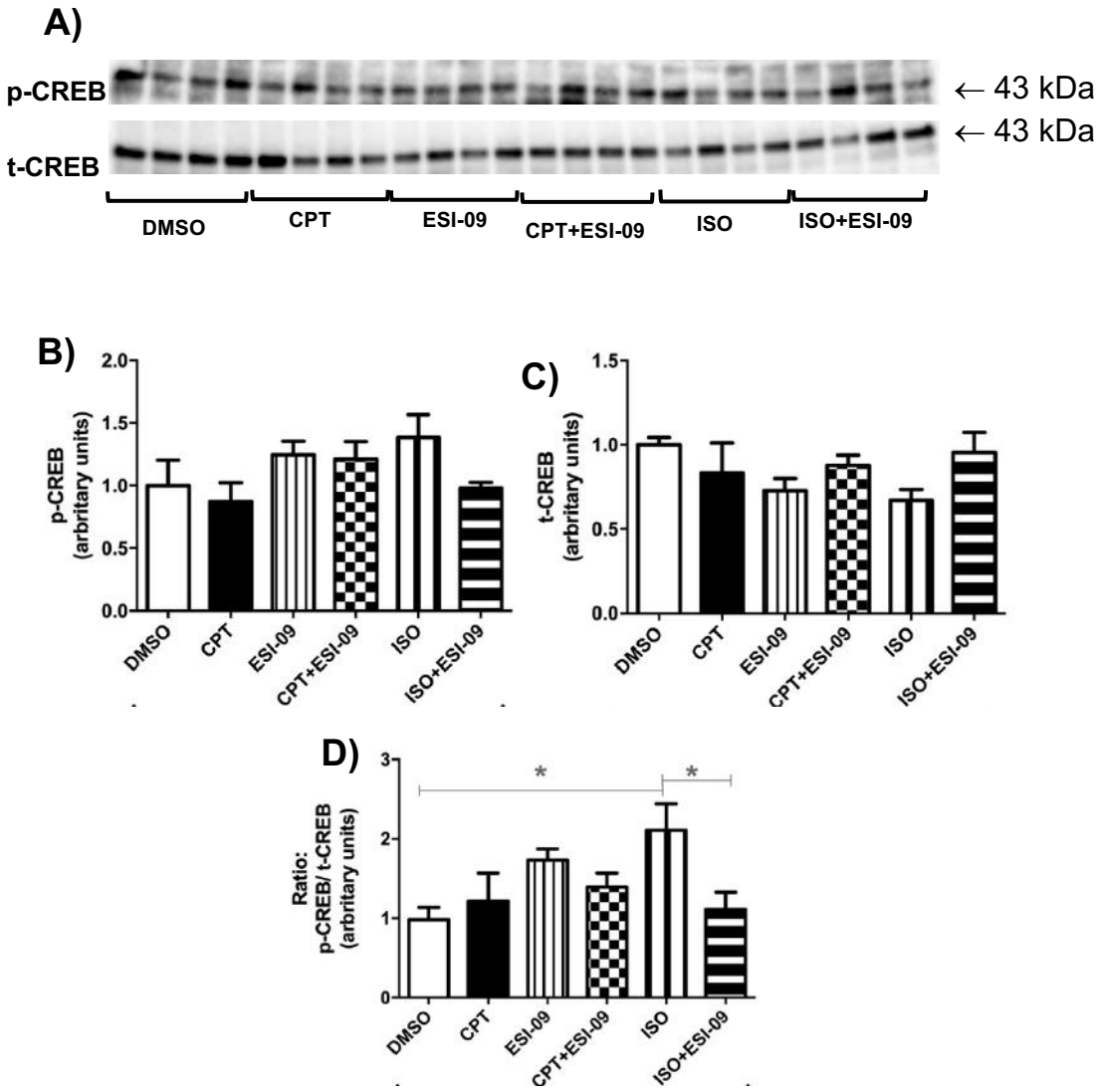

Figure 4. 17 Aortic CREB phosphorylation and expression in CD groups exposed to different treatments.

(A), representative western blots for total CREB and phosphorylated CREB; (B), phosphorylated CREB; (C), total CREB; (D), phospho/total ratio for CREB in rat thoracic aortas (without perivascular fat). All values are expressed as mean ± SEM. n = 4 per group. * P < 0.05 .

Figure 4.18 demonstrates phosphorylated CREB, total CREB and phospho: total CREB ratio for aortas from HC groups. There were no significant differences among the groups.

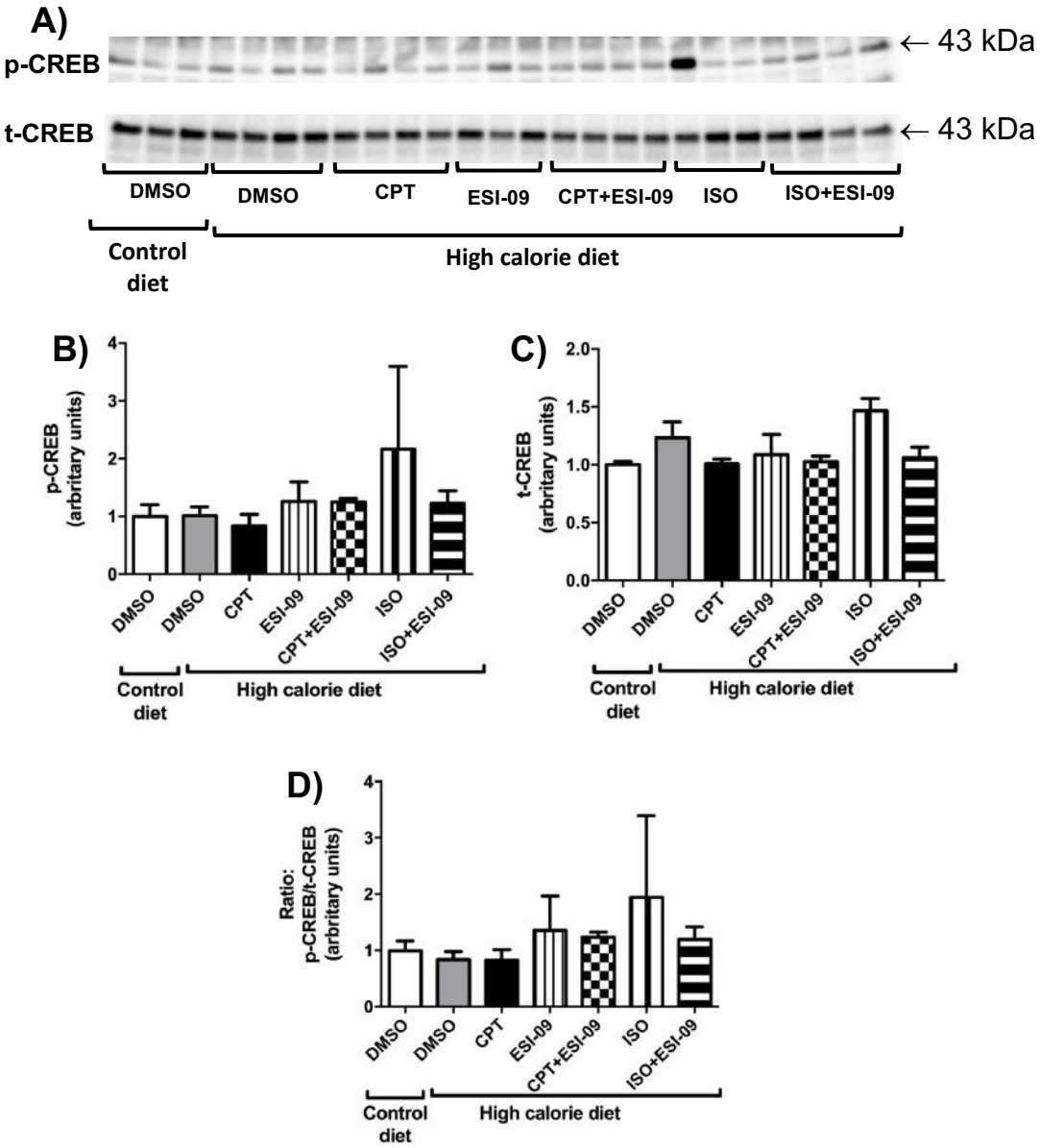

Figure 4. 18 Aortic CREB phosphorylation and expression in HC groups exposed to different treatments

A), representative western blots for total CREB and phosphorylated CREB; (B), phosphorylated CREB; (C), total CREB; (D), phospho/total ratio for CREB in rat thoracic aortas (without perivascular fat). All values are expressed as mean ± SEM. n = 3-4 per group.

4.4 Discussion

The aim of this study was to elucidate a putative role Epac signalling in *ex vivo* thoracic aortas of a rat model of high calorie diet-induced obesity. This study has demonstrated that a high-calorie diet (HC) had no effect on PE and ACh induced vascular reactivity. Beta-adrenergic stimulation with ISO and selective Epac stimulation significantly improved vasorelaxation in HC and CD aortas which was abolished by an Epac inhibitor ESI-09. Furthermore, CPT directly induced vasorelaxation in a dose-dependent manner in both HC and CD group and this effect was NOS-dependent, as it was abolished by L-NAME (NOS inhibitor). Acute stimulation of Epac with CPT (2 µM) had no effect on PKB and eNOS phosphorylation in HC. However, ESI-09 significantly reduced the PKB phosphorylation in CD aortas suggesting that blocking Epac activity may have a detrimental effect on the PKB pathway. Furthermore, ESI-09 significantly increased stress-activated kinase AMPK in both HC and CD aortas.

4.4.1 The role of Epac in vascular reactivity

In this study, Wistar rats fed with an HC showed significant increases in body weight and intraperitoneal fat which may be an indication of overweight/obesity. This was followed by an elevation in non-fasting glucose concentration and insulin resistance (HOMA-IR index) after 16 weeks on diet (as previously discussed in Chapter 3, section 3.4.1). Previous studies have reported the harmful effects of excessively high energy diets on vascular function. For example, both high-fat diet (HFD) and high sucrose diet have been shown to induce adiposity and oxidative stress which can lead to the development of endothelial dysfunction (Sweazea *et al*., 2010). In our study, we found no changes in vascular reactivity between the HC and CD rat aortas. We demonstrated that L-NAME attenuated ACh-induced relaxation in both CD and HC groups and therefore confirmed NOS dependence. The L-NAME pro-contractile and anti-relaxation on endothelium function was the same in both diet groups, thus HC did not adversely affect the endothelial function. Poncelas *et al.* (2015) have demonstrated that even 6 months of feeding high-fat diet in mice could not alter vascular reactivity between control and the high-fat group (Poncelas *et al*., 2015).

There is growing interest in the role of cAMP and in particular the Epac signalling pathway in cardiovascular health (Lezoualc'H *et al*., 2016). Therefore, in our study, we were interested in the role of Epac on vascular reactivity of rat aortas *(ex vivo)* pre-exposed to "obesogenic" high energy diets. We investigated the effect of beta-adrenergic stimulation on aortic vascular reactivity in aortas exposed to a 16 week high-calorie diet (HC). The beta-adrenergic agonist ISO activates the second messenger cAMP (Stamper *et al*., 2009), which could activate downstream cascades PKA and Epac. It has been shown that aortic rings from 1 week ISO-treated *(in vivo)* Wistar rats had an increase in the contraction response to PE but the relaxation response to ACh remained unchanged (Davel *et al*., 2006). In our study, we found similar results with an acute 15 minutes stimulation of the beta-adrenergic receptor with ISO (0.1 μM), with an increase in PE-induced vasocontraction in CD aortas but no effects on relaxation. However, Cuíñas and colleagues (2016) suggests that activation of PKA and Epac by cAMP in vascular smooth muscle cells led to a decline in intracellular Ca^{2+} stores thereby reducing Ca^{2+} availability for vasocontraction (Cuíñas *et al*., 2016). On the other hand, we found that ISO administration to HC aortas did not affect the PE-induced vasocontraction but improved the response to ACh induced vasorelaxation. Epac1/2 inhibition with ESI-09 reduced these effects of beta-adrenergic stimulation on vascular reactivity in both HC and CD aortas.

From these findings, we could conclude that the vasorelaxation in HC aortas was mediated, at least in part, by Epac. However since the effect was only partial, this does not exclude the effect of PKA. In rat aortas, PKA was reported to be involved in endothelium-dependent vasorelaxation induced by stimulation of beta-adrenergic receptors (Ferro *et al*., 2004). The study by García-Morales and colleagues (2014) demonstrated a role for PKA in vascular smooth muscle in relaxation from healthy Wistar rats aortas by directly activating PKA with is agonist 6-Benz-cAMP suggesting that PKA activates eNOS to catalyse the release of NO in the vascular smooth muscle cells (García-Morales *et al*., 2014). They further investigated the participation of Epac on cAMP vasorelaxation effect and found that the Epac activator CPT significantly relaxed PE pre-contracted aortas with or without endothelium suggesting that Epac vasorelaxation act via both the endothelium as well as directly on the vascular smooth muscle cells (García-Morales *et al*., 2014). Other studies have shown that Epac

activators can relax not only vascular type but also the non-vascular type of smooth muscle cells (Roscioni *et al.*, 2011). In our study, the selective Epac activation with CPT (2 μM) did not affect PE induced vasocontraction in CD aortas. However, the Epac activation was anti-contractile in HC aortas with a reduced maximal vasoconstrictor (E_{max}) response to PE.

The present study showed that Epac activation with CPT, even at the low concentration of 2 μM, increased the sensitivity of both CD and HC aortas to ACh-induced relaxation. This was abolished by Epac inhibitor ESI-09 in both CD and HC aortas. It has been shown that, in the vascular smooth muscle cell and endothelium, Epac (Rap1B) is required for the maintenance of vascular tone and blood pressure (Lakshmikanthan *et al*., 2014). Therefore, our study confirms that Epac plays an important role in vascular smooth muscle relaxation even in the context of "obesity".

We further investigated the mechanism of Epac's vasorelaxation effect by blocking NOS with L-NAME and then exposed the aortic rings to a cumulative concentrations of CPT (1, 2, 5 and 10 μM) only. CPT relaxed both CD and HC aortas via NOS (Figure 4.7). In the endothelium and vascular smooth cells, Epac can directly mediate vasorelaxation through regulation of Ca^{2+}-sensitive and ATP-sensitive K^+ channels (Purves *et al*., 2009; Roberts *et a*l., 2013). For arterial smooth muscle relaxation, Epac activates eNOS which catalyses the release of NO from the vascular endothelial cells which is a potent vasodilator (García-Morales *et al*., 2014).

4.4.2 Molecular mechanisms: signalling pathways

Vascular function/tone is regulated through various signalling pathways, and cAMP and cGMP are considered to be the main second messengers involved (Morgado *et al*., 2012). Epac (cAMP-GEF) serves as guanine nucleotide exchange factors (GEFs) for the small G-protein (Rap1 and Rap2). Rap1 is a key regulator of endothelial barrier function (Aslam *et al*., 2014; Birukova *et al.*, 2010, 2008, 2007; Pannekoek *et al*., 2014) ,vascular tone, (Lakshmikanthan *et al.*, 2014; Roberts *et al*., 2013; Roscioni *et a*l., 2011; Zieba e*t al*., 2011), VSMC proliferation (Hewer *et al*., 2011), and vascular remodelling (Yokoyama *et al.*, 2010, 2008b, 2008a). In this regard, it is necessary to understand the molecular mechanism of cAMP-Epac/Rap1 in pathology (obesity/high-

fat induced endothelium dysfunction). In this study, we investigated the involvement of signalling pathways, in particular the cAMP-Epac/Rap pathway in aortas from male Wistar rat after a 16 week exposure to a HC. In addition, the Epac/Rap pathway was activated in *ex vivo* isolated aortas by the administration of an Epac agonist CPT (2μM). In the current study, Rap-GDP (inactive Rap) expression did not differ between the diet groups. Epac1/Rap1 is required for NO release and endothelium function (Chrzanowska-Wodnicka, 2017; García-Morales *et al*., 2014; Lakshmikanthan *et al*., 2014). Rap1 deficiency in mice aortas is associated with an increase in oxidative stress and impaired endothelium-dependent NO production (Wong *et a*l., 2018). In human endothelial cells, eNOS was activated by both PKA and Epac via the PI3K/PKB pathway (García-Morales *et al*., 2017). In the endothelium, the insulin-dependent NO production via insulin receptor substrate 1 (IRS1) activates PI3K/PKB pathway, which in turn phosphorylates eNOS at ser1177 (Arce-Esquivel. *et al*., 2013). However, an increase in circulating free fatty acids as observed in obesity and type 2 diabetes patients can lead to insulin resistance, thus compromising the IRS1-PI3K/PKB-eNOS pathway (Capurso and Capurso, 2012; Imrie *et al*., 2010).

In this study, the diet and Epac activation with CPT showed no significant changes in PKB and eNOS phosphorylation and expression in rat aortas (without PVAT). However, ESI-09 inhibition reduced PKB phosphorylation in both CD and HC. These findings suggest that blocking Epac activity with ESI-09 may have detrimental effects on PKB and possibly also the eNOS pathway. In HC aortas, a significant increase in phosphorylated :total PKB was noted upon cAMP elevation with isoproterenol (ISO) and coincubation with ESI-09 did not reverse the effect, thus suggesting the involvement of PKA (García-Morales *et al*., 2017). Interestingly, ISO effects on HC phosphorylated :total eNOS were abolished by co-incubation of ISO and ESI-09. Thus, suggesting that both Epac and PKB are involved in PKB-eNOS phosphorylation in rat aortas from the HC group. Furthermore, Epac activation with CPT did not affect MEK-ERK1/2 phosphorylation and expression in either CD or HC aortas. The Ras/Raf/MEK-ERK1/2 pathway is known to play a crucial role in endothelial function (proliferation and migration during angiogenesis) (Hood *et al.*, 2003; Liu *et al*., 2001; Srinivasan *et al.*, 2009). In HC aortas, beta-adrenoreceptor activation with ISO showed an increase in phosphorylated :total ERK1/2. Furthermore, co-incubation of ISO and ESI-09

reversed the phosphorylated: total ERK1/2 ratio suggesting the involvement of Epac. Cai and co-worker (2008) suggested that the ERK1/2- myosin light chain kinase (MLCK) pathway is involved in CaMKII cytoskeleton reorganization and barrier function in both macrovascular and microvascular endothelial cells (Cai *et al*., 2008).

We further investigated a possible association between Epac and the stress-activated kinase AMPK. In the present study, there were no differences in AMPK phosphorylation and expression between the CD and HC aortas. ISO and CPT did not affect phosphorylation and expression of this metabolic censor in the aortas. Surprisingly, Epac inhibition with ESI-09 significantly increased AMPK phosphorylation and phosphorylated: total ratio in both CD and HC aortas. In the previous chapter (Chapter 3, section 3.3.5.9), the ESI-09 also increased AMPK phosphorylation in hearts from the HC diet group. Further, the hearts went to contracture and cardiac function was lost. Therefore, the increase in AMPK might be due to intracellular stress such as hypoxia and ATP depletion within the cells (Nagata *et al*., 2003). However, the ESI-09 effect on AMPK requires further investigation. On the other hand, García-Prieto and colleagues (2015) have demonstrated that high-fat diet induced endothelial dysfunction was associated with a downregulation of the AMPK/PI3K/PKB/eNOS signalling pathway (García-Prieto *et al*., 2015). Furthermore, both PKB and AMPK are known to be involved in the activation of eNOS at Ser^{1177} by cAMP elevating agents (Hashimoto *et al*., 2006; Tanano *et al.*, 2013; Zhang and Hintze, 2006). AMPK inhibition eradicates eNOS Ser^{1177} phosphorylation and NO production in human umbilical vein endothelial cells (Han *et al.*, 2015). This suggests that AMPK contributes to NO production in endothelial cells. However, García-Morales and co-workers (2017) showed that Epac and PKB activated eNSO phosphorylation at Ser^{1177} via PKB, independent of AMPK, CaMKII activation or increased cytoplasmic Ca^{2+} concentration (García-Morales *et al*., 2017).

Furthermore, Epac activation with CPT did not affect CREB phosphorylation and expression in either the HC or the CD group. However, beta-adrenergic stimulation with ISO resulted in the phosphorylation of CREB, a downstream effector on PKA, and surprisingly this effect was abolished by ESI-09.

In conclusion, agonist-induced Epac activation improved vasorelaxation via NOS in both control and diet-induced obese rats. These effects were independent of obesity.

Chapter Five

The role of Epac signalling in palmitic and oleic acid induce endothelial dysfunction

5.1 Introduction

Elevated levels of free fatty acids (FFAs) in the blood circulation are associated with an increased risk of CVD and, are closely related to obesity and type 2 diabetes mellitus (Boden, 2011, 2008; Egan *et al*., 2001). Overconsumption of dietary fats induce obesity, increase serum FFAs and induce lipotoxicity and insulin resistance *in vivo* animal models (Liu *et al*., 2015). For *in vitro* studies, FFAs are used to mimic *in vivo* high fat diet-induced lipotoxicity (Liu *et al*., 2015). Abnormal elevation of FFAs has been shown to induce oxidative stress followed by an increase in inflammatory markers, which results in insulin resistance and impaired endothelial function (Boden, 2008; Ellies *et al*., 2013; Fratantonio *et al*., 2015). Furthermore, excessive FFAs including palmitic acid (PA), are significant sources of reactive oxygen species (ROS) in vascular cells, leading to oxidative stress, a crucial step in the development of endothelial dysfunction (Ghosh *et al*., 2017). Endothelial dysfunction can be described as reduced production and/or availability of nitric oxide (NO) (as described in Chapter 4, Section 4.1). Saturated FFAs such as PA have been associated with the downregulation of eNOS in porcine aortic endothelial cells (Van Vickle, 2005). Furthermore, FFAs overload inhibits Ca^{2+} signalling and NO production in endothelial cells (Esenabhalu *et al*., 2003). Previous studies have demonstrated the role of the cAMP-Epac pathway in vascular structure and function including endothelial cell barrier function, regulation of vascular tone, smooth muscle vasorelaxation and inflammation (Cullere *et al*., 2005; Lezoualc'H *et al*., 2016; Purves *et al*., 2009; Roberts *et al*., 2013; Sands *et al*., 2006). However, to our knowledge, this is the first study investigating the effect of the cAMP-Epac pathway in obesity/FFAs induced endothelial dysfunction. In this chapter, it was aimed to establish an *in vitro* model of FFAs (obesity)-induced endothelial dysfunction and to explore the role of the cAMP-Epac pathway in this model. To achieve the aim, rat aortic endothelial cells (RAECs) were treated with saturated fatty acids, palmitic acid (PA) and monounsaturated fatty

acid, oleic acid (OA) to induce endothelial dysfunction. In addition, the cells were treated with an Epac agonist, CPT and Epac antagonist, ESI-09, respectively.

5.2 Material and methods:

Materials:

Cell Applications, San Diego, CA, USA)

1. Rat endothelial cell growth medium (catalogue number: #R211-500)
2. Rat endothelial cell Basal medium (catalogue number: #R210-500)
3. Foetal bovine serum (FBS) (catalogue number: #026-100)

Thermo Fisher Scientific, MA, USA

1. Gibco™ Trypsin 2.5%, no phenol red (catalogue number: #15090046)
2. Gibco™ Attachment factor (catalogue number: #S006100)
3. Dihydrorhodamine-1, 2, 3 (DHR-123) (catalogue number: #D23806)
4. Dihydroethidium (DHE) (catalogue number: #D11347)

Sigma-Aldrich (St Louis, Mo, USA)

1. 8-pCPT-2'-O-Me-cAMP (CPT): Epac agonist. (catalogue number: #C8988)
2. Dimethyl Sulfoxide (DMSO) (catalogue number: #276855)
3. Oleic acid (OA) (catalogue number: #O1008)
4. Palmitic acid (PA) (catalogue number: #P0500)
5. Diethylamine NONOate diethylammonium salt (DEA/NO) (catalogue number: D5431)
6. 4,5-diaminofluorescein-2/diacetate (DAF-2/DA) (catalogue number: D2813)
7. Propidium Iodide (PI) (catalogue number: #P4170)

Biolog Life Science Institute (Bremen, Germany)

1. ESI-09: Epac antagonist (catalogue number: #B133-05)

5.2.1 Rat aortic endothelial cells (RAECs)

RAECs were purchased from VEC Technologies (Rensselaer, New York, USA). On arrival the cells were given fresh rat endothelial cell growth medium in a 75 mm^2 flask and allowed to grow until confluent in a standard tissue culture incubator (Forma Series II, Thermo Electron Corporation, Waltham, MA, USA) and maintained at 37 °C in a 40 – 60% humidity with 5% CO_2. For the first passage, the cells were subcultured into 5 x 25 mm^2 flasks and allowed to grow until confluent. From the second (P1) , third (P2) to the fourth passage (P3), the cells were trypsinized (3 minutes with 0.25% trypsin) and suspended in a freezing medium (90 % foetal bovine serum (FBS), 5 % growth medium and 5 % DMSO) (Genis, 2014). Aliquots were then stored in liquid nitrogen for experimental use as shown in Figure 5.1.

5.2.2 Seeding of cells

Stored RAEC's were seeded in 35 mm petri dishes pre-coated with an attachment factor and given a fresh growth medium, and incubated in a standard tissue culture incubator until confluency. Every second day the RAECs were washed twice with phosphate buffered saline, PBS (137 mM NaCl, 2.68 mM KCl, 8.33 mM Na_2HPO_4, 1.47 mM KH_2PO_4, pH 7.4), and given fresh growth medium. The RAECs were regularly monitored by light microscopic to validate purity by observing a typical monolayer, cobblestone appearance exhibited by cultured endothelial cells (Figure 5.2)(Westcott, 2015). When the RAECs reached (90-100%) confluency, the cells were passaged to the next generation in a 1:2 ratio (Figure 5.1) (Genis, 2014).

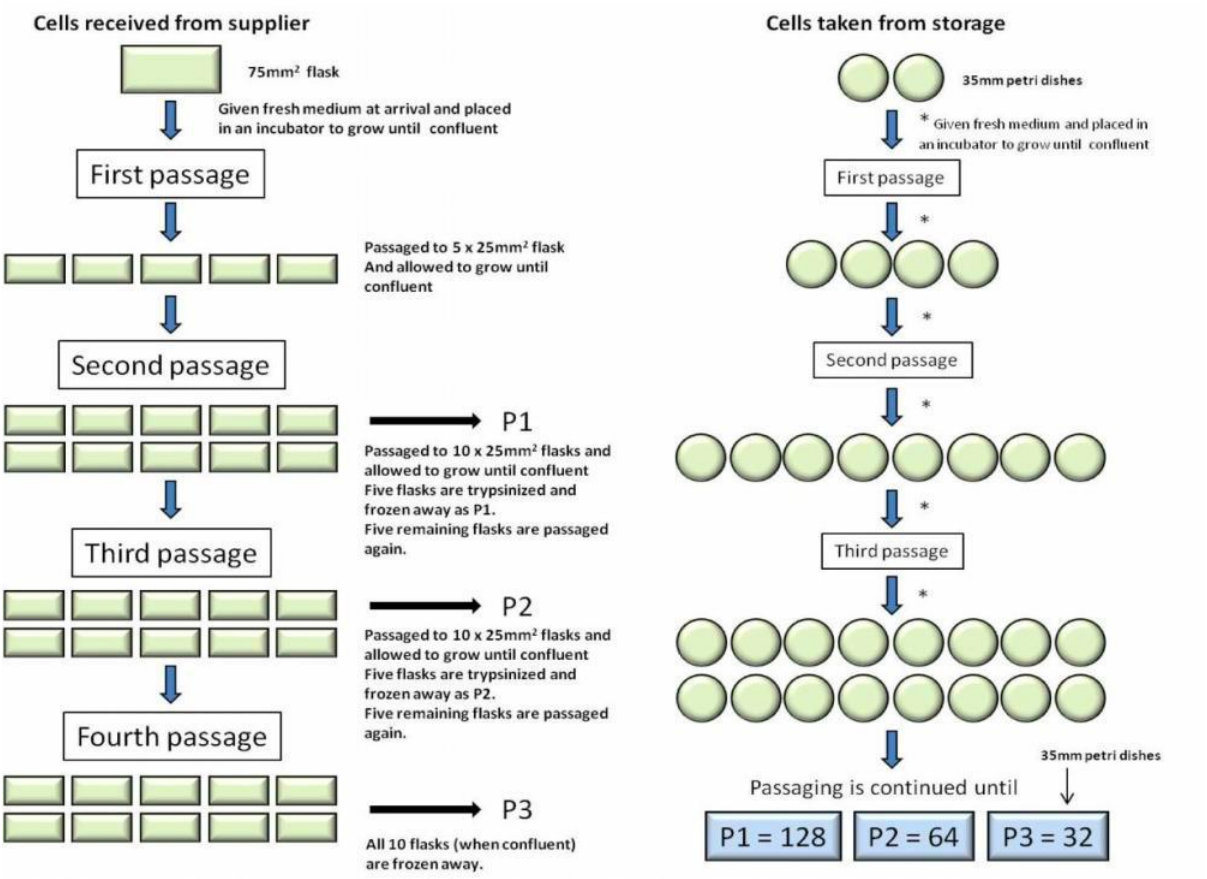

Figure 5. 1 Passaging and cell aliquot storage procedures (Genis, 2014)

5.2.3 Passaging of cells

Briefly, the cells were washed twice with PBS and trypsinized to detach cells from the bottom of gelatin-containing attachment factor-coated 35 mm petri dishes. Detached cells were then immediately transferred into a 15 ml conical tube containing growth media and centrifuged at 1000 rpm for 3 minutes at 4°C. The supernatant (medium containing trypsin) was then aspirated and pellet (cells) was transferred into a fresh growth medium and seeded into the next generation. The P3 generations of cells (stored cells) were also passaged until the seventh generation and used for plate reader assays (5-diaminofluorescein-2/diacetate (DAF-2/DA), Propidium Iodide (PI) and dihydrorhodamine 123 (DHR)) (Figure 5.3). All experiments were repeated thrice, each time using a new P3 generation of cells (plate reader assays), thus three biological repeats.

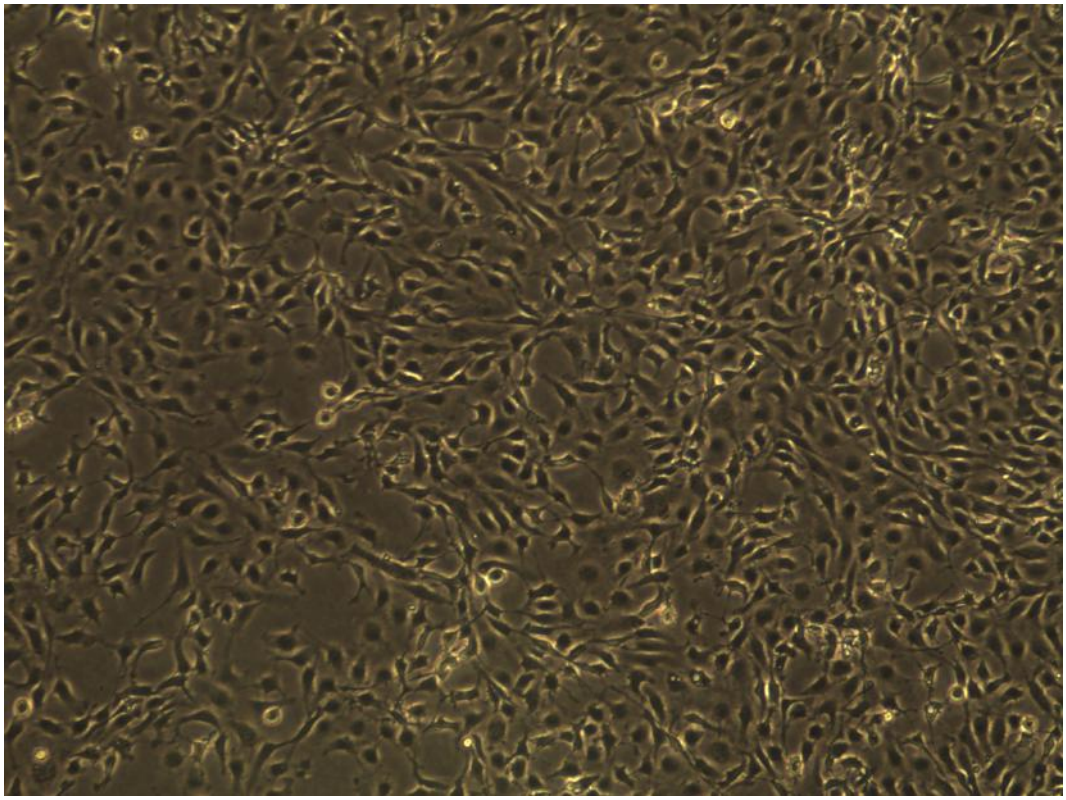

Figure 5. 2 Micrograph of RAECs morphology in culture (10x magnification; Carl Zeiss inverted microscope, West Germany).

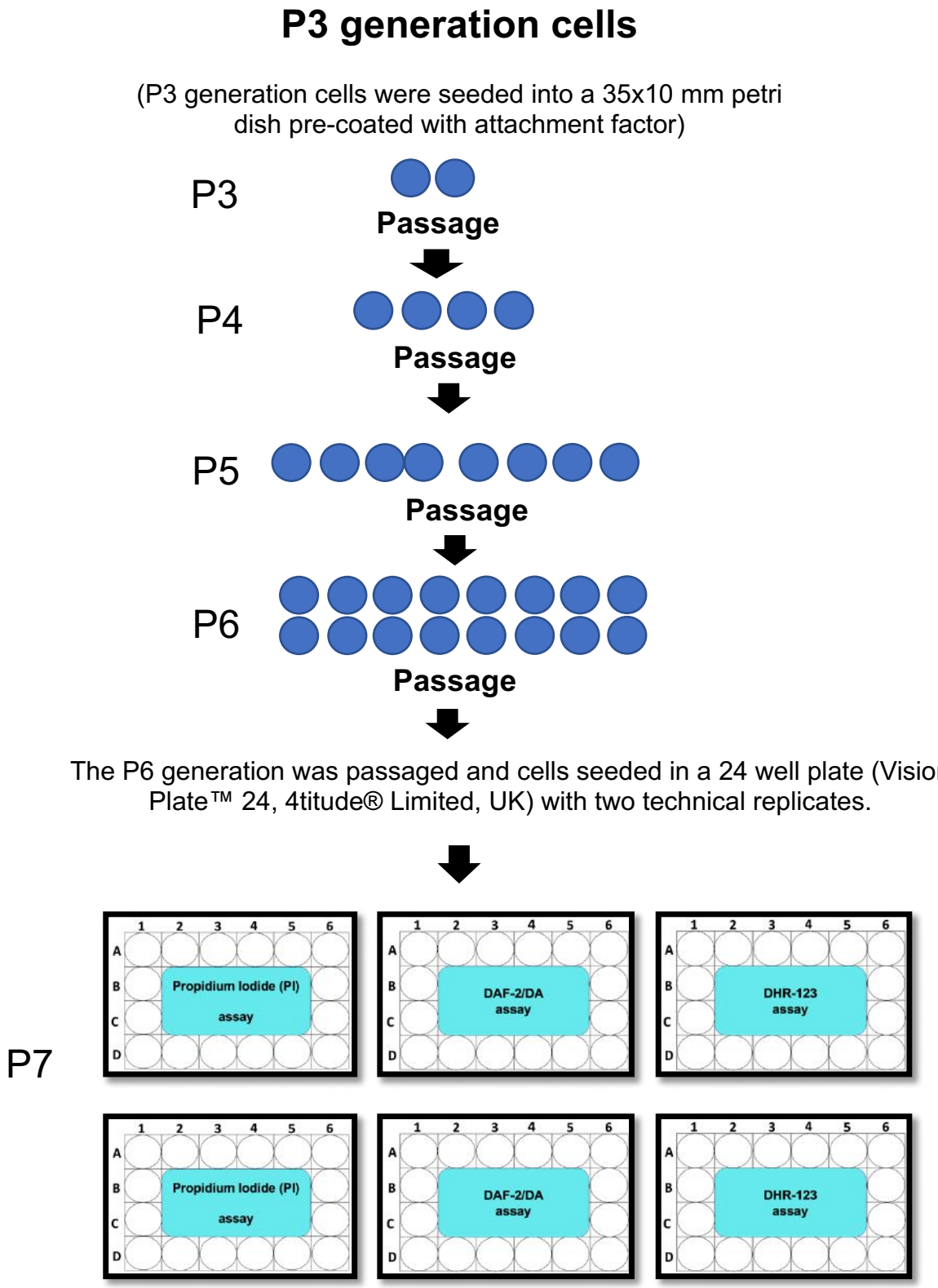

Figure 5. 3 Passaging of cells from P3 generation to the 7th generation for plate reader assays (two 35 x10 mm petri dish goes to one 24 well plate).

5.2.4. Preparation of drugs and free fatty acids (FFA)

Palmitic acid (0.256 g) (*Sigma-Aldrich*, St Louis, Mo, USA) and Oleic acid (0.282 g) (*Sigma-Aldrich*, St Louis, Mo, USA) were dissolved in 100% ethanol (5 ml) to make a 200 mM stock of each. CPT (5 mg) (*Sigma-Aldrich*, St Louis, Mo, USA) was dissolved in distilled water (9.846 ml) to make 1 mM stock. ESI-09 (1.654 mg) (*Sigma-Aldrich*, St Louis, Mo, USA) was dissolved in DMSO (100 µl) to create a 50 mM stock.

5.2.5 Treatment of cells

For all experiments, the RAECs were allowed to grow up 80% confluency. The cells were then serum-starved for 24 hours with rat endothelial cell basal medium (containing 0% FBS) (Cell Applications, Inc, San Diego). The purpose of serum starvation is to synchronise the cells in different stages of the cell cycle to the G_0 phase (Langan and Chou, 2011). After 24 hours, the basal medium containing 0% FBS was aspirated.

The cells are incubated in rat endothelial cell growth medium (containing 10% FBS) (*Cell Applications*, San Diego, CA, USA) for 24 hours in control groups. For treatment groups, the rat endothelium growth medium was supplemented with 50 µM – 500 µM palmitic acid or 50 µM – 500 µM oleic acid or the combination (palmitic acid + oleic acid) to establish a model of obesity/FFA-induced endothelial dysfunction (Figure 5.4).

Furthermore, cells were divided into control/”Lean” groups and FFA/”Obese” groups and treated with different concentrations of an Epac agonist (CPT 2, µM – 10 µM) or an Epac antagonist (ESI-09, 1 µM – 10 µM) for a period of 24 hours (Figure 5.5).

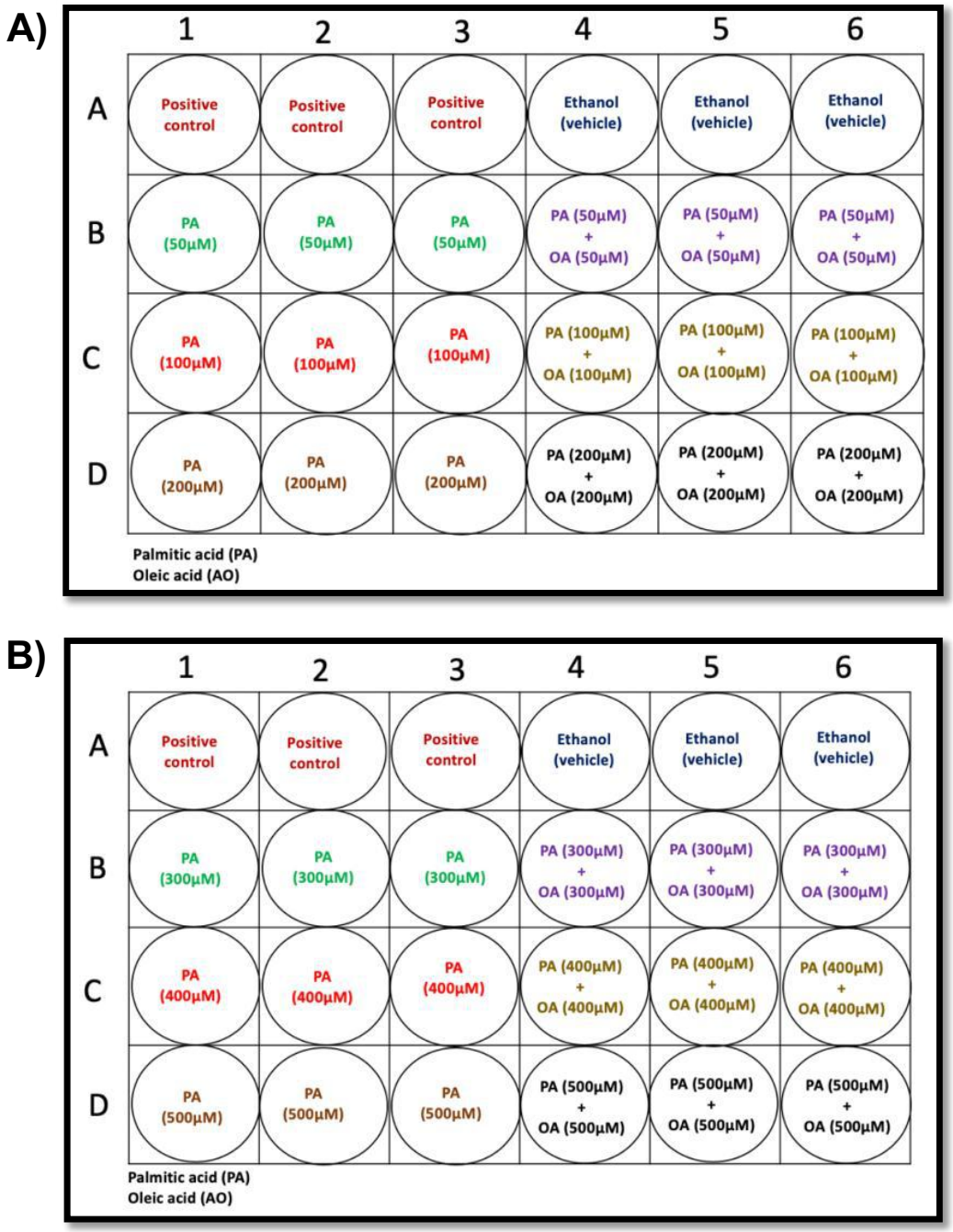

Figure 5. 4 Plate reader experimental setup for cells with different FFA concentrations.

A), 50 μM – 200 μM FFA dosages and B), 300 μM – 500 μM FFA dosages, Ethanol 0.1% (vehicle). Palmitic acid (PA) and oleic acid (OA). Positive controls: Diethylamine NONOate diethyl ammonium salt (DEA/NO 100 μM) for *DAF-2/DA assay,* Peroxynitrite (100 μM) for DHR-123 assay, distilled water for PI assay.

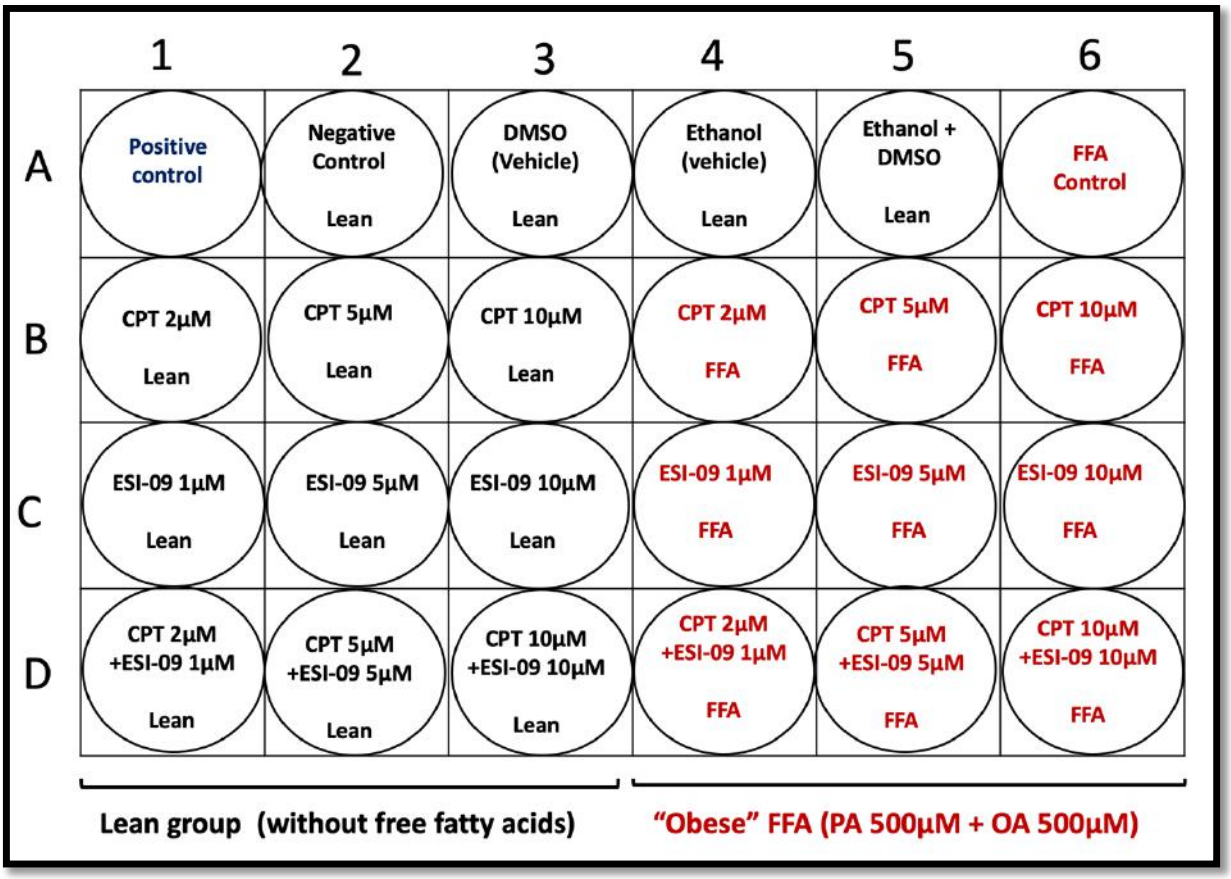

Figure 5. 5 Plate reader experimental setup for cells with different drug concentrations in combination with "Lean" (without free fatty acids) and "Obese" (with palmitic acid, PA and oleic acid, OA) groups.

Positive controls: Diethylamine NONOate diethyl ammonium salt **(DEA/NO 100 µM)** for *DAF-2/DA assay,* **Peroxynitrite (100 µM)** for DHR-123 assay, **distilled water** for PI assay.

5.2.6 Plate reader assays

After a 24 hour treatment period, the cells were fully confluent and ready for the plate reader assays. The assays included, (a) NO measurements using DAF-2/DA, (b) oxidative stress measurements using DHR-123 (dihydrorhodamine 123) and (c) cell viability measurements using PI (Propidium Iodide).

5.2.6 (a) NO measurements: DAF-2/DA

After a 24 hour treatment, the growth medium containing the drugs was aspirated from 24 well plates. The plates were then washed once with PBS followed by incubation with DAF-2/DA (10 µM) for 2 hours at 37ºC. DAF-2/DA is a cell permeable fluorescent NO indicator. It reacts to NO to yield the highly fluorescent triazolofluorescein (DAF-2T) (Zhou and He, 2011).

In the final 30 minutes of the 2 hour incubation period, a Diethylamine NONOate diethyl ammonium salt (DEA/NO 100 µM) (Sigma-Aldrich, St. Louis, MO, USA) was added in the positive control well (Genis, 2014). DEA/NO is a known NO donor.

After two hours, the DAF-2/DA probe was aspirated from all wells and the cells were resuspended in PBS. The fluorescence was measured using a FLUOstar Omega microplate reader (*BMG LABTECH*, Ortenberg, Germany) (at 485 nm excitation and 520 nm emission.

The fluorescence intensity of the positive control and treatment groups are expressed as a percentage of vehicle control (ethanol). (Figure 5.6).

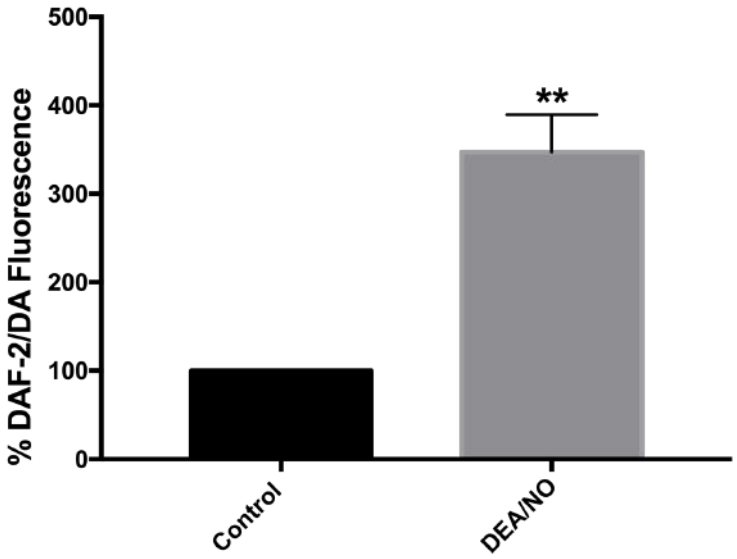

Figure 5. 6 Effects of treatment with the NO donor, DEA/NO (positive control) to validate the NO-specificity of DAF-2/DA.

DAE/NO (100 μM) showed a significant increase in fluorescent intensity compared to vehicle control (Ethanol),** P<0.01 vs. control (ethanol).

5.2.6 (b) Oxidative stress measurement: DHR-123

After 24 hours, the cells were washed with PBS once and DHR-123 (5μM) (*Sigma-Aldrich*, St Louis, Mo, USA) was added and incubated for 3 hours at 37ºC. DHR-123 is an uncharged nonfluorescent intracellular ROS indicator that can freely diffuse across membranes and be oxidized to form a cationic rhodamine 123 which localizes in the mitochondria and exhibits green fluorescence (Henderson and Chappell, 1993). DHR-123 has previously shown to be sensitive to oxidants including peroxynitrite (Valez *et al*., 2013).

After an hour, authentic peroxynitrite (100 μM) was added to the positive control well and incubated for the final 2 hours of the total 3 hours at 37ºC. Peroxynitrite is a biological oxidant that can damage a wide range of molecules in cells including DNA and proteins. After 3 hours, the fluorescence was immediately read on the FLUOstar Omega plate reader at 485nm excitation and 520nm emission. The fluorescence intensity was calculated as in section 5.2.6 (a) (Figure 5.7).

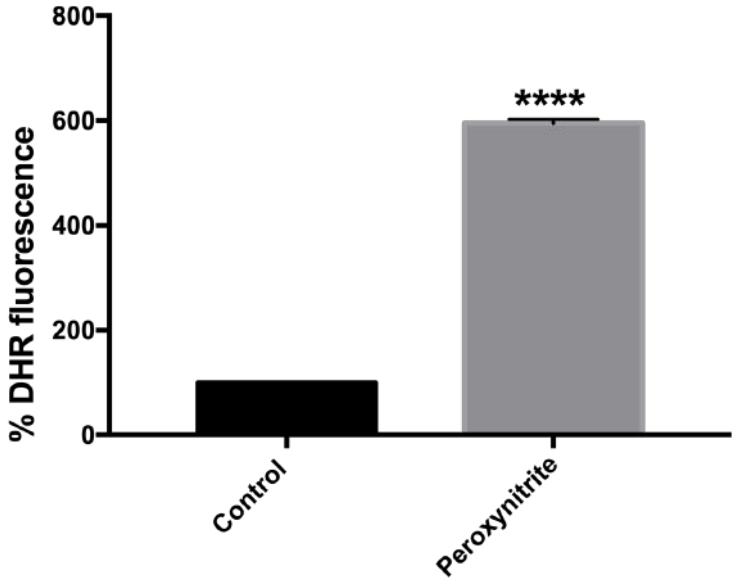

Figure 5. 7 Effects of treatment with authentic peroxynitrite (positive control) to validate the relative peroxynitrite-specificity of DHR-123.

Cells treated with peroxynitrite (100 μM) showed a significant increase in DHR fluorescence intensity, an indication of cellular oxidative stress.****P<0.0001 vs. control (ethanol).

5.2.6 (c) Cell viability: Propidium iodide (PI)

PI is an indicator of cell death (apoptosis and necrosis) (Crowley *et al.*, 2016; Wilkins *et al*., 2002). PI is a large molecule and cannot cross the cell membranes of normal healthy cells. Therefore in apoptotic and necrotic cells, when cell membranes have lost their integrity, PI can penetrate cells and bind to DNA in the nucleus and a fluorescent reaction is elicited (Wilkins *et al.*, 2002). Cells that are fluorescent with PI are assumed to be damaged. Cells treated with distilled water were included as positive controls. Distilled water causes the cells to swell and burst through osmosis and allows the PI to bind to DNA and change colour.

After 24 hours, the cells were washed with PBS and 900 μL of PBS was added to each well except for the wells used as positive controls. For the latter, 900μL of distilled water was used. Propidium iodide (PI) (5 μM) (100μL in 900 μL) was added to each well to have an equal volume of 1ml per well and the plates were incubated for 15 minutes. After 15 minutes, the fluorescence was immediately read on the FLUOstar Omega plate reader at 544nm excitation and 640nm emission. The fluorescence intensity was calculated as in section 5.2.6 (a). (Figure 5.8).

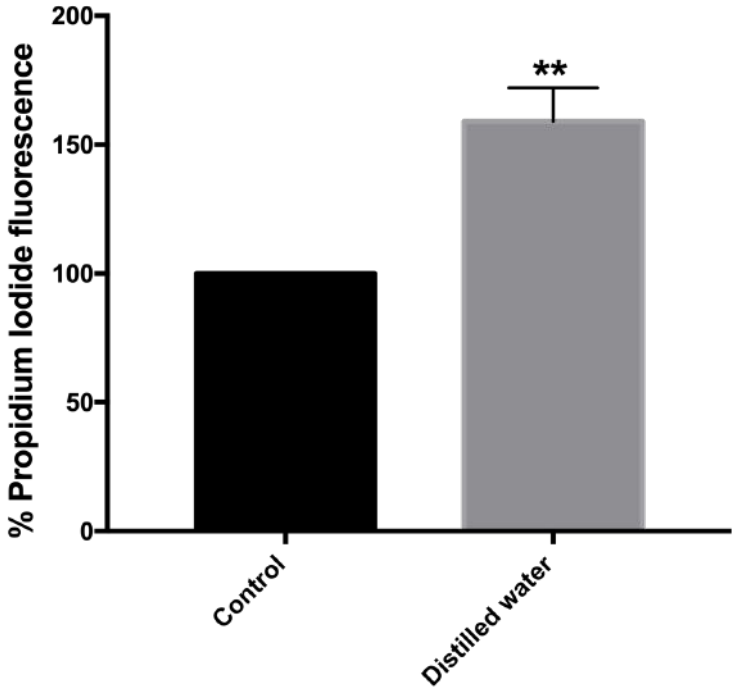

Figure 5. 8 Propidium iodide validation.

The RAECs treated with distilled water had a significant increase in PI fluorescence intensity which indicates cell death. **P<0.01 vs. control (ethanol).

5.2.7 Statistical analysis

Fluorescence values from the positive control and treatment groups were expressed as a percentage of the vehicle control fluorescence. All values are expressed as mean ± standard error of the mean (SEM) and Graph Pad Prism™ 6 was used for statistical analyses. Comparisons of groups were performed by ANOVA (one-way or two-way) followed by Bonferroni's post-test or student's t-tests where applicable. Significance was established at a p-value of <0.05.

5.3 Results

5.3.1 Effect of FFA on RAECs: Dose-response

The P7 generation RAECs were treated with different concentrations of palmitic acid (PA) or oleic acid (OA) or the combination of PA+OA for 24 hours with the aim of inducing endothelial dysfunction. Figure 5.9 (A and B) represents NO production using the DAF-2/DA fluorescent probe. NO production was reduced in RAECs treated with a combination of FFA (PA+OA) although the differences were not significant. However, this was a pilot study with an n-value of 2 per group. We then saw a significant difference with larger n-value of three per group (Figure 5.10).

Figure 5.9 (C and D) represents fluorescence readings with the DHR probe. There were no significant differences between the groups. Furthermore, there were also no differences in cell viability as measured with PI fluorescent probe (Figure 5.9 E and F).

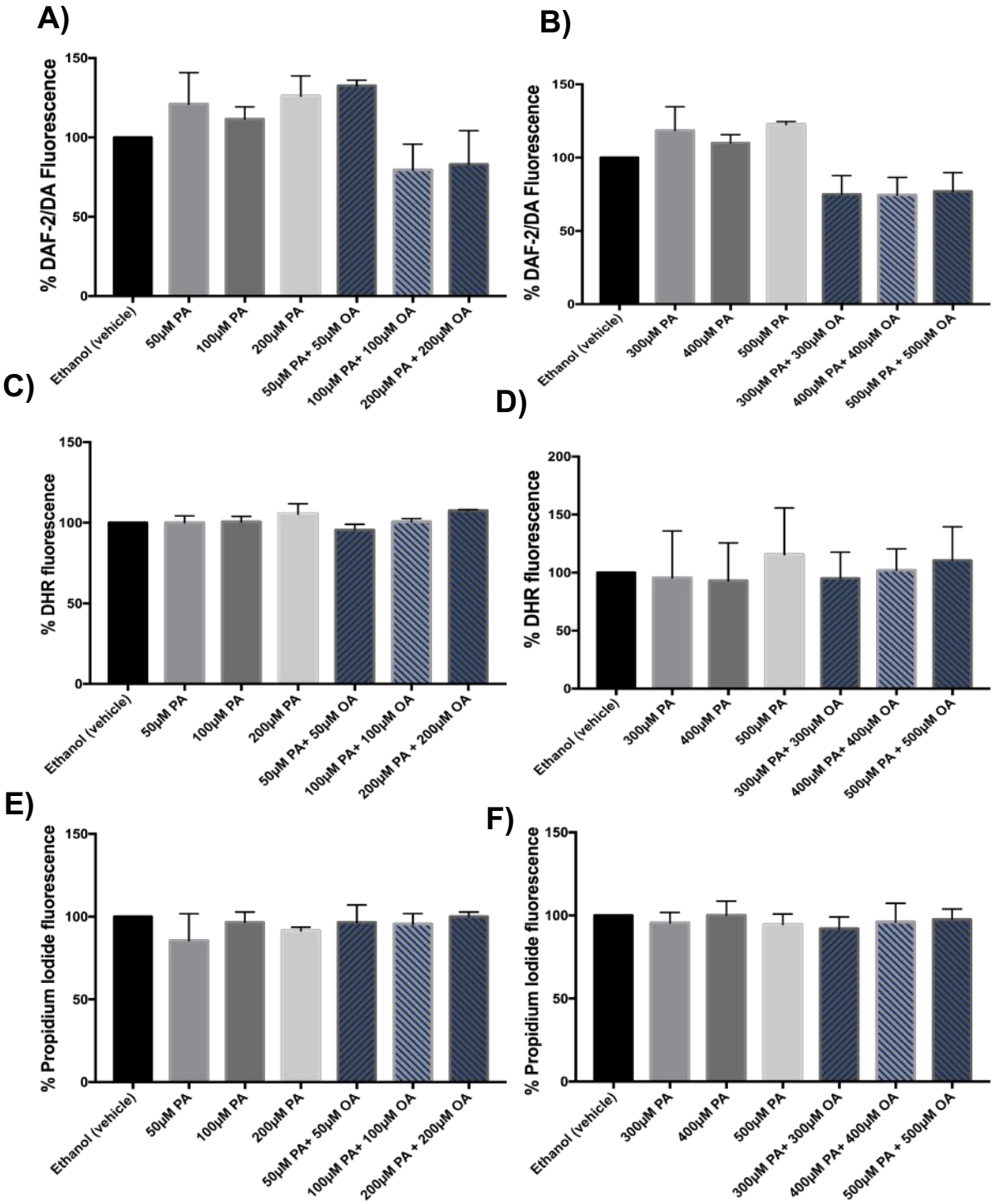

Figure 5. 9 Effect of different concentrations of PA (50 µM – 500 µM) and the combination of PA + OA (50 µM – 500 µM) on RAECs.

A and B), NO production as measured by DAF-2/DA fluorescence; C and D), % DHR fluorescence cells; E and F), % Propidium iodide fluorescence cells. All values are expressed as a percentage of the Ethanol (0.1%)(vehicle). n = 2 per group.

5.3.2 Effect of Epac modulation in healthy and FFA-treated RAECs: Dose-response of drugs

For a dose-response of drugs on the RAECs, the P7 generation were treated with FFAs (500 µM PA + 500 µM OA) and different dosages of Epac activator (CPT: [2 µM, 5 µM, 10 µM]) and/or Epac inhibitor (ESI-09: [1 µM, 5 µM, 10 µM]) for 24 hours. The production of NO, oxidative stress and cell viability were measured using the appropriate fluorescent probes.

5.3.2 (a) NO production

Figure 5.10 A represents NO production as measured by DAF-2/DA fluorescence intensity in RAECs treated with CPT [2 µM] and ESI-09 [1 µM]. Epac activation with CPT [2 µM] significantly increased NO production compared to control (CPT [2 µM]: 129.3 ± 5.8% vs. Control: 100%, $P<0.1$). Epac inhibition with ESI-09 [1 µM] significantly reversed the CPT [2 µM] effect on NO production (CPT [2 µM]: 129.3 ± 5.8% vs. CPT [2 µM] + ESI-09 [1 µM]: 102.7 ± 5%, $P<0.01$). RAECs treated with FFA had a significant reduction in NO production compared to nontreated cells (FFA: 60.3 ± 1.2% vs. Ethanol (vehicle): 101.7 ± 2.7%, $P<0.0001$).
However, neither Epac activation nor inhibition had a significant effect on FFA-treated cells (Figure 5.10 A, B, C).

Figure 5.10 B represents NO production as measured by DAF-2/DA fluorescence intensity in RAECs treated with CPT [5µM] and ESI-09 [5µM]. The [5 µM] CPT concentration also increased NO production in RAECs compared to control (CPT [5 µM]: 124.7 ± 1.2% vs. control: 100%, $P<0.01$). However, inhibition with [5 µM] ESI-09 did not affect NO production.

Figure 5.10 C represents NO production as measured by DAF-2/DA fluorescence intensity in RAECs treated with CPT [10µM] and ESI-09 [10µM]. CPT [10 µM] increased NO production when compared to control RAECs (CPT [10 µM]: 131 ± 7% vs. control: 100%, $P<0.01$) while the co-treatment with ESI-09 [10 µM] reversed the CPT [10 µM] effect on NO production (CPT [10µM]: 131 ± 7% vs. CPT [10 µM] + ESI-09 [10 µM]: 110.7 ± 7.9%, $P<0.05$).

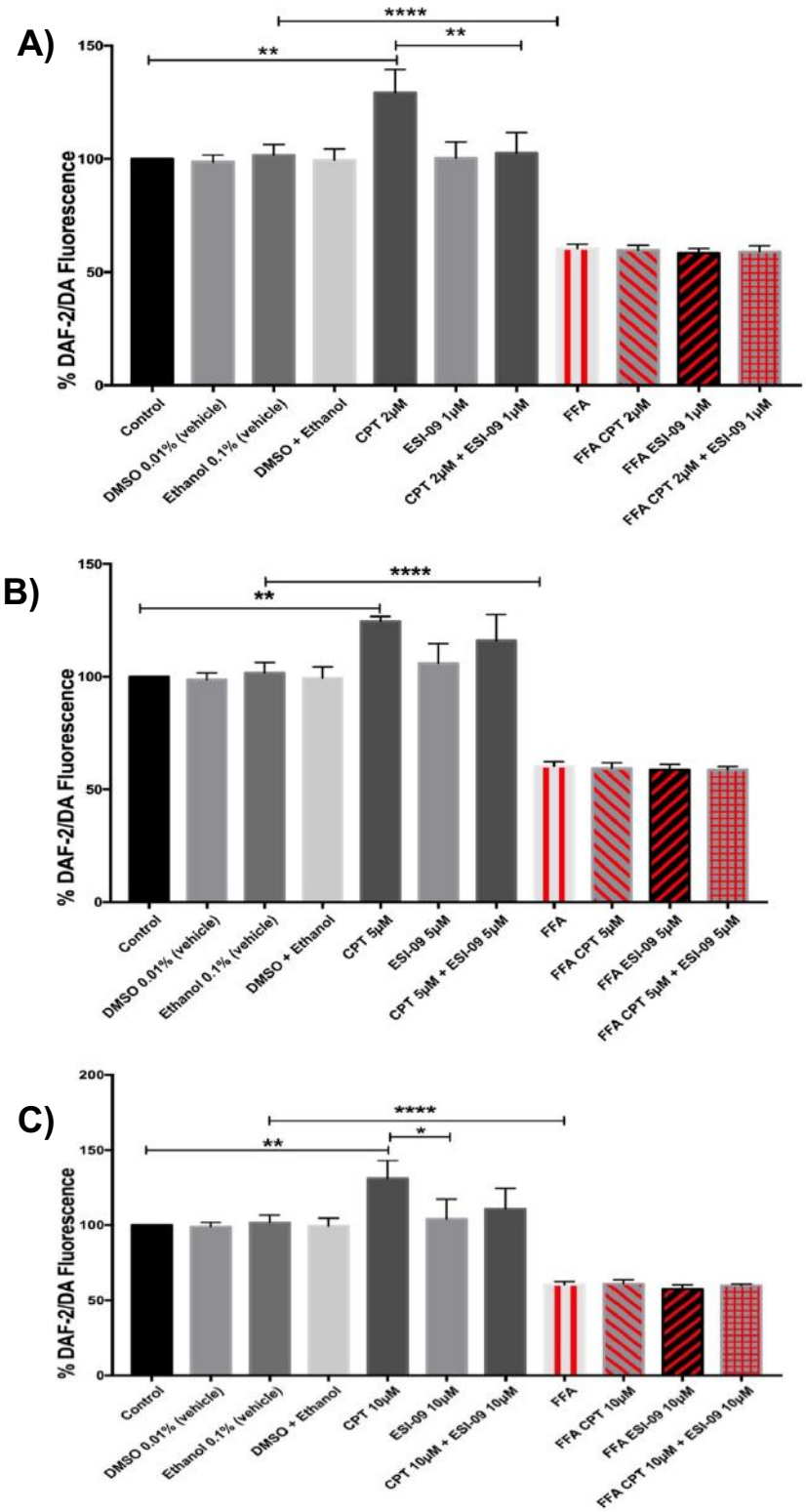

Figure 5. 10 Effect of Epac modulation in healthy and FFA-treated (500μM PA + 500μM OA) cells. Intracellular NO production as measured by DAF-2/DA fluorescence after24hr of treatment with A) CPT, 2 μM and ESI-09, 1 μM; B) CPT 5μM and ESI-09, 5 μM; C) CPT, 10 μM and ESI-09, 10 μM. All values are expressed as the percentage of the control. n = 3 per group.*P<0.05, **P<0.01, ****P<0.0001.

5.3.2 (b) ROS production

Figure 5.11A represents ROS production as measured by DHR fluorescence intensity in RAECs treated with CPT [2μM] and ESI-09 [1μM]. The RAECs treatment with FFAs showed no significant differences in ROS production when compared to ethanol (vehicle). RAECs co-treated with CPT [2 μM] and ESI-09 [1 μM] had an increased percentage DHR fluorescence intensity compared to DMSO (vehicle) (CPT [2 μM] + ESI-09: [1 μM]: 99.3 ± 1.1% vs. DMSO: 96 ± 2.5%, $P<0.05$).
However, neither Epac activation nor inhibition had a significant effect on FFA-treated cells (Figure 5.11 A, B, C).

Figure 5.11B represents ROS production as measured by DHR fluorescence intensity in RAECs treated with CPT [5μM] and ESI-09 [5μM]. Epac activation with CPT [5 μM] reduced the percentage DHR fluorescence intensity compared to control (CPT [5 μM]: 87.67 ± 1.5% vs. control: 100%, $P<0.001$). Furthermore, co-treatment of CPT [5 μM] with ESI-09 [5 μM] reversed the effects of CPT [5 μM] on ROS production (CPT [5 μM] + ESI-09 [5 μM]: 93.7 ± 1.6% vs. CPT [5 μM]: 87.67 ± 1.5%, $P<0.05$). The RAECs treatment with FFAs showed no significant differences in ROS production when compared to ethanol (vehicle).

Figure 5.11C represents ROS production as measured by DHR fluorescence intensity in RAECs treated with CPT [10 μM] and ESI-09 [10 μM]. CPT [10 μM] reduced the percentage DHR fluorescence intensity compared to control (CPT [10 μM]: 85.67 ± 2.6% vs. control: 100%, $P<0.05$). The RAECs treatment with FFAs showed no significant differences in percentage DHR intensity compared to ethanol (vehicle).

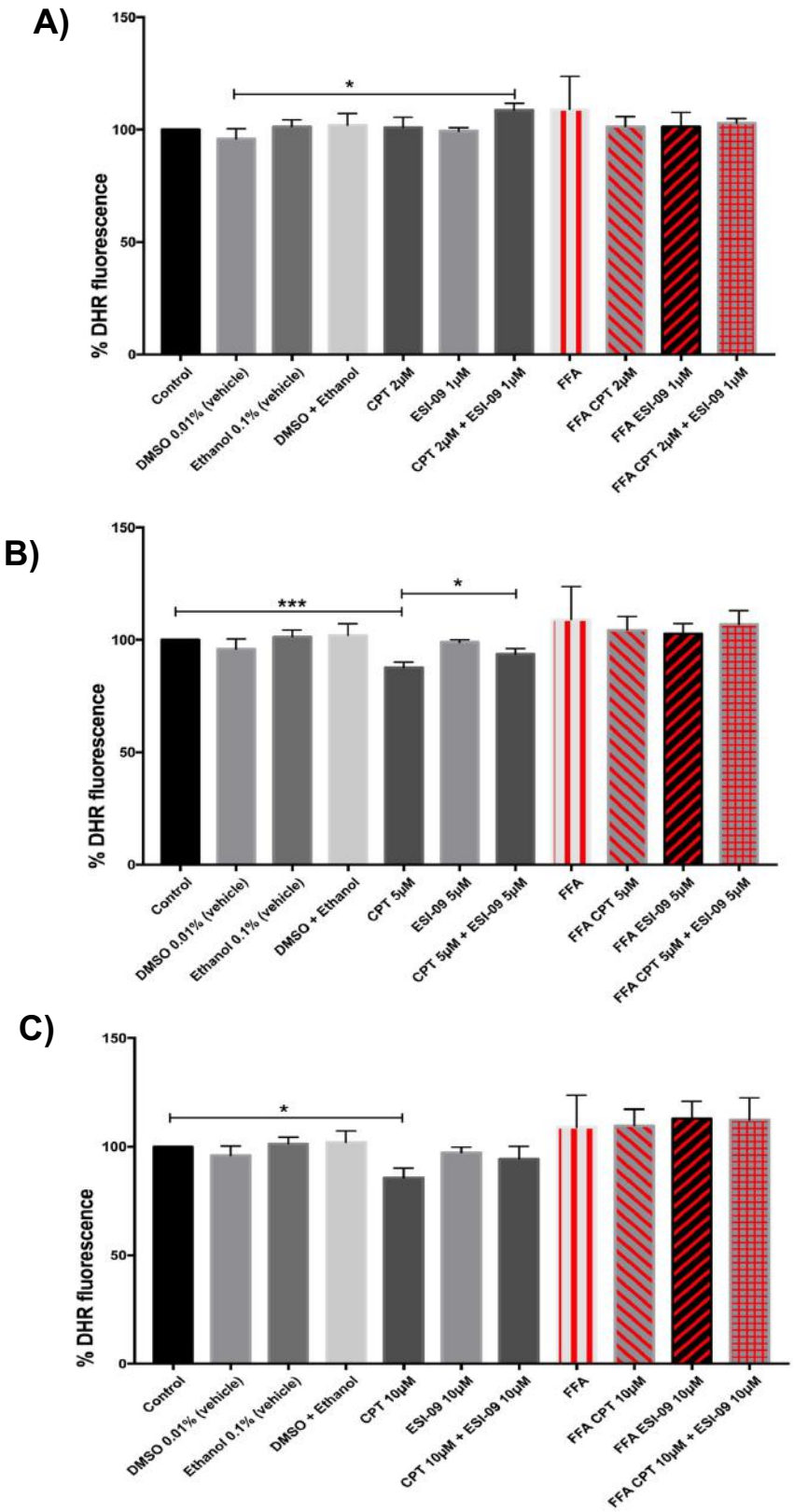

Figure 5. 11 Effect of Epac modulation in healthy and FFA-treated (500μM PA + 500μM OA) cells.

ROS production as measured by % DHR fluorescence after 24hr of treatment with: A) CPT, 2 μM and ESI-09, 1 μM; B) CPT, 5 μM and ESI-09, 5 μM; C) CPT, 10 μM and ESI-09, 10 μM. All values are expressed as the percentage of the control. n = 3 per group.*P<0.05, ***P<0.001.

5.3.2 (c) Cell viability

Figure 5.12A represents cell viability as measured by PI fluorescence intensity in RAECs treated with CPT [2 μM] and ESI-09 [1 μM]. RAECs treated with FFA had a significant decrease in PI fluorescence intensity compared to non-treated cells (FFA: 69.33 ± 1.455 vs. Ethanol: 101.7 ± 5.21%, $P<0.001$). Epac activation with CPT [2 μM] had no effect on cell viability.
Furthermore, neither Epac activation nor inhibition had a significant effect on FFA-treated cells (Figure 5.12 A, B, C).

Figure 5.12B represents cell viability as measured by PI fluorescence intensity in RAECs treated with CPT [5 μM] and ESI-09 [5 μM]. Epac activation with CPT [5μM] had no effect cell viability. Epac inhibition with ESI-09 showed a significant reduction in PI fluorescence intensity compared to DMSO (vehicle control) (ESI-09: 88 ± 2.31% vs. DMSO: 106 ± 0.57%, $P<0.05$; ESI-09 + CPT: 85.33 ± 5.21% vs. DMSO: 106 ± 0.57%, $P<0.01$).

Figure 5.12C represents cell viability as measured by PI fluorescence intensity in RAECs treated with CPT [10 μM] and ESI-09 [10 μM]. Epac activation with CPT [10 μM] had no effect cell viability. Epac inhibition with ESI-09 showed a significant reduction in PI fluorescence intensity compared to DMSO (vehicle control) (ESI-09: 86.67 ± 2.0% vs. DMSO: 106 ± 0.57%, $P<0.01$; ESI-09 + CPT: 89.33 ± 3.48% vs. DMSO: 106 ± 0.57%, $P<0.01$).

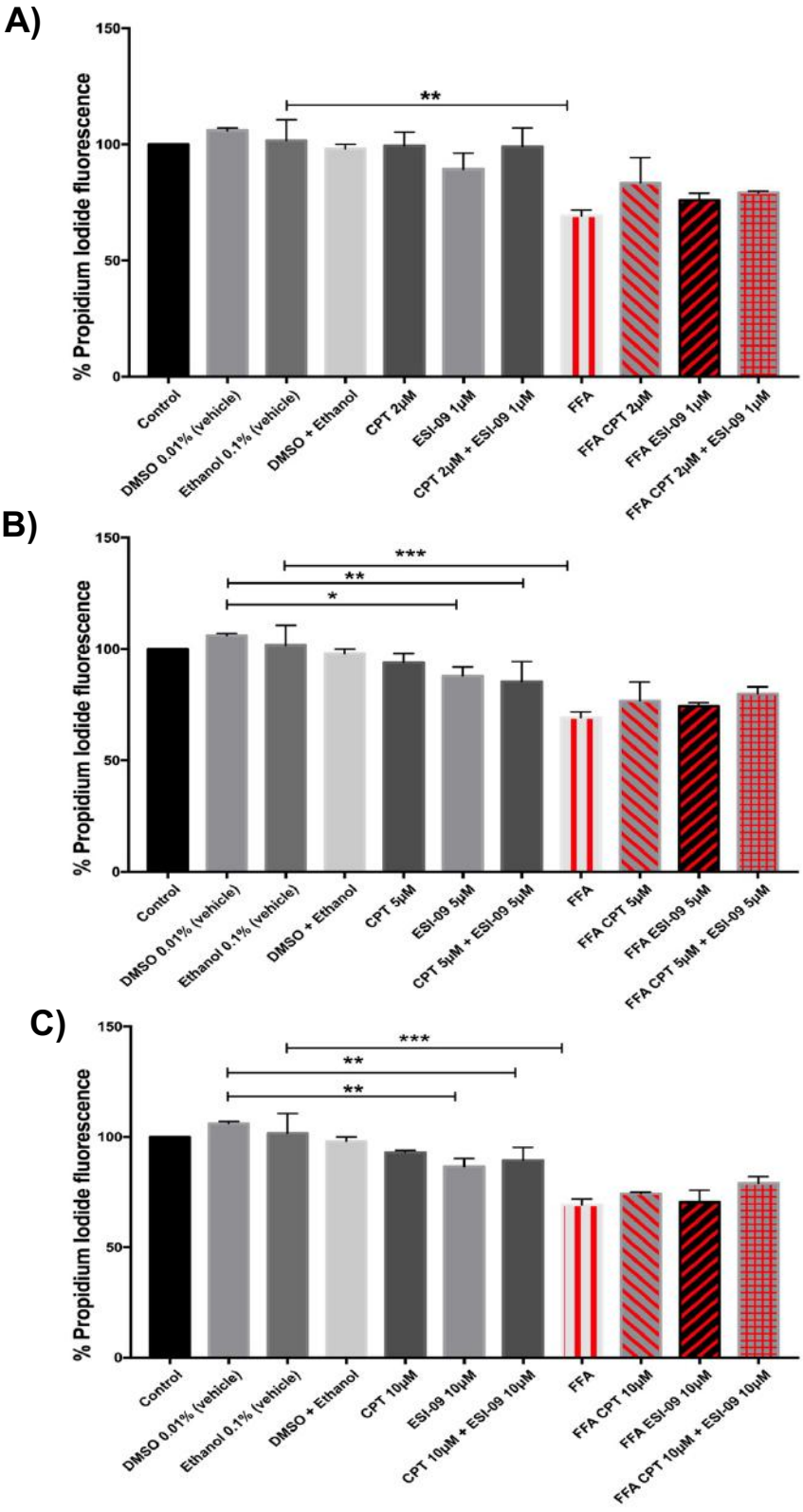

Figure 5. 12 Effect of Epac modulation in healthy and FFA-treated (500μM PA + 500μM OA) cells.

Cell viability as measured by PI fluorescence intensity after 24hr of treatment with: **A)** CPT, 2 μM and ESI-09, 1 μM; **B)** CPT, 5 μM and ESI-09, 5 μM; **C)** CPT, 10 μM and ESI-09, 10 μM. All values are expressed as the percentage of the control. n = 3 per group.*P<0.05, ***P<0.001.

5.4 Discussion

In this study we aimed to establish an *in vitro* model of FFAs induced endothelial dysfunction and to explore the role of the cAMP-Epac pathway in this model. To achieve the aim, RAECs were treated with saturated fatty acids, palmitic acid (PA) and monounsaturated fatty acid, oleic acid (OA) to induce endothelial dysfunction. In addition, the cells were treated with an Epac agonist, CPT and Epac antagonist, ESI-09, respectively. We have demonstrated that Epac activation with CPT improved NO production/availability and reduced intracellular ROS in normal RAECs. However, CPT did not reverse the detrimental effects on FFAs on RAECs.

5.4.1. FFAs induced endothelial dysfunction

In this study, we used palmitic acid (PA) with an aim to establish a model of endothelial dysfunction. Previous studies have shown that PA causes oxidative stress and inflammation, and leads to insulin resistance and impairment of endothelial function (Batumalaie *et al*., 2016; Chen *et al*., 2019; Lee *et al*., 2014; Li *et al*., 2018). Furthermore, the unsaturated FFAs OA and linoleic acid inhibit Ca^{2+} mediated- NO production/release in endothelial cells demonstrating their role in the development of endothelial dysfunction (Kuroda *et al*., 2001). In the present study, endothelial function was assessed by investigating NO production, ROS production and cell viability in RAECs treated with different concentrations of FFAs. PA (50 µM - 500 µM) did not induce endothelial dysfunction after 24hours treatment. It has been reported that elevation in OA leads to an increase in mitochondrial ROS and a reduced nitric oxide synthase (eNOS) activity in endothelial cells (Gremmels *et al*., 2015). Therefore, we combined PA and OA, and a reduction (not significant, n = 2 per group) in NO availability was noticed from the concentration of (PA 100µM + OA 100 µM to PA 500µM + OA 500µM). However, with an increased n-value (n = 3), FFAs significantly reduced NO production at the concentration of (PA 500 µM + OA 500 µM)(Figure 5.10). The ROS production and cell viability did not change, we therefore, decided to use the combination of PA and OA at the concentration of 500 µM each for the future studies.

5.4.2 The role cAMP-Epac pathway on FFA-induced endothelial dysfunction

The present study showed that the chronic exposure of RAECs to FFAs for 24 hours had a detrimental effect on NO production (Figure 5.10A, B and C). These findings suggest that elevated FFAs have an inhibitory role on NO production in endothelial cells. In a study by Steinberg and co-workers (Steinberg *et al*., 1997), it was shown that high concentrations of circulating FFAs were closely associated with an impairment of endothelium-dependent vasodilation while endothelium-independent vasodilation was not affected. These findings confirmed the detrimental role of FFAs on endothelial NO production. Furthermore, Van Vickle and colleagues (Van Vickle, 2005) demonstrated a reduction in eNOS protein expression in porcine aortic endothelial when exposed to PA and stearic acid which may affect NO availability. Inhibitory effects of FFAs on eNOS activity and eNOS mRNA expression were also observed in RAECs was suggested to be through oxidative stress and inflammation (Yu *et al.*, 2008). Surprisingly, there were no significant changes in ROS production/oxidative stress between FFA-treated and control RAECs (Figure 5.11A, B, C). Therefore, we can speculate that the FFAs were not effective enough to produce ROS in this pilot study. Furthermore, this model needs to be optimized and the use of bovine serum albumin bind the FFAs could be beneficial to carry FFAs into the cell.

We found that Epac activation with different concentrations of a selective agonist CPT [2 µM, 5 µM and 10 µM] significantly increased DAF-2/DA fluorescence (indicative of NO production) in non-FFA-treated RAECs as compared to untreated cells. This effect was abolished by the Epac inhibitor, ESI-09 [1 µM and 10 µM] (Figure 5.10A, B and C). These findings suggest that Epac activation may increase eNOS activity, which resulted in an increased endothelium-dependent NO bioavailability. Other studies suggested that both Epac and PKA play a dual role in eNOS activity and NO release in human umbilical vein endothelial cells (HUVEC) (García-Morales *et al*., 2017, 2014).

Oxidative stress reduces NO release and lessens endothelium-dependent vasodilatation (Pierini and Bryan, 2015). Furthermore, increased intracellular ROS is closely associated with the development of endothelial dysfunction and atherosclerosis (Boden, 2008; Cai and Harrison, 2000). In the present study, the

increased NO production observed in RAECs treated with CPT was associated with a decrease in intracellular ROS (Figure 511B and C). This effect was abolished with co-treatment with ESI-09 [5 μM] (Figure 5.11B). In other cell types, Epac has been demonstrated to be involved in mitochondrial ROS production (Remans *et al*., 2006, 2004). For example, Epac2-Rap1 inhibition with (ESI-05) in cardiomyocytes lead to an increased mitochondrial ROS production and CaMKII activation (Yang *et al*., 2016). Another study demonstrated that pharmacological activation of Epac with CPT reduced ROS production and prevented apoptosis in tubular epithelium after exposure to I/R injury (Stokman *et al*., 2014). Furthermore, hyperglycaemia downregulates Rap1 expression and activation which leads to renal tubular cells injury via a mechanism that includes an overproduction of mitochondrial ROS (Xiao *et al*., 2014). In another study, it was demonstrated that the Epac-Rap pathway is essential in preventing and restoring barrier function after an inflammatory cytokine-induced retinal vascular permeability (Ramos *et al*., 2018). Furthermore, Epac1 is considered to be a therapeutic target for vascular endothelial cells due to its ability to attenuate proinflammatory cytokines (Barker *et al.*, 2017). Therefore, we have demonstrated in this study that a selective Epac activation with CPT in RAECs plays a significant role in the reduction of intracellular ROS and the increase in NO availability.

Furthermore, FFA-induced ROS production is associated with an increased monocyte expression of CD11b and adhesion of monocyte to endothelial cells, this is a critical mechanism in early development of atherosclerosis (Mestas and Ley, 2008; Zhang *et al.*, 2006). However, in our study, there were no significant changes in ROS production among the groups treated with FFAs and CPT.

In conclusion, Epac activation with CPT improved NO production/availability and reduced intracellular ROS in normal RAECs. However, CPT did not reverse the detrimental effects on FFAs on RAECs.

Chapter Six

Conclusions, limitations and future directions

6.1 Summary of the findings

The first aim of the study was to elucidate the role of Epac in myocardial ischaemia-reperfusion injury of *ex vivo* hearts of a rat model of normal body weight. We demonstrated that Epac activation with CPT pre- or post- ischaemia protects the hearts against I/R injury. Furthermore, pharmacological inhibition of the RISK pathway suggested partial involvement of ERK1/2 and PKB in CPT-induced cardioprotection (reduced infarct size). The cardioprotective mechanism is not clear, as the western blot data indicated that CPT/Epac stimulation could not activate ERK 1/2 or PKB (RISK pathway). However, co-treatment with CPT and ESI-09 reduced the phosphorylation of both ERK1/2 and PKB compared to untreated hearts. Therefore even though CPT's effect on the RISK pathway was inconclusive, Epac inhibition with 5 μM ESI-09 negatively affected the RISK pathway. Suggesting that Epac-mediated cardioprotection partially involves the RISK pathway.

The second aim of the study was to elucidate the role of Epac in myocardial ischaemia-reperfusion injury of *ex vivo* hearts of a rat model of high-calorie diet-induced obesity and insulin resistance. We have demonstrated that male Wister rats fed with a HC diet for 16 weeks developed characteristics of the metabolic syndrome including increased body weight gain compared to control diet animals, increased IP, elevated non-fasting glucose levels, increased HOMA-IR and glucose intolerance. However, the hearts from the HC group did not present with altered cardiac function at stabilization nor post I/R. The HC diet also had no detrimental effect on infarct size. In addition, co-treatment of CPT with the RISK pathway inhibitors suggested that CPT-mediated protection, based on post ischaemic recovery of cardiac function and infarct size was partially mediated by PKB and ERK1/2 in the CD group, but mainly by PKB in the HC group. However, we found no association between infarct size data and the protein expression and phosphorylation of PKB. Suggesting that alternative cardioprotection

pathway need to be investigated e.g. connexins (Schulz *et al*., 2007) or the survivor activating factor enhancement (SAFE) pathway (Lecour, 2009). Interestingly, CPT activated CaMKII in the HC group but not eNOS and therefore this needs further elucidation. Epac inhibitor (ESI-09, 5 μM) was detrimental to cardiac function and this was associated with decreased phosphorylated ERK1/2 in both diets, decreased phosphorylated GSK-3β in CD, increased phosphorylated AMPK in both diets, increased PARP cleavage in CD and increased autophagy (phosphorylated ULK-1) in CD.

The third aim was to investigate the role of Epac signalling in *ex vivo* thoracic aortas of a rat model of high-calorie diet-induced obesity and insulin resistance. The HC diet did not exert detrimental effects on vascular function. CPT treated aortas had a significant improvement in ACh-induced vasorelaxation and Epac inhibition with ESI-09 abolished the CPT vasorelaxant effect. Most importantly, CPT directly induced vasorelaxation in a dose-dependent manner in both HC and CD group and this effect was NOS-dependent, as it was abolished by L-NAME (NOS inhibitor). Interestingly, ESI-09 also increased the phosphorylation of the stress kinase AMPK. However, the western blot data did not give conclusive results which limited our conclusion on the mechanism through which Epac induce vasorelaxation.

The fourth aim was to investigate the role of Epac signalling in palmitic and oleic acid-induced endothelial dysfunction in RAECs. We have demonstrated that Epac activation with CPT improved NO production/availability and reduced intracellular ROS in normal RAECs. However, CPT did not reverse the detrimental effects on FFAs on RAECs.

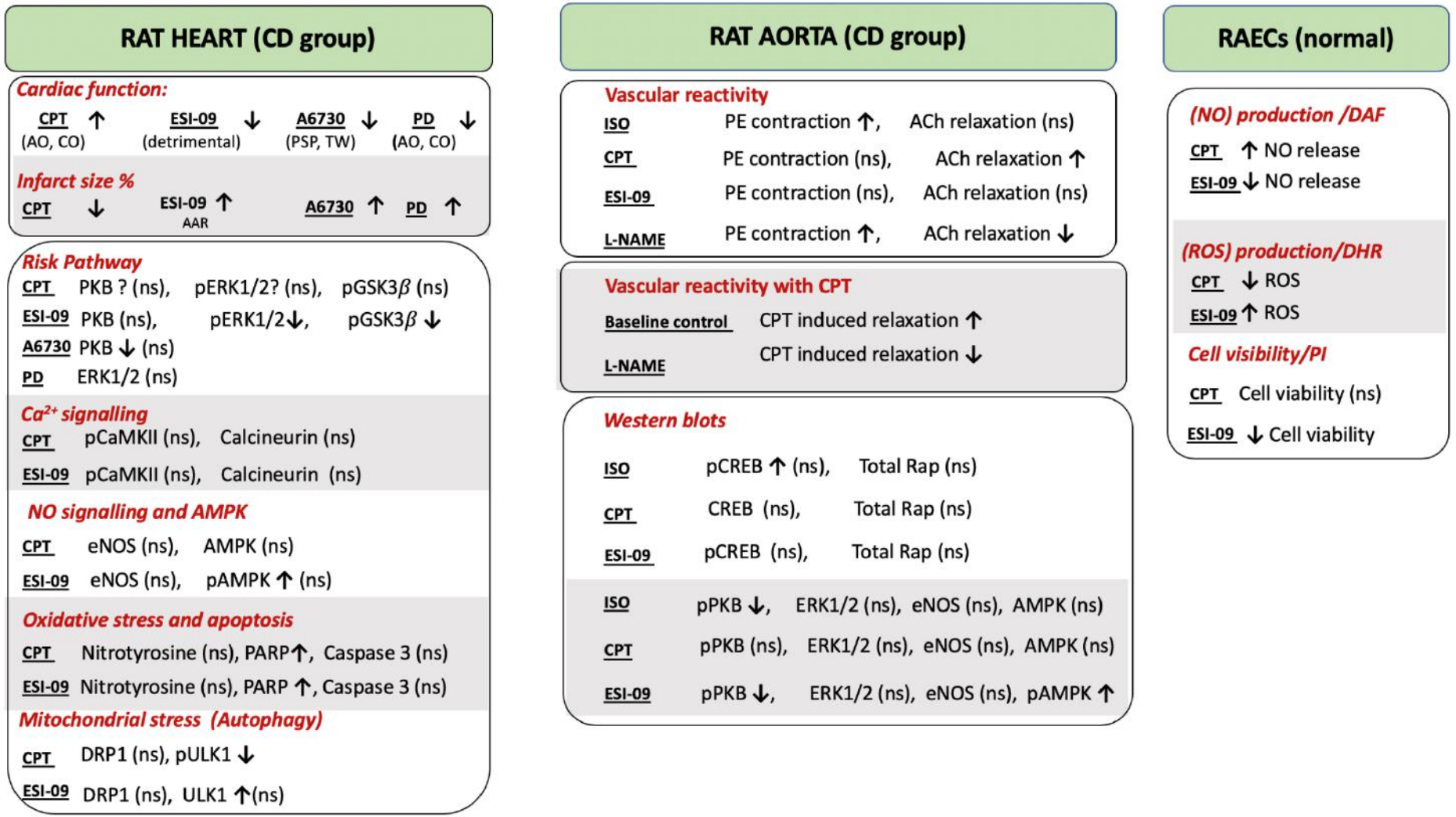

Figure 6. 1 Summary of the findings: CD group. ("ns"= not significant)

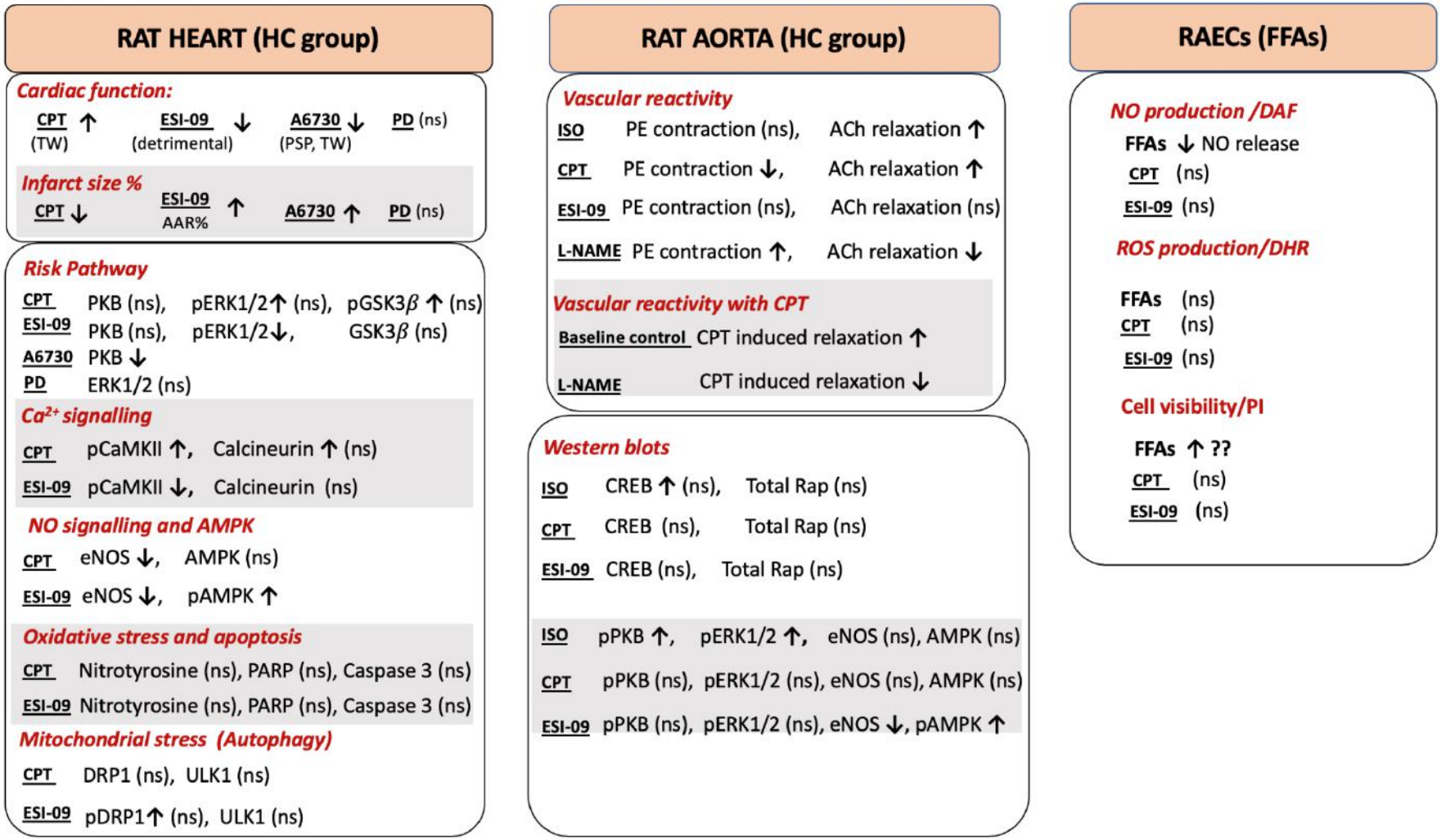

Figure 6. 2 Summary of the findings: HC group. ("ns"= not significan)

6.2 Conclusions

The novelty of this study lies in the role of Epac in the cardiovascular system (heart and vascular tissues) of diet-induced obese rats and isolated cells treated with FFA, and the possible mechanisms involved. In this regard, acute Epac activation with CPT (2 µM) at reperfusion is cardioprotective against I/R injury in *ex vivo* isolated hearts of diet-induced obese rats. Furthermore, direct Epac stimulation improves the endothelium-dependent vascular reactivity of diet-induced obese rats. To our knowledge, this is the first such observation. Previous studies have pointed towards the effects of Epac prior to I/R injury. However, Epac's cardioprotective mechanisms still need further elucidation and therefore we propose the following mechanisms. The first speculated mechanism is that Epac-mediated cardioprotection partially involves the RISK pathway (ERK1/2 and PKB) as demonstrated by the infarct size data. Furthermore, inhibition of Epac with ESI-09 reduced phosphorylated ERK1/2 in both diets suggesting an impaired ERK signalling. Unfortunately, the PKB Western blot data was inconclusive and need to be repeated in future work. The second speculated mechanism is the possibility that Epac's vasorelaxant effects are mediated via NOS but this also needs verification since the western blots could not give a clear answer. Interestingly, Epac activation with CPT significantly increased NO production and reduced intracellular ROS in normal RAECs which further supports its role NOS activity.

Collectively, enhancing Epac signalling post-I/R injury reduces myocardial infarction in *ex vivo* isolated hearts, partially via the RISK pathway. These effects were attenuated by both Epac and the RISK pathway inhibitors. Furthermore, enhanced Epac signalling improved the vasculature responsiveness in *ex vivo* rat aortas and the presence of Epac and NOS inhibitors abolished the effect. In addition, Epac activation increased NO production and reduced ROS generation in RAECs. Thus, suggests that Epac signalling may be considered as a potential future therapeutic target in the prevention of I/R injury and endothelial dysfunction.

6.3 Limitations

a) The HC diet was not associated with altered cardiac function at stabilization nor post I/R and could not induce endothelial dysfunction. This suggests that the diet programme used in the study was not sufficiently harmful to induce overt and measurable markers of injury in the hearts and aortas. Despite this, several significant observations were made showing that the diet was able to exert partial effects, which allowed to draw some meaningful conclusions.

b) Having one control (DMSO vehicle control) was a limiting factor since one of our drugs was dissolved in distilled water. However, DMSO is regarded as a safe solvent in low concentrations (Sanmartín-Suárez *et al*., 2011).

c) Epac-mediated cardioprotective effects could be either Epac1 or Epac2. We did not study the role of the individual isoforms in this study, only the overall effect of Epac.

d) The Epac inhibitor ESI-09 was detrimental to hearts with the result that we could not measure the cardiac function.

e) The n-value in western blot experiments was low due to the large number of treatment groups and limited number of wells per gel. Furthermore, the Western blot data was not (always?) conclusive.

f) Another challenge was to establish a working model of FFA-induced endothelial dysfunction in the cultured endothelial cells. PA alone did not induce endothelial dysfunction and the combination of PA and OA was potentially excessively detrimental to the RAECs compared to the vehicle control. As a result, Epac activation with CPT could not reverse the adverse effects of FFAs.

g) Another limitation of this study was the cell viability assay (PI). The assay includes a washing step before measuring the fluorescence. The dead endothelial cells detached from the plate surfaces and will be lost during the washing steps. Therefore, PI fluorescence in the ESI-09 and FFAs treated cells

was significantly lower because the necrotic cells are washed away. Therefore, the results in figure 5.12A, B and C may not be a true representation of cell viability.

6.4 Future studies and contribution

Our findings indicate the complexity of Epac-mediated cardioprotection and therefore emphasizes the importance of future mechanistic studies of Epac in the cardiovascular system. Such studies should include:

a) The use of an *in vivo* animal model in which overt obesity/insulin resistance/ cardiomyopathy/ endothelial dysfunction has been induced to evaluate the role of Epac.

b) Mechanistic studies to further elucidate the role of Epac on the RISK pathway

c) Alternative cardioprotective pathways such connexins and SAFE pathway should also be investigated.

~~d)~~ We also demonstrated the detrimental effects of the Epac inhibitor ESI-09, which was associated with an increased stress kinase AMPK in both hearts and aortas, and therefore this needs further investigation.

e) We demonstrated that Epac activation with CPT reduced autophagy (ULK1 Ser555) and co-treatment ESI-09 abolished the effect in CD group but not HC group. Therefore, this suggests that an association exists between Epac and autophagy and this needs further investigation.

f) Optimization of the FFA-induced endothelial dysfunction model in cultured endothelial cells, and the protocol which should include binding of PA and OA to bovine serum albumin. This will be beneficial to the study since our observation is based on healthy RAECs.

g) Additional assays (like MTT and flow cytometry) to measure apoptosis and cell viability in RAECs could be beneficial to the study.

h) Western blot studies are needed to validate the role of Epac in NO production in RAECs.

Appendix A

Supplementary data

Table A. 1 Characteristics of the Diet Models: Weekely food consumption, water intake and non-fasting blood glucose.

Parameter	Unit	CD	n	HC	n
Food consumption					
Week 1-10	g	17.62±0.36	40	23.41±0.52***	40
Week 11-16	g	17.76±0.44	20	21.10±0.92***	20
Week 1-16	g	18.00±0.54	20	22.30±1.27***	20
Water intake					
Week 1-10	mL	29.09±0.90	40	19.85±0.64***	40
Week 11-16	mL	29.76±0.88	20	20.25±0.76***	20
Week 1-16	mL	29.74±0.74	20	19.55±0.58***	20
Non-fasting blood glucose Week 16	mM	6.88±0.11	63	7.78±0.14***	65

***p<0.001. vs. CD group.

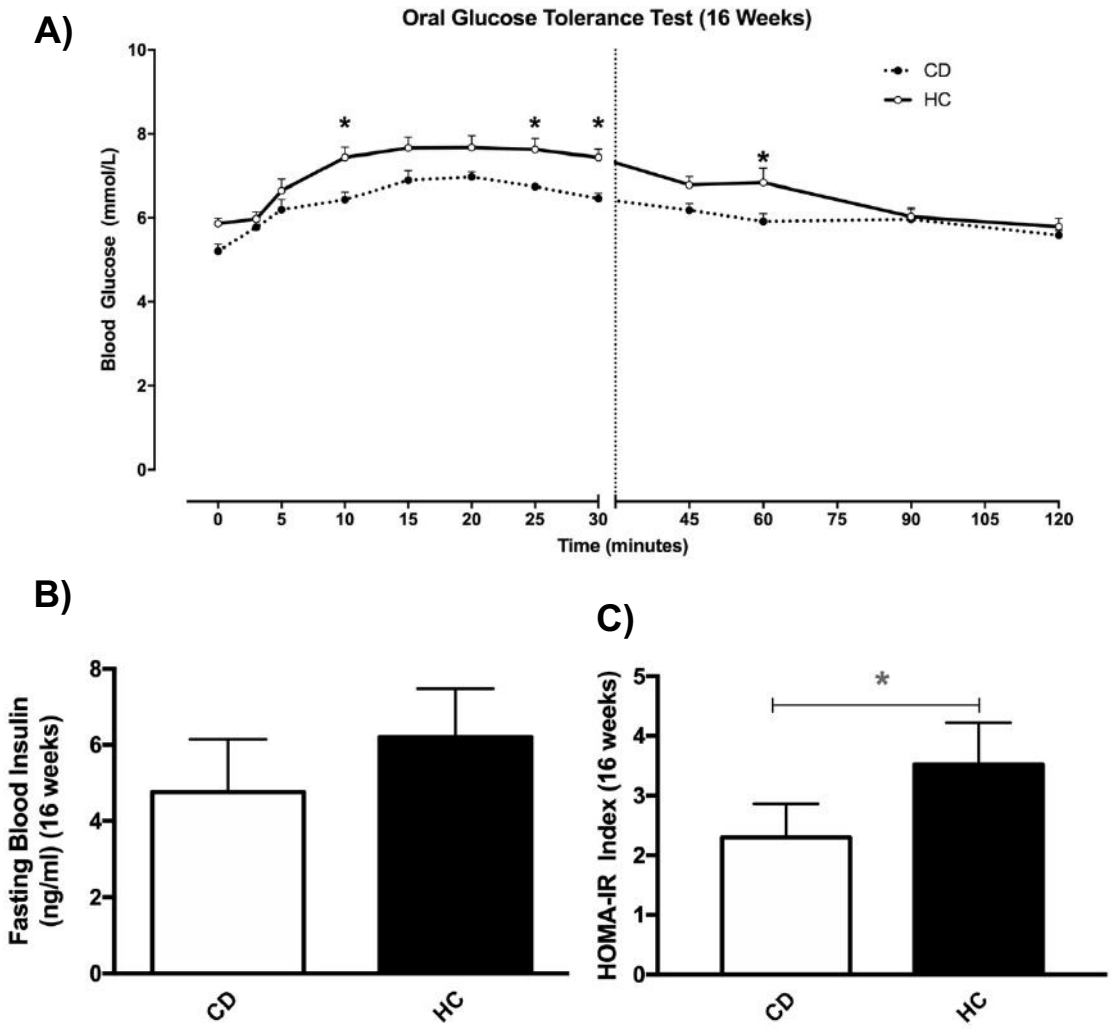

Figure A. 1 Oral glucose tolerance test, fasting blood insulin concentrations and HOMA-IR of male Wistar rats at 16 weeks of feeding high calorie diet (HC).

(A), Oral glucose tolerance test; (B), fasting blood insulin concentrations; (C), Homeostatic model for insulin resistance (HOMA-IR). *P<0.05. n = 6-12

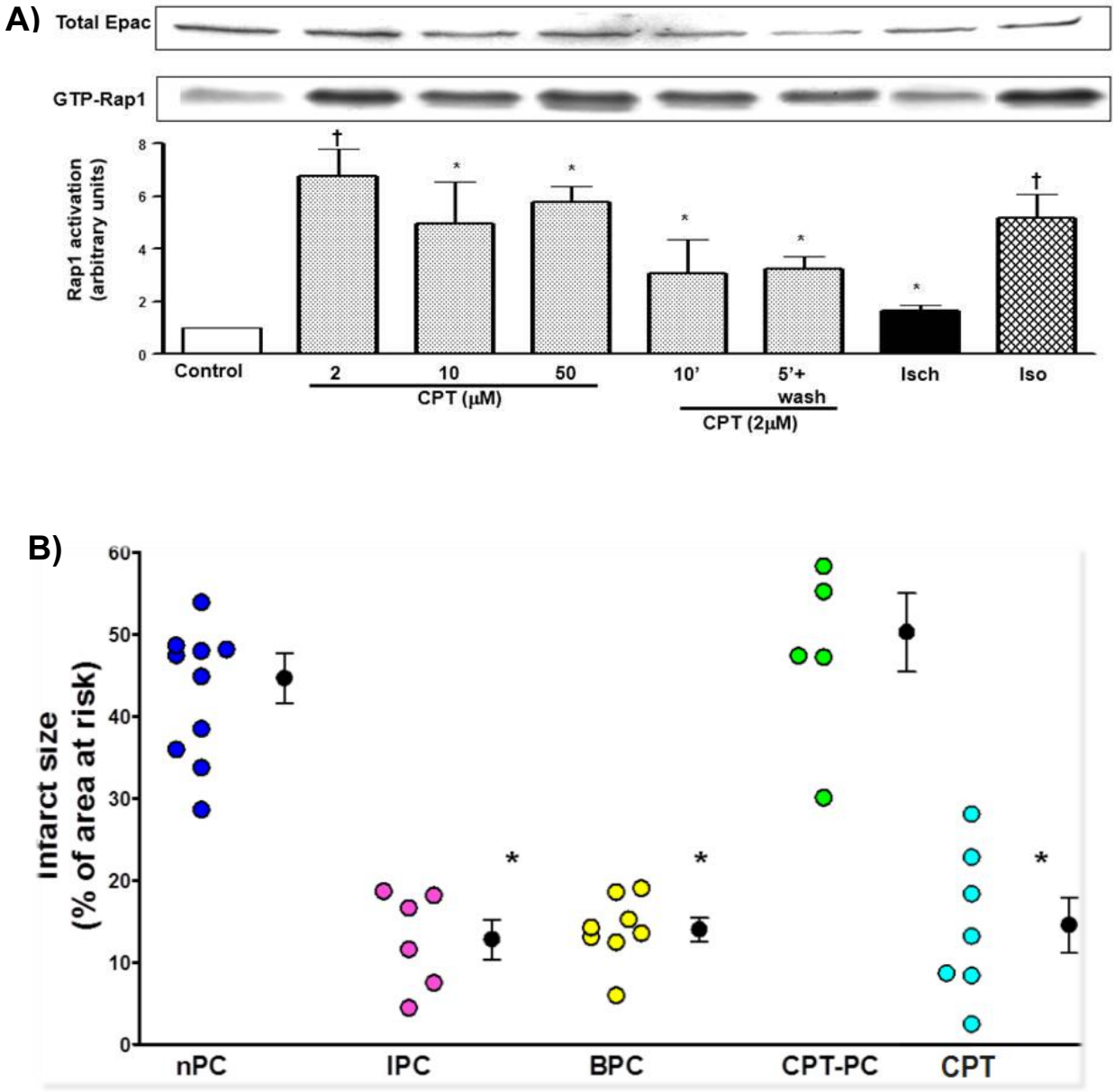

Figure A. 2 **(A),** Effect of CPT on Rap1 Activation and expression **(B),** nPC = non-Preconditioning; IPC = Ischaemic Preconditioning; BPC = Beta-Preconditioning; CPT-PC = Epac agonist Preconditioning; CPT = Epac agonist Pre-treatment. *p < 001 vs. nPC.

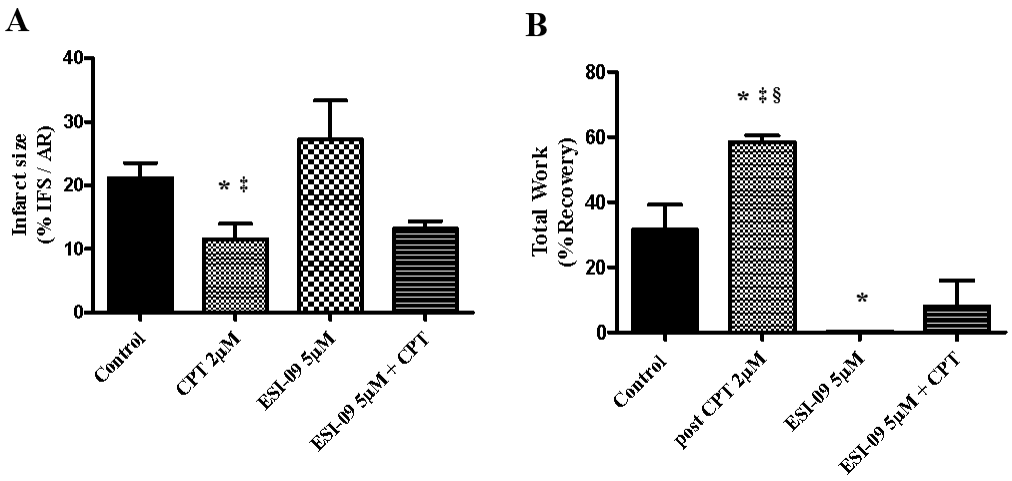

Figure A. 3 Ischaemic hearts post-treated with agonist (8-CPT-2'-O-Me-cAMP) CPT, novel selective Epac1 antagonist ESI-09 and untreated ischaemic hearts

(A) Infarct sizes expressed as % (IFS/AR) Infarct size /Area at risk, (B) Total work expressed as % recovery. Data are means ± SEM. *p < 0.05 vs. control; ‡P < 0.05 vs. ESI-09 5μM; §P < 0.05 vs. ESI-09 5μM + CPT 2μM.

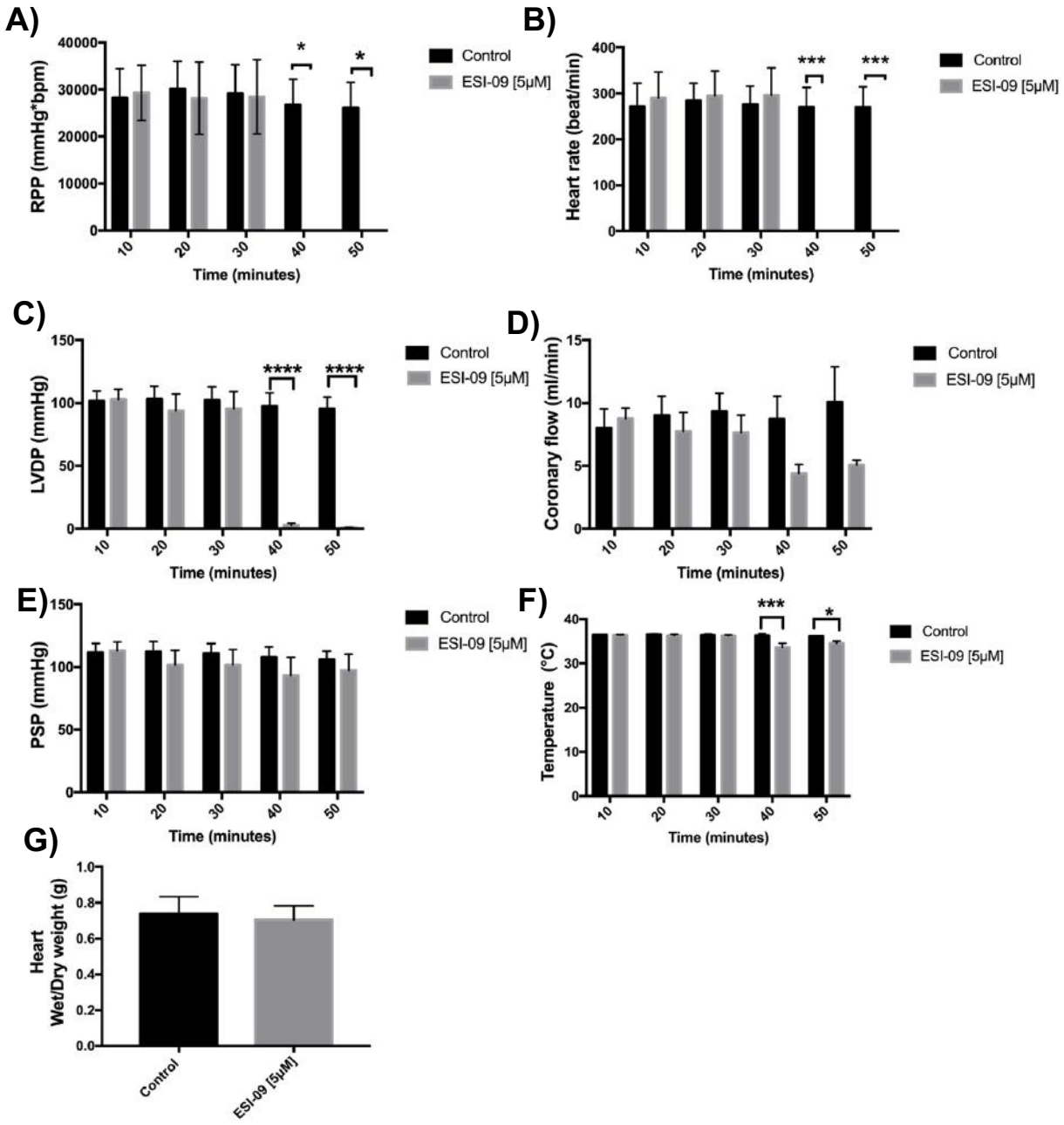

Figure A. 4 Cardiac function of male Wistar rats of normal weight (Langendorff "balloon model").

The hearts were treated with an Epac inhibitor ESI-09 [5µM] and monitored for 50 minutes. **(A),** Rate Pressure Product (RPP = LVDP × heart rate); **(B),** Heart rate; (C), Left ventricular developed pressure (LVDP = systolic pressure − end-diastolic pressure); **(D),** Coronary flow; **(E),** Peak systolic pressure (PSP); **(F),** Temperature; **(G),** Heart wet weight/dry weight. Data are means ± SEM. *p < 0.05; ***P<0.001; ****P<0.0001. n = 5.

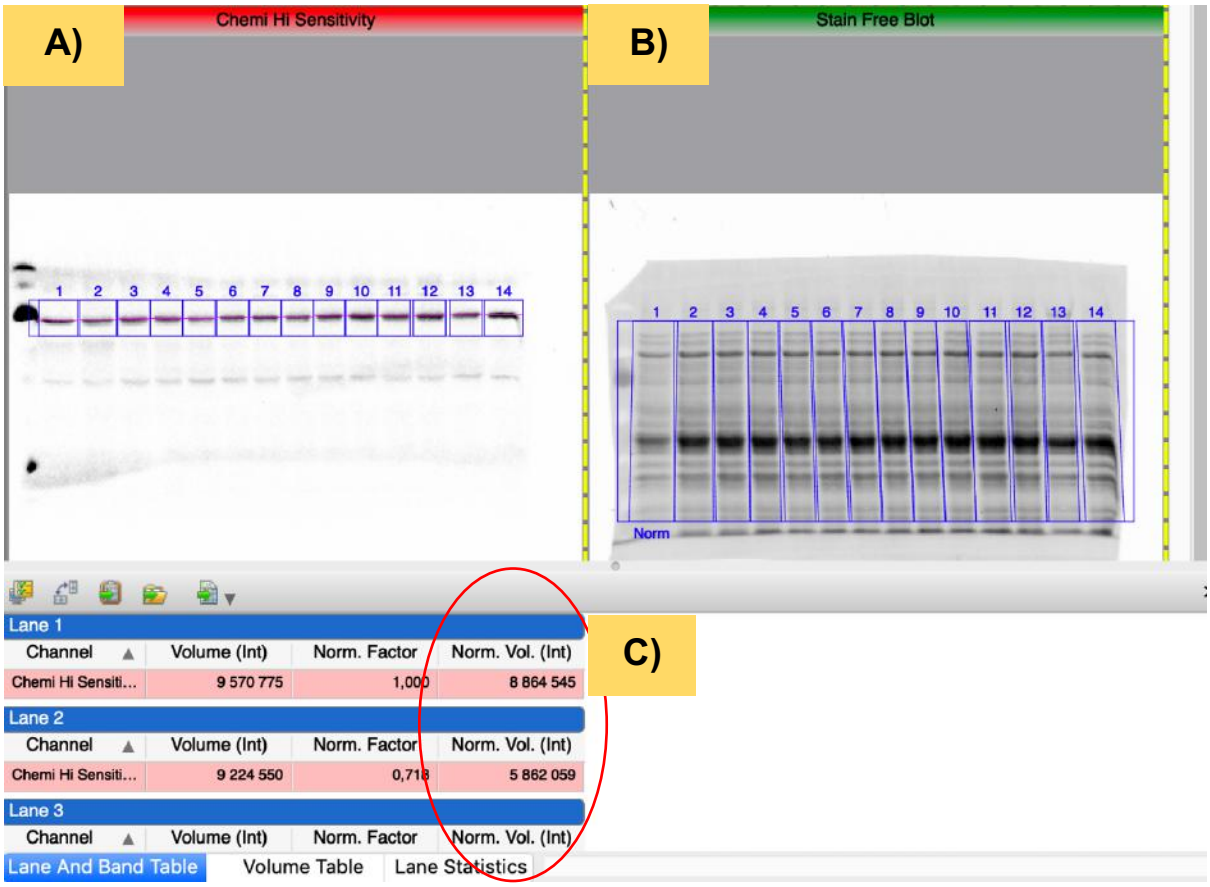

Figure A. 5 Western blot normalization.

(A) Specific protein signal enhanced with a ECL (Chemi Hi Sensitivity), (B) Stain-free blot, (C) The software detects bands and calculates normalisation volume intensities.

Table A. 2 STANDARD RAT CHOW DIET COMPOSITION

microchem
Specialized Lab Services
Co .Reg. 2007/010539/07 Vat No. 4330239049

1st Floor, Fairweather House,
176 Sir Lowry Road,
Cape Town
8001
Telephone : +27 21 465-6996/7
E-mail: chem@microchem.co.za

ilac-MRA sanas Testing Laboratory T0393

CERTIFICATE OF ANALYSIS

Client's Reporting Address:
Department of Food Science
Private Bag X1
Matieland
7602

Client's Telephone #: 021 938 9391
Client's Fax #:

Our Lab Ref #: 2013-06-25-039 **Our Sample ID :** AC92365
Client: Stellenbosch University
Requested by: Prof A Lochner
E-mail address: alo@sun.ac.za
Product: Control Chow
Sampling Method
Barcode
No of Samples:
Production Date: 24/06/2013
Sample Condition: SEALED
Date Received: 25/06/2013
Date Validated: 16/07/2013
Client Samp #: 1
Batch Code:
Sell By Date:
Order Number: PROF A LOCHNER

ANALYSIS RESULTS	1	2	Average	MoU (%)	Test Method Ref
Moisture (g/100g)	10.95	10.84	10.9	0.70	S.O.P.C. No. 1#
Ash (g/100g)	5.66	5.72	5.7	5.00	S.O.P.C. No. 2#
Total Fat (g/100g)	4.65	4.91	4.8	2.60	S.O.P.C. No. 25#
Saturated Fat (g/100g)	0.87	0.91	0.9	2.60	S.O.P.C. No. 25#
Mono-Unsaturated Fat (g/100g)	1.42	1.51	1.5	2.60	S.O.P.C. No. 25#
Poly-Unsaturated Fat (g/100g)	2.37	2.50	2.4	2.60	S.O.P.C. No. 25#
Trans Fatty Acids (g/100g)	0.000	0.000	0.00	2.60	S.O.P.C. No. 25#
Omega 3 Fatty Acids (g/100g)	0.23	0.25	0.2	2.60	S.O.P.C. No. 25#
ALA (g/100g)	0.23	0.25	0.2	2.60	S.O.P.C. No. 25#
EPA (g/100g)	0.00	0.00	0.0	2.60	S.O.P.C. No. 25#
DHA (g/100g)	0.00	0.00	0.0	2.60	S.O.P.C. No. 25#
DPA (g/100g)	0.00	0.00	0.0		S.O.P.C. No. 25#
Omega 6 Fatty acids (g/100g)	2.13	2.25	2.2	2.60	S.O.P.C. No. 25#
Cholesterol (mg/100 g)	2.99	2.94	3	4.70	S.O.P.C. No. 26#
% Protein (6.25)	16.96	17.22	17.1	1.90	S.O.P.C. No. 36#
Nitrogen (g/100g)	2.71	2.75	2.7	1.90	S.O.P.C. No. 36#
Total Dietary Fibre (g/100g)	26.98	26.88	26.9	1.30	S.O.P.C. No. 20#
% Carbohydrate	34.80	34.43	34.6	C*	S.O.P.C. No. 21
Total Sugar (g/100g)	6.65	6.54	6.6	2.90	S.O.P.C. No. 27#
Fructose (g/100g)	0.51	0.49	0.5	2.90	S.O.P.C. No. 27#
Glucose (g/100g)	0.76	0.77	0.8	2.90	S.O.P.C. No. 27#
Sucrose (g/100g)	5.39	5.28	5.3	2.90	S.O.P.C. No. 27#
Maltose (g/100g)	0.00	0.00	0.0	2.90	S.O.P.C. No. 27#
Lactose (g/100g)	0.00	0.00	0.0	2.90	S.O.P.C. No. 27#
Energy (kJ/100 g)	1268	1275	1272		S.O.P.C. No. 22
Sodium (mg/100 g)	188.75	178.40	184	7.56	S.O.P.C. No. 45#

COMMENTS

Confirmed by: P Rubuz Date: 16-Jul-13
Technical Signatory

These results relate only to the items tested. Total Dietary Fibre content determined by AOAC Method 991.43
MoU = Measurement of Uncertainty. C* = By calculation.
 # = SANAS Accredited Method.
Tests without the # mark in this report are "Not SANAS Accredited" and are not included in the SANAS Schedule of Accreditation for this laboratory.
Opinions and interpretations expressed herein are outside the scope of SANAS accreditation. This certificate shall not be reproduced except with the approval of the laboratory. The integrity of results reported are only valid from sample receipt by the laboratory.

Page 1 of 1

Table A. 3 HIGH-CALORIC DIET COMPOSITION

microchem
Specialized Lab Services
Co .Reg. 2007/010539/07 Vat No. 4330239049

1st Floor, Fairweather House,
176 Sir Lowry Road,
Cape Town
8001
Telephone : +27 21 465-6996/7
E-mail: chem@microchem.co.za

ilac-MRA sanas Testing Laboratory T0393

CERTIFICATE OF ANALYSIS

Client's Reporting Address:
Department of Food Science
Private Bag X1
Matieland
7602

Client's Telephone #: 021 938 9391
Client's Fax #:

Our Lab Ref #:	2013-06-25-039	**Our Sample ID :**	AC92366
Client:	Stellenbosch University		
Requested by:	Prof A Lochner		
E-mail address:	alo@sun.ac.za		
Product:	Sucrose Diet		
Sampling Method			
Barcode		Client Samp #:	2
No of Samples:		Batch Code:	
Production Date:	24/06/2013		
Sample Condition:	SEALED	Sell By Date:	2013/06/26
Date Received:	25/06/2013		
Date Validated:	16/07/2013	Order Number:	PROF A LOCHNER

ANALYSIS RESULTS	1	2	Average	MoU (%)	Test Method Ref
Moisture (g/100g)	29.83	29.31	29.6	0.70	S.O.P.C. No. 1#
Ash (g/100g)	2.75	2.93	2.8	5.00	S.O.P.C. No. 2#
Total Fat (g/100g)	4.53	4.76	4.6	2.60	S.O.P.C. No. 25#
Saturated Fat (g/100g)	2.74	2.92	2.8	2.60	S.O.P.C. No. 25#
Mono-Unsaturated Fat (g/100g)	1.05	1.12	1.1	2.60	S.O.P.C. No. 25#
Poly-Unsaturated Fat (g/100g)	0.75	0.73	0.7	2.60	S.O.P.C. No. 25#
Trans Fatty Acids (g/100g)	0.032	0.044	0.04	2.60	S.O.P.C. No. 25#
Omega 3 Fatty Acids (g/100g)	0.07	0.07	0.1	2.60	S.O.P.C. No. 25#
ALA (g/100g)	0.07	0.07	0.1	2.60	S.O.P.C. No. 25#
EPA (g/100g)	0.00	0.00	0.0	2.60	S.O.P.C. No. 25#
DHA (g/100g)	0.00	0.00	0.0	2.60	S.O.P.C. No. 25#
DPA (g/100g)	0.00	0.00	0.0		S.O.P.C. No. 25#
Omega 6 Fatty acids (g/100g)	0.68	0.66	0.7	2.60	S.O.P.C. No. 25#
Cholesterol (mg/100 g)	10.32	10.46	10	4.70	S.O.P.C. No. 26#
% Protein (6.25)	9.23	9.61	9.4	1.90	S.O.P.C. No. 36#
Nitrogen (g/100g)	1.48	1.54	1.5	1.90	S.O.P.C. No. 36#
Total Dietary Fibre (g/100g)	7.69	7.68	7.7	1.30	S.O.P.C. No. 20#
% Carbohydrate	45.97	45.71	45.8	C*	S.O.P.C. No. 21
Total Sugar (g/100g)	28.06	27.43	27.7	2.90	S.O.P.C. No. 27#
Fructose (g/100g)	0.76	0.78	0.8	2.90	S.O.P.C. No. 27#
Glucose (g/100g)	0.90	0.91	0.9	2.90	S.O.P.C. No. 27#
Sucrose (g/100g)	23.58	22.99	23.3	2.90	S.O.P.C. No. 27#
Maltose (g/100g)	0.00	0.00	0.0	2.90	S.O.P.C. No. 27#
Lactose (g/100g)	2.82	2.75	2.8	2.90	S.O.P.C. No. 27#
Energy (kJ/100 g)	1168	1178	1173		S.O.P.C. No. 22
Sodium (mg/100 g)	91.7	103	97.4	7.56	S.O.P.C. No. 45#

COMMENTS

Confirmed by: P Rubuz Date: 16-Jul-13
Technical Signatory

These results relate only to the items tested. Total Dietary Fibre content determined by AOAC Method 991.43
MoU = Measurement of Uncertainty. C* = By calculation.
 # = SANAS Accredited Method.
Tests without the # mark in this report are "Not SANAS Accredited" and are not included in the SANAS Schedule of Accreditation for this laboratory.
Opinions and interpretations expressed herein are outside the scope of SANAS accreditation. This certificate shall not be reproduced except with the approval of the laboratory. The integrity of results reported are only valid from sample receipt by the laboratory.

Page 1 of 1

Figure A. 6 Ethical approval.

UNIVERSITEIT·STELLENBOSCH·UNIVERSITY
jou kennisvennoot • your knowledge partner

Protocol Approval

Date: 07-Oct-2015

PI Name: Marais, Erna E

Protocol #: SU-ACUD14-00020

Title:

Dear Erna Marais, the Progress Report, was reviewed on 06-Oct-2015 by the Research Ethics Committee: Animal Care and Use via committee review procedures and was approved. Please note that this clearance is only valid for a period of twelve months. Ethics clearance of protocols spanning more than one year must be renewed annually through submission of a progress report, up to a maximum of three years.

Applicants are reminded that they are expected to comply with accepted standards for the use of animals in research and teaching as reflected in the South African National Standards 10386: 2008. The SANS 10386: 2008 document is available on the Division for Research Developments website www.sun.ac.za/research.

As provided for in the Veterinary and Para-Veterinary Professions Act, 1982. It is the principal investigator's responsibility to ensure that all study participants are registered with or have been authorised by the South African Veterinary Council (SAVC) to perform the procedures on animals, or will be performing the procedures under the direct and continuous supervision of a SAVC-registered veterinary professional or SAVC-registered para-veterinary professional, who are acting within the scope of practice for their profession.

Please remember to use your protocol number, SU-ACUD14-00020 on any documents or correspondence with the REC: ACU concerning your research protocol.

Please note that the REC: ACU has the prerogative and authority to ask further questions, seek additional information, require further modifications or monitor the conduct of your research.

Any event not consistent with routine expected outcomes that results in any unexpected animal welfare issue (death, disease, or prolonged distress) or human health risks (zoonotic disease or exposure, injuries) must be reported to the committee, by creating an Adverse Event submission within the system.

We wish you the best as you conduct your research.

If you have any questions or need further help, please contact the REC: ACU secretariat at WABEUKES@SUN.AC.ZA or 0218089003.

Sincerely,

Winston Beukes

REC: ACU Secretariat

Research Ethics Committee: Animal Care and Use

REFERENCES

Aasakiran, M., 2007. β -Adrenergic receptor signaling in cardiac function and heart failure. McGill J. Med. 10, 99–104.

Acehan, D., Jiang, X., Morgan, D.G., Heuser, J.E., Wang, X., Akey, C.W., 2004. Three-dimensional structure of the apoptosome. Mol. Cell 9, 423–432.

Ahsan, H., 2013. 3-Nitrotyrosine: A biomarker of nitrogen free radical species modified proteins in systemic autoimmunogenic conditions. Hum. Immunol. 74, 1392–1399.

Ai, X., Curran, J.W., Shannon, T.R., Bers, D.M., Pogwizd, S.M., 2005. Ca2+/calmodulin-dependent protein kinase modulates cardiac ryanodine receptor phosphorylation and sarcoplasmic reticulum Ca2+ leak in heart failure. Circ. Res. 97, 1314–1322.

Almahariq, M., Tsalkova, T., Mei, F.C., Chen, H., Zhou, J., Sastry, S.K., Schwede, F., Cheng, X., 2012. A novel EPAC-specific inhibitor suppresses pancreatic cancer cell migration and invasion. Mol. Pharmacol. 83, 122–128.

Alpert, M.A., Lambert, C.R., Panayiotou, H., Terry, B.E., Cohen, M. V., Massey, C. V., Hashimi, M.W., Mukerji, V., 1995. Relation of duration of morbid obesity to left ventricular mass, systolic function, and diastolic filling, and effect of weight loss. Am. J. Cardiol. 76, 1194–1197.

Ambrose, J.A., Singh, M., 2015. Pathophysiology of coronary artery disease leading to acute coronary syndromes. F1000Prime Rep. 7.

Amin, A., Maleki, M., 2012. Positive inotropes in heart failure: A review article. Heart Asia 4, 16–22.

Arce-Esquivel., A.A., Bunker., A.K., Mikus., C.R., Laughlin., M.H., 2013. Insulin resistance and endothelial dysfunction: macro and microangiopathy. In: Type 2 Diabetes. InTech, p. https://doi.org/10.5772/56475.

Ardehali, H., Sabbah, H.N., Burke, M.A., Sarma, S., Liu, P.P., Cleland, J.G.F., Maggioni, A., Fonarow, G.C., Abel, E.D., Campia, U., Gheorghiade, M., 2012. Targeting myocardial substrate metabolism in heart failure: Potential for new therapies. Eur. J. Heart Fail. 14, 120–129.

Argaud, L., Gateau-Roesch, O., Muntean, D., Chalabreysse, L., Loufouat, J., Robert,

D., Ovize, M., 2005. Specific inhibition of the mitochondrial permeability transition prevents lethal reperfusion injury. J. Mol. Cell. Cardiol. 38, 367–374.

Aronson, D., Nassar, M., Goldberg, T., Kapeliovich, M., Hammerman, H., Azzam, Z.S., 2010. The impact of body mass index on clinical outcomes after acute myocardial infarction. Int. J. Cardiol. 145, 476–480.

Aslam, M., Tanislav, C., Troidl, C., Schulz, R., Hamm, C., Gündüz, D., 2014. cAMP controls the restoration of endothelial barrier function after thrombin-induced hyperpermeability via Rac1 activation. Physiol. Rep. 2, e12175.

Baines, C.P., Kaiser, R.A., Purcell, N.H., Blair, N.S., Osinska, H., Hambleton, M.A., Brunskill, E.W., Sayen, M.R., Gottlieb, R.A., Dorn, G.W., Bobbins, J., Molkentin, J.D., 2005. Loss of cyclophilin D reveals a critical role for mitochondrial permeability transition in cell death. Nature 434, 658–662.

Bakker, S.J.L., Ijzerman, R.G., Teerlink, T., Westerhoff, H. V., Gans, R.O.B., Heine, R.J., 2000. Cytosolic triglycerides and oxidative stress in central obesity: The missing link between excessive atherosclerosis, endothelial dysfunction, and β-cell failure? Atherosclerosis 148, 17–21.

Balligand, J.-L., Feron, O., Dessy, C., 2009. eNOS activation by physical forces: From short-term regulation of contraction to chronic remodeling of cardiovascular tissues. Physiol. Rev. 89, 481–534.

Banerjee, U., Cheng, X., 2015. Exchange protein directly activated by cAMP encoded by the mammalian rapgef3 gene: Structure, function and therapeutics. Gene 570, 157–167.

Baradaran, A., 2012. Lipoprotein(a), type 2 diabetes and nephropathy; the mystery continues. J. Nephropathol. 1, 126–129.

Barker, G., Parnell, E., van Basten, B., Buist, H., Adams, D., Yarwood, S., 2017. The potential of a novel class of EPAC-selective agonists to combat cardiovascular inflammation. J. Cardiovasc. Dev. Dis. 4, 22.

Bastien, M., Poirier, P., Lemieux, I., Després, J.P., 2014. Overview of epidemiology and contribution of obesity to cardiovascular disease. Prog. Cardiovasc. Dis. 56, 369–381.

Batumalaie, K., Amin, M.A., Murugan, D.D., Sattar, M.Z.A., Abdullah, N.A., 2016. Withaferin A protects against palmitic acid-induced endothelial insulin resistance and dysfunction through suppression of oxidative stress and inflammation. Sci. Rep. 6, 27236.

Baxter, G.F., Mocanu, M.M., Brar, B.K., Latchman, D.S., Yellon, D.M., 2001. Cardioprotective effects of transforming growth factor-β1 during early reoxygenation or reperfusion are mediated by p42/p44 MAPK. J. Cardiovasc. Pharmacol. 38, 930–939.

Behrendt, D., Ganz, P., 2002. Endothelial function. Am. J. Cardiol. 90, L40–L48.

Bers, D.M., 2007. Calcium cycling and signaling in cardiac myocytes. Annu. Rev. Physiol. 70, 23–49.

Berthouze, M., Laurent, A.C., Breckler, M., Lezoualc'h, F., 2011. New perspectives in cAMP-signaling modulation. Curr. Heart Fail. Rep. 8, 159–167.

BioRad Laboratories, 2019. Stain-Free Imaging Technology [WWW Document]. BioRad. URL https://www.bio-rad.com/en-za/applications-technologies/stain-free-imaging-technology?ID=NZ0G1815 (accessed 9.30.19).

Birukova, A.A., Burdette, D., Moldobaeva, N., Xing, J., Fu, P., Birukov, K.G., 2010. Rac GTPase is a hub for protein kinase A and Epac signaling in endothelial barrier protection by cAMP. Microvasc. Res. 79, 128–138.

Birukova, A.A., Zagranichnaya, T., Alekseeva, E., Bokoch, G.M., Birukov, K.G., 2008. EpacRap and PKA are novel mechanisms of ANP-induced Rac-mediated pulmonary endothelial barrier protection. - Birukova et al. - Journal of cellular physiology - 2008.pdf. J. Cell. Physiol. 215, 715–724.

Birukova, A.A., Zagranichnaya, T., Fu, P., Alekseeva, E., Chen, W., Jacobson, J.R., Birukov, K.G., 2007. Prostaglandins PGE2and PGI2promote endothelial barrier enhancement via PKA- and Epac1/Rap1-dependent Rac activation. Exp. Cell Res. 313, 2504–2520.

Boden, G., 2008. Obesity and FFAs. Endocrinol Metab Clin North Am 37, 635.

Boden, G., 2011. Obesity, insulin resistance and free fatty acids. Curr. Opin. Endocrinol. Diabetes Obes. 18, 139–143.

Boengler, K., Hilfiker-Kleiner, D., Heusch, G., Schulz, R., 2010. Inhibition of permeability transition pore opening by mitochondrial STAT3 and its role in myocardial ischemia/reperfusion. Basic Res. Cardiol. 105, 771–785.

Bos, J.L., 2006. Epac proteins: multi-purpose cAMP targets. Trends Biochem. Sci. 31, 680–686.

Bradford, M.M., 1976. A rapid and sensitive method for the quantitation of microgram quantities of protein utilizing the principle of protein-dye binding. Anal. Biochem. 72, 248–254.

Brette, F., Blandin, E., Simard, C., Guinamard, R., Salle, L., 2013. Epac activator critically regulates action potential duration by decreasing potassium current in rat adult ventricle. J. Mol. Cell. Cardiol. 57, 96–105.

Briaud, I., Kelpe, C.L., Johnson, L.M., Tran, P.O.T., Poitout, V., 2002. Differential effects of hyperlipidemia on insulin secretion in islets of langerhans from hyperglycemic versus normoglycemic rats. Diabetes 51, 662–668.

British Heart Foundation, 2019. Cardiovascular disease (CVD) [WWW Document]. Br. Hear. Found. URL https://www.bhf.org.uk/informationsupport/conditions/cardiovascular-disease (accessed 9.26.19).

Brocheriou, V., Hagège, A.A., Oubenaïssa, A., Lambert, M., Mallet, V.O., Duriez, M., Wassef, M., Kahn, A., Menasché, P., Gilgenkrantz, H., 2000. Cardiac functional improvement by a human Bcl-2 transgene in a mouse model of ischemia/reperfusion injury. J. Gene Med. 2, 326–333.

Brown, L.M., Rogers, K.E., Aroonsakool, N., McCammon, J.A., Insel, P.A., 2014. Allosteric inhibition of Epac: Computationalmodeling and experimental validationtoidentify allosteric sites and inhibitors. J. Biol. Chem. 289, 29148–29157.

Brutsaert, D.L., 2015. Cardiac endothelial-myocardial signaling: Its role in cardiac growth, contractile performance, and rhythmicity. Physiol. Rev. 83, 59–115.

Buja, L.M., 2005. Myocardial ischemia and reperfusion injury. Cardiovasc. Pathol. 14, 170–175.

Cai, H., Harrison, D.G., 2000. Endothelial dysfunction in cardiovascular diseases: The role of oxidant stress. Circ. Res. 87, 840–844.

Cai, H., Liu, D., Garcia, J.G.N., 2008. CaM Kinase II-dependent pathophysiological signalling in endothelial cells. Cardiovasc. Res. 77, 30–34.

Capurso, C., Capurso, A., 2012. From excess adiposity to insulin resistance: The role of free fatty acids. Vascul. Pharmacol. 57, 91–97.

Carbone, S., Canada, J.M., Billingsley, H.E., Siddiqui, M.S., Elagizi, A., Lavie, C.J., 2019. Obesity paradox in cardiovascular disease: where do we stand? Vasc. Health Risk Manag. 15, 89–100.

Cazorla, O., Lucas, A., Poirier, F., Lacampagne, A., Lezoualc'h, F., 2009. The cAMP binding protein Epac regulates cardiac myofilament function. Proc. Natl. Acad. Sci. 106, 14144–14149.

Chaitanya, G.V., Alexander, J.S., Babu, P.P., 2010. PARP-1 cleavage fragments: Signatures of cell-death proteases in neurodegeneration. Cell Commun. Signal. 8.

Chavez, A., Smith, M., Mehta, D., 2011. New insights into the regulation of vascular permeability. Int. Rev. Cell Mol. Biol. 290, 205–248.

Chen, H., Ding, C., Wild, C., Liu, H., Wang, T., White, M.A., Cheng, X., Zhou, J., 2013. Efficient synthesis of ESI-09, a novel non-cyclic nucleotide EPAC antagonist. Tetrahedron Lett. 54, 1546–1549.

Chen, H., Tsalkova, T., Mei, F.C., Hu, Y., Cheng, X., Zhou, J., 2012. 5-Cyano-6-oxo-1,6-dihydro-pyrimidines as potent antagonists targeting exchange proteins directly activated by cAMP. Bioorganic Med. Chem. Lett. 22, 4038–4043.

Chen, H.T., Yang, C.X., Li, H., Zhang, C.J., Wen, X.J., Zhou, J., Fan, Y.L., Huang, T., Zeng, Y.M., 2008. Cardioprotection of sevoflurane postconditioning by activating extracellular signal-regulated kinase 1/2 in isolated rat hearts. Acta Pharmacol. Sin. 29, 931–941.

Chen, P., Liu, H., Xiang, H., Zhou, J., Zeng, Z., Chen, R., Zhao, S., Xiao, J., Shu, Z., Chen, S., Lu, H., 2019. Palmitic acid-induced autophagy increases reactive oxygen species via the Ca2+/PKCα/NOX4 pathway and impairs endothelial function in human umbilical vein endothelial cells. Exp. Ther. Med. 17, 2425–2432.

Chen, Z., Chua, C.C., Ho, Y.S., Hamdy, R.C., Chua, B.H., 2001. Overexpression of Bcl-2 attenuates apoptosis and protects against myocardial I/R injury in transgenic mice. Am. J. Physiol. Heart Circ. Physiol. 280, H2313-20.

Cheng, X., Ji, Z., Tsalkova, T., Mei, F., 2008. Epac and PKA: A tale of two intracellular cAMP receptors. Acta Biochim. Biophys. Sin. (Shanghai). 40, 651–662.

Chipuk, J.E., Moldoveanu, T., Llambi, F., Parsons, M.J., Green, D.R., 2010. The BCL-2 Family Reunion. Mol. Cell 37, 299–310.

Chong, Y.H., Ng, T.K.W., 1991. Effects of palm oil on cardiovascular risk. Med. J. Malaysia 46, 41–50.

Chrzanowska-Wodnicka, M., 2017. Rap1 in endothelial biology. Curr. Opin. Hematol. 24, 248–255.

Cittadini, A., Monti, M.G., Iaccarino, G., Di Rella, F., Tsichlis, P.N., Di Gianni, A., Strömer, H., Sorriento, D., Peschle, C., Trimarco, B., Saccà, L., Condorelli, G.,

2006. Adenoviral gene transfer of Akt enhances myocardial contractility and intracellular calcium handling. Gene Ther. 13, 8–19.

Clark, K., 2003. Obesity and the risk of heart failure. J. Insur. Med. 35, 59–60.

Clarke, S.J., McStay, G.P., Halestrap, A.P., 2002. Sanglifehrin A acts as a potent inhibitor of the mitochondrial permeability transition and reperfusion injury of the heart by binding to cyclophilin-D at a different site from cyclosporin A. J. Biol. Chem. 277, 34793–34799.

Clavijo, L.C., Pinto, T.L., Kuchulakanti, P.K., Torguson, R., Chu, W.W., Satler, L.F., Kent, K.M., Suddath, W.O., Pichard, A.D., Waksman, R., 2006. Metabolic syndrome in patients with acute myocardial infarction is associated with increased infarct size and in-hospital complications. Cardiovasc. Revascularization Med. 7, 7–11.

Cohen, M. V., Downey, J.M., 2007. Cardioprotection: Spotlight on PKG. Br. J. Pharmacol. 152, 833–834.

Cohen, M. V., Yang, X.M., Downey, J.M., 1999. Smaller infarct after preconditioning does not predict extent of early functional improvement of reperfused heart. Am. J. Physiol. - Hear. Circ. Physiol. 277.

Condorelli, G., Drusco, A., Stassi, G., Bellacosa, A., Roncarati, R., Iaccarino, G., Russo, M.A., Gu, Y., Dalton, N., Chung, C., Latronico, M.V.G., Napoli, C., Sadoshima, J., Croce, C.M., Ross, J., 2002. Akt induces enhanced myocardial contractility and cell size in vivo in transgenic mice. Proc. Natl. Acad. Sci. U. S. A. 99, 12333–12338.

Condorelli, G., Roncarati, R., Ross, J., Pisani, A., Stassi, G., Todaro, M., Trocha, S., Drusco, A., Gu, Y., Russo, M.A., Frati, G., Jones, S.P., Lefer, D.J., Napoli, C., Croce, C.M., 2001. Heart-targeted overexpression of caspase3 in mice increases infarct size and depresses cardiac function. Proc. Natl. Acad. Sci. U. S. A. 98, 9977–9982.

Courilleau, D., Bisserier, M., Jullian, J.C., Lucas, A., Bouyssou, P., Fischmeister, R., Blondeau, J.P., Lezoualc'h, F., 2012. Identification of a tetrahydroquinoline analog as a pharmacological inhibitor of the cAMP-binding protein Epac. J. Biol. Chem. 287, 44192–44202.

Crabtree, G.R., 1999. Generic signals and specific outcomes: Signaling through Ca2+, calcineurin, and NF-AT. Cell 96, 611–614.

Crowley, L.C., Scott, A.P., Marfell, B.J., Boughaba, J.A., Chojnowski, G.,

Waterhouse, N.J., 2016. Measuring cell death by propidium iodide uptake and flow cytometry. Cold Spring Harb. Protoc. 2016, 647–651.

Cuíñas, A., García-Morales, V., Viña, D., Gil-Longo, J., Campos-Toimil, M., 2016. Activation of PKA and Epac proteins by cyclic AMP depletes intracellular calcium stores and reduces calcium availability for vasoconstriction. Life Sci. 155, 102–109.

Cullere, X., Shaw, S.K., Andersson, L., Hirahashi, J., Luscinskas, F.W., Mayadas, T.N., 2005. Regulation of vascular endothelial barrier function by Epac, a cAMP-activated exchange factor for Rap GTPase. Blood 105, 1950–5.

Davel, A.P.C., Kawamoto, E.M., Scavone, C., Vassallo, D. V., Rossoni, L. V., 2006. Changes in vascular reactivity following administration of isoproterenol for 1 week: A role for endothelial modulation. Br. J. Pharmacol. 148, 629–639.

Davidson, S.M., Hausenloy, D., Duchen, M.R., Yellon, D.M., 2006. Signalling via the reperfusion injury signalling kinase (RISK) pathway links closure of the mitochondrial permeability transition pore to cardioprotection. Int. J. Biochem. Cell Biol. 38, 414–419.

de Groot, H., Rauen, U., 2007. Ischemia-reperfusion injury: Processes in pathogenetic networks: A review. Transplant. Proc. 39, 481–484.

de Lucia, C., Eguchi, A., Koch, W.J., 2018. New insights in cardiac β-Adrenergic signaling during heart failure and aging. Front. Pharmacol. 9, 904.

De Rooij, J., Rehmann, H., Van Triest, M., Cool, R.H., Wittinghofer, A., Bos, J.L., 2000. Mechanism of regulation of the Epac family of cAMP-dependent RapGEFs. J. Biol. Chem. 275, 20829–20836.

De Rooij, J., Zwartkruis, F.J.T., Verheijen, M.H.G., Cool, R.H., Nijman, S.M.B., Wittinghofer, A., Bos, J.L., 1998. Epac is a Rap1 guanine-nucleotide-exchange factor directly activated by cyclic AMP. Nature 396, 474–477.

Deanfield, J.E., Halcox, J.P., Rabelink, T.J., 2007. Endothelial function and dysfunction: Testing and clinical relevance. Circulation 115, 1285–1295.

Degterev, A., Huang, Z., Boyce, M., Li, Y., Jagtap, P., Mizushima, N., Cuny, G.D., Mitchison, T.J., Moskowitz, M.A., Yuan, J., 2005. Chemical inhibitor of nonapoptotic cell death with therapeutic potential for ischemic brain injury. Nat. Chem. Biol. 1, 112–119.

Dejana, E., Orsenigo, F., 2013. Endothelial adherens junctions at a glance. J. Cell Sci. 126, 2545–2549.

Díaz-Vegas, A., Espinoza, A., Cofré, C., Sánchez-Aguilera, P., 2018. Eccentric resistance training reduces both non-response to exercise and cardiovascular risk factors in adult with overweight or obesity. Sci. Sport. 33, 245–252.

Diaz, M.N., Frei, B., Vita, J.A., Keaney, J.F., 2002. Antioxidants and Atherosclerotic Heart Disease. N. Engl. J. Med. 337, 408–416.

Dimmeler, S., Fleming, I., Fisslthaler, B., Hermann, C., Busse, R., Zeiher, A.M., 1999. Activation of nitric oxide synthase in endothelial cells by Akt- dependent phosphorylation. Nature 399, 601–605.

Disatnik, M.H., Ferreira, J.C.B., Campos, J.C., Gomes, K.S., Dourado, P.M.M., Qi, X., Mochly-Rosen, D., 2013. Acute inhibition of excessive mitochondrial fission after myocardial infarction prevents long-term cardiac dysfunction. J. Am. Heart Assoc. 2.

Domínguez-Rodríguez, A., Ruiz-Hurtado, G., Sabourin, J., Gómez, A.M., Alvarez, J.L., Benitah, J.P., 2015. Proarrhythmic effect of sustained EPAC activation on TRPC3/4 in rat ventricular cardiomyocytes. J. Mol. Cell. Cardiol. 87, 74–78.

Donner, D., Headrick, J.P., Peart, J.N., du Toit, E.F., 2012. Obesity improves myocardial ischaemic tolerance and RISK signalling in insulin-insensitive rats. Dis. Model. Mech. 6, 457–466.

Donner, D., Headrick, J.P., Peart, J.N., Du Toit, E.F., 2013. Obesity improves myocardial ischaemic tolerance and RISK signalling in insulin-insensitive rats. DMM Dis. Model. Mech. 6, 457–466.

du Toit, E.F., Nabben, M., Lochner, A., 2005. A potential role for angiotensin II in obesity induced cardiac hypertrophy and ischaemic/reperfusion injury. Basic Res. Cardiol. 100, 346–354.

du Toit, E.F., Smith, W., Muller, C., Strijdom, H., Stouthammer, B., Woodiwiss, A.J., Norton, G.R., Lochner, A., 2008. Myocardial susceptibility to ischemic-reperfusion injury in a prediabetic model of dietary-induced obesity. Am. J. Physiol. Circ. Physiol. 294, H2336–H2343.

Duncker, D.J., Bache, R.J., 2008. Regulation of coronary blood flow during exercise. Physiol. Rev. 88, 1009–1086.

Duquesnes, N., Derangeon, M., Métrich, M., Lucas, A., Mateo, P., Li, L., Morel, E., Lezoualc'h, F., Crozatier, B., 2010. Epac stimulation induces rapid increases in connexin43 phosphorylation and function without preconditioning effect. Pflugers Arch. Eur. J. Physiol. 460, 731–741.

Edland, F., Wergeland, A., Kopperud, R., Åsrud, K.S., Hoivik, E.A., Witsø, S.L., Æsøy, R., Madsen, L., Kristiansen, K., Bakke, M., Døskeland, S.O., Jonassen, A.K., 2016. Long-term consumption of an obesogenic high fat diet prior to ischemia-reperfusion mediates cardioprotection via Epac1-dependent signaling. Nutr. Metab. 13, 1–11.

Egan, B.M., Greene, E.L., Goodfriend, T.L., 2001. Nonesterified fatty acids in blood pressure control and cardiovascular complications. Curr. Hypertens. Rep. 3, 107–116.

Ellies, L.G., Johnson, A., Olefsky, J.M., 2013. Obesity, inflammation, and insulin resistance. In: Obesity, Inflammation and Cancer. Springer New York, pp. 1–23.

Enserink, J.M., Christensen, A.E., De Rooij, J., Van Triest, M., Schwede, F., Genieser, H.G., Døskeland, S.O., Blank, J.L., Bos, J.L., 2002. A novel Epac-specific cAMP analogue demonstrates independent regulation of Rap1 and ERK. Nat. Cell Biol. 4, 1–6.

Esenabhalu, V.E., Schaeffer, G., Graier, W.F., 2003. Free fatty acid overload attenuates Ca2+ signaling and NO production in endothelial cells. Antioxidants Redox Signal. 5, 147–153.

Essop, M.F., Anna Chan, W.Y., Valle, A., García-Palmer, F.J., Du Toit, E.F., 2009. Impaired contractile function and mitochondrial respiratory capacity in response to oxygen deprivation in a rat model of pre-diabetes. Acta Physiol. 197, 289–296.

Ferdinandy, P., Hausenloy, D.J., Heusch, G., Baxter, G.F., Schulz, R., 2014. Interaction of risk factors, comorbidities, and comedications with ischemia/reperfusion injury and cardioprotection by preconditioning, postconditioning, and remote conditioning. Pharmacol. Rev. 66, 1142–1174.

Ferro, A., Coash, M., Yamamoto, T., Rob, J., Ji, Y., Queen, L., 2004. Nitric oxide-dependent β 2-adrenergic dilatation of rat aorta is mediated through activation of both protein kinase A and Akt. Br. J. Pharmacol. 143, 397–403.

Flammer, A.J., Lüscher, T.F., 2010. Human endothelial dysfunction: EDRFs. Pflugers Arch. Eur. J. Physiol. 459, 1005–1013.

Förstermann, U., Kleinert, H., 1995. Nitric oxide synthase: expression and expressional control of the three isoforms. Naunyn. Schmiedebergs. Arch. Pharmacol. 352, 351–364.

Frangogiannis, N.G., 2015. Pathophysiology of myocardial infarction. Compr.

Physiol. 5, 1841–1875.

Fratantonio, D., Speciale, A., Ferrari, D., Cristani, M., Saija, A., Cimino, F., 2015. Palmitate-induced endothelial dysfunction is attenuated by cyanidin-3-O-glucoside through modulation of Nrf2/Bach1 and NF-κB pathways. Toxicol. Lett. 239, 152–160.

Freedman, N.J., Lefkowitz, R.J., 2004. Anti-β1-adrenergic receptor antibodies and heart failure: Causation, not just correlation. J. Clin. Invest. 113, 1379–1382.

Fukuda, M., Williams, K.W., Gautron, L., Elmquist, J.K., 2011. Induction of leptin resistance by activation of cAMP-Epac signaling. Cell Metab. 13, 331–339.

Fullmer, T.M., Pei, S., Zhu, Y., Sloan, C., Manzanares, R., Henrie, B., Pires, K.M., Cox, J.E., Abel, E.D., Boudina, S., 2013. Insulin suppresses ischemic preconditioning-mediated cardioprotection through Akt-dependent mechanisms. J. Mol. Cell. Cardiol. 64, 20–29.

Galluzzi, L., Vitale, I., Abrams, J.M., Alnemri, E.S., Baehrecke, E.H., Blagosklonny, M. V., Dawson, T.M., Dawson, V.L., El-Deiry, W.S., Fulda, S., Gottlieb, E., Green, D.R., Hengartner, M.O., Kepp, O., Knight, R.A., Kumar, S., Lipton, S.A., Lu, X., Madeo, F., Malorni, W., Mehlen, P., Nũez, G., Peter, M.E., Piacentini, M., Rubinsztein, D.C., Shi, Y., Simon, H.U., Vandenabeele, P., White, E., Yuan, J., Zhivotovsky, B., Melino, G., Kroemer, G., 2012. Molecular definitions of cell death subroutines: Recommendations of the Nomenclature Committee on Cell Death 2012. Cell Death Differ. 19, 107–120.

García-Morales, V., Cuíñas, A., Elíes, J., Campos-Toimil, M., 2014. PKA and Epac activation mediates cAMP-induced vasorelaxation by increasing endothelial NO production. Vascul. Pharmacol. 60, 95–101.

García-Morales, V., Luaces-Regueira, M., Campos-Toimil, M., 2017. The cAMP effectors PKA and Epac activate endothelial NO synthase through PI3K/Akt pathway in human endothelial cells. Biochem. Pharmacol. 145, 94–101.

García-Prieto, C.F., Hernández-Nuño, F., Rio, D. Del, Ruiz-Hurtado, G., Aránguez, I., Ruiz-Gayo, M., Somoza, B., Fernández-Alfonso, M.S., 2015. High-fat diet induces endothelial dysfunction through a down-regulation of the endothelial AMPK-PI3K-Akt-eNOS pathway. Mol. Nutr. Food Res. 59, 520–532.

Genis, A., 2014. Exposure of cardiac microvascular endothelial cells to harmful stimuli: A study of the cellular responses and mechanisms. Stellenbosch University.

Gersh, B.J., Stone, G.W., White, H.D., Holmes, D.R., 2005. Pharmacological facilitation of primary percutaneous coronary intervention for acute myocardial infarction: Is the slope of the curve the shape of the future? J. Am. Med. Assoc. 293, 979–986.

Ghosh, A., Gao, L., Thakur, A., Siu, P.M., Lai, C.W.K., 2017. Role of free fatty acids in endothelial dysfunction. J. Biomed. Sci. 24.

Gimbrone, M.A., García-Cardeña, G., 2016. Endothelial cell dysfunction and the pathobiology of atherosclerosis. Circ. Res. 118, 620–636.

Gong, B., Shelite, T., Mei, F.C., Ha, T., Hu, Y., Xu, G., Chang, Q., Wakamiya, M., Ksiazek, T.G., Boor, P.J., Bouyer, D.H., Popov, V.L., Chen, J., Walker, D.H., Cheng, X., 2013. Exchange protein directly activated by cAMP plays a critical role in bacterial invasion during fatal rickettsioses. Proc. Natl. Acad. Sci. 110, 19615–19620.

Gottlieb, R.A., Mentzer, R.M., 2013. Autophagy: An affair of the heart. In: Heart Failure Reviews. pp. 575–584.

Gremmels, H., Bevers, L.M., Fledderus, J.O., Braam, B., Jan Van Zonneveld, A., Verhaar, M.C., Joles, J.A., 2015. Oleic acid increases mitochondrial reactive oxygen species production and decreases endothelial nitric oxide synthase activity in cultured endothelial cells. Eur. J. Pharmacol. 751, 67–72.

Grover-Páez, F., Zavalza-Gómez, A.B., 2009. Endothelial dysfunction and cardiovascular risk factors. Diabetes Res. Clin. Pract. 84, 1–10.

Grundy, S.M., 2012. Pre-diabetes, metabolic syndrome, and cardiovascular risk. J. Am. Coll. Cardiol. 59, 635–643.

Gupte, A.A., Minze, L.J., Reyes, M., Ren, Y., Wang, X., Brunner, G., Ghosn, M., Cordero-Reyes, A.M., Ding, K., Pratico, D., Morrisett, J., Shi, Z.Z., Hamilton, D.J., Lyon, C.J., Hsueh, W.A., 2013. High-fat feeding-induced hyperinsulinemia increases cardiac glucose uptake and mitochondrial function despite peripheral insulin resistance. Endocrinology 154, 2650–2662.

Gustafson, L.A., Kuipers, F., Wiegman, C., Sauerwein, H.P., Romijn, J.A., Meijer, A.J., 2002. Clotibrate improves glucose tolerance in fat-fed rats but decreases hepatic glucose consumption capacity. J. Hepatol. 37, 425–431.

Gustafsson, Å.B., Gottlieb, R.A., 2009. Autophagy in ischemic heart disease. Circ. Res. 104, 150–158.

Hajjar, D.P., Gotto, A.M., 2013. Biological relevance of inflammation and oxidative

stress in the pathogenesis of arterial diseases. Am. J. Pathol. 182, 1474–1481.

Haluzik, M., Gavrilova, O., Leroith, D., 2004. Peroxisome proliferator-activated receptor-α deficiency does not alter insulin sensitivity in mice maintained on regular or high-fat diet: Hyperinsulinemic-euglycemic clamp studies. Endocrinology 145, 1662–1667.

Hamacher-Brady, A., Brady, N.R., Gottlieb, R.A., 2006. Enhancing macroautophagy protects against ischemia/reperfusion injury in cardiac myocytes. J. Biol. Chem. 281, 29776–29787.

Hamacher-Brady, A., Brady, N.R., Logue, S.E., Sayen, M.R., Jinno, M., Kirshenbaum, L.A., Gottlieb, R.A., Gustafsson, Å.B., 2007. Response to myocardial ischemia/reperfusion injury involves Bnip3 and autophagy. Cell Death Differ. 14, 146–157.

Han, F., Zhang, S., Hou, N., Wang, D., Sun, X., 2015. Irisin improves endothelial function in obese mice through the AMPK-eNOS pathway. Am. J. Physiol. Heart Circ. Physiol. 309, H1501–H1508.

Hansson, G.K., 2001. Immune mechanisms in atherosclerosis. Arterioscler. Thromb. Vasc. Biol. 21, 1876–1890.

Hashimoto, A., Miyakoda, G., Hirose, Y., Mori, T., 2006. Activation of endothelial nitric oxide synthase by cilostazol via a cAMP/protein kinase A- and phosphatidylinositol 3-kinase/Akt-dependent mechanism. Atherosclerosis 189, 350–357.

Hausenloy, D.J., Duchen, M.R., Yellon, D.M., 2003. Inhibiting mitochondrial permeability transition pore opening at reperfusion protects against ischaemia-reperfusion injury. Cardiovasc. Res. 60, 617–625.

Hausenloy, D.J., Ong, S.B., Yellon, D.M., 2009. The mitochondrial permeability transition pore as a target for preconditioning and postconditioning. Basic Res. Cardiol. 104, 189–202.

Hausenloy, D.J., Yellon, D.M., 2007. Preconditioning and postconditioning: United at reperfusion. Pharmacol. Ther. 116, 173–191.

He, H., Liu, X., Lv, L., Liang, H., Leng, B., Zhao, D., Zhang, Y., Du, Z., Chen, X., Li, S., Lu, Y., Shan, H., 2014. Calcineurin suppresses AMPK-dependent cytoprotective autophagy in cardiomyocytes under oxidative stress. Cell Death Dis. 5.

Hegyi, B., Bányász, T., Izu, L.T., Belardinelli, L., Bers, D.M., Chen-Izu, Y., 2018. β-

adrenergic regulation of late Na+ current during cardiac action potential is mediated by both PKA and CaMKII. J. Mol. Cell. Cardiol. 123, 168–179.

Henderson, L.M., Chappell, J.B., 1993. Dihydrorhodamine 123: a fluorescent probe for superoxide generation? Eur. J. Biochem. 217, 973–980.

Heusch, G., 2015. Molecular basis of cardioprotection signal transduction in ischemic pre-, post-, and remote conditioning. Circ. Res. 116, 674–699.

Heusch, G., Gersh, B.J., 2017. The pathophysiology of acute myocardial infarction and strategies of protection beyond reperfusion: A continual challenge. Eur. Heart J. 38, 774–784.

Heusch, G., Libby, P., Gersh, B., Yellon, D., Böhm, M., Lopaschuk, G., Opie, L., 2014. Cardiovascular remodelling in coronary artery disease and heart failure. Lancet 383, 1933–1943.

Hewer, R.C., Sala-Newby, G.B., Wu, Y.J., Newby, A.C., Bond, M., 2011. PKA and Epac synergistically inhibit smooth muscle cell proliferation. J. Mol. Cell. Cardiol. 50, 87–98.

Higashi, Y., 2015. Assessment of Endothelial Function. Int. Heart J. 56, 125–134.

Hirase, T., Node, K., 2011. Endothelial dysfunction as a cellular mechanism for vascular failure. Am. J. Physiol. Circ. Physiol. 302, H499–H505.

Hochhauser, E., Cheporko, Y., Yasovich, N., Pinchas, L., Offen, D., Barhum, Y., Pannet, H., Tobar, A., Vidne, B.A., Birk, E., 2007. Bax deficiency reduces infarct size and improves long-term function after myocardial infarction. Cell Biochem. Biophys. 47, 11–19.

Hochhauser, E., Kivity, S., Offen, D., Maulik, N., Otani, H., Barhum, Y., Pannet, H., Shneyvays, V., Shainberg, A., Goldshtaub, V., Tobar, A., Vidne, B.A., 2015. Bax ablation protects against myocardial ischemia-reperfusion injury in transgenic mice. Am. J. Physiol. Circ. Physiol. 284, H2351–H2359.

Honegger, K.J., Capuano, P., Winter, C., Bacic, D., Stange, G., Wagner, C.A., Biber, J., Murer, H., Hernando, N., 2006. Regulation of sodium-proton exchanger isoform 3 (NHE3) by PKA and exchange protein directly activated by cAMP (EPAC). Proc. Natl. Acad. Sci. 103, 803–808.

Hood, J.D., Frausto, R., Kiosses, W.B., Schwartz, M.A., Cheresh, D.A., 2003. Differential αv integrin-mediated Ras-ERK signaling during two pathways of angiogenesis. J. Cell Biol. 162, 933–943.

Horimatsu, T., Kim, H.W., Weintraub, N.L., 2017. The role of perivascular adipose

tissue in non-atherosclerotic vascular disease. Front. Physiol. 8.

Hu, C., Huang, Y., Li, L., 2017. Drp1-dependent mitochondrial fission plays critical roles in physiological and pathological progresses in mammals. Int. J. Mol. Sci. 18.

Huang, C.Y., Lai, C.H., Kuo, C.H., Chiang, S.F., Pai, P.Y., Lin, J.Y., Chang, C.F., Viswanadha, V.P., Kuo, W.W., Huang, C.Y., 2018. Inhibition of ERK-Drp1 signaling and mitochondria fragmentation alleviates IGF-IIR-induced mitochondria dysfunction during heart failure. J. Mol. Cell. Cardiol. 122, 58–68.

Huisamen, B., Dietrich, D., Bezuidenhout, N., Lopes, J., Flepisi, B., Blackhurst, D., Lochner, A., 2012. Early cardiovascular changes occurring in diet-induced, obese insulin-resistant rats. Mol. Cell. Biochem. 368, 37–45.

HuisamenB, Pêrel, S.J.C., Friedrich, S.O., Salie, R., Strijdom, H., Lochner, A., 2011. ANG II type I receptor antagonism improved nitric oxide production and enhanced eNOS and PKB/Akt expression in hearts from a rat model of insulin resistance. Mol. Cell. Biochem. 349, 21–31.

Hwang, M., Go, Y., Park, J.H., Shin, S.K., Song, S.E., Oh, B.C., Im, S.S., Hwang, I., Jeon, Y.H., Lee, I.K., Seino, S., Song, D.K., 2017. Epac2a-null mice exhibit obesity-prone nature more susceptible to leptin resistance. Int. J. Obes. 41, 279–288.

Iacobellis, G., Sharma, A.M., 2007. Epicardial adipose tissue as new cardio-metabolic risk marker and potential therapeutic target in the metabolic syndrome. Curr. Pharm. Des. 13, 2180–2184.

Iacobellis, G., Zaki, M.C., Garcia, D., Willens, H.J., 2014. Epicardial fat in atrial fibrillation and heart failure. Horm. Metab. Res. 46, 587–590.

Imrie, H., Abbas, A., Kearney, M., 2010. Insulin resistance, lipotoxicity and endothelial dysfunction. Biochim. Biophys. Acta - Mol. Cell Biol. Lipids 1801, 320–326.

Jenkins, D.P., Pugsley, W.B., Yellon, D.M., 1995. Ischaemic preconditioning in a model of global ischaemia: Infarct size limitation, but no reduction of stunning. J. Mol. Cell. Cardiol. 27, 1623–1632.

Jonassen, A.K., Sack, M.N., Mjøs, O.D., Yellon, D.M., 2001. Myocardial protection by insulin at reperfusion requires early administration and is mediated via Akt and p70s6 kinase cell-survival signaling. Circ. Res. 89, 1191–1198.

Juhaszova, M., Zorov, D.B., Kim, S.H., Pepe, S., Fu, Q., Fishbein, K.W., Ziman,

B.D., Wang, S., Ytrehus, K., Antos, C.L., Olson, E.N., Sollott, S.J., 2004. Glycogen synthase kinase-3β mediates convergence of protection signalling to inhibit the mitochondrial permeability transition pore. J. Clin. Invest. 113, 1535–1549.

Kahn, S.E., Hull, R.L., Utzschneider, K.M., 2006. Mechanisms linking obesity to insulin resistance and type 2 diabetes. Nature 444, 840–846.

Kai, A.K.L., Lam, A.K.M., Chen, Y., Tai, A.C.P., Zhang, X., Lai, A.K.W., Yeung, P.K.K., Tam, S., Wang, J., Lam, K.S., Vanhoutte, P.M., Bos, J.L., Chung, S.K.S.S.M., Xu, A., Chung, S.K.S.S.M., 2013. Exchange protein activated by cAMP 1 (Epac1)-deficient mice develop β-cell dysfunction and metabolic syndrome. FASEB J. 27, 4122–4135.

Kaltman, A.J., Goldring, R.M., 1976. Role of circulatory congestion in the cardiorespiratory failure of obesity. Am. J. Med. 60, 645–653.

Kamo, T., Akazawa, H., Komuro, I., 2015. Cardiac nonmyocytes in the hub of cardiac hypertrophy. Circ. Res. 117, 89–98.

Kandala, N.B., Manda, S.O.M., Tigbe, W.W., Mwambi, H., Stranges, S., 2014. Geographic distribution of cardiovascular comorbidities in South Africa: a national cross-sectional analysis. J. Appl. Stat. 41, 1203–1216.

Kannengiesser, G.J., Opie, L.H., Van Der Werff, T.J., 1979. Impaired cardiac work and oxygen uptake after reperfusion of regionally ischaemic myocardium. J. Mol. Cell. Cardiol. 11, 197–207.

Kato, Y., Yokoyama, U., Fujita, T., Umemura, M., Kubota, T., Ishikawa, Y., 2019. Epac1 deficiency inhibits basic fibroblast growth factor-mediated vascular smooth muscle cell migration. J. Physiol. Sci. 69, 175–184.

Kaur, S., Kong, C.H.T., Cannell, M.B., Ward, M.L., 2016. Depotentiation of intact rat cardiac muscle unmasks an Epac-dependent increase in myofilament Ca2+ sensitivity. Clin. Exp. Pharmacol. Physiol. 43, 88–94.

Kawasaki, H., Springett, G.M., Mochizuki, N., Toki, S., Nakaya, M., Matsuda, M., Housman, D.E., Graybiel, A.M., 1998. A family of cAMP-binding proteins that directly activate Rap1. Science (80-.). 282, 2275–2279.

Kenchaiah, S., Evans, J.C., Levy, D., Wilson, P.W.F., Benjamin, E.J., Larson, M.G., Kannel, W.B., Vasan, R.S., 2002. Obesity and the risk of heart failure. N. Engl. J. Med. 347, 305–313.

Khaliulin, I., Bond, M., James, A.F., Dyar, Z., Amini, R., Johnson, J.L., Suleiman,

M.S., 2017. Functional and cardioprotective effects of simultaneous and individual activation of protein kinase A and Epac. Br. J. Pharmacol. 174, 438–453.

Khaliulin, I., Halestrap, A.P., Bryant, S.M., Dudley, D.J., James, A.F., Suleiman, M.S., 2014. Clinically-relevant consecutive treatment with isoproterenol and adenosine protects the failing heart against ischaemia and reperfusion. J. Transl. Med. 12.

Khaliulin, I., Parker, J.E., Halestrap, A.P., 2010. Consecutive pharmacological activation of PKA and PKC mimics the potent cardioprotection of temperature preconditioning. Cardiovasc. Res. 88, 324–333.

Kim, H.S., Cho, J.E., Hwang, K.C., Shim, Y.H., Lee, J.H., Kwak, Y.L., 2010. Diabetes mellitus mitigates cardioprotective effects of remifentanil preconditioning in ischemia-reperfused rat heart in association with anti-apoptotic pathways of survival. Eur. J. Pharmacol. 628, 132–139.

Klee, C.B., Ren, H., Wang, X., 1998. Regulation of the calmodulin-stimulated protein phosphatase, calcineurin. J. Biol. Chem. 273, 13367–13370.

Ku, C.S., Lin, S.L., Wang, D.J., Chang, S.K., Lee, W.J., 1994. Left ventricular filling in young normotensive obese adults. Am. J. Cardiol. 73, 613–615.

Kuroda, R., Hirata, K.I., Kawashima, S., Yokoyama, M., 2001. Unsaturated free fatty acids inhibit Ca 2+ mobilization and NO release in endothelial cells. Kobe J. Med. Sci. 47, 211–219.

Lacerda, L., McCarthy, J., Mungly, S.F.K., Lynn, E.G., Sack, M.N., Opie, L.H., Lecour, S., 2010. TNFα protects cardiac mitochondria independently of its cell surface receptors. Basic Res. Cardiol. 105, 751–762.

Lakshmikanthan, S., Zieba, B.J., Ge, Z.D., Momotani, K., Zheng, X., Lund, H., Artamonov, M. V., Maas, J.E., Szabo, A., Zhang, D.X., Auchampach, J.A., Mattson, D.L., Somlyo, A. V., Chrzanowska-Wodnicka, M., 2014. Rap1b in smooth muscle and endothelium is required for maintenance of vascular tone and normal blood pressure. Arterioscler. Thromb. Vasc. Biol. 34, 1486–1494.

Lambert, J.P., Nicholson, C.K., Amin, H., Amin, S., Calvert, J.W., 2014. Hydrogen sulfide provides cardioprotection against myocardial/ischemia reperfusion injury in the diabetic state through the activation of the RISK pathway. Med. Gas Res. 4.

Langan, T.J., Chou, R.C., 2011. Synchronization of mammalian cell cultures by

serum deprivation. Methods Mol. Biol. 761, 75–83.

Lanktree, M.B., Hegele, R.A., 2017. Metabolic syndrome. Genomic Precis. Med. Prim. Care Third Ed. 283–299.

Lastra, G., Manrique, C., 2015. Perivascular adipose tissue, inflammation and insulin resistance: link to vascular dysfunction and cardiovascular disease. Horm. Mol. Biol. Clin. Investig. 22, 19–26.

Laudette, M., Zuo, H., Lezoualc'h, F., Schmidt, M., 2018. Epac Function and cAMP Scaffolds in the Heart and Lung. J. Cardiovasc. Dev. Dis. 5, 9.

Lauer, M.L., Andsrson, K.M., Kannel, W.B., Levy, D., 2010. The impact of obesity on left ventricular mass and geometry. J. Am. Coll. Cardiol. 17, A293.

Lauffenburger, D.A., Horwitz, A.F., 1996. Cell migration: A physically integrated molecular process. Cell 84, 359–369.

Lecour, S., 2009. Activation of the protective Survivor Activating Factor Enhancement (SAFE) pathway against reperfusion injury: Does it go beyond the RISK pathway? J. Mol. Cell. Cardiol. 47, 32–40.

Lee, C.-H., Lee, S.-D., Ou, H.-C., Lai, S.-C., Cheng, Y.-J., 2014. Eicosapentaenoic acid protects against palmitic acid-induced endothelial dysfunction via activation of the AMPK/eNOS pathway. Int. J. Mol. Sci. 15, 10334–10349.

Lee, T.M., Lin, S.Z., Chang, N.C., 2013. Both PKA and Epac pathways mediate N-acetylcysteine-induced connexin43 preservation in rats with myocardial Infarction. PLoS One 8.

Lehrke, M., Kahles, F., Makowska, A., Tilstam, P. V., Diebold, S., Marx, J., Stöhr, R., Hess, K., Endorf, E.B., Bruemmer, D., Marx, N., Findeisen, H.M., 2015. PDE4 inhibition reduces neointima formation and inhibits VCAM-1 expression and histone methylation in an Epac-dependent manner. J. Mol. Cell. Cardiol. 81, 23–33.

Leitinger, N., 2003. Oxidized phospholipids as modulators of inflammation in atherosclerosis. Curr. Opin. Lipidol. 14, 421–430.

Lejay, A., Fang, F., John, R., Van, J.A.D., Barr, M., Thaveau, F., Chakfe, N., Geny, B., Scholey, J.W., 2016. Ischemia reperfusion injury, ischemic conditioning and diabetes mellitus. J. Mol. Cell. Cardiol. 91, 11–22.

Lerman, A., Zeiher, A.M., 2005. Endothelial function: Cardiac events. Circulation 111, 363–368.

Lewis, A.E., Aesoy, R., Bakke, M., 2016. Role of EPAC in cAMP-mediated actions in

adrenocortical cells. Front. Endocrinol. (Lausanne). 7, 63.

Lezoualc'H, F., Fazal, L., Laudette, M., Conte, C., 2016. Cyclic AMP sensor EPAC proteins and their role in cardiovascular function and disease. Circ. Res. 118, 881–897.

Li, C.-Y., Wang, L.-X., Dong, S.-S., Hong, Y., Zhou, X.-H., Zheng, W.-W., Zheng, C., 2018. Phlorizin exerts direct protective effects on palmitic acid (PA)-induced endothelial dysfunction by activating the PI3K/AKT/eNOS signaling pathway and increasing the levels of nitric oxide (NO). Med. Sci. Monit. Basic Res. 24, 1–9.

Li, C., Jackson, R.M., 2013. Reactive species mechanisms of cellular hypoxia-reoxygenation injury. Am. J. Physiol. Physiol. 282, C227–C241.

Li, Y., Konings, I.B.M., Zhao, J., Price, L.S., de Heer, E., Deen, P.M.T., 2008. Renal expression of exchange protein directly activated by cAMP (Epac) 1 and 2. Am. J. Physiol. Physiol. 295, F525–F533.

Lim, S.Y., Davidson, S.M., Mocanu, M.M., Yellon, D.M., Smith, C.C.T., 2007. The cardioprotective effect of necrostatin requires the cyclophilin-D component of the mitochondrial permeability transition pore. Cardiovasc. Drugs Ther. 21, 467–469.

Lin, L., Zhang, M., Yan, R., Shan, H., Diao, J., Wei, J., 2017. Inhibition of Drp1 attenuates mitochondrial damage and myocardial injury in Coxsackievirus B3 induced myocarditis. Biochem. Biophys. Res. Commun. 484, 550–556.

Little, G.H., Saw, A., Bai, Y., Dow, J., Marjoram, P., Simkhovich, B., Leeka, J., Kedes, L., Kloner, R.A., Poizat, C., 2009. Critical Role of Nuclear Calcium/Calmodulin-dependent Protein Kinase IIδB in Cardiomyocyte Survival in Cardiomyopathy. J. Biol. Chem. 284, 24857–24868.

Liu, J., Lloyd, S.G., 2013. High-fat, low-carbohydrate diet alters myocardial oxidative stress and impairs recovery of cardiac function after ischemia and reperfusion in obese rats. Nutr. Res. 33, 311–321.

Liu, T.W., Heden, T.D., Matthew Morris, E., Fritsche, K.L., Vieira-Potter, V.J., Thyfault, J.P., 2015. High-fat diet alters serum fatty acid profiles in obesity prone rats: Implications for in vitro studies. Lipids 50, 997–1008.

Liu, W., Liu, Y., Lowe Jr, W.L., 2001. The role of phosphatidylinositol 3-kinase and the mitogen-activated protein kinases in insulin-like growth factor-I-mediated effects in vascular endothelial cells. Endocrinology 142, 1710–1719.

Lochner, A., Genade, S., Moolman, J.A., 2003. Ischemic preconditioning: Infarct size

is a more reliable endpoint than functional recovery. Basic Res. Cardiol. 98, 337–346.

Lochner, A., Genade, S., Tromp, E., Podzuweit, T., Moolman, J.A., 1999. Ischemic preconditioning and the β-adrenergic signal transduction pathway. Circulation 100, 958–966.

Lønborg, J., Kelbæk, H., Vejlstrup, N., Jørgensen, E., Helqvist, S., Saunamäki, K., Clemmensen, P., Holmvang, L., Treiman, M., Jensen, J.S., Engstrøm, T., 2010. Cardioprotective effects of ischemic postconditioning in patients treated with primary percutaneous coronary intervention, evaluated by magnetic resonance. Circ. Cardiovasc. Interv. 3, 34–41.

Maarman, G., Marais, E., Lochner, A., Du Toit, E.F., 2012. Effect of chronic CPT-1 inhibition on myocardial ischemia-reperfusion injury (I/R) in a model of diet-induced obesity. Cardiovasc. Drugs Ther. 26, 205–216.

Makaula, S., Lochner, A., Genade, S., Sack, M.N., Awan, M.M., Opie, L.H., 2005. H-89, a non-specific inhibitor of protein kinase A, promotes post-ischemic cardiac contractile recovery and reduces infarct size. J. Cardiovasc. Pharmacol. 45, 341–347.

Mandini, S., Collini, G., Grazzi, G., Lavezzi, E., Mazzoni, G., Conconi, F., 2018. Reduction in risk factors for cardiovascular diseases and long-lasting walking habit in sedentary male and female subjects following 1 year of guided walking. Sport Sci. Health 14, 121–126.

Mangmool, S., Denkaew, T., Parichatikanond, W., Kurose, H., 2017. β-Adrenergic receptor and insulin resistance in the heart. Biomol. Ther. 25, 44–56.

Mangmool, S., Hemplueksa, P., Parichatikanond, W., Chattipakorn, N., 2015. Epac is required for GLP-1R-mediated inhibition of oxidative stress and apoptosis in cardiomyocytes. Mol. Endocrinol. 29, 583–596.

Marais, E., Genade, S., Strijdom, H., Moolman, J.A., Lochner, A., 2001. p38 MAPK activation triggers pharmacologically-induced β-adrenergic preconditioning, but not ischaemic preconditioning. J. Mol. Cell. Cardiol. 33, 2157–2177.

Marín-García, J., 2016. Cell death in the pathogenesis and progression of heart failure. Heart Fail. Rev. 21, 117–121.

Martí, M.L., 2016. The metabolic syndrome. Prensa Med. Argent. 102, 353–376.

Martínez, P., Gómez-López, G., García, F., Mercken, E., Mitchell, S., Flores, J.M., DeCabo, R., Blasco, M.A., 2013. RAP1 protects from obesity through its

extratelomeric role regulating gene expression. Cell Rep. 3, 2059–2074.

Mathers, C.D., Loncar, D., 2006. Projections of global mortality and burden of disease from 2002 to 2030. PLoS Med. 3, e442.

Matsui, T., Tao, J., Del Monte, F., Lee, K.H., Li, L., Picard, M., Force, T.L., Franke, T.F., Hajjar, R.J., Rosenzweig, A., 2001. Akt activation preserves cardiac function and prevents injury after transient cardiac ischemia in vivo. Circulation 104, 330–335.

Matsui, Y., Takagi, H., Qu, X., Abdellatif, M., Sakoda, H., Asano, T., Levine, B., Sadoshima, J., 2007. Distinct roles of autophagy in the heart during ischemia and reperfusion: roles of AMP-activated protein kinase and Beclin 1 in mediating autophagy. Circ. Res. 100, 914–22.

Mayer, P., Hinze, A.V., Harst, A., Von Kügelgen, I., 2011. A2B receptors mediate the induction of early genes and inhibition of arterial smooth muscle cell proliferation via Epac. Cardiovasc. Res. 90, 148–156.

McAlindon, E., Bucciarelli-Ducci, C., Suleiman, M.S., Baumbach, A., 2015. Infarct size reduction in acute myocardial infarction. Heart 101, 155–160.

McKean, J.S., Murray, F., Gibson, G., Shewan, D.A., Tucker, S.J., Nixon, G.F., 2015. The cAMP-producing agonist beraprost inhibits human vascular smooth muscle cell migration via exchange protein directly activated by cAMP. Cardiovasc. Res. 107, 546–555.

McKean, J.S., Shewan, D., Gibson, G., Nixon, G.F., 2013. Exchange protein activated by cAMP (Epac) inhibits human vascular smooth muscle cell migration. Proc. Physiol. Soc. 975P-975P.

McPhee, I., Gibson, L.C.D., Kewney, J., Darroch, C., Stevens, P.A., Spinks, D., Cooreman, A., MacKenzie, S.J., 2005. Cyclic nucleotide signalling: a molecular approach to drug discovery for Alzheimer's disease. Biochem. Soc. Trans. 33, 1330.

Md Hashim, N.H., 2015. Drugs and the cardiovascular system. Pharmacol. Basis Acute Care 7, 89–100.

Messerli, F.H., Nunez, B.D., Ventura, H.O., Snyder, D.W., 1987. Overweight and sudden death: Increased ventricular ectopy in cardiopathy of obesity. Arch. Intern. Med. 147, 1725–1728.

Mestas, J., Ley, K., 2008. Monocyte-endothelial cell interactions in the development of atherosclerosis. Trends Cardiovasc. Med. 18, 228–232.

Métrich, M., Berthouze, M., Morel, E., Crozatier, B., Gomez, A.M., Lezoualc'h, F., 2010. Role of the cAMP-binding protein Epac in cardiovascular physiology and pathophysiology. Pflugers Arch. Eur. J. Physiol. 459, 535–546.

Métrich, M., Lucas, A., Gastineau, M., Samuel, J.L., Heymes, C., Morel, E., Lezoualc'h, F., 2008. Epac mediates β-adrenergic receptor-induced cardiomyocyte hypertrophy. Circ. Res. 102, 959–965.

Mika, D., Leroy, J.Ô., Vandecasteele, G., Fischmeister, R., 2012. PDEs create local domains of cAMP signaling. J. Mol. Cell. Cardiol. 52, 323–329.

Mizushima, N., Levine, B., Cuervo, A.M., Klionsky, D.J., 2008. Autophagy fights disease through cellular self-digestion. Nature 451, 1069–1075.

Mocanu, M.M., Baxter, G.F., Yellon, D.M., 2000. Caspase inhibition and limitation of myocardial infarct size: Protection against lethal reperfusion injury. Br. J. Pharmacol. 130, 197–200.

Mohan, P., Brutsaert, D.L., Paulus, W.J., Sys, S.U., 1996. Myocardial contractile response to nitric oxide and cGMP. Circulation 93, 1223–1229.

Morel, E., Marcantoni, A., Gastineau, M., Birkedal, R., Rochais, F., Garnier, A., Lompré, A.M., Vandecasteele, G., Lezoualc'h, F., 2005. cAMP-binding protein Epac induces cardiomyocyte hypertrophy. Circ. Res. 97, 1296–1304.

Morgado, M., Cairrão, E., Santos-Silva, A.J., Verde, I., 2012. Cyclic nucleotide-dependent relaxation pathways in vascular smooth muscle. Cell. Mol. Life Sci. 69, 247–266.

Murakami, M., Simons, M., 2009. Regulation of vascular integrity. J. Mol. Med. 87, 571–582.

Murry, C.E., Jennings, R.B., Reimer, K.A., 1986. Preconditioning with ischemia: A delay of lethal cell injury in ischemic myocardium. Circulation 74, 1124–1136.

Nagata, D., Mogi, M., Walsh, K., 2003. AMP-activated protein kinase (AMPK) signaling in endothelial cells is essential for angiogenesis in response to hypoxic stress. J. Biol. Chem. 278, 31000–31006.

Nakagawa, T., Shimizu, S., Watanabe, T., Yamaguchi, O., Otsu, K., Yamagata, H., Inohara, H., Kubo, T., Tsujimoto, Y., 2005. Cyclophilin D-dependent mitochondrial permeability transition regulates some necrotic but not apoptotic cell death. Nature 434, 652–658.

Nasa, Y., Toyoshima, H., Ohaku, H., Hashizume, Y., Sanbe, A., Takeo, S., 1996. Impairment of cGMP- and cAMP-mediated vasorelaxations in rats with chronic

heart failure. Am. J. Physiol. 271, H2228–H2237.

NIH, 2019. Ischemic Heart Disease [WWW Document]. Natl. Inst. Heal. Hear. Dis. URL https://www.nhlbi.nih.gov/health-topics/ischemic-heart-disease (accessed 8.28.19).

Niimura, M., Miki, T., Shibasaki, T., Fujimoto, W., Iwanaga, T., Seino, S., 2009. Critical role of the N-terminal cyclic AMP-binding domain of Epac2 in its subcellular localization and function. J. Cell. Physiol. 219, 652–658.

Nishino, Y., Webb, I.G., Davidson, S.M., Ahmed, A.I., Clark, J.E., Jacquet, S., Shah, A.M., Miura, T., Yellon, D.M., Avkiran, M., Marber, M.S., 2008. Glycogen synthase kinase-3 inactivation is not required for ischemic preconditioning or postconditioning in the mouse. Circ. Res. 103, 307–314.

Nojilana, B., Bradshaw, D., Pillay-van Wyk, V., Msemburi, W., Somdyala, N., Joubert, J.D., Groenewald, P., Laubscher, R., Dorrington, R.E., 2016. Persistent burden from non-communicable diseases in South Africa needs strong action. South African Med. J. 106, 436.

Odia, O.J., 2015. Palm oil and the heart: A review. World J. Cardiol. 7, 144.

Oestreich, E.A., Malik, S., Goonasekera, S.A., Blaxall, B.C., Kelley, G.G., Dirksen, R.T., Smrcka, A. V., 2009. Epac and phospholipase Cε regulate Ca 2+ release in the heart by activation of protein kinase Cε and calcium-calmodulin kinase II. J. Biol. Chem. 284, 1514–1522.

Oestreich, E.A., Wang, H., Malik, S., Kaproth-Joslin, K.A., Blaxall, B.C., Kelley, G.G., Dirksen, R.T., Smrcka, A. V., 2007. Epac-mediated activation of phospholipase Cε plays a critical role in β-adrenergic receptor-dependent enhancement of Ca2+ mobilization in cardiac myocytes. J. Biol. Chem. 282, 5488–5495.

Ofengeim, D., Yuan, J., 2013. Regulation of RIP1 kinase signalling at the crossroads of inflammation and cell death. Nat. Rev. Mol. Cell Biol. 14, 727–736.

Okumura, S., Fujita, T., Cai, W., Jin, M., Namekata, I., Mototani, Y., Jin, H., Ohnuki, Y., Tsuneoka, Y., Kurotani, R., Suita, K., Kawakami, Y., Hamaguchi, S., Abe, T., Kiyonari, H., Tsunematsu, T., Bai, Y., Suzuki, S., Hidaka, Y., Umemura, M., Ichikawa, Y., Yokoyama, U., Sato, M., Ishikawa, F., Izumi-Nakaseko, H., Adachi-Akahane, S., Tanaka, H., Ishikawa, Y., 2014. Epac1-dependent phospholamban phosphorylation mediates the cardiac response to stresses. J. Clin. Invest. 124, 2785–2801.

Oldenburg, O., Qin, Q., Krieg, T., Yang, X.M., Philipp, S., Critz, S.D., Cohen, M. V.,

Downey, J.M., 2004. Bradykinin induces mitochondrial ROS generation via NO, cGMP, PKG, and mitoKATP channel opening and leads to cardioprotection. Am. J. Physiol. - Hear. Circ. Physiol. 286.

Ong, S.B., Subrayan, S., Lim, S.Y., Yellon, D.M., Davidson, S.M., Hausenloy, D.J., 2010. Inhibiting mitochondrial fission protects the heart against ischemia/reperfusion injury. Circulation 121, 2012–2022.

Oni, T., Youngblood, E., Boulle, A., McGrath, N., Wilkinson, R.J., Levitt, N.S., 2015. Patterns of HIV, TB, and non-communicable disease multi-morbidity in peri-urban South Africa- a cross sectional study. BMC Infect. Dis. 15.

Ozen., G., Daci., A., Norel., X., Topal., G., 2015. Human perivascular adipose tissue dysfunction as a cause of vascular disease: Focus on vascular tone and wall remodeling. Eur. J. Pharmacol. 766, 16–24.

Paiva, M.A., Gonçalves, L.M., Providência, L.A., Davidson, S.M., Yellon, D.M., Mocanu, M.M., 2010. Transitory activation of AMPK at reperfusion protects the ischaemic-reperfused rat myocardium against infarction. Cardiovasc. Drugs Ther. 24, 25–32.

Paiva, M.A., Rutter-Locher, Z., Gonçalves, L.M., Providência, L.A., Davidson, S.M., Yellon, D.M., Mocanu, M.M., 2011. Enhancing AMPK activation during ischemia protects the diabetic heart against reperfusion injury. Am. J. Physiol. - Hear. Circ. Physiol. 300.

Palmer, D., Tsoi, K., Maurice, D.H., 1998. Synergistic inhibition of vascular smooth muscle cell migration by phosphodiesterase 3 and phosphodiesterase 4 inhibitors. Circ. Res. 82, 852–861.

Palmer, R.M.J., Ashton, D.S., Moncada, S., 1988. Vascular endothelial cells synthesize nitric oxide from L-arginine. Nature 333, 664–666.

Pannekoek, W.J., Post, A., Bos, J.L., 2014. Rap1 signaling in endothelial barrier control. Cell Adhes. Migr. 8, 100–107.

Park, Y.S., Choi, S.E., Koh, H.C., 2018. PGAM5 regulates PINK1/Parkin-mediated mitophagy via DRP1 in CCCP-induced mitochondrial dysfunction. Toxicol. Lett. 284, 120–128.

Parnell, E., Palmer, T.M., Yarwood, S.J., 2015. The future of EPAC-targeted therapies: Agonism versus antagonism. Trends Pharmacol. Sci. 36, 203–214.

Patterson, C.E., Lum, H., Schaphorst, K.L., Verin, A.D., Garcia, J.G., 2000. Regulation of endothelial barrier function by the cAMP-dependent protein

kinase. Endothelium 7, 287–308.

Peng, W., Zhang, Y., Zheng, M., Cheng, H., Zhu, W., Cao, C.M., Xiao, R.P., 2010. Cardioprotection by CaMKII-δB is mediated by phosphorylation of heat shock factor 1 and subsequent expression of inducible heat shock protein 70. Circ. Res. 106, 102–110.

Penna, C., Mancardi, D., Rastaldo, R., Losano, G., Pagliaro, P., 2007. Intermittent activation of bradykinin B2 receptors and mitochondrial KATP channels trigger cardiac postconditioning through redox signaling. Cardiovasc. Res. 75, 168–177.

Pereira, L., Bare, D.J., Galice, S., Shannon, T.R., Bers, D.M., 2017. β-Adrenergic induced SR Ca2 + leak is mediated by an Epac-NOS pathway. J. Mol. Cell. Cardiol. 108, 8–16.

Pereira, L., Métrich, M., Fernández-velasco, M., Lucas, A., Leroy, J., Perrier, R., Morel, E., Fischmeister, R., Richard, S., Bénitah, J.P., Lezoualc'h, F., Gómez, A.M., 2007. The cAMP binding protein Epac modulates Ca2+ sparks by a Ca2+/calmodulin kinase signalling pathway in rat cardiac myocytes. J. Physiol. 583, 685–694.

Pereira, L., Ruiz-Hurtado, G., Morel, E., Laurent, A.C., Métrich, M., Domínguez-Rodríguez, A., Lauton-Santos, S., Lucas, A., Benitah, J.P., Bers, D.M., Lezoualc'h, F., Gómez, A.M., 2012. Epac enhances excitation-transcription coupling in cardiac myocytes. J. Mol. Cell. Cardiol. 52, 283–291.

Perin, E.C., Silva, G. V., 2004. Stem cell therapy for cardiac diseases. Curr. Opin. Hematol. 11, 399–403.

Pi-Sunyer, X., 2009. The medical risks of obesity. Postgrad. Med. 121, 21–33.

Pierce, K.L., Premont, R.T., Lefkowitz, R.J., 2002. Seven-transmembrane receptors. Nat. Rev. Mol. Cell Biol. 3, 639–650.

Pierini, D., Bryan, N.S., 2015. Nitric oxide availability as a marker of oxidative stress. Methods Mol. Biol. 1208, 63–71.

Pinton, P., Giorgi, C., Siviero, R., Zecchini, E., Rizzuto, R., 2008. Calcium and apoptosis: ER-mitochondria Ca2+ transfer in the control of apoptosis. Oncogene 27, 6407–6418.

Poirier, P., 2007. Adiposity and cardiovascular disease: Are we using the right definition of obesity? Eur. Heart J. 28, 2047–2048.

Poirier, P., Alpert, M.A., Fleisher, L.A., Thompson, P.D., Sugerman, H.J., Burke,

L.E., Marceau, P., Franklin, B.A., 2009. Cardiovascular evaluation and management of severely obese patients undergoing surgery: A science advisory from the american heart association. Circulation 120, 86–95.

Poncelas, M., Inserte, J., Vilardosa, Ú., Rodriguez-Sinovas, A., Bañeras, J., Simó, R., Garcia-Dorado, D., 2015. Obesity induced by high fat diet attenuates postinfarct myocardial remodeling and dysfunction in adult B6D2F1 mice. J. Mol. Cell. Cardiol. 84, 154–161.

Ponsioen, B., Zhao, J., Riedl, J., Zwartkruis, F., van der Krogt, G., Zaccolo, M., Moolenaar, W.H., Bos, J.L., Jalink, K., 2004. Detecting cAMP-induced Epac activation by fluorescence resonance energy transfer: Epac as a novel cAMP indicator. EMBO Rep. 5, 1176–1180.

Poppe, H., Rybalkin, S.D., Rehmann, H., Hinds, T.R., Tang, X.B., Christensen, A.E., Schwede, F., Genieser, H.G., Bos, J.L., Doskeland, S.O., Beavo, J.A., Butt, E., 2008. Cyclic nucleotide analogs as probes of signaling pathways [1]. Nat. Methods 5, 277–278.

Port, J.D., Bristow, M.R., 2001. Altered beta-adrenergic receptor gene regulation and signaling in chronic heart failure. J. Mol. Cell. Cardiol. 33, 887–905.

Prados-Torres, A., Calderón-Larrañaga, A., Hancco-Saavedra, J., Poblador-Plou, B., Van Den Akker, M., 2014. Multimorbidity patterns: A systematic review. J. Clin. Epidemiol. 67, 254–266.

Pretorius, S., Stewart, S., Sliwa, K., 2017. Lessons from the Heart of Soweto Study and future directions. SA Hear. 8.

Privett, K., Kunert, M.P., Lombard, J.H., 2004. Vascular Phenotypes: High throughput characterization of vascular reactivity in rats conditioned on 0.4 % and 4.0 % NaCl diet. Med. Coll. Wisconsin (User manu.

Puddey, I.B., Rakic, V., Dimmitt, S.B., Beilin, L.J., 1999. Influence of pattern of drinking on cardiovascular disease and cardiovascular risk factors - A review. Addiction 94, 649–663.

Purves, G.I., Kamishima, T., Davies, L.M., Quayle, J.M., Dart, C., 2009. Exchange protein activated by cAMP (Epac) mediates cAMP-dependent but protein kinase A-insensitive modulation of vascular ATP-sensitive potassium channels. J. Physiol. 587, 3639–3650.

Rafieian-Kopaei, M., Setorki, M., Doudi, M., Baradaran, A., Nasri, H., 2014. Atherosclerosis: process, indicators, risk factors and new hopes. Int. J. Prev.

Med. 5, 927–46.

Rahmati-Najarkolaei, F., Pakpour, A.H., Saffari, M., Hosseini, M.S., Hajizadeh, F., Chen, H., Yekanineja, M.S., 2017. Determinants of lifestyle behavior in Iranian adults with prediabetes: Applying the theory of planned behavior. Arch. Iran. Med. 20, 198–204.

Ramos, C.J., Lin, C., Liu, X., Antonetti, D.A., 2018. The EPAC-Rap1 pathway prevents and reverses cytokineinduced retinal vascular permeability. J. Biol. Chem. 293, 717–730.

Rampersad, S.N., Ovens, J.D., Huston, E., Umana, M.B., Wilson, L.S., Netherton, S.J., Lynch, M.J., Baillie, G.S., Houslay, M.D., Maurice, D.H., 2010. Cyclic AMP phosphodiesterase 4D (PDE4D) tethers EPAC1 in a vascular endothelial cadherin (VE-Cad)-based signaling complex and controls cAMP-mediated vascular vermeability. J. Biol. Chem. 285, 33614–33622.

Rehmann, H., 2013. Epac-inhibitors: facts and artefacts. Sci. Rep. 3, 3032.

Rehmann, H., Schwede, F., Doøskeland, S.O., Wittinghofer, A., Bos, J.L., 2003. Ligand-mediated activation of the cAMP-responsive guanine nucleotide exchange factor Epac. J. Biol. Chem. 278, 38548–38556.

Remans, P.H.J., Gringhuis, S.I., van Laar, J.M., Sanders, M.E., Papendrecht-van der Voort, E.A.M., Zwartkruis, F.J.T., Levarht, E.W.N., Rosas, M., Coffer, P.J., Breedveld, F.C., Bos, J.L., Tak, P.P., Verweij, C.L., Reedquist, K.A., 2004. Rap1 signaling is required for suppression of Ras-generated reactive oxygen species and protection against oxidative stress in T lymphocytes. J. Immunol. 173, 920–931.

Remans, P.H.J., Wijbrandts, C.A., Sanders, M.E., Toes, R.E., Breedveld, F.C., Tak, P.P., Van Laar, J.M., Reedquist, K.A., 2006. CTLA-4Ig suppresses reactive oxygen species by preventing synovial adherent cell-induced inactivation of Rap1, a Ras family GTPase mediator of oxidative stress in rheumatoid arthritis T cells. Arthritis Rheum. 54, 3135–3143.

Ritchie, S.A., Connell, J.M.C., 2007. The link between abdominal obesity, metabolic syndrome and cardiovascular disease. Nutr. Metab. Cardiovasc. Dis. 17, 319–326.

Roberts, O.L., Kamishima, T., Barrett-Jolley, R., Quayle, J.M., Dart, C., 2013. Exchange protein activated by cAMP (Epac) induces vascular relaxation by activating Ca2+-sensitive K+ channels in rat mesenteric artery. J. Physiol. 591,

5107–5123.

Roberts, O.L.L., Dart, C., 2014. cAMP signalling in the vasculature: the role of Epac (exchange protein directly activated by cAMP). Biochem. Soc. Trans. 42, 89–97.

Rogier van der Velde, A., Meijers, W.C., de Boer, R.A., 2015. Biomarkers: Cardiovascular biomarkers: translational aspects of hypertension, atherosclerosis, and heart failure in drug development. In: Principles of Translational Science in Medicine: From Bench to Bedside: Second Edition. Elsevier Inc., pp. 167–183.

Romero-Corral, A., Montori, V.M., Somers, V.K., Korinek, J., Thomas, R.J., Allison, T.G., Mookadam, F., Lopez-Jimenez, F., 2006. Association of bodyweight with total mortality and with cardiovascular events in coronary artery disease: a systematic review of cohort studies. Lancet 368, 666–678.

Romero-Corral, A., Somers, V.K., Sierra-Johnson, J., Jensen, M.D., Thomas, R.J., Squires, R.W., Allison, T.G., Korinek, J., Lopez-Jimenez, F., 2007. Diagnostic performance of body mass index to detect obesity in patients with coronary artery disease. Eur. Heart J. 28, 2087–2093.

Roscioni, S.S., Maarsingh, H., Elzinga, C.R.S., Schuur, J., Menzen, M., Halayko, A.J., Meurs, H., Schmidt, M., 2011. Epac as a novel effector of airway smooth muscle relaxation. J. Cell. Mol. Med. 15, 1551–1563.

Rossello, X., Yellon, D.M., 2016. A critical review on the translational journey of cardioprotective therapies! Int. J. Cardiol. 220, 176–184.

Ruiz-Hurtado, G., Domínguez-Rodríguez, A., Pereira, L., Fernández-Velasco, M., Cassan, C., Lezoualc'h, F., Benitah, J.P., Gómez, A.M., 2012. Sustained Epac activation induces calmodulin dependent positive inotropic effect in adult cardiomyocytes. J. Mol. Cell. Cardiol. 53, 617–625.

Ruiz-Hurtado, G., Morel, E., Domínguez-Rodríguez, A., Llach, A., Lezoualc'h, F., Benitah, J.P., Gomez, A.M., 2013. Epac in cardiac calcium signaling. J. Mol. Cell. Cardiol. 58, 162–171.

Runkle, E.A., Mu, D., 2013. Tight junction proteins: From barrier to tumorigenesis. Cancer Lett. 337, 41–48.

Salie, R., Alsalhin, A.K.H., Marais, E., Lochner, A., 2019. Cardioprotective effects of beta3-adrenergic receptor (β3-AR) pre-, per-, and post-treatment in ischemia–reperfusion. Cardiovasc. Drugs Ther. 33, 163–177.

Salie, R., Huisamen, B., Lochner, A., 2014. High carbohydrate and high fat diets

protect the heart against ischaemia/reperfusion injury. Cardiovasc. Diabetol.

Salie, R., Moolman, J.A., Lochner, A., 2011. The role of β-adrenergic receptors in the cardioprotective effects of beta-preconditioning (βPC). Cardiovasc. Drugs Ther. 25, 31–46.

Sanchis-Gomar, F., Perez-Quilis, C., Leischik, R., Lucia, A., 2016. Epidemiology of coronary heart disease and acute coronary syndrome. Ann. Transl. Med. 4.

Sands, W.A., Woolson, H.D., Milne, G.R., Rutherford, C., Palmer, T.M., 2006. Exchange protein activated by cyclic AMP (Epac)-mediated induction of suppressor of cytokine signaling 3 (SOCS-3) in vascular endothelial cells. Mol. Cell. Biol. 26, 6333–6346.

Sanmartín-Suárez, C., Soto-Otero, R., Sánchez-Sellero, I., Méndez-Álvarez, E., 2011. Antioxidant properties of dimethyl sulfoxide and its viability as a solvent in the evaluation of neuroprotective antioxidants. J. Pharmacol. Toxicol. Methods 63, 209–215.

Sassone-Corsi, P., 2012. The Cyclic AMP pathway. Cold Spring Harb. Perspect. Biol. 4.

Schmidt, M., Dekker, F.J., Maarsingh, H., 2013. Exchange protein directly activated by cAMP (epac): A multidomain cAMP mediator in the regulation of diverse biological functions. Pharmacol. Rev. 65, 670–709.

Schulman, D., Latchman, D.S., Yellon, D.M., 2015. Urocortin protects the heart from reperfusion injury via upregulation of p42/p44 MAPK signaling pathway. Am. J. Physiol. Circ. Physiol. 283, H1481–H1488.

Schulz, R., Boengler, K., Totzeck, A., Luo, Y., Garcia-Dorado, D., Heusch, G., 2007. Connexin 43 in ischemic pre- and postconditioning. Heart Fail. Rev. 12, 261–266.

Schwede, F., Bertinetti, D., Langerijs, C.N., Hadders, M.A., Wienk, H., Ellenbroek, J.H., de Koning, E.J.P., Bos, J.L., Herberg, F.W., Genieser, H.G., Janssen, R.A.J., Rehmann, H., 2015. Structure-guided design of selective Epac1 and Epac2 agonists. PLoS Biol. 13.

Sciarretta, S., Zhai, P., Shao, D., Maejima, Y., Robbins, J., Volpe, M., Condorelli, G., Sadoshima, J., 2012. Rheb is a Critical Regulator of Autophagy During Myocardial Ischemia. Circulation 125, 1134–1146.

Segers, V.F.M., Brutsaert, D.L., De Keulenaer, G.W., 2018. Cardiac remodeling: Endothelial cells have more to say than just NO. Front. Physiol. 9.

Shimabukuro, M., Hirata, Y., Tabata, M., Dagvasumberel, M., Sato, H., Kurobe, H., Fukuda, D., Soeki, T., Kitagawa, T., Takanashi, S., Sata, M., 2013. Epicardial adipose tissue volume and adipocytokine imbalance are strongly linked to human coronary atherosclerosis. Arterioscler. Thromb. Vasc. Biol. 33, 1077–1084.

Skålén, K., Gustafsson, M., Knutsen Rydberg, E., Hultén, L.M., Wiklund, O., Innerarity, T.L., Boren, J., 2002. Subendothelial retention of atherogenic lipoproteins in early atherosclerosis. Nature 417, 750–754.

Srinivasan, R., Zabuawala, T., Huang, H., Zhang, J., Gulati, P., Fernandez, S., Karlo, J.C., Landreth, G.E., Leone, G., Ostrowski, M.C., 2009. Erk1 and erk2 regulate endothelial cell proliferation and migration during mouse embryonic angiogenesis. PLoS One 4.

Stamper, R.L., Lieberman, M.F., Drake, M. V, Stamper, R.L., Lieberman, M.F., Drake, M. V, 2009. The adrenergic system and adrenergic agonists. Becker-Shaffer's Diagnosis Ther. Glaucomas 376–391.

Statista, 2017. Urbanization in South Africa 2017 [WWW Document]. URL https://www.statista.com/statistics/455931/urbanization-in-south-africa/ (accessed 10.4.18).

Steinberg, H.O., Brechtel, G., Johnson, A., Fineberg, N., Baron, A.D., 1994. Insulin-mediated skeletal muscle vasodilation is nitric oxide dependent. J. Clin. Invest. 94, 1172–1179.

Steinberg, H.O., Tarshoby, M., Monestel, R., Hook, G., Cronin, J., Johnson, A., Bayazeed, B., Baron, A.D., 1997. Elevated circulating free fatty acid levels impair endothelium-dependent vasodilation. J. Clin. Invest. 100, 1230–1239.

Stokman, G., Qin, Y., Booij, T.H., Ramaiahgari, S., Lacombe, M., Dolman, M.E.M., Van Dorenmalen, K.M.A., Teske, G.J.D., Florquin, S., Schwede, F., Van De Water, B., Kok, R.J., Price, L.S., 2014. Epac-rap signaling reduces oxidative stress in the tubular epithelium. J. Am. Soc. Nephrol. 25, 1474–1485.

Stossel, T.P., 1993. On the crawling of animal cells. Science (80-.). 260, 1086–1094.

Surinkaew, S., Aflaki, M., Takawale, A., Chen, Y., Qi, X.Y., Gillis, M.A., Shi, Y.F., Tardif, J.C., Chattipakorn, N., Nattel, S., 2019. Exchange protein activated by cyclic-adenosine monophosphate (Epac) regulates atrial fibroblast function and controls cardiac remodelling. Cardiovasc. Res. 115, 94–106.

Sutherland, E.W., Rall, T.W., 1958. Fractionation and characterization of a cyclic adenine ribonucleotide formed by tissue particles. J. Biol. Chem. 232, 1077–91.

Svensjö, E., Bouskela, E., 2018. Endothelial Barrier: Factors That Regulate Its Permeability. Endothel. Cardiovasc. Dis. Vasc. Biol. Clin. Syndr. 37–48.

Sweazea, K.L., Lekic, M., Walker, B.R., 2010. Comparison of mechanisms involved in impaired vascular reactivity between high sucrose and high fat diets in rats. Nutr. Metab. 7.

Tai, W., Shi, E., Yan, L., Jiang, X., Ma, H., Ai, C., 2012. Diabetes abolishes the cardioprotection induced by sevoflurane postconditioning in the rat heart in vivo: Roles of glycogen synthase kinase-3β and its upstream pathways. J. Surg. Res. 178, 96–104.

Tanano, I., Nagaoka, T., Omae, T., Ishibazawa, A., Kamiya, T., Ono, S., Yoshida, A., 2013. Dilation of porcine retinal arterioles to cilostazol: roles of eNOS phosphorylation via cAMP/protein kinase A and AMP-activated protein kinase and potassium channels. Invest. Ophthalmol. Vis. Sci. 54, 1443–1449.

Tavafi, M., 2013. Complexity of diabetic nephropathy pathogenesis and design of investigations. J Ren. Inj Prev 2, 59–62.

Taylor, S.C., Posch, A., 2014. The design of a quantitative western blot experiment. Biomed Res. Int. 2014.

Teringova, E., Tousek, P., 2017. Apoptosis in ischemic heart disease. J. Transl. Med. 15, 87.

Thim, T., Bentzon, J.F., Kristiansen, S.B., Simonsen, U., Andersen, H.L., Wassermann, K., Falk, E., 2006. Size of myocardial infarction induced by ischaemia/reperfusion is unaltered in rats with metabolic syndrome. Clin. Sci. 110, 665–671.

Tibazarwa, K., Ntyintyane, L., Sliwa, K., Gerntholtz, T., Carrington, M., Wilkinson, D., Stewart, S., 2009. A time bomb of cardiovascular risk factors in South Africa: Results from the Heart of Soweto Study “Heart Awareness Days.” Int. J. Cardiol. 132, 233–239.

Tong, H., Imahashi, K., Steenbergen, C., Murphy, E., 2002. Phosphorylation of glycogen synthase kinase-3β during preconditioning through a phosphatidylinositol-3-kinase-dependent pathway is cardioprotective. Circ. Res. 90, 377–379.

Tousoulis, D., Kampoli, A.-M., Tentolouris Nikolaos Papageorgiou, C., Stefanadis,

C., 2011. The role of nitric oxide on endothelial function. Curr. Vasc. Pharmacol. 10, 4–18.

Tsalkova, T., Gribenko, A. V., Cheng, X., 2010. Exchange protein directly activated by cyclic AMP isoform 2 is not a direct target of sulfonylurea drugs. Assay Drug Dev. Technol. 9, 88–91.

Tsalkova, T., Mei, F.C., Li, S., Chepurny, O.G., Leech, C.A., Liu, T., Holz, G.G., Woods, V.L., Cheng, X., 2012. Isoform-specific antagonists of exchange proteins directly activated by cAMP. Proc. Natl. Acad. Sci. 109, 18613–18618.

Tsang, A., Hausenloy, D.J., Mocanu, M.M., Carr, R.D., Yellon, D.M., 2005. Preconditioning the diabetic heart: The importance of Akt phosphorylation. Diabetes 54, 2360–2364.

Turer, A.T., Hill, J.A., 2010. Pathogenesis of myocardial ischemia-reperfusion injury and rationale for therapy. Am. J. Cardiol. 106, 360–368.

Ulucan, C., Wang, X., Baljinnyam, E., Bai, Y., Okumura, S., Sato, M., Minamisawa, S., Hirotani, S., Ishikawa, Y., 2007. Developmental changes in gene expression of Epac and its upregulation in myocardial hypertrophy. Am. J. Physiol. Circ. Physiol. 293, H1662–H1672.

Valez, V., Cassina, A., Batinic-Haberle, I., Kalyanaraman, B., Ferrer-Sueta, G., Radi, R., 2013. Peroxynitrite formation in nitric oxide-exposed submitochondrial particles: Detection, oxidative damage and catalytic removal by Mn-porphyrins. Arch. Biochem. Biophys. 529, 45–54.

Van Vickle, G., 2005. The effect of free fatty acids on endothelial cells. University of Missouri, Columbia.

Vandenabeele, P., Galluzzi, L., Vanden Berghe, T., Kroemer, G., 2010. Molecular mechanisms of necroptosis: An ordered cellular explosion. Nat. Rev. Mol. Cell Biol. 11, 700–714.

Vela, D., Buja, L.M., Madjid, M., Burke, A., Naghavi, M., Willerson, J.T., Casscells, S.W., Litovsky, S., 2007. The role of periadventitial fat in atherosclerosis: An adipose subset with potential diagnostic and therapeutic implications. Arch. Pathol. Lab. Med. 131, 481–487.

Vestweber, D., 2012. Relevance of endothelial junctions in leukocyte extravasation and vascular permeability. Ann. N. Y. Acad. Sci. 1257, 184–192.

Vianello, E., Dozio, E., Bandera, F., Schmitz, G., Nebuloni, M., Longhi, E., Tacchini, L., Guazzi, M., Corsi Romanelli, M.M., 2019. Dysfunctional EAT thickness may

promote maladaptive heart remodeling in CVD patients through the ST2-IL33 system, directly related to EPAC protein expression. Sci. Rep. 9.

Vinten-Johansen, J., Zatta, A.J., Jiang, R., Shi, W., 2013. Lethal myocardial reperfusion injury. Manag. Myocard. Reperfus. Inj. 51–85.

Vliem, M.J., Ponsioen, B., Schwede, F., Pannekoek, W.-J., Riedl, J., Kooistra, M.R.H., Jalink, K., Genieser, H.-G., Bos, J.L., Rehmann, H., 2008. 8-pCPT-2′-O-Me-cAMP-AM: An improved Epac-selective cAMP analogue. ChemBioChem 9, 2052–2054.

Vossler, M.R., Yao, H., York, R.D., Pan, M.G., Rim, C.S., Stork, P.J.S., 1997. cAMP activates MAP kinase and Elk-1 through a B-Raf- and Rap1-dependent pathway. Cell 89, 73–82.

Wang, D., Uhrin, P., Mocan, A., Waltenberger, B., Breuss, J.M., Tewari, D., Mihaly-Bison, J., Huminiecki, Ł., Starzyński, R.R., Tzvetkov, N.T., Horbańczuk, J., Atanasov, A.G., 2018. Vascular smooth muscle cell proliferation as a therapeutic target. Part 1: molecular targets and pathways. Biotechnol. Adv. 36, 1586–1607.

Wang, J.X., Jiao, J.Q., Li, Q., Long, B., Wang, K., Liu, J.P., Li, Y.R., Li, P.F., 2011. MiR-499 regulates mitochondrial dynamics by targeting calcineurin and dynamin-related protein-1. Nat. Med. 17, 71–78.

Wang, X., Luo, C., Cheng, X., Lu, M., 2017. Lithium and an EPAC-specific inhibitor ESI-09 synergistically suppress pancreatic cancer cell proliferation and survival. Acta Biochim. Biophys. Sin. (Shanghai). 49, 573–580.

Wei, C.-D., Li, Y., Zheng, H.-Y., Tong, Y.-Q., Dai, W., 2013. Palmitate induces H9c2 cell apoptosis by increasing reactive oxygen species generation and activation of the ERK1/2 signaling pathway. Mol. Med. Rep. 7, 855–861.

Wensley, I., Salaveria, K., Bulmer, A.C., Donner, D.G., Du Toit, E.F., 2013. Myocardial structure, function and ischaemic tolerance in a rodent model of obesity with insulin resistance. Exp. Physiol. 98, 1552–1564.

Westcott, C., 2015. Investigating the cholesterol-independent (pleiotropic) effects of selected hypolipidaemic agents in functional and dysfunctional endothelial cells. Stellenbosch University.

Wever, K.E., Hooijmans, C.R., Riksen, N.P., Sterenborg, T.B., Sena, E.S., Ritskes-Hoitinga, M., Warlé, M.C., 2015. Determinants of the efficacy of cardiac ischemic preconditioning: A systematic review and meta-analysis of animal

studies. PLoS One 10.

Wever, K.E., Menting, T.P., Rovers, M., van der Vliet, J.A., Rongen, G.A., Masereeuw, R., Ritskes-Hoitinga, M., Hooijmans, C.R., Warlé, M., 2012. Ischemic preconditioning in the animal kidney, a systematic review and meta-analysis. PLoS One 7.

Whelan, R.S., Konstantinidis, K., Wei, A.-C., Chen, Y., Reyna, D.E., Jha, S., Yang, Y., Calvert, J.W., Lindsten, T., Thompson, C.B., Crow, M.T., Gavathiotis, E., Dorn, G.W., O'Rourke, B., Kitsis, R.N., 2012. Bax regulates primary necrosis through mitochondrial dynamics. Proc. Natl. Acad. Sci. 109, 6566–6571.

WHO, 2018a. Cardiovascular diseases (CVDs) [WWW Document]. URL https://www.who.int/en/news-room/fact-sheets/detail/cardiovascular-diseases-(cvds) (accessed 10.4.18).

WHO, 2018b. World Health Organization - Noncommunicable Diseases (NCD) Country Profiles, 2018 [WWW Document]. https://www.who.int/nmh/countries/zaf_en.pdf?ua=1. URL https://www.who.int/nmh/countries/zaf_en.pdf (accessed 10.4.18).

Wilkins, B.J., Molkentin, J.D., 2002. Calcineurin and cardiac hypertrophy: Where have we been? Where are we going? J. Physiol. 541, 1–8.

Wilkins, R.C., Kutzner, B.C., Truong, M., Sanchez-Dardon, J., McLean, J.R.N., 2002. Analysis of radiation-induced apoptosis in human lymphocytes: Flow cytometry using Annexin V and propidium iodide versus the neutral comet assay. Cytometry 48, 14–19.

Wong, K.H.K., Cai, Y., Ying, F., Chen, X., Vanhoutte, P.M., Tang, E.H.C., 2018. Deletion of Rap1 disrupts redox balance and impairs endothelium-dependent relaxations. J. Mol. Cell. Cardiol. 115, 1–9.

Wormser, D., Kaptoge, S., Di Angelantonio, E., Wood, A.M., Pennells, L., Thompson, A., Sarwar, N., Kizer, J.R., Lawlor, D.A., Nordestgaard, B.G., Ridker, P., Salomaa, V., Stevens, J., Woodward, M., Sattar, N., Collins, R., Thompson, S.G., Whitlock, G., Danesh, J., Folsom, A.R., Chambless, L.E., Panagiotakos, D.B., Pitsavos, C., Chrysohoou, C., Stefanadis, C., Atkins, R., Barr, E.L.M., Shaw, J.E., Zimmet, P.Z., Whincup, P.H., Wannamethee, S.G., Morris, R.W., Kiechl, S., Willeit, J., Oberhollenzer, F., Mayr, A., Ebrahim, S., Yarnell, J., Gallacher, J., Nietert, P.J., Sutherland, S.E., Bachman, D.L., Keil, J.E., Mukamal, K.J., De Boer, I.H., Tybjærg-Hansen, A., Frikke-Schmidt, R.,

Giampaoli, S., Palmieri, L., Panico, S., Vanuzzo, D., Pilotto, L., De La Cámara, A.G., Rubio, M.A., Blazer, D.G., Guralnik, J.M., Phillips, C.L., Khaw, K.T., Harald, K., Jousilahti, P., Vartiainen, E., D'Agostino, R.B., Vasan, R.S., Fox, C.S., Pencina, M.J., Dankner, H.R., Chetrit, A., Lubin, F., Wilhelmsen, L., Eriksson, H., Svärdsudd, K., Welin, L., Rosengren, A., Lappas, G., Björkelund, C., Lissner, L., Bengtsson, C., Strandberg, T.E., Tilvis, R.S., Miettinen, T.A., Kiyohara, Y., Arima, H., Doi, Y., Ninomiya, T., Dekker, J.M., Nijpels, G., Stehouwer, C.D.A., Rimm, E.B., Pai, J.K., Iso, H., Kitamura, A., Yamagishi, K., Noda, H., Deeg, D., Poppelaars, J.L., Psaty, B.M., Shea, S., Döring, A., Koenig, W., Meisinger, C., Verschuren, W.M.M., Blokstra, A., Bueno-De-Mesquita, H.B., Fletcher, A., Gillum, R.F., Mussolino, M., Hankinson, S.E., Manson, J.E., Davidson, K.W., Kirkland, S., Shaffer, J.A., Korin, M.R., Sato, S., Bakker, S.J.L., Gansevoort, R.T., Hillege, H.L., Amouyel, P., Arveiler, D., Evans, A., Ferrières, J., Barrett-Connor, E., Wingard, D.L., Bettencourt, R., Witteman, J., Kardys, I., Tiemeier, H., Hofman, A., Tunstall-Pedoe, H., Tavendale, R., Lowe, G.D.O., Howard, B. V., Zhang, Y., Best, L., Umans, J., Onat, A., Hergenç, G., Can, G., Nakagawa, H., Sakurai, M., Nakamura, K., Morikawa, Y., Njølstad, I., Mathiesen, E.B., Løchen, M.L., Wilsgaard, T., ørnlöv, J., Sundström, J., Risérus, U., Ingelsson, E., Wassertheil-Smoller, S., Manson, J.E., Brunner, E., Shipley, M., Buring, J., Walker, M., Watson, S., Alexander, M., Butterworth, A.S., Franco, O.H., Gao, P., Gobin, R., Haycock, P., Kondapally Seshasai, S.R., Lewington, S., White, I.R., 2011. Separate and combined associations of body-mass index and abdominal adiposity with cardiovascular disease: Collaborative analysis of 58 prospective studies. Lancet 377, 1085–1095.

Wu, Q., Wang, T., Chen, S., Zhou, Q., Li, H., Hu, N., Feng, Y., Dong, N., Yao, S., Xia, Z., 2018. Cardiac protective effects of remote ischaemic preconditioning in children undergoing tetralogy of fallot repair surgery: A randomized controlled trial. Eur. Heart J. 39, 1028–1037.

Xia, Z., Li, H., Irwin, M.G., 2016. Myocardial ischaemia reperfusion injury: the challenge of translating ischaemic and anaesthetic protection from animal models to humans. Br. J. Anaesth. 117, ii44–ii62.

Xiao, L., Zhu, X., Yang, S., Liu, F., Zhou, Z., Zhan, M., Xie, P., Zhang, D., Li, J., Song, P., Kanwar, Y.S., Sun, L., 2014. Rap1 ameliorates renal tubular injury in diabetic nephropathy. Diabetes 63, 1366–1380.

Yan, J., Mei, F.C., Cheng, H., Lao, D.H., Hu, Y., Wei, J., Patrikeev, I., Hao, D., Stutz, S.J., Dineley, K.T., Motamedi, M., Hommel, J.D., Cunningham, K.A., Chen, J., Cheng, X., 2013. Enhanced leptin sensitivity, reduced adiposity, and improved glucose homeostasis in mice lacking exchange protein directly activated by cyclic AMP isoform 1. Mol. Cell. Biol. 33, 918–26.

Yang, Z., Kirton, H.M., Al-Owais, M., Thireau, J., Richard, S., Peers, C., Steele, D.S., 2016. Epac2-Rap1 signaling regulates reactive oxygen species production and susceptibility to cardiac arrhythmias. Antioxid. Redox Signal. 27, 117–132.

Yaspelkis, B.B., Davis, J.R., Saberi, M., Smith, T.L., Jazayeri, R., Singh, M., Fernandez, V., Trevino, B., Chinookoswong, N., Wang, J., Shi, Z.Q., Levin, N., 2001. Leptin administration improves skeletal muscle insulin responsiveness in diet-induced insulin-resistant rats. Am. J. Physiol. - Endocrinol. Metab. 280.

Yellon, D.M., Alkhulaifi, A.M., Pugsley, W.B., 1993. Preconditioning the human myocardium. Lancet 342, 276–277.

Yellon, D.M., Baxter, G.F., 1999. Reperfusion injury revisited: Is there a role for growth factor signaling in limiting lethal reperfusion injury? Trends Cardiovasc. Med. 9, 245–249.

Yokoyama, U., Minamisawa, S., Ishikawa, Y., 2010. Regulation of vascular tone and remodeling of the ductus arteriosus. J. Smooth Muscle Res. 46, 77–87.

Yokoyama, U., Minamisawa, S., Quan, H., Akaike, T., Jin, M., Otsu, K., Ulucan, C., Wang, X., Baljinnyam, E., Takaoka, M., Sata, M., Ishikawa, Y., 2008a. Epac1 is upregulated during neointima formation and promotes vascular smooth muscle cell migration. Am. J. Physiol. Circ. Physiol. 295, H1547–H1555.

Yokoyama, U., Minamisawa, S., Quan, H., Akaike, T., Suzuki, S., Jin, M., Jiao, Q., Watanabe, M., Otsu, K., Iwasaki, S., Nishimaki, S., Sato, M., Ishikawa, Y., 2008b. Prostaglandin E2-activated Epac promotes neointimal formation of the rat ductus arteriosus by a process distinct from that of cAMP-dependent protein kinase A. J. Biol. Chem. 283, 28702–28709.

Ytrehus, K., Liu, Y., Tsuchida, A., Miura, T., Liu, G.S., Yang, X.M., Herbert, D., Cohen, M. V, Downey, J.M., 1994. Rat and rabbit heart infarction: effects of anesthesia, perfusate, risk zone, and method of infarct sizing. Am. J. Physiol. 267, H2383–H2390.

Yu, J.S.L., Cui, W., 2016. Proliferation, survival and metabolism: The role of PI3K/AKT/ mTOR signalling in pluripotency and cell fate determination. Dev.

143, 3050–3060.

Yu, S., Chen, Y., Chen, S., Ye, N., Li, Y., Sun, Y., 2018. Klotho inhibits proliferation and migration of angiotensin II-induced vascular smooth muscle cells (VSMCs) by modulating NF-κB p65, Akt, and extracellular signal regulated kinase (ERK) signaling activities. Med. Sci. Monit. 24, 4851–4860.

Yu, Y. rong, Li, H. liang, Zhang, X. xun, 2008. Effects of free fatty acids on nitric oxide synthase activity and mRNA expression in endothelial cell of SD rat aorta. J. Sichuan Univ. (Medical Sci. Ed. 39, 193–196.

Zhai, P., Sciarretta, S., Galeotti, J., Volpe, M., Sadoshima, J., 2011. Differential roles of gsk-3β during myocardial ischemia and ischemia/reperfusion. Circ. Res. 109, 502–511.

Zhang, C.L., Katoh, M., Shibasaki, T., Minami, K., Sunaga, Y., Takahashi, H., Yokoi, N., Iwasaki, M., Miki, T., Seino, S., 2009. The cAMP sensor epac2 is a direct target of antidiabetic sulfonylurea drugs. Science (80-.). 325, 607–610.

Zhang, W.Y., Schwartz, E., Wang, Y., Attrep, J., Li, Z., Reaven, P., 2006. Elevated concentrations of nonesterified fatty acids increase monocyte expression of CD11b and adhesion to endothelial cells. Arterioscler. Thromb. Vasc. Biol. 26, 514–519.

Zhang, X.P., Hintze, T.H., 2006. cAMP signal transduction induces eNOS activation by promoting PKB phosphorylation. Am. J. Physiol. - Hear. Circ. Physiol. 290.

Zhang, Y.H., Casadei, B., 2012. Sub-cellular targeting of constitutive NOS in health and disease. J. Mol. Cell. Cardiol. 52, 341–350.

Zhao, Y., Vanhoutte, P.M., Leung, S.W.S., 2015. Vascular nitric oxide: Beyond eNOS. J. Pharmacol. Sci. 129, 83–94.

Zhou, X., He, P., 2011. Improved measurements of intracellular nitric oxide in intact microvessels using 4,5-diaminofluorescein diacetate. Am. J. Physiol. - Hear. Circ. Physiol. 301.

Zhu, H., Tannous, P., Johnstone, J.L., Kong, Y., Shelton, J.M., Richardson, J.A., Le, V., Levine, B., Rothermel, B.A., Hill, J.A., 2007. Cardiac autophagy is a maladaptive response to hemodynamic stress. J. Clin. Invest. 117, 1782–1793.

Zhu, M., Feng, J., Lucchinetti, E., Fischer, G., Xu, L., Pedrazzini, T., Schaub, M.C., Zaugg, M., 2006. Ischemic postconditioning protects remodeled myocardium via the PI3K-PKB/Akt reperfusion injury salvage kinase pathway. Cardiovasc. Res. 72, 152–162.

Zhu, Y., Chen, H., Boulton, S., Mei, F., Ye, N., Melacini, G., Zhou, J., Cheng, X., 2015. Biochemical and pharmacological characterizations of ESI-09 based EPAC inhibitors: Defining the ESI-09 “therapeutic window.” Sci. Rep. 5.

Zieba, B.J., Artamonov, M. V., Jin, L., Momotani, K., Ho, R., Franke, A.S., Neppl, R.L., Stevenson, A.S., Khromov, A.S., Chrzanowska-Wodnicka, M., Somlyo, A. V., 2011. The cAMP-responsive Rap1 guanine nucleotide exchange factor, Epac, induces smooth muscle relaxation by down-regulation of RhoA activity. J. Biol. Chem. 286, 16681–16692.

Zitvogel, L., Kepp, O., Kroemer, G., 2010. Decoding cell death signals in inflammation and immunity. Cell 140, 798–804.

Zweier, J.L., Talukder, M.A.H., 2006. The role of oxidants and free radicals in reperfusion injury. Cardiovasc. Res. 70, 181–190.